

Université du Québec
Institut National de la Recherche Scientifique
Institut Armand-Frappier

**NOVEL INSIGHTS INTO BIPHENYL ANALOGS METABOLISM BY THE
BACTERIAL BIPHENYL CATABOLIC PATHWAY**

Par
Thi Thanh My Pham

Thèse présentée pour l'obtention du grade
Philosophiae doctor (Ph.D) en biologie

Jury d'évaluation

Président du jury
et examinateur interne

François Lépine
INRS- Institut Armand-Frappier

Examineur externe

Mohamed Hijri
Institut de recherche en biologie végétale,
Centre sur la biodiversité, Université de
Montréal, Montréal, Québec, Canada

Examineur externe

Peter C.K. Lau
Institut de recherche en biotechnologie du
Conseil national de recherches Canada,
Montréal, Québec, Canada

Directeur de recherche

Michel Sylvestre
INRS-Institut Armand-Frappier

Acknowledgements

Coming from a developing country, with a background in chemistry, speaking neither English nor French, I am writing my thesis to obtain a Doctorate degree in biology. I mention this only so that you can appreciate the challenge this presented my director, Prof. Michel Sylvestre. Without his invaluable support and patience, I would not be here now. Michel has always listened to my problems, answered my many questions, offered advice and supported as well as provided me access to all the materials and equipment which allowed me to accomplish my research. For all these reasons, I wish to thank you Michel: You have given me the opportunity to enrich my life.

It was also my good fortune to work with Diane Barriault, Jean-Patrick Toussaint, Marie-Ève Rivard, Concetta Restieri, Fatemeh Afkhami, Letian Song, Noutcheka St-Felix and Youbin Tu, all of whom shared with me their knowledge, experience and especially their kindness. They provided me the techniques which allowed me to work, both in the fields of biochemistry and molecular biology. I would also like to thank Audrey Lemelin and Nancy Johanna Pino Rodriguez. Both interns assisted me greatly even though our time spent together was brief.

I would also like to mention the support of Sameer Al-Abdul-Wahid at QANUC NMR Facility (McGill University) for his help in NMR analysis, and Prof. Éric Déziel (INRS-Institut Armand-Frappier) for the use of his Bioscreen C system.

In addition, I would like to thank the Institut National de la Recherche Scientifique (INRS) and Vietnam Academy of Science and Technology (VAST) for partial financial support of my studies. Also I give thanks to Prof. Lê Quốc Sinh, Prof. Alain Fournier, Prof. Châu Văn Minh and Prof. Vũ Thị Bích who are responsible for the program.

Table of contents

TABLE OF CONTENTS.....	I
LIST OF FIGURES	IX
LIST OF TABLES	XIII
LIST OF ABBREVIATIONS	XV
RÉSUMÉ	1
SUMMARY	5
1. INTRODUCTION	7
1.1. The biphenyl catabolic pathway and its importance in polychlorinated biphenyls degradation and metabolic engineering	7
1.2. Problems facing the application of the biphenyl catabolic pathway.....	10
1.3. Rhizoremediation	11
1.4. Objectives of the project	13
1.5. Thesis presentation	15
2. LITERATURE REVIEW	17
2.1. Biphenyl catabolic pathway.....	17
<i>2.1.1. General description of the pathway.....</i>	<i>17</i>
<i>2.1.1.1. Upper and lower pathways of the biphenyl catabolic pathway.....</i>	<i>17</i>
<i>2.1.1.2. Enzymes of the biphenyl catabolic pathway</i>	<i>19</i>
<i>2.1.1.3. Isolated bacteria containing biphenyl catabolic pathway.....</i>	<i>20</i>
<i>2.1.1.4. Regulation of bph genes</i>	<i>22</i>
<i>2.1.2. Biphenyl dioxygenase (BPDO).....</i>	<i>26</i>
<i>2.1.2.1. Structure of BPDO</i>	<i>26</i>

2.1.2.2. Biphenyl dioxygenase mechanism of action	29
2.1.2.3. Mechanistic functioning	31
2.2. Polychlorinated biphenyls: Environmental issues and methods of destruction	37
2.2.1. Polychlorinated biphenyls.....	37
2.2.1.1. Structure, properties and usage of PCBs	37
2.2.1.2. Effects of PCBs on health	37
2.2.1.3. Polychlorinated biphenyls destruction technologies.....	38
2.2.1.3.1. Non-biological processes	38
2.2.1.3.2. Biological processes.....	38
2.2.1.3.2.1. Factors affecting the microbial degradation of PCBs	39
2.2.1.3.2.2. Microbial processes for the degradation of PCBs.....	40
2.2.1.3.2.3. Phyto- and rhizoremediation processes for the degradation of PCBs..	42
2.2.2. Rhizoremediation of PCBs	43
2.2.2.1. Plant-rhizobacteria relationship.....	43
2.2.2.1.1. Role of rhizobacteria.....	43
2.2.2.1.2. Role of plants.....	44
2.2.2.1.3. Rhizoremediation studies.....	46
2.2.3. Engineering the biphenyl catabolic pathway and plants to degrade PCBs.....	48
2.2.3.1. Engineering biphenyl catabolic pathway enzymes	49
2.2.3.2. Engineering plants	50
2.2.3.3. Other processes that can be combined with biphenyl catabolic pathway to better degrade PCBs	51
2.3. Manufacturing flavonoids via BPDOs	52
2.3.1. Green way to manufacture molecules.....	52
2.3.2. Flavonoids.....	54
2.3.3. Transformations of some common flavonoids.....	55
2.3.3.1. Flavonoids transformation by fungi and streptomyces	55
2.3.3.2. Flavonoids transformations by BPDOs.....	58
2.3.4. Engineering BPDOs for manufacturing flavonoids	63
3. PRESENTATION OF ARTICLE 1	65
3.1. The context of the article.....	65
3. 2. Contribution of the student to article 1.....	65
3.3. Article 1	66

3.4. Résumé	67
3.5. Abstract	68
3.6. Introduction	69
3.7 Materials and methods.....	71
3.7.1. <i>Bacterial strains, culture media and chemicals</i>	71
3.7.2. <i>Identification of strain U22, U23A and U24 and amplification of bphA gene.....</i>	72
3.7.3. <i>Axenic culture for the production of root exudates</i>	72
3.7.4. <i>Flavonoids detection and identification from root exudates by HPLC, LC-MS and GC-MS.....</i>	74
3.7.5. <i>Growth of R. erythropolis U23A and other isolates on root exudates</i>	75
3.7.6. <i>PCB congener degradation</i>	75
3.7.7. <i>Metabolism of flavanone by biphenyl-induced cells of strain U23A.....</i>	77
3.7.8. <i>4-Chlorobiphenyl degradation assay</i>	77
3.7.9. <i>Motility assays.....</i>	78
3.7.10. <i>Chemotaxis assay</i>	79
3.7.11. <i>Binding assays: microbial adhesion test on hydrocarbons/sand</i>	79
3.7.12. <i>Root colonization assay</i>	80
3.8. Results	81
3.8.1. <i>Isolation and identification</i>	81
3.8.2. <i>Bacterial growth on root exudates and flavonoids detection by HPLC</i>	82
3.8.3. <i>PCB and 4CB degradation by cells grown on root exudates</i>	82
3.8.4. <i>Metabolism of flavonoids by strain U23A</i>	85
3.8.5. <i>Induction of U23A biphenyl catabolic enzymes by flavanone</i>	87
3.8.6. <i>Motility, binding, and colonization assays.....</i>	89
3.9. Discussion	92
3.10. Acknowledgements	96
 4. PRESENTATION OF ARTICLE 2	 97
4.1. The context of article 2.....	97
4.2. Contribution of the student to article 2.....	98
4.3. Article 2	99

4.4. Résumé	100
4.5. Abstract	101
4.6. Introduction	102
4.7. Materials and methods.....	105
4.7.1. Bacterial strains, plasmids, and chemicals.....	105
4.7.2. Whole-cell assays to determine the ability of <i>P. pnomenusa</i> B356 and <i>B. xenovorans</i> LB400 to metabolize flavanone.....	105
4.7.3. Assays to identify the metabolites produced from flavone, flavanone, and isoflavone by <i>BphAE_{B356}</i> , <i>BphAE_{LB400}</i> and <i>BphAE_{p4}</i> , and to determine their kinetics parameters.....	106
4.7.4. Assays to assess the ability of flavone, flavanone, and isoflavone to induce the biphenyl catabolic pathway of strains B356 and LB400.....	106
4.7.5. Docking and structure analysis	107
4.8. Results	108
4.8.1. Metabolism of flavanone by biphenyl-induced resting cells of strains B356 and LB400	108
4.8.2. Induction of the biphenyl catabolic pathway of strain B356 and LB400 by flavonoids	109
4.8.3. Metabolites produced from flavonoids by purified <i>BphAE_{B356}</i> , <i>BphAE_{LB400}</i> , and <i>BphAE_{p4}</i>	112
4.8.4. Kinetic parameters of purified <i>BphAE_{B356}</i> , <i>BphAE_{LB400}</i> , and <i>BphAE_{p4}</i> toward flavone, flavanone, and isoflavone	117
4.8.5. Structural analysis of docked flavonoids at active sites of <i>BphAE_{B356}</i> , <i>BphAE_{LB400}</i> , and <i>BphAE_{p4}</i>	119
4.9. Discussion	126
4.10. Acknowledgements	129
 5. PRESENTATION OF ARTICLE 3	 131
5.1. The context of the article.....	131
5.2. Contribution of the student to article 3.....	132
5.3. Article 3	133
5.4. Résumé	134

5.5. Abstract	135
5.6. Introduction	136
5.7. Materials and methods.....	138
5.7.1. <i>Bacterial strains, plasmids, chemicals and general protocols</i>	138
5.7.2. <i>Assays to assess ability of diphenylmethane and benzophenone to support growth of strains B356 and LB400 and to induce their biphenyl catabolic pathway.....</i>	139
5.7.3. <i>Analysis of the metabolites produced from diphenylmethane and benzophenone by strains B356 and LB400 and by enzymes of their biphenyl catabolic pathway</i>	140
5.7.4. <i>Assays to identify diphenylmethane and benzophenone metabolites produced from BphAE_{B356}, BphAE_{LB400} and BphAE_{p4} and to determine their steady-state kinetics</i>	141
5.7.5. <i>Purification and NMR analysis of 2,2',3,3'-tetrahydroxybenzophenone</i>	141
5.7.6. <i>Docking and structure analysis</i>	142
5.8. Results	143
5.8.1. <i>Growth of P. pnomenusa B356 and B. xenovorans LB400 on diphenylmethane and benzophenone.....</i>	143
5.8.2. <i>Metabolism of diphenylmethane and benzophenone by P. pnomenusa B356.....</i>	146
5.8.3. <i>Metabolism of diphenylmethane by purified BphAE_{B356}, BphAE_{LB400}, and BphAE_{p4}</i>	149
5.8.4. <i>Benzophenone metabolism by purified BphAE_{B356}, BphAE_{LB400}, and BphAE_{p4}</i>	154
5.8.5. <i>Docking experiments with diphenylmethane and benzophenone</i>	155
5.9. Discussion	158
5.10. Acknowledgements	162
5.11. Supplemental materials	163
 6. PRESENTATION OF ARTICLE 4	 173
6.1. <i>The context of the article.....</i>	173
6.2. <i>Contribution of the student to article 4.....</i>	174
6.3. <i>Article 4</i>	175
6.4. <i>Résumé</i>	176
6.5. <i>Abstract</i>	177

6.6. Introduction	178
6.7. Materials and methods	181
6.7.1. Bacterial strains, plasmids, chemicals and general protocols	181
6.7.2. Whole cell assays to assess the metabolism of the various hydroxychlorobiphenyls by the biphenyl catabolic pathway enzymes	181
6.7.3. Purification and NMR analysis of 3,4-dihydroxy-4'-chlorobiphenyl, 3,4,5-trihydroxy-4'-chlorobiphenyl, and 4-(4-chlorophenyl)-cis-5,6-dihydroxycyclohex-3-en-1-one	182
6.7.4. Docking and structure analysis	183
6.8. Results	184
6.8.1. Analysis of metabolites produced from 4-hydroxy-4'-chlorobiphenyl by purified B356 BPDO	184
6.8.2. Analysis of the metabolites produced from 4-hydroxy-4'-chlorobiphenyl by biphenyl-induced resting cells of strain B356	186
6.8.3. Identity of metabolite 3, 4 and 7	187
6.8.4. Metabolism of 4-hydroxy-4'-chlorobiphenyl by E. coli cells expressing B356 BPDO	192
6.8.5. Docking experiments and suggested pathway for the metabolism of 4-hydroxy-4'-chlorobiphenyl	192
6.8.6. Metabolism of other para-hydroxy- or hydroxychlorobiphenyls	197
6.8.6.1. Metabolism of 4,4'-dihydroxybiphenyl by biphenyl-induced cells of strain B356	197
6.8.6.2. Metabolism of 3-hydroxy-4,4'-dichlorobiphenyl	199
6.8.6.3. Metabolism of 3,3'-dihydroxy-4,4'-dichlorobiphenyl	202
6.9. Discussion	204
6.10. Acknowledgements	207
 7. DISCUSSION	 209
7.1. Biphenyl catabolic pathway for the degradation of PCBs	209
Biphenyl catabolic pathway and PSMs	209
Exploiting PSMs to promote PCBs rhizoremediation	212
Degradation of hydroxychlorobiphenyls by the biphenyl catabolic pathway	214
7.2. Biphenyl catabolic pathway for molecular manufacturing	216
7.3. Mechanistic interactions between BPDOs and substrates	218

8. CONCLUSION	221
----------------------------	------------

ANNEX	247
--------------------	------------

Article 1

Plant secondary metabolites in *Arabidopsis thaliana* root exudats detected by HPLC

Article 2

Article 3

Bioscreen C system

List of figures

Figure 1.1: The first four enzymatic steps of the bacterial biphenyl catabolic pathway.	7
Figure 1.2: General chemical structure of PCBs.....	8
Figure 1.3: Phylogenetic analysis of BPDOs primary sequences.....	9
Figure 2.1: The bacterial upper and lower biphenyl catabolic pathway.	19
Figure 2.2: Organization of <i>bph</i> gene clusters encoding enzymes of biphenyl catabolic pathway in several bacteria.	23
Figure 2.3: Transcriptional regulatory system of <i>bph</i> and <i>sal</i> gene clusters in <i>P. pseudoalcaligenes</i> KF707.	25
Figure 2.4: Structure of one α - β dimers of BphAE _{B356}	27
Figure 2.5: Structure of BphAE _{B356} heterohexamer.	28
Figure 2.6: Active site of BphAE _{B356} containing biphenyl as substrate.....	28
Figure 2.7: Catalytic reaction of BPDO	29
Figure 2.8: The three components of a NDO..	30
Figure 2.9: Putative reaction mechanisms and the intermediates of the oxygenation of the substrate by NDO.....	31
Figure 2.10: C-terminal portion of the α subunit of LB400 and KF707 BPDOs.....	33
Figure 2.11: Structure around the bound substrate in BphA1 _{RHA1}	34
Figure 2.12: Superposition of segments of the crystal structure of BphAE _{LB400} with its biphenyl-bound form, and of BphAE _{p4} with its 2,6-dichlorobiphenyl-bound form	36
Figure 2.13: Potential reductive dechlorination pathway of 2,2',4,4',5-pentachlorobiphenyl.	40
Figure 2.14: Molecular structures of three classes of flavonoids	54
Figure 2.15: Skeleton of some common flavonoids	54
Figure 2.16: Microbial transformation of isoflavanone and isoflavone.....	56
Figure 2.17: Microbial transformation of flavanone	57
Figure 2.18: Biotransformation of flavone.	58

Figure 2.19: Biotransformation of certain flavonoids by BPDO _{LB400} and by BPDO _{KF707}	59
Figure 2.20: Transformation of flavonoid by cells of <i>E. coli</i> carrying <i>bphA1</i> (2072), <i>bphA2</i> , <i>bphA3</i> , <i>bphA4</i> , <i>bphB</i> , and <i>bphC</i> genes.....	62
Figure 2.21 : Biotransformation of isoflavan-4-ol by BPDO of <i>P. pseudoalcaligenes</i> KF707..	63
Figure 3.1: Axenic culture system for the growth of <i>A. thaliana</i> and the collection of root exudates.	73
Figure 3.2: Amount of 4-chlorobenzoic acid produced.....	83
Figure 3.3: Total ion chromatogram showing the peaks of the two metabolites produced from flavanone	86
Figure 3.4: Amount of 4-chlorobenzoic acid produced.....	89
Figure 3.5: Chemotaxis movement of <i>R. erythropolis</i> U23A towards tryptone or <i>A. thaliana</i> root exudates	90
Figure 3.6: Number of CFUs of <i>R. erythropolis</i> U23A or <i>P. fluorescens</i> F113 remaining in sand or associated to roots of <i>M. sativa</i> (alfalfa)	91
Figure 4.1: BPDO reaction and structures of flavanone, flavone and isoflavone.....	103
Figure 4.2: Amounts of 4-chlorobenzoic acid produced.	111
Figure 4.3: Total ion chromatogram showing the peaks of metabolites produced from flavanone and flavone.....	116
Figure 4.4: Total ion chromatogram showing the peaks of metabolites produced from isoflavone	116
Figure 4.5: Superposition of catalytic center residues of the flavone-docked and biphenyl-bounded forms of BphAE _{B356} ; two flavone-docked forms of BphAE _{p4} and the top-ranked flavone-docked form of BphAE _{B356} ; two flavone-docked forms of BphAE _{p4} and the biphenyl-bound form of BphAE _{LB400}	120
Figure 4.6: Superposition of catalytic center residues of the flavanone-docked and flavone-docked forms of BphAE _{B356} ; the top-ranked flavanone-docked form of BphAE _{p4} and the top-ranked flavanone-docked form of BphAE _{LB400}	122
Figure 4.7: Superposition of catalytic center residues of the top-ranked isoflavone-docked and flavone-docked forms of BphAE _{B356} ; the top-ranked isoflavone-docked forms of BphAE _{p4} and of BphAE _{B356} ; the top-ranked isoflavone-docked forms of BphAE _{LB400} and of BphAE _{B356}	125

Figure 5.1: Biphenyl catabolic pathway enzymes and metabolites	136
Figure 5.2: Growth curves of strain B356	145
Figure 5.3: Total ion chromatograms of metabolites produced from diphenylmethane and benzophenone.....	149
Figure 5.4: Total ion chromatograms of metabolites produced from diphenylmethane and benzophenone.....	153
Figure 5.5: NMR structural features of the hydroxylated metabolites obtained from benzophenone.....	155
Figure 5.6: Superposition of catalytic center residues of benzophenone-docked and biphenyl-bound forms of BphAE _{B356} ; diphenylmethane-docked and biphenyl-bound forms of BphAE _{B356} ; benzophenone-docked and biphenyl-bound forms of BphAE _{LB400} ; biphenyl-bound form of BphAE _{LB400} and the benzophenone-docked BphAE _{B356}	157
Figure 5.7: Profile of metabolites generated during the oxidation of diphenylmethane or benzophenone.....	159
Figure 5S1: Mass spectrum of the TMS-derived of 7-phenyl HODA.....	163
Figure 5S2: Mass spectrum of the TMS-derived of 7-phenyl DODA.....	164
Figure 5S3: Mass spectrum of the TMS-derived acidic metabolite produced from benzophenone by biphenyl-induced cells of strain B356.....	165
Figure 5S4: Mass spectrum of a <i>n</i> BuB-derived of 3-benzylcyclohexa-3,5-diene-1,2-diol....	166
Figure 5S5: Mass spectrum of a <i>n</i> BuB-derived metabolite of 3-[(5,6-dihydroxycyclohexa-1,3-dien-1-yl)methyl]cyclohexa-3,5-diene-1,2-diol.....	167
Figure 5S6: Mass spectrum of the TMS-derived of 2,3-dihydroxydiphenylmethane.....	168
Figure 5S7: Mass spectrum of the TMS-derived of 2,2',3,3'-tetrahydroxydiphenylmethane.	169
Figure 5S8: Mass spectrum of the <i>n</i> BuB-derived of 3-benzoylcyclohexa-3,5-diene-1,2-diol.	170
Figure 5S9: Mass spectrum of the TMS-derived metabolite of 2,3-dihydroxybenzophenone.	171
Figure 5S10: Mass spectrum of the TMS-derived of 2,2',3,3'-tetrahydroxybenzophenone.	172
Figure 6.1: The first four enzymatic steps of the bacterial biphenyl catabolic pathway.	179

Figure 6.2: Total ion chromatogram of the metabolites produced from 4-hydroxy-4'-chlorobiphenyl.....	186
Figure 6.3: NMR coupling constants and HMBC correlations of metabolite 7, metabolite 4, metabolite 3A, and metabolite 3B.	189
Figure 6.4: Superposition of catalytic center residues of 4-hydroxy-4'-chlorobiphenyl-docked and biphenyl-bound forms of BphAE _{B356}	194
Figure 6.5: Proposed profile of metabolites produced from 4-hydroxy-4'-chlorobiphenyl	196
Figure 6.6: Proposed profile of metabolites produced from 3-hydroxy-4,4'-dichlorobiphenyl	201
Figure 6.7: Proposed profile of metabolites produced from 3,3'-dihydroxy-4,4'-dichlorobiphenyl.....	203

List of tables

Table 2.1: Recorded rhizoremediation attempts for PCBs degradation.....	47
Table 2.2: Studies using PSMs to enhance PCBs removal	48
Table 2.3: The transformation of some flavonoids by engineered BPDOs	61
Table 3.1: List of PCBs and their concentrations in a mixture of 18 congeners.....	76
Table 3.2: Effect of carbon source on the PCB-degrading ability of <i>R. erythropolis</i> U23A toward the PCB congeners found in a mixture of 18.....	84
Table 4.1: Mass spectral features of the butylboronate-derived metabolites produced from flavanone and flavone by BphAE _{B356} , BphAE _{LB400} and BphAE _{p4}	114
Table 4.2: Steady-state kinetic parameters of BphAE _{B356} , BphAE _{LB400} , and BphAE _{p4} toward flavanone, flavone, and isoflavone	118
Table 5.1: Plasmids used in the study	138
Table 5.2: Steady-state kinetic parameters of BphAE _{B356} , BphAE _{LB400} , and BphAE _{p4} toward diphenylmethane and benzophenone	153
Table 6.1: Metabolites produced from 4-hydroxy-4'-chlorobiphenyl by B356 BPDO.....	185
Table 6.2: NMR features of metabolite 7	188
Table 6.3: ¹³ C and ¹ H chemical shifts and HMBC correlations of metabolite 3	191
Table 6.4: Metabolites produced from 4,4'-dihydroxybiphenyl by strain B356 BPDO.....	198
Table 6.5: Metabolites produced from 3-hydroxy-4,4'-dichlorobiphenyl and from 3,3'-dihydroxy-4,4'-dichlorobiphenyl by strain B356 and its BPDO.....	200

List of abbreviations

¹³ C NMR	Carbon-13 nuclear magnetic resonance
16S rRNA	16S ribosomal RNA
¹ H NMR	Proton nuclear magnetic resonance
2,3-DDHBD	2,3-dihydro-2,3-dihydroxybiphenyl-2,3-dehydrogenase
2,3-DHBD	2,3-dihydroxybiphenyl-1,2-dioxygenase
3D-QSAR	Three-dimensional quantitative structure-activity relationship
4-CBA	4-chlorobenzoic acid
7-phenyl DODA	2-hydroxy-6,7-dioxo-7-phenylheptanoic acid
7-phenyl HODA	2-hydroxy-6-oxo-7-phenylhepta-2,4-dienoic acid
Ala	Alanine
Arg	Arginine
Art.	Article
Asp	Aspartic acid
BCL	Benzoate-CoA ligase
BenABCD	Benzoate 1,2-dioxygenase and benzoate dihydrodiol dehydrogenase
BLAST	Basic local alignment search tool
BLASTn	Nucleotide-nucleotide BLAST
BLASTp	Protein-protein BLAST
BPDO	Biphenyl dioxygenase
BphAE	Terminal oxygenase
BphB	2,3-DDHBD
BphC	2,3-DHBD
BphD	HODA hydrolase
BphF	Ferredoxin
BphG	Ferredoxin reductase
BphH	2-hydroxypenta-2,4-dienoate hydratase
BphI	Acylating acetaldehyde dehydrogenase
BphJ	4-hydroxy-2-oxovalerate aldolase
BSTFA	<i>N,O</i> -bis(trimethylsilyl)trifluoroacetamide

CFU	Colony-forming unit
Chlorophenyl-HODA	2-hydroxy-6-oxo-6-[4'-chlorophenyl]-hexa-2,4-dienoic acid
Cys	Cysteine
Cl	Chlorine
COSY	Correlation spectroscopy
d	Doublet
dd	Doublet of doublets
DDD	1,1-dichloro-2,2-(4-chlorophenyl)ethane
DDT	1,1,1-trichloro-2,2-bis(4-chlorophenyl)ethane
DMSO	Dimethyl sulfoxide
DNA	Deoxyribonucleic acid
DPM	Diphenylmethane
EI	Electron impact
ESP+	Electrospray positive mode
Fe	Iron
GC	Guanine-cytosine
GC-MS	Gas chromatography–mass spectrometry
Gln	Glutamine
Glu	Glutamic acid
Gly	Glycine
H ⁺	Proton
H ₂ PO ₄ ⁻	Dihydrophosphate
HCl	Hydrochloric acid
His	Histidine
HMBC	Heteronuclear multiple bond correlation
HMSA	2-hydroxymuconate semialdehyde
HODA	2-hydroxy-6-oxo-6-phenylhexa-2,4-dienoic acid
HODA Hydrolase	2-hydroxy-6-oxo-phenylhexa-2,4-dienoate hydrolase
HPLC	High-performance liquid chromatography
HPO ₄ ²⁻	Hydrophosphate
Ile	Isoleucine

INRS	Institut national de la recherche scientifique
IPTG	Isopropyl β -D-1-thiogalactopyranoside
IUPAC	International union of pure and applied chemistry
J	Coupling constant
LB	Luria-Bertani
LC-MS	Liquid chromatography–mass spectrometry
M	Molecular weight
M ⁺	Molecular ion
M9	Basal medium
MATH	Microbial adhesion to hydrocarbons
MATS	Microbial adhesion to silica sand
MES	Morpholinethanesulfonic
Met	Methionine
MM30	Minimal mineral medium number 30
Mr	Relative molecular mass
N ₂	Nitrogen molecule
Na acetate	Sodium acetate
NaCl	Sodium chloride
NAD	Nicotinamide adenine dinucleotide
NADH	Reduced form of nicotinamide adenine dinucleotide
NADP ⁺	Nicotinamide adenine dinucleotide phosphate
NADPH	Reduced form of nicotinamide adenine dinucleotide phosphate
NahAab	Oxygenase of naphthalene dioxygenase
NahAc	Ferredoxin of naphthalene dioxygenase
NahAd	Ferredoxin reductase of naphthalene dioxygenase
NaOH	Sodium hydroxide
<i>n</i> BuB	<i>n</i> -Butylboronate
NCBI	National center for biotechnology information
NDO	Naphthalene dioxygenase
NH ₄ Cl	Ammonium chloride
NMR	Nuclear magnetic resonance

NSERC	Natural sciences and engineering research council of canada
O ₂	Oxygen
OD	Optical density
ox	Oxidant
PBS	Phosphate buffer solution
PCB	Polychlorinated biphenyl
PCR	Polymerase chain reaction
PDB	Protein data bank
PGPR	Plant growth-promoting rhizobacteria
pH	Potential hydrogen
Phe	Phenylalanine
ppm	Parts per million
PSM	Plant secondary metabolite
red	Reductant
RO	Rieske-type dioxygenase
RT	Retention time
S	Sulfur
SD	Standard deviation
SE	Standard error
Ser	Serine
Thr	Threonine
TMS	Trimethylsilyl
TOCSY	Total correlation spectroscopy
TodC1	Toluene dioxygenase α subunit
Tyr	Tyrosine
U.S.	United States
UV	Ultraviolet
v/v	Volume to volume
Val	Valine
w/v	Weight to volume

Résumé

La voie catabolique du biphényle a été grandement étudiée en raison de sa capacité à dégrader les biphényles polychlorés (BPC) en cométabolisme et de son application potentielle pour la fabrication de produits chimiques fins. Bien que de nombreux progrès aient déjà été réalisés, plusieurs problèmes restent à résoudre avant que nous puissions mettre à profit cette voie efficacement, pour l'une ou l'autre de ces deux applications. En ce qui concerne la dégradation des BPC, le nombre limité de substrats qui peuvent être métabolisés, le besoin du biphényle pour induire la voie ainsi que d'une source de carbone pour soutenir la croissance bactérienne comptent parmi les principaux facteurs qui peuvent limiter le processus. En ce qui concerne l'utilisation des enzymes pour la fabrication de produits chimiques fins, il sera nécessaire d'augmenter le nombre de substrats que chaque enzyme peut métaboliser ainsi que d'améliorer leurs paramètres cinétiques envers les substrats désirés. L'augmentation de l'éventail d'analogues du biphényle que les enzymes de la voie peuvent métaboliser impliquera sans aucun doute, des approches d'ingénierie génétique. Cependant, plusieurs autres problèmes limitant la dégradation bactérienne des BPC, pourraient être surmontés en faisant appel à la rhizoremédiation qui est un procédé de décontamination basé sur l'interaction entre les plantes et les rhizobactéries qui leur sont associées.

Les exsudats de racines contiennent des métabolites secondaires des plantes (MSP) qui sont connus pour stimuler la dégradation bactérienne des BPC. Cependant, les mécanismes par lesquels ces produits chimiques interagissent avec la voie catabolique du biphényle sont mal connus. Par conséquent, afin d'assurer le succès des procédés de rhizoremédiation, il faudra accroître notre compréhension des mécanismes d'interactions entre les exsudats des plantes et la voie catabolique du biphényle des bactéries auxquelles elles sont associées. L'identification des MSP spécifiques capables de stimuler la dégradation des BPC pourra aider à optimiser le processus. Toutefois, afin d'aider à élaborer les stratégies qui pourraient assurer un rendement de rhizoremédiation optimale, une meilleure connaissance des propriétés catalytiques des enzymes de la voie envers ces produits chimiques sera nécessaire. Dans ce travail, nous nous sommes concentrés sur la biphényle dioxygénase (BPDO), le premier enzyme de la voie catabolique du biphényle. Cet enzyme

détermine l'éventail des analogues du biphenyle que la voie peut métaboliser. De plus, il catalyse l'une des réactions biochimiques les plus difficiles, soit l'introduction de deux atomes d'oxygène dans un cycle aromatique.

Compte tenu de ces prémisses, nous avons examiné l'interaction entre la voie catabolique du biphenyle de trois souches bactériennes et quelques analogues du biphenyle sélectionnés, dont certains flavonoïdes, le diphénylméthane et la benzophénone. Les flavonoïdes sont des MSP bien connus alors que le diphénylméthane et la benzophénone sont des contaminants environnementaux et de plus, ils peuvent servir de squelette carboné pour certains MSP. De manière plus précise, nous avons déterminé si ces composés pouvaient induire la voie catabolique du biphenyle de *Rhodococcus erythropolis* U23A, de *Pandoraea pnomenusa* B356 et de *Burkholderia xenovorans* LB400 et nous avons vérifié la capacité des enzymes de cette voie catabolique à métaboliser ces composés. Sur la base des homologies génétiques des enzymes de leur voie catabolique du biphenyle, chacune de ces trois bactéries appartient à un groupe phylogénétique différent.

Nos données montrent que, parmi les flavonoïdes testés, la flavanone et l'isoflavone étaient respectivement aussi efficaces que le biphenyle pour induire la capacité des souches U23A et B356 à dégrader les BPC. En outre, de façon notable, le diphénylméthane a pu non seulement induire la voie catabolique du biphenyle de la souche B356, mais aussi soutenir sa croissance. Cependant, aucun des composés testés n'était capable d'induire la voie du biphenyle de la souche LB400. Bien que les composés testés n'étaient pas tous capables d'induire la voie catabolique du biphenyle de ces souches ou de soutenir leur croissance, ils étaient tous cométabolisés à des degrés divers par leurs enzymes de dégradation du biphenyle. Une comparaison des propriétés catalytiques des BPDO de B356 et de LB400 a permis de constater que, contrairement à la BPDO de LB400 qui métabolise mal ces composés, la BPDO de B356 métabolise ces composés aussi efficacement que le biphenyle. Une analyse structurale comparative des complexes modélisés BPDO-substrats obtenus par amarrage moléculaire nous a permis d'identifier quelques-unes des caractéristiques de la BPDO de B356 qui pouvaient expliquer sa performance supérieure à celle de LB400. L'ensemble de nos résultats appuie l'hypothèse selon laquelle chacune des trois branches phylogénétiques auxquelles se rattachent les voies cataboliques du biphenyle/chlorobiphenyle aurait évolué de façon divergente chez les bactéries, en vue de servir chacune, une fonction écophysiologique distincte qui n'est pas liée à la dégradation du biphenyle. Ceci implique que

l'efficacité des procédés de rhizoremédiation dépend grandement des souches bactériennes choisies pour le traitement, celles-ci devant répondre adéquatement aux MPS produits par les plantes avec lesquelles on voudra les associer.

Un deuxième objectif de notre travail était d'étudier le métabolisme des hydroxychlorobiphényles par la voie catabolique du biphényle. Nous avons comparé la capacité des souches B356 et LB400 à transformer quatre hydroxychlorobiphényles substitués en position *para* sur les deux noyaux (le 4,4'-dihydroxybiphényle, le 4-hydroxy-4'-chlorobiphényle, le 3-hydroxy-4,4'-dichlorobiphényle, et le 3,3'-dihydroxy-4,4'-dichlorobiphényle). Pour chacun de ces quatre substrats, aucun des métabolites dihydrodihydroxybiphényles attendus n'a été détecté, mais plusieurs métabolites inattendus ont été détectés et identifiés. Les données suggèrent que les métabolites dihydrodihydroxy générés par ces contaminants sont instables et se réarrangent pour générer des métabolites culs-de-sac, dont certains pourraient être préoccupants pour l'environnement. L'étude apporte un nouvel éclairage sur le devenir de ces dérivés des polychlorobiphényles dans l'environnement.

Summary

The biphenyl catabolic pathway in bacteria has been extensively studied because of its ability to cometabolically degrade polychlorinated biphenyls (PCBs) and its potential application to manufacture fine chemicals. Although many achievements have been obtained, several problems need to be overcome before we can use this pathway efficiently for both applications. With respect to the degradation of PCBs, the limited substrate range, the need for biphenyl to induce the pathway and for a carbon source to support bacterial growth are among the major factors that may limit the process. With respect to the use of the enzymes for manufacturing fine chemicals, the enzymes substrate range needs to be expanded and reaction rates toward the desired substrates need to be increased. Expanding the range of biphenyl analogs that the pathway enzymes can metabolize will require enzyme engineering. However, several of the other problems that limit bacterial PCB remediation, may be overcome by exploiting a process, called rhizoremediation, which is based on the interaction between plants and their associated rhizobacteria.

Plant exudates contain plant secondary metabolites (PSMs) that are known to promote the bacterial degradation of PCBs. However, the bases by which these chemicals interact with the biphenyl catabolic pathway are largely unknown. Therefore, successful application of the rhizoremediation process will require a better understanding about the mechanistic interactions between plants exudates and the biphenyl catabolic pathway of their associated bacteria. Identifying the individual PSMs that may promote or induce PCB degradation may help to optimize the process. However, in order to help determining strategies that may further improve the rhizoremediation process, better knowledge about catalytic properties of the pathway enzymes toward these chemicals will be required. In this work, we focused on the biphenyl dioxygenase (BPDO) the first enzyme of the biphenyl catabolic pathway. This enzyme determines the range of biphenyl analogs that the pathway can metabolize and it also catalyzes one of the most difficult biochemical reactions, the introduction of two oxygen atoms onto an aromatic ring structure.

Given these premises, in this work, we have examined the interaction between the biphenyl catabolic pathway of three bacterial strains and selected biphenyl analogs, including flavonoids, diphenylmethane and benzophenone. Flavonoids are well-known PSMs whereas, diphenylmethane and benzophenone are both environmental contaminants and in addition, they may also serve as carbon skeleton for some PSMs. Precisely, we have determined

whether these compounds can induce the biphenyl catabolic pathway of *Rhodococcus erythropolis* U23A, *Pandoraea pnomenusa* B356, and *Burkholderia xenovorans* LB400 and we have verified whether their biphenyl catabolic enzymes can metabolize these compounds. Each of the three bacteria belongs to a different phylogenetic cluster with respect to their biphenyl-degrading pathway.

Our data showed that among the tested flavonoids, flavanone and isoflavone were respectively, as potent as biphenyl to induce the PCB-degrading ability of strains U23A and B356. In addition, remarkably, diphenylmethane was able to not only induce the biphenyl pathway of strain B356 but also support its growth. However, none of the tested compounds were able to induce the biphenyl pathway of strain LB400. Although not all of the tested compounds were able to either induce the biphenyl catabolic pathway or support the growth of the three bacterial strains, they were all cometabolized, though to various extents by their biphenyl degrading enzymes. When comparing the catalytic properties of B356 and LB400 BPDOs, notably, we found that unlike LB400 BPDO that metabolized these compounds poorly, those of B356 BPDO were in the same range as for biphenyl. Structural analysis of docked BPDOs allowed us to identify some of the B356 BPDO features that were responsible for its better performance than LB400 BPDO. Together, our results are consistent with the hypothesis that three phylogenetically distinct biphenyl/chlorobiphenyl-degrading pathways have evolved divergently in bacteria and each may serve distinct ecophysiological functions not related to biphenyl degradation. This implies that the efficiency of rhizoremediation processes will depend on the choice of appropriate bacterial strains responding to the specific PSMs produced by the plants with which they are associated.

A second objective of our work was to study the metabolism of hydroxychlorobiphenyls by the biphenyl catabolic pathway. We compared the ability of strain B356 and LB400 to transform four doubly *para*-substituted hydroxy-chlorobiphenyls (4,4'-dihydroxybiphenyl, 4-hydroxy-4'-chlorobiphenyl, 3-hydroxy-4,4'-dichlorobiphenyl and 3,3'-dihydroxy-4,4'-dichlorobiphenyl). For all four substrates, the expected dihydrodihydroxybiphenyl metabolites were not detected and unexpected metabolites were produced and identified. Data suggested that the dihydrodihydroxy metabolites generated from these environmental contaminants are unstable and they rearrange to generate dead-end metabolites that may be of concern for the environment. The study brings more insights about the likely fate of these polychlorobiphenyls derivatives in the environment.

1. Introduction

1.1. The biphenyl catabolic pathway and its importance in polychlorinated biphenyls degradation and metabolic engineering

The biphenyl catabolic pathway is a four enzymatic-step pathway used by bacteria to transform biphenyl to benzoic acid (238, 316) (**Figure 1.1**). The first step is initiated by the biphenyl dioxygenase (BPDO) (encoded by *bhAEFG*). This enzyme inserts two atoms of oxygen onto two vicinal *-ortho,-meta* carbons of one of the two aromatic rings to produce *cis*-2,3-dihydro-2,3-dihydroxybiphenyl. The oxidized ring is then re-aromatized by the 2,3-dihydro-2,3-dihydroxybiphenyl-2,3-dehydrogenase (2,3-DDHBD) encoded by *bphB*. The catechol product is then further metabolized by two enzymes, the 2,3-dihydroxybiphenyl-1,2-dioxygenase (2,3-DHBD) encoded by *bphC* and the 2-hydroxy-6-oxo-phenylhexa-2,4-dienoate hydrolase (HODA hydrolase) encoded by *bphD*, generating as end-products benzoic acid and 2-hydroxypenta-2,4-dienoic acid. The biphenyl catabolic pathway has been studied since the early 1970s, because of its potential to degrade polychlorinated biphenyls (PCBs) which count among the major priority pollutants worldwide. Recently, this catabolic pathway has also been investigated because of its importance in the domain of metabolic engineering.

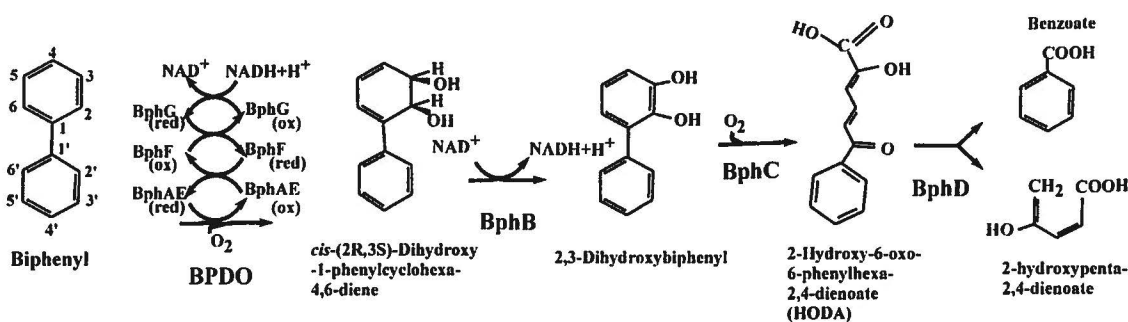


Figure 1.1: The first four enzymatic steps of the bacterial biphenyl catabolic pathway.

Polychlorinated biphenyls are unnatural chemicals that were released in the environment from the 1930s until late 1970s. These chemicals were synthesized principally for industrial purposes. Their desirable physical and chemical properties such as thermal and chemical stability, dielectric property, and fire resistance, made them become common compounds used in industry (252). However, due to these properties, they are very persistent in the environment. Since PCBs may cause serious health effects on human and animal, their usage is now banned. However, despite of the synthesis and usage restrictions, PCBs still persist in the environment. In some areas, their concentrations are largely above their maximal allowable toxic levels (127, 166). General structure of PCBs was shown in **Figure 1.2**.

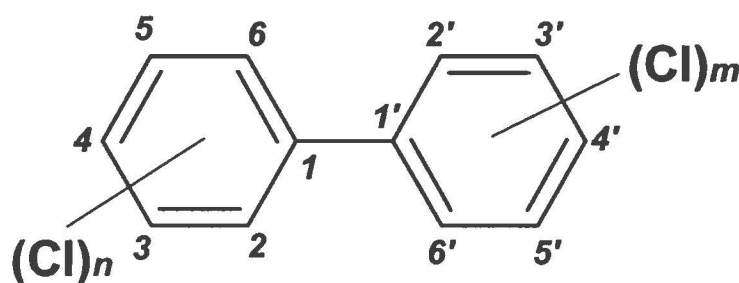


Figure 1.2: General chemical structure of PCBs ($1 \leq m + n \leq 10$)

Microbial catabolic pathways play an essential role in recycling organic matters in the environment. They are very versatile and able to completely degrade most of organic compounds on earth. However, only a few of these pathways may potentially metabolize PCBs. Among them, the most studied one is the bacterial biphenyl catabolic pathway. As mentioned above, this pathway contains four enzymatic steps. The most important and most studied enzyme of this pathway is the BPDO which initiates the degradation process and thus limits the range of PCB congeners degraded by the pathway. Therefore, the mechanism in which its active site interacts with substrate is of particular interest. On the basis of their primary sequence alignments, three distinct phylogenetic clusters were identified from the bacterial BPDOs (345) (**Figure 1.3**), each one seems to have different catalytic properties toward biphenyl analogs (300). Therefore, comparing the structures and biochemical

properties of members of each of these clusters may help getting more insights about the mechanistic functioning of this class of enzymes.

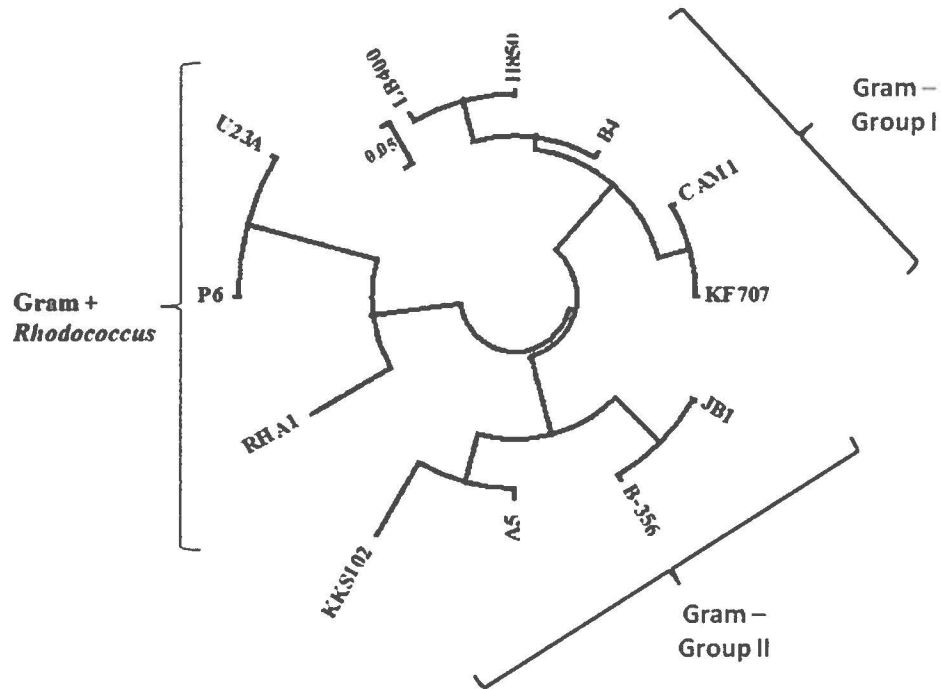


Figure 1.3: Phylogenetic analysis of BPDOs primary sequences. The sequence accession numbers are: B356 (*P. pnomenusa* B356) [CTU47637] (7); JB1 (*Burkholderia* sp. JB1) [CAA08985] (233); A5 (*Cupriavidus oxalaticus* A5) [CAD61140] (263); KKS102 (*Pseudomonas* sp. KKS102) [Q52438] (153); KF707 (*Pseudomonas alcaligenes* KF707) [AAF22429] (97); CAM1 (*Pseudomonas* sp. CAM1) [AAK14781] (190); B4 (*Pseudomonas* sp. B4) [AAB88813] (64); H850 (*Ralstonia eutropha* H850) [AJ544525] (26); LB400 (*B. xenovorans* LB400) [YP556409] (24); RHA1 (*Rhodococcus jostii* RHA1) [YP707265] (187); P6 (*Rhododoccus globerulus* P6) [CAA56346] (96); U23A (*R. erythropolis* U23A) [HQ412801] (330).

Besides their importance for environmental decontamination processes, microbial enzymes may serve as biocatalysts for the synthesis of fine chemicals and pharmaceutical products. By using enzymes, chemical synthesis processes are milder, require less energy, structure isomerization and rearrangement are minimized as well pollutants production. Recently, along with the development of DNA sequencing, gene expression profiling and high throughput enzyme structure analysis technologies and with the advent of metabolic reactions' databases, biocatalysts became available to the emerging domain of metabolic engineering. This process aims at converting raw materials into valuable chemicals through sequential enzymatic reactions. Keasling, J.D. (2010) proposed that "In any future, metabolic engineering will soon rival and potentially eclipse synthetic organic chemistry" (148).

In our work, we paid particular attention to flavonoids which are plant secondary metabolites (PSMs), for two reasons. First, these compounds have molecular structures similar to biphenyl, the substrate and inducer of the biphenyl catabolic pathway. Second, they have recently attracted considerable attention in the disciplines of nutrition, food science, and pharmacology due to their beneficial effects on human health, with diverse physiological and pharmacological activities such as anti-oxidative, anti-cancer, anti-allergic, anti-inflammatory, anti-platelet, antiviral, antifungal, anti-hemolytic, anti-ischemic, estrogenic (84, 219, 253). With regard to these beneficial activities, some hydroxy-flavonoids are more potent than simple flavonoids (44, 142). However, regiospecific hydroxylation of the aromatic ring is one of the most challenging reactions in organic synthesis (224). To this end, BPDOs have featured an ability to regiospecifically hydroxylate many aromatic substrates. Therefore, these enzymes are promising biocatalysts for the synthesis of novel flavonoid derivatives.

1.2. Problems facing the application of the biphenyl catabolic pathway

Biphenyl catabolic pathway enzymes are promising tools for designing efficient biological processes for the decontamination of PCBs as well as in biocatalytic processes for the synthesis of organic chemicals. However, there are several problems that need to be

solved in order to expand the applications of this pathway. In the context of industrial biocatalysts, it is necessary to increase the enzymes specificities toward substrates, as well as the performance of the catalytic reaction. Improving biocatalytic processes, will thus require better insights about the enzymes structural features involved in substrate binding and catalytic reaction. With respect to the PCB decontamination processes, a major issue is the range of PCB congeners that the biphenyl catabolic pathway can metabolize and which depends upon the number and position of chlorine atoms on the aromatic ring. Therefore, expanding substrate range is one of the difficulties that need to be solved. Another issue is that expression of the biphenyl catabolic pathway enzymes requires biphenyl or other fortuitous compounds as inducer. In addition, since PCBs are cometabolized, an alternative carbon source is required to support bacterial growth during the PCB-degrading process. Finally, PCBs are very hydrophobic and poorly bioavailable therefore these pollutants and bacteria are unevenly distributed in soil. This strongly reduces PCBs accessibility to bacteria for their transform action.

In order to expand the range of PCBs metabolized by the biphenyl catabolic enzymes, it is better to use directed evolution since natural evolution is slow. Thus, understanding mechanistic interactions between the degrading enzyme and the various substrates is essential. Other issues such as: inducers, carbon source, and the bioavailability of PCBs that limite the application of this pathway for PCB remediation processes may be solved by exploiting plants and their interacting rhizospheric microorganisms. Certain PSMs that plants excrete via their root exudates may act as inducers of the biphenyl catabolic pathway while other root exudates components may serve as carbon source. On the other hand, plants may also help dislocate PCBs from the subsurface to the rhizosphere zone where they are in direct contact with rhizobacteria that may degrade them.

1.3. Rhizoremediation

Rhizoremediation is a process involving microorganisms and plants to degrade pollutants in the rhizosphere. Although both plants and microbes play an important role in this process, in most case, rhizobacteria are considered as the main contributors.

Rhizosphere is a narrow region of soil that has an intimate contact with the root system of plants, wherein the plants and microorganisms interact. It has been well documented that a broad range of organic compounds are released into the rhizosphere by plant roots via root exudation. These compounds include sugars, amino acids, organic acids, nucleotides, enzymes, as well as PSMs (39). Some of them are known to promote microbial growth and therefore in the rhizosphere, microbes are 10-100 times more abundant than in bulk soil (soil which is not part of the rhizosphere) (199). This ratio may be even up to 1,000-2,000 times in soils containing a large amount of roots (199). These microbes, in return, produce plant growth promoters to support plant growth and also they release antibiotics that may protect plants from pathogens (63, 181). PSMs are believed to play an essential role in the rhizosphere as they may act as signal molecules to control the various steps involved in the microbial root colonization process. In this respect, it has been suggested that PSMs themselves would modulate the quantity and quality of these signal molecules by controlling appropriate microbial catabolic pathways (273).

Plant secondary metabolites are important components of the root exudates. Among them, flavonoids and terpenoids are two common classes. Several studies have provided lines of evidence that several terpenoids and flavonoids may promote bacterial PCB degradation. Gilbert et al. (1997) (103) investigated the ability of *Arthrobacter sp.* B1B to grow and degrade PCBs in soils enriched with natural sources of terpenoids (orange peels, eucalyptus leaves, ivy leaves and spearmint leaves). Results showed that plant terpenoids may be useful to enhance the rate of PCBs degradation by bacteria in soil. A more direct example about the ability of PSMs to trigger biphenyl catabolic pathway was observed by Narasimhan and colleagues (216). According to their work, *Pseudomonas putida* PML2, a phenylpropanoid-utilizing and PCB-degrading rhizobacterium, was able to remove PCBs in rhizosphere of wild-type *Arabidopsis thaliana*, more efficiently than that of its mutant that excreted less flavonoids.

These studies provide lines of evidence that some PSMs may act as fortuitous inducers of the bacterial biphenyl catabolic pathway. The structural similarities of PSMs with biphenyl and the data suggesting that they may act as inducers of the pathway may be used as an evidence supporting the hypothesis proposed by Focht (1995) (79) that the bacterial biphenyl catabolic pathway may serve ecological functions related to the metabolism of not

only biphenyl but also of many biphenyl analogs in soil. Therefore, although this hypothesis has never been clearly demonstrated, the biphenyl catabolic pathway may count among the microbial metabolic pathways proposed by Shaw et al. (2006) (285) which would be involved in the maintenance of PSMs in soils.

1.4. Objectives of the project

Getting more insights about how the biphenyl catabolic pathway responds to PSMs may be useful in identifying among PSMs, the biphenyl analogs that would possibly act as inducer for this pathway. Furthermore, investigating the catalytic properties of the pathway enzymes toward these chemicals can provide insights on the ecophysiological role of this pathway and it will allow us, to better define strategies that can be successfully applied to the rhizoremediation process. In addition, the information will improve our knowledge in order to design novel, better performing engineered enzymes for the degradation of PCBs and related pollutants and enzymes that may be useful as catalysts for the production of novel bioactive molecules from existing PSMs.

As illustrated on **Figure 1.3**, three phylogenetically distinct biphenyl-degrading bacterial groups have been recognized on the basis of BPDOs sequence alignment. These groups may also differ with respect to their mechanism of regulation. In this context and with regard to the rhizoremediation process, our major objective was **to determine how bacterial representatives of each of these groups would response to selected biphenyl analogs including flavonoids and diphenylmethane and benzophenone**, which may serve as carbon skeleton for PSMs.

Three bacterial strains, each of which belongs to a distinct phylogenetic group of biphenyl-degrading bacteria were chosen for this study. *R. erythropolis* U23A is a biphenyl-degrading rhizobacteria isolated in the course of this study. *P. pnomenusa* B356 and *B. xenovorans* LB400 are two Gram-negative bacteria that were not shown to be able to colonize plant roots but which have been extensively studied over the years.

With regard to not only the rhizoremediation process, but also to the potential application of these catabolic pathways for biocatalytic purposes, our second objective consisted at **examining the metabolite profile generated from these selected flavonoids by the biphenyl catabolic pathway and examining some of the BPDO structure features influencing the enzyme catalytic properties toward these substrates.**

Our results clearly showed that some flavonoids could act as inducer of the biphenyl catabolic pathway of certain bacteria. In addition, these compounds could be efficiently cometabolized by those bacteria. More interesting, we found that certain bacteria could use their biphenyl catabolic pathway to grow on certain of these biphenyl analogs such as diphenylmethane. Since BPDO is the enzyme that determines the range of substrates the pathway can metabolize, in this work, we have also used modeled structures to identify some of the BPDO residues and protein atoms that are involved in the binding of these substrates analogs. Together, results raised the question on the assumption that biphenyl catabolic pathway has evolved to principally metabolize biphenyl in one hand, and on the other hand, these results supported our hypothesis mentioned at the beginning that the pathway may have evolved to serve other ecophysiological roles than biphenyl degradation.

Over the last decades, much attention has been paid to the degradation of PCBs by the biphenyl catabolic pathway. However, few studies have been devoted to hydroxychlorobiphenyls which are increasingly considered as a new class of contaminants. These chemicals are released in PCB-contaminated sites as a result PCBs metabolism by plants and animals. Therefore, in order to get a better insight about the overall fate of PCBs in the environment, we defined as an indirectly related objective, to investigate **the metabolism of hydroxychlorobiphenyls by the biphenyl catabolic pathway.** In this work, we focused on the doubly-*para* substituted hydroxychlorobiphenyls because preliminary work had indicated that the dihydrodihydroxy metabolites derived from these biphenyl analogs may be unstable and prone to generate dead-end metabolites that may accumulate in the environment.

1.5. Thesis presentation

The thesis is presented as the scientific article-form for the Doctorate in Biology program at INRS. Section 2 of the thesis (Literature review) introduces the current knowledge about the biphenyl catabolic pathway including information about biphenyl-degrading bacteria, enzymes of the pathway, and the applications of the pathway in the PCB-rhizoremediation process as well as in manufacturing molecules. The results obtained and the methods used in this work are then introduced in the sections 3, 4, 5 and 6, in three published and one submitted articles. Section 7, the last section of the thesis, serves as a general discussion of all results obtained as well as the perspectives of the project.

2. Literature review

2.1. Biphenyl catabolic pathway

2.1.1. General description of the pathway

2.1.1.1. Upper and lower pathways of the biphenyl catabolic pathway

The biphenyl catabolic pathway has been studied since the early 1970s because of its potential ability to degrade PCBs, which are among the most serious environmental pollutants worldwide (94, 309) as well as its promising role in manufacturing molecules (278, 289).

The biphenyl catabolic pathway, also called the upper biphenyl pathway transforms biphenyl to benzoic acid and 2-hydroxypenta-2,4-dienoic acid (8, 128, 129, 312). The two key intermediates are then metabolized by lower biphenyl pathways. The bacterial upper and lower biphenyl catabolic pathways are shown in **Figure 2.1**.

Benzoic acid and 2-hydroxypenta-2,4-dienoic acid pathways, which metabolize the end products of the biphenyl upper pathway are shown in **Figure 2.1**. 2-Hydroxypenta-2,4-dienoic acid is transformed to acetyl-CoenzymeA by a series of enzymes including 2-hydroxypenta-2,4-dienoate hydratase (BphH), acylating acetaldehyde dehydrogenase (BphI) and 4-hydroxy-2-oxovalerate aldolase (BphJ) (238). Since this product can be used directly by the Krebs cycle, the 2-hydroxypenta-2,4-dienoic acid pathway may allow the growth of bacterial strain on the substrate.

Benzoic acid is mineralized normally via catechol by a pathway involving a benzoate 1,2-dioxygenase and a benzoate dihydrodiol dehydrogenase (113) or unusually via benzoyl-CoenzymeA by a pathway involving a benzoate-CoenzymeA ligase in various bacteria including *B. xenovorans* strain LB400 (53, 100) (**Figure 2.1**).

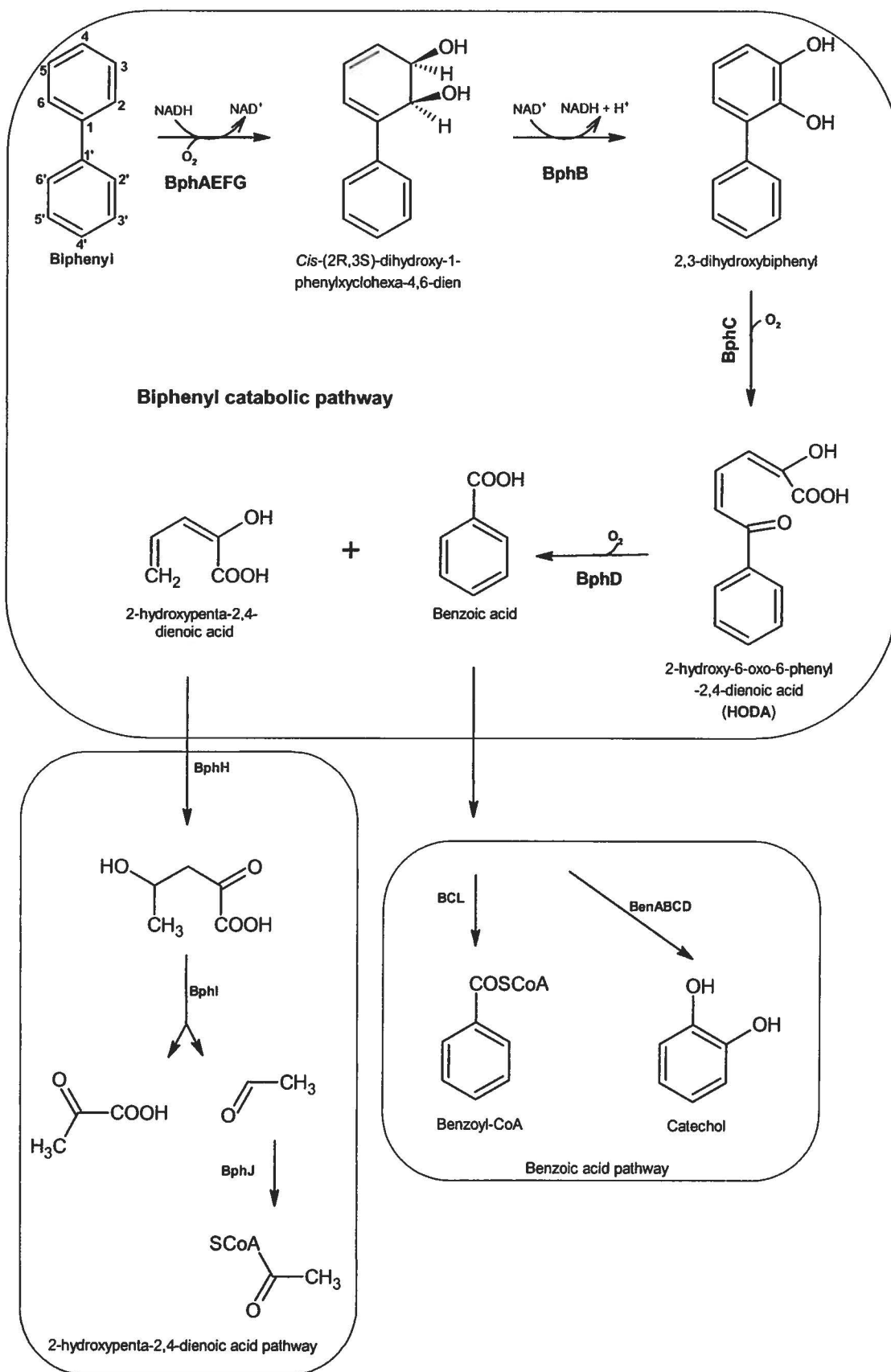


Figure 2.1: The bacterial upper and lower biphenyl catabolic pathway. The lower pathway is composed of the 2-hydroxypenta-2,4-dienoic acid and the benzoic acid pathways. BphAEFG: Biphenyl 2,3-dioxygenase; BphB: *cis* -2,3-dihydro-2,3-dihydroxybiphenyl dehydrogenase; BphC: 2,3-dihydroxybiphenyl 1,2-dioxygenase; BphD: 2-hydroxy-6-oxo-6-phenylhexa-2,4-dienoate (HODA) hydrolase (5); BphH: 2-hydroxypenta-2,4-dienoate hydratase; BphI: acylating acetaldehyde dehydrogenase; BphJ: 4-hydroxy-2-oxovalerate aldolase; BCL: benzoate-CoenzymeA ligase; BenABCD: benzoate 1,2-dioxygenase and benzoate dihydrodiol dehydrogenase (238). The genes designations are those of *B. xenovorans* LB400.

Although in this work, we are interested in the upper pathway, the lower ones are also important for the degradation of chlorinated pollutants that may generate, as end-products, chlorobenzoates (297) or chlorocatechols (338), which are toxic for microorganisms. The lower pathways are also important because they determine the ability of biphenyl analogs to support microbial growth. In this regard, biphenyl can only be mineralized if the lower pathways enzymes are up regulated by a metabolite of the upper pathway.

2.1.1.2. Enzymes of the biphenyl catabolic pathway

Biphenyl catabolic pathway (upper pathway) contains four steps catalyzed by four enzymes, including the biphenyl dioxygenase (BPDO); the 2,3-dihydro-2,3-dihydroxybiphenyl dehydrogenase (2,3-DDHBD); the 2,3-dihydroxybiphenyl 1,2-dioxygenase (2,3-DHBD) and the 2-hydroxy-6-oxo-6-phenylhexa-2,4-dienoate hydrolase (HODA) (Figure 2.1).

The first enzyme, BPDO catalyzes the first step of the pathway. This enzyme is critical in determining the substrate specificity of PCB-degrading bacteria (5) therefore it is the most important and most studied enzymes of the pathway. This enzyme can metabolize not only biphenyl and PCBs but also other persistent organic pollutants such as 1,1,1-trichloro-2,2-bis(4-chlorophenyl)ethane (DDT) (169), dibenzofuran (206), chlorodibenzofurans (164) and several flavonoids (44, 271, 278). A better understanding of the BPDO's structure will be very helpful in designing newer and more efficient biocatalysts to degrade pollutants or

produce compounds of pharmaceutical, industrial or agricultural interest. More details about this enzyme are discussed in section 2.1.2.

The second enzyme of biphenyl catabolic pathway, 2,3-DDHBD (or BphB), is a dehydrogenase that catalyzes the dehydrogenation of the first metabolite of the pathway. This enzyme metabolizes a wide range of BPDO's products generated from biphenyl, PCBs, naphthalene, dibenzofuran and flavonoids (22, 142, 205). Its versatility can be explained by the plasticity of the catalytic cavity allowing conformational changes during the reaction to accommodate various substrates (57).

The third enzyme is the 2,3-DHBD (or BphC) that cleaves catechol metabolite formed by the 2,3-DDHBD. This enzyme is less versatile than 2,3-DDHBD, thus it cannot transform *meta-para* dihydroxy metabolites (68). Moreover, this enzyme was shown to be inhibited by 3-chlorocatechol, a metabolite that unfortunately may be produced by the lower biphenyl pathway when PCBs with chlorine atom at position 3 are used as substrate (297). These two limitations can cause an incomplete-degradation of contaminants or other substrates.

The last enzyme, HODA hydrolase (or BphD) catalyzes the hydrolysis of the metabolite produced by 2,3-DHBD. Similar to BPDO, this enzyme has been intensively studied. It has been crystallized (126, 215) and its catalytic mechanism has been investigated as well (125, 255). The catalytic capacity of this enzyme varies among biphenyl-degrading bacteria. HODA hydrolase of strain LB400 transforms HODAs that contain chlorine atoms on the phenyl ring but poorly metabolizes the ones bearing chlorine atoms on the dienoate moiety. In contrast, BphD from *R. globerulus* P6 catalyses the hydrolysis of 9-Cl, 10-Cl and 9,10-diCl HODAs efficiently. Moreover, BphD_{LB400} is strongly inhibited by 3-Cl HODA and less by 4-Cl HODA, while BphD_{P6} is more sensitive toward 4-Cl HODA than toward 3-Cl HODA (269).

2.1.1.3. Isolated bacteria containing biphenyl catabolic pathway

Several bacterial strains were isolated and identified as biphenyl-degrading organisms. We will describe below some of those strains, that have been extensively studied, and that are also the subjects of this work.

P. pnomenusa B356 (formerly *Comamonas testosteria* B356 (344)), isolated from domestic wastewater treatment sludge in Quebec, Canada (8), is one of the most interesting strains for the degradation of PCBs as well as for other persistent organic pollutants because of not only its higher specific activity toward biphenyl than any other biphenyl-degrading bacteria but also its remarkable ability to metabolize and cometabolize certain flavonoids and other biphenyl analogs including DDT, 2,6-dichlorobiphenyl, 2,4,4'-trichlorobiphenyl (106, 169). This bacterium catalyzes the degradation of dichlorobiphenyls in order of priority *meta*- > *ortho*- > *para*- substituted (20, 134).

B. xenovorans LB400 (109) (formerly *Pseudomonas* sp. LB400 (101), or *Burkholderia fungorum* LB400) has been extensively studied. This bacterium was isolated from a PCBs contaminated soil sample. *B. xenovorans* LB400 can efficiently transform a broad range of substrates, especially the *ortho*-substituted PCBs congeners that contain up to six chlorines (207). It can also catalyze the transformation of certain 2,5-substituted congeners, such as 2,2',5,5'-tetrachlorobiphenyl to 3,4-dihydroxylated metabolites (130). Interestingly, LB400 has also the capacity to catalyze the dehalogenation of certain 2-chloro congeners to yield 2,3-dihydroxybiphenyls (270).

Another well studied Gram-negative strain is *P. pseudoalcaligenes* KF707, discovered on a site surrounding a PCB manufacturing factory in Japan (97). The biphenyl genes of this strain are very closely related to those of strain LB400. However unlike strain LB400, this bacterium metabolizes preferentially PCB congeners containing chlorine atoms at *para*- and *meta*- positions (155) rather than *ortho*- substituted congeners (101). Other strains such as *C. necator* H850 isolated from a sludge sample of Hudson River (New York), prefers *ortho*-substituted PCBs (26) and *Acidovorax* sp. KKS102 isolated from a land near a refinery in Japan, degrades both *ortho*- and *para*- substituted PCBs (227).

R. erythropolis U23A, a Gram-positive bacterium, was isolated recently from the rhizosphere of plant grown on a site artificially contaminated with PCBs and its characterization is part of this thesis (330). This strain was shown to exhibit a chemotactic response toward PSMs released in *A. thaliana* root exudates. And more interestingly, it can use *A. thaliana* root exudates as source of carbon to support its growth. The biphenyl catabolic pathway in this strain could be induced by flavanone as strongly as by biphenyl, the traditional inducer, and at the same time, flavanone was metabolized by this bacterial

pathway (330). Whole-cells of strain U23A induced by biphenyl degrade well PCB congeners bearing up to four chlorine atoms (2,3,2',3'- and 2,3',4,4'-tetrachlorobiphenyls) (330). Although *R. erythropolis* U23A was isolated only few years ago (in 2011) (330), its competences in degrading soil pollutants are very promising and need more studies to be fully explored.

R. jostii RHA1 isolated from soil contaminated with hexachlorocyclohexane has also been extensively studied (280). This strain shows an ability to degrade a wide range of PCB congeners. It was able to transform 45 of 62 PCBs congeners, including tri-, tetra-, penta-, and even octachlorobiphenyls (280, 281). This strain can effectively transform both *ortho*- and *para*- substituted PCB congeners as well. Its high PCB-degrading potential was explained by the gene duplications of not only PCBs degradation genes (137, 360) but also regulatory genes (320).

One more Gram-positive bacterium which has been well studied is *R. globerulus* P6 isolated from Lake Mendota (Wisconsin, US) sediment (96). *R. globerulus* P6 metabolizes more efficiently PCB congeners with chlorine at *meta*- position such as 3,3'-dichlorobiphenyl than congeners with chlorine at *para*- position (40). The strain hardly transforms double *ortho*- congeners (40, 196).

On the basis of the phylogenetic analysis of BPDOs primary sequences, these bacteria were classified in three distinct clusters (344, 357) (**Figure 1.3**). The Gram-negative group I contains *B. xenovorans* LB400 and *P. pseudoalcaligenes* KF707. The Gram-negative group II includes *P. pnomenusa* B356 and *Acidovorax* sp. KKS102. The three Gram-positive strains, *R. jostii* RHA1, *R. erythropolis* U23A, *R. globerulus* P6, and the closely related *Rhodococcus* sp. M5 (170) belong to the third distinct group. Each group seems to have a different capacity to transform pollutants (300).

2.1.1.4. Regulation of *bph* genes

The genetic organization of *bph* genes of selected biphenyl-degrading bacteria is shown in **Figure 2.2**. *B. xenovorans* LB400 and *P. pseudoalcaligenes* KF707 have a similar *bph* gene organization (70, 122, 319, 352, 353). The similarity of *bph* gene clusters suggests that gene clusters can be transferred among soil bacteria (94). For these bacteria, the genes coding the biphenyl catabolic upper pathway (*bphAEFGBCD*) and biphenyl catabolic lower pathway (*bphKHJI*) are grouped together.

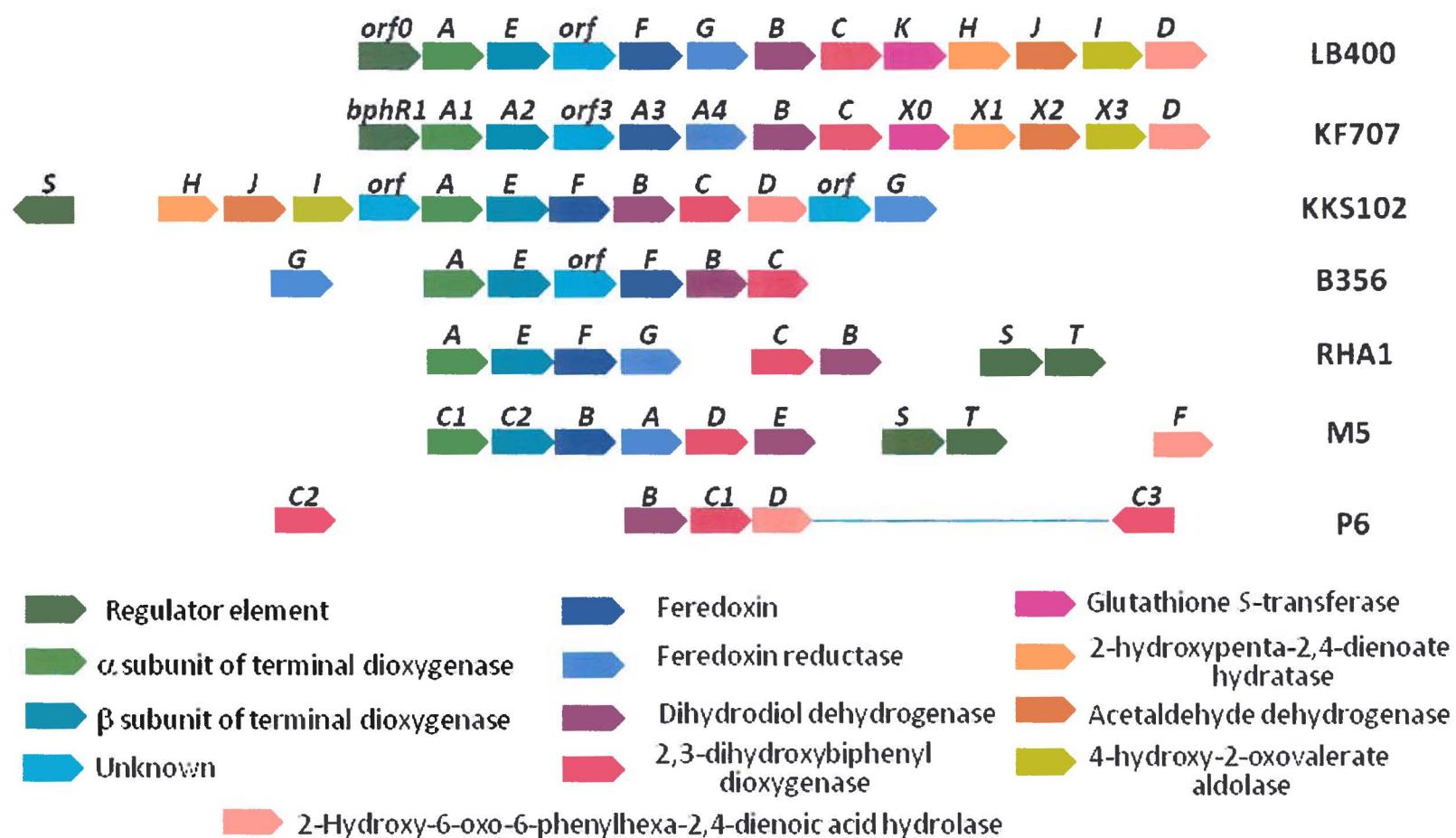


Figure 2.2: Organization of *bph* gene clusters encoding enzymes of biphenyl catabolic pathway in several bacteria. *B. xenovorans* LB400 (70, 122); *P. pseudoalcaligenes* KF707 (319, 352, 353); *P. pnumenusa* B356 (314); *R. jostii* RHA1 (187, 286, 360); *R. globerulus* P6 (14), *Rhodococcus* sp. M5 (170, 171) and *Acidovorax* sp. KKS102 (92). Since genes were designated differently for different organisms, we have referenced homologous genes by a same color.

P. pnomenusa B356 and *Acidovorax* sp. (formally *Pseudomonas* sp. (92)) KKS102 exhibit a similar gene organization where *bphG* is located outside of the *bphAEF* gene cluster (314). Unlike other strains, *R. globerulus* P6 contains two more *bphC* genes (*bphC2* and *bphC3*) encoding 2,3-dihydroxybiphenyl dioxygenases that *meta*-cleave the aromatic ring (14). The existence of multiple *bphC* genes may help to increase the range of PCBs that can be metabolized by this strain (157, 337). The current knowledge shows *bph* gene clusters are significantly different in term of gene organization which is reflected by the fact that the regulatory mechanisms differ considerably among the various PCB-degrading bacteria.

Although the gene organization of many biphenyl catabolic pathways has been well characterized, little is known about the regulation of their expression. One of the most studied regulatory mechanisms of the *bph* genes is that of *P. pseudoalcaligenes* KF707 (90, 352, 353).

KF707 utilizes both biphenyl and salicylate as sole source of carbon. In this strain, the regulation of the *bph* operon is interrelated with that of the *sal* operon, which is located 6.6-kb downstream of the *bph* genes, through a mechanism involving the regulatory genes *bphR1* and *bphR2* (353). The *bphR1* gene is located just upstream of *bphABC*, while the *bphR2* is located just upstream of *sal* operon (94). The BphR1 protein, a GntR-type regulator, was shown to act as an activator of its own gene (*bphR1*), and of *bphX1X2X3* (designated as *bphHJI* in LB400, **Figure 2.2**) and *bphD*. BphR2, a LysR-type regulatory protein, controls the transcription of *bphR1* and *bphABC* (352). In the absence of both biphenyl and salicylate, BphR2 binds to *bphR2* operator and represses *bphR2* transcription while BphR1 binds to the operator of the *sal* gene cluster to repress the genes. Under these conditions, *bph* and *sal* genes are not transcribed. In the presence of biphenyl, BphR2 binds to the operators of *bphR1* and of the *bphA1A2A3A4BC* (designated as *bphAEFGBC* in LB400, **Figure 2.2**) cluster to activate their transcription. HODA is thus produced from biphenyl, and this metabolite further promotes the transcription of *bphR1* to produce BphR1, which activates its own transcription and the transcription of *bphX0X1X2X3* and *bphD*. At the same time, BphR1 still represses *sal* gene. In the presence of salicylate, 2-hydroxymuconate semialdehyde (HMSA) is produced. This metabolite binds to BphR1 releasing it from the *sal* promoter to suppress *sal* gene repression. Under these conditions, BphR2 is highly expressed in the presence of

HMSA and it binds to *sal* operator to activate the *sal* gene (94, 98). The transcriptional regulatory system of the *bph* and *sal* gene clusters of strain KF707 is shown in **Figure 2.3**.

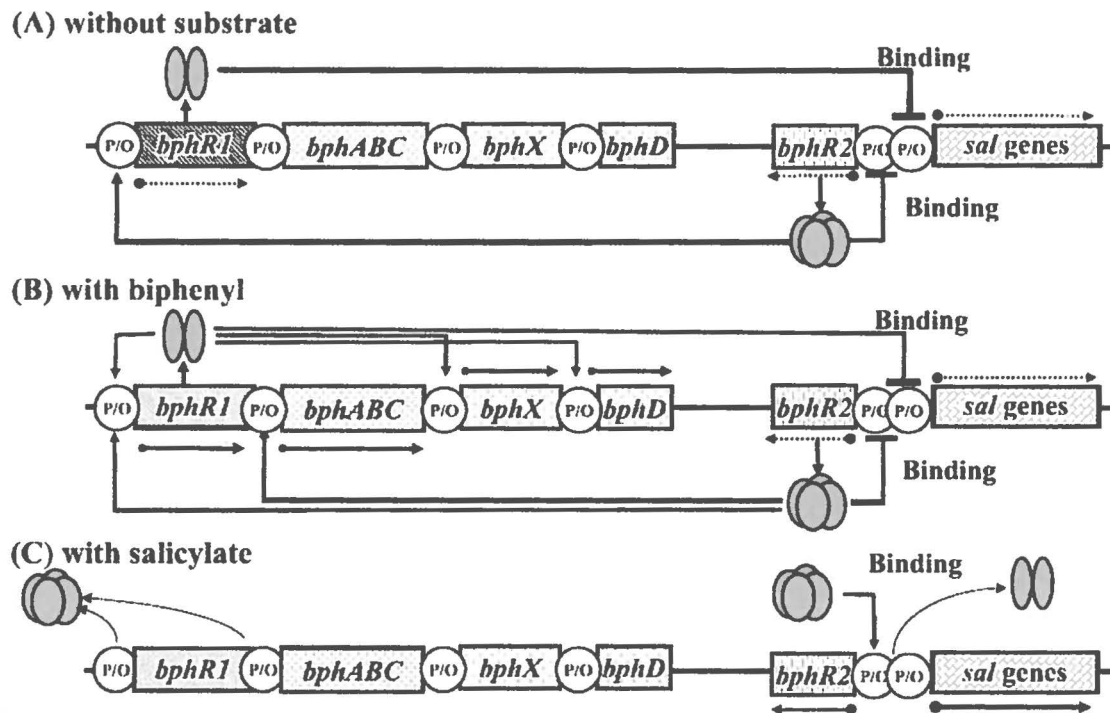


Figure 2.3: Transcriptional regulatory system of *bph* and *sal* gene clusters in *P. pseudoalcaligenes* KF707. The drawing has been reproduced from Fujihara et al. (2006) (90).

In the case of *B. xenovorans* LB400 (27), the regulation involves gene *orf0* which exhibits 85% of DNA sequence homology with *bphR1* of strain KF707. Unlike BphR1, data suggest that in the presence of biphenyl, Orf0 may be a positive regulator of all *bph* genes (27, 53). However, further work is required to clarify the precise role of Orf0 and other possible regulatory genes that were up-regulated during the growth of strain LB400 on biphenyl (53).

Similar to the *bph* genes of strain KF707, those of strain *Acidovorax* sp. KKS102 are also induced by HODA (228). In strain KKS102, the *bph* operon is regulated by pE promoter

located upstream of *bphE* gene. This promoter is negatively controlled by BphS, a GntR family repressor, produced by *bphS*, which is also located upstream region of *bphE* (**Figure 2.2**). In the absence of HODA, BphS binds to the pE promoter to repress the transcription of *bph* operon. This repression is released in the presence of HODA (227).

A two-component regulatory system of *bpdS* and *bpdT* was identified from the region between *bpdE* and *bpdF* (170) and downstream *bphB* (321) of *Rhodococcus* sp. M5 and *R. jostii* RHA1, respectively (**Figure 2.2**). In strain M5, BpdS and BpdT regulate the transcription of the *bph* operon (*bpdC1C2BADEF*- designated as *bphAEFGCB* in LB400, **Figure 2.2**) in which BphS acts as a sensor histidine kinase and BphT acts as a response regulator (170). In strain RHA1, biphenyl activates the *bphS* product (BphS), BphS then activates BphT by phosphorylation. The activated BphT promotes the transcription initiation from P_{bphA1} and the expression of the *bphAEFGCB* genes is induced (321).

2.1.2. Biphenyl dioxygenase (BPDO)

2.1.2.1. Structure of BPDO

BPDO is a Rieske-type three-component enzyme. It comprises a terminal oxygenase which is an iron sulfur protein, a ferredoxin (encoded by *bphF*) and a ferredoxin reductase (encoded by *bphG*). The terminal oxygenase includes a large subunit (subunit α , encoded by *bphA*) and a small subunit (subunit β , encoded by *bphE*) (**Figure 2.4**) (128, 129, 309). The terminal oxygenase (herein designated as BphAE) is directly responsible for the catalytic activity whereas the ferredoxin (BphF) and the ferredoxin reductase (BphG) are responsible for transporting electrons from NADH to BphAE.

The oxygenase component is a $\alpha_3\beta_3$ heterohexamer formed by the association of 3 α (BphA, $M_r = 51,000$) and 3 β subunits (BphE, $M_r = 22,000$) (129, 134) (**Figure 2.5**). Like the other aryl-hydroxylating dioxygenases, BphAE (also called BphA1A2) hexamers take a mushroom-like shape with the three α subunits making the head and three β subunits making the tip of the mushroom (61, 74, 99, 106, 138). Each α subunit comprises a Rieske-type [2Fe-2S] His₂Cys₂ cluster and coordinates a Fe(II) ion via the side chains of conserved His, His, and Asp residues. The mononuclear Fe also binds with one water molecule (129, 165). BphG

($M_r = 43,000$) is a flavoprotein and belongs to the glutathione reductase family (275). The crystal structure analysis of BphF ($M_r = 12,000$) showed that it is a small iron-sulfur protein and has a typical Rieske-type ferredoxin fold (273).

The crystal structures of BphAE from *B. xenovorans* LB400, *P. pnomenusa* B356 and *R. jostii* RHA1 have now been elucidated. The Protein Data Bank coordinate files of BphAE_{LB400} (165), BphAE_{B356} (106, 169) and BphA1A2_{RHA1} (99) are available. **Figure 2.4** shows the structure of one α - β dimer of BphAE_{B356} with one α subunit (green) and one β subunit (pale cyan).

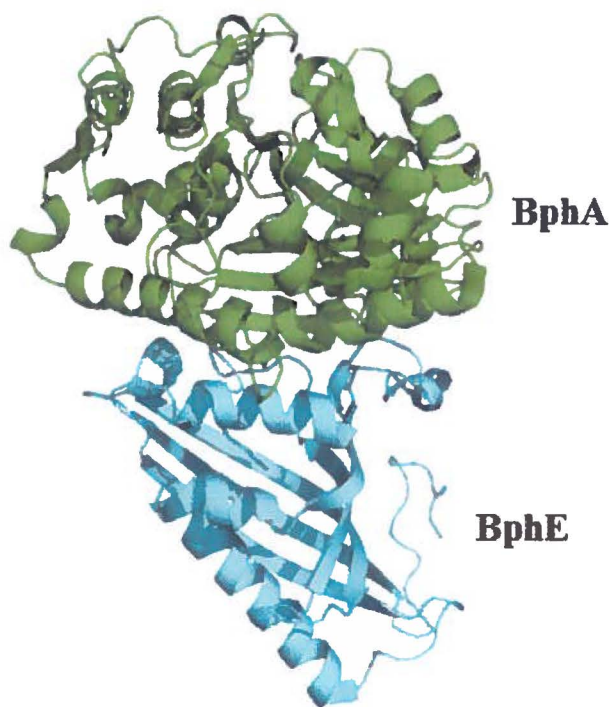


Figure 2.4: Structure of one α (green)- β (pale cyan) dimers of BphAE_{B356}. Image obtained by PyMOL software using the RCBS Protein Data Bank PDB entry 3GZX.

The catalytic center of BphAE contains many essential amino acids (**Figure 2.6**). Any mutations affecting these residues will inactivate completely the enzyme. The four residues that compose the Rieske center of BphAE_{B356} are: His123, His102, Cys100 and Cys120. They correspond to His121, His100, Cys98, Cys118 of BphAE_{RHA1} and His123, His102, Cys100, Cys120 of BphAE_{LB400}. The three residues coordinating to Fe^{2+} of BphAE_{B356} are His233,

His239 and Asp386. For BphAE_{LB400} and BphAE_{RHA1}, these three residues are: His233 and His239, His224 and His230, Asp388 and Asp378, respectively.

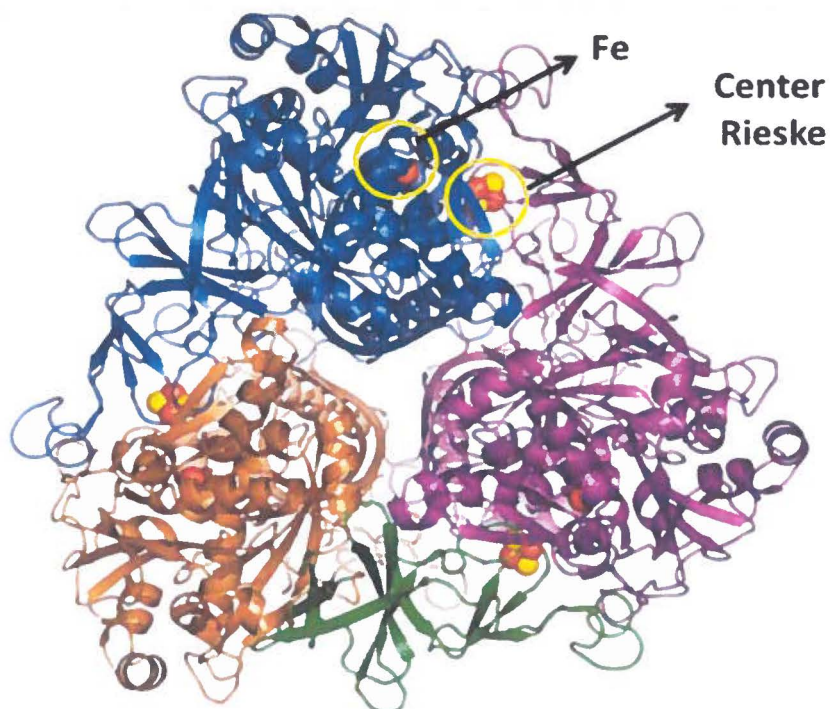


Figure 2.5: Structure of BphAE_{B356} heterohexameric. Image was taken from Colbert et al. (2013) (46).

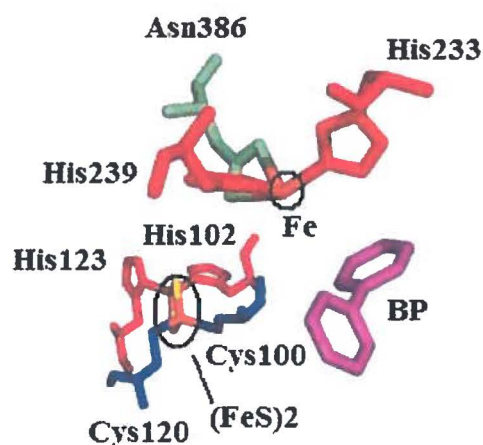


Figure 2.6: Active site of BphAE_{B356} containing biphenyl (BP) as substrate. The figure shows the residues of the Rieske (Fe₂-S₂) cluster and those that coordinate to Fe²⁺. Image obtained by PyMOL software using RCBS Protein Data Bank PDB entry 3GZX.

2.1.2.2. Biphenyl dioxygenase mechanism of action

The mechanism by which electrons are transferred from NADH to the ferredoxin component of BPDO of strain *Acidovorax sp.* KKS102, has been studied by Senda et al. (2007) (274). Crystal structure of reaction intermediates of the enzyme components showed that, initially, two electrons are transferred from NADH to BphG. BphG then delivers one electron at a time to the Rieske center of BphF. BphF acts like an electron-transport shuttle between BphG and BphAE (Figure 2.7). The mechanism is similar to that of naphthalene dioxygenase (NDO) (75) shown in Figure 2.8.

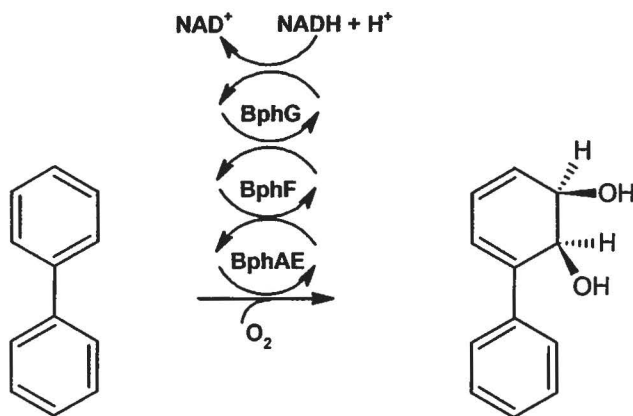


Figure 2.7: Catalytic reaction of BPDO

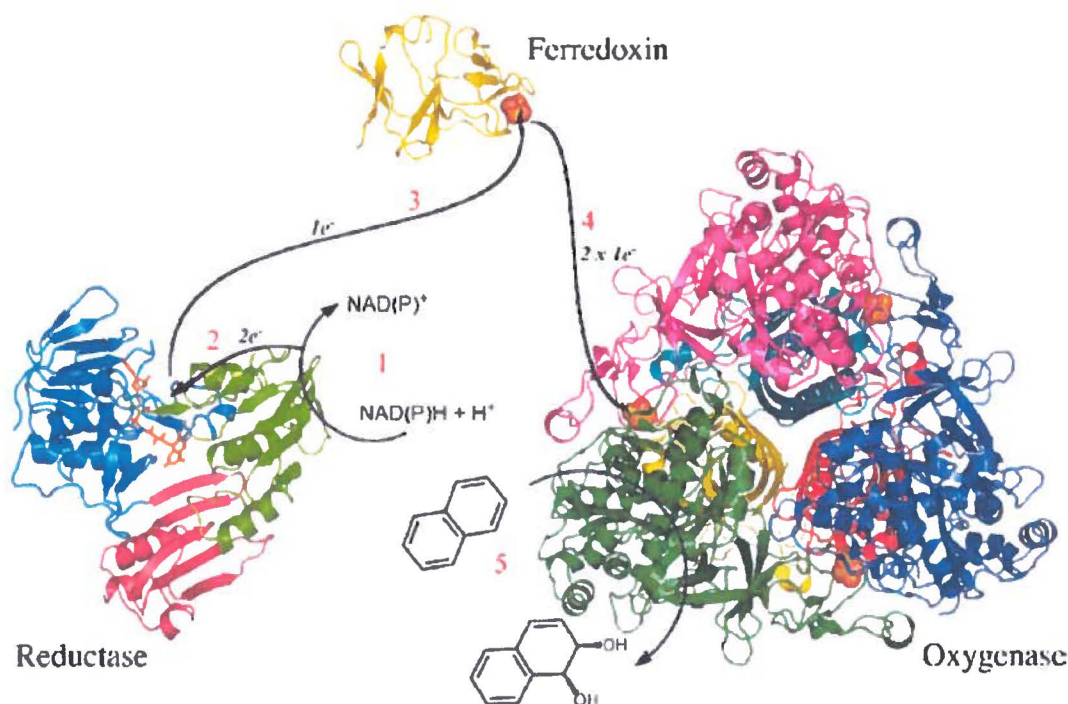


Figure 2.8: The three components of a NDO. The ferredoxin reductase (NahAd) oxidizes NAD(P)H to NADP⁺ and captures 2 electrons (step 1). The flavin retains the electrons (step 2). The ferredoxin (NahAc) then shuttles the electron from the reductase to the oxygenase (NahAab) (step 3 and 4). The substrate is then oxygenated at the mononuclear iron site to form the product (step 5). Image was taken from Ferraro et al. (2005) (75).

The BPDO catalytic reaction is initiated by the binding of substrate to the active center and of oxygen to the ferrous ion. There are two hypothetical catalytic processes for the substrate oxidation by the non-heme-iron center of the Rieske-type dioxygenases (248). These two processes are illustrated in **Figure 2.9**.

End-on attack mode: An iron peroxo is formed and it attacks directly the substrate to produce the intermediate Fe-O-O-substrate complex. Then, the O-O bond of the complex is broken and the intermediate may undergo a reduction to form a monohydroxy-substrate. In this case, it is not clear whether the peroxo reacts by introducing one oxygen atom at a time

or by introducing both oxygen atoms together on the substrate to yield the dihydrodihydroxy product (37, 348).

Side-on attack mode: The feroxo group is protonated twice from water or from surrounding amino acids, forming a highly reactive Fe(V)=O(OH) named oxo. In this case, both oxygens atoms of the oxo intermediates attack the substrate, side-on, simultaneously, to generate the *cis*-dihydrodihydroxy product (144). Crystal structure analysis of *Pseudomonas* *sp.* NCIB 9816-4 NDO provided strong evidence that the reaction mechanism of Rieske-type oxygenase proceeds through a side-on mechanism and would explain the formation of a *cis*-dihydrodihydroxy metabolite.

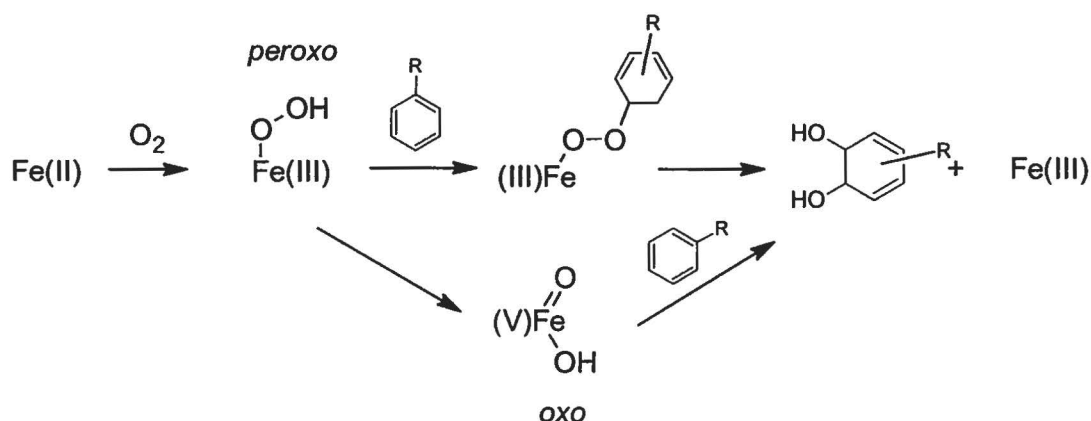


Figure 2.9: Putative reaction mechanisms and the intermediates of the oxygenation of the substrate by NDO, which may also apply to BPDO.

2.1.2.3. Mechanistic functioning

Many studies have been attempted to understand insight about the mechanistic functioning of BPDOs. These studies focused on substrate specificities and enzyme activities of BPDOs and their variants. The results obtained help us to decipher some of the mechanisms by which these enzymes evolve and also provide us some advance approaches to engineer better performing biocatalysts.

BphA is crucially responsible for recognizing and binding with substrates (40, 69), however, there are few reports that suggest an involvement of BphE in substrate recognition (130). The significant contribution of BphA to the catalytic reaction was demonstrated by Erickson and Mondello (69, 70) and by Taira et al. (1992) (319) with two important observations: (a) A hybrid dioxygenase comprised of TodC1BphEFG was generated by replacing BphA by TodC1 from the *Pseudomonas putida* F1 toluene dioxygenase α subunit. The enzyme displayed the same substrate specificity as the parent toluene dioxygenase (95, 120). (b) The chimeric BPDO constructed by replacing BphA_{KF707} by BphA_{LB400} in BPDO_{KF707} had the ability to metabolize the same range of PCBs as that of BPDO_{LB400} parent (155). Thus, exchanging BphA_{KF707} of BPDO_{KF707} which differs from BphA_{LB400} by only 20 amino acids on a total of 460, generated an hybrid exhibiting the catalytic properties of BphA_{LB400}.

Further studies revealed that a relatively small number of these 20 amino acids determine the substrates specificities of these two BPDOs. Based on site-directed mutagenesis experiments, Mondello et al. (1997) (208) identified four short segments of BphA (designated as region I, II, III and IV) that were involved in determining the range of substrate's analogs used by the enzyme (**Figure 2.10**). These four regions were all located on the C-terminal domain of the oxygenase large subunit. Changing these regions of BphA_{LB400} by those of BphA_{KF707} generated hybrids with a narrow substrate range that was similar to that of BPDO_{KF707}. Among them, the section of seven amino acids, termed region III, is of particular interest. Also, the most active mutants were obtained from multiple residues alteration in region III. This suggests that the effects of these mutations are cooperative.

Many reports revealed that by changing single residues near the active site, the specificities and regiospecificities of Rieske-type aryl hydroxylating dioxygenases could be improved (230, 303, 307). These single residues make contact with the substrate (residue Ile326 of BphA_{RIIAI} corresponding to Phe336 of BphA_{LB400}) or are too distant to interact directly with the substrate (residue Gly325 of BphA_{RHAI} corresponding to Thr335 of BphA_{LB400} and residue 377 of BphA_{LB400} (307)). Despite their distance from the substrate, they were all shown to modulate the reaction turnover rates and regiospecificities toward PCB congeners. Crystal structure analysis has helped to explain how some of these residues may influence the catalytic property of dioxygenases.

Recently, the crystal structure of BPDOs oxygenase component from *B. xenovorans* LB400 (BphAE_{LB400}), *P. pnomenus* B356 (BphAE_{B356}); *R. jostii* (BphA1A2_{RHAI}); *Sphingobium yanoikuyae* B1 (BphA1A2_{B1}) and of closely related dioxygenases involved in naphthalene, cumene or toluene have been reported (61, 88, 99, 106, 146, 165, 365). These reports provide us a clearer view on the mechanistic insight of the BPDOs' function.

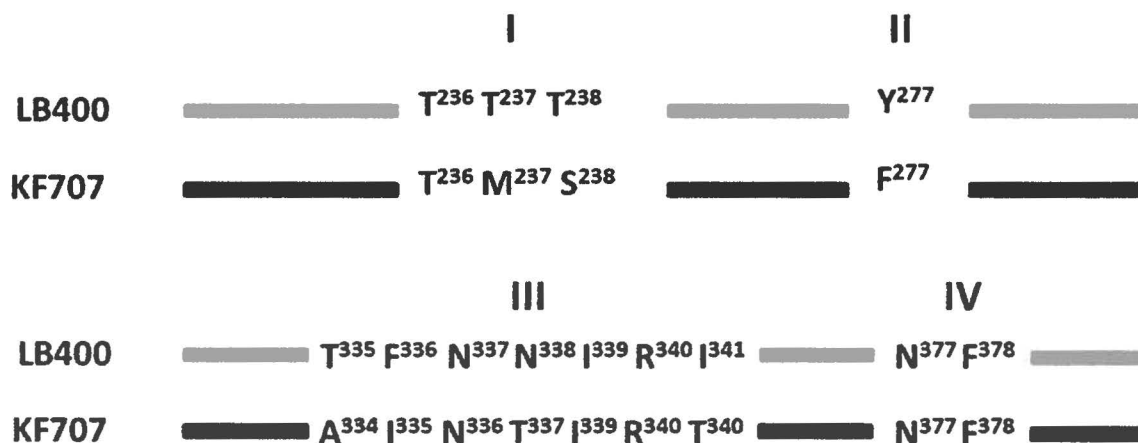


Figure 2.10: C-terminal portion of the α subunit of LB400 and KF707 BPDOs showing the amino acid residues that are presumed to be involved in substrate specificity toward PCBs. Image was modified from Sylvestre (2004) (309).

According to Furusawa et al. (2004) (99), in the substrate-binding pocket of BphA1A2_{RHAI}, there are significant conformational changes of several protein residues upon substrate binding that are likely required to accommodate the substrate in the catalytic pocket. The residues in the substrate-binding pocket of BphA1A2_{RHAI} can be roughly classified into three groups (**Figure 2.11**), which respectively, seem to have an important role in the catalytic reaction, orientation/conformation of the substrate, and conformational changes of the substrate-binding pocket. The first group contains residues Gln217, Phe218, His224, His230, and Asp378 of BphA1A2_{RHAI}, which are located around Fe⁺⁺ (amino acids highlighted in blue in **Figure 2.11**). These amino acids are likely important in the catalytic reaction and are well conserved in all BPDOs. Belonging to the second group are residues

Leu323, Ile326, Thr328, Thr367, Phe368, and Phe374, which are located between the β -sheet core and the bound substrate (red residues in **Figure 2.11**). These residues are presumed to modulate the orientation/conformation of the bound substrate. The amino acids in the last group (shown in yellow in **Figure 2.11**) are located in the remaining area of the substrate-binding pocket and they are less conserved among other related enzymes. These amino acids show significant conformational changes upon substrate binding, which is important to accommodate various substrates. The cooperative actions of residues with different characters in the three groups seem to determine the substrate specificity of the enzyme.

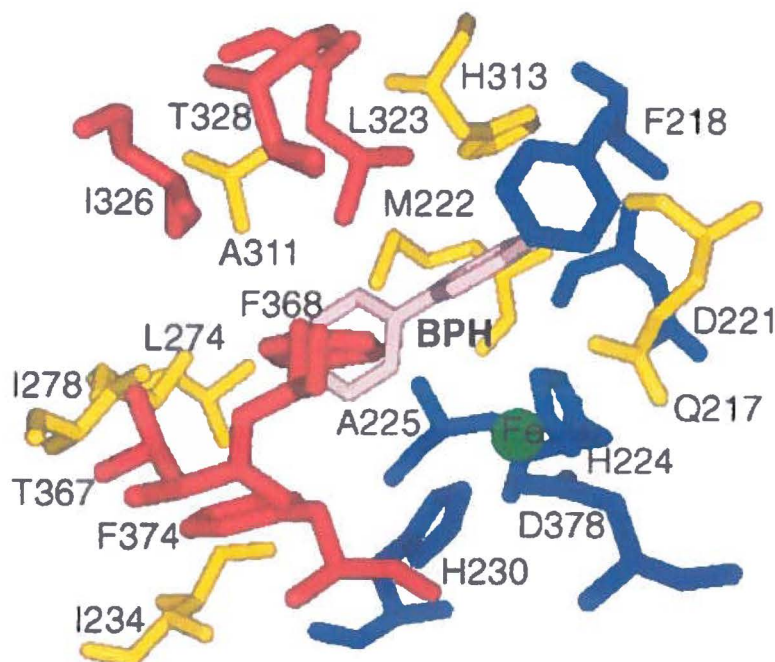


Figure 2.11: Structure around the bound substrate in BphA1_{RIIA1}. Blue: Residues located around Fe^{++} and conserved among the related enzymes; Red: The residues may be responsible for the substrate specificity for PCB congeners; Yellow: The remaining residues. The biphenyl molecule (BP) and the Fe^{++} are shown in pink and green, respectively. Image was taken from Furusawa et al. (2004) (99).

One mechanism to enhance the enzyme catalytic capacity is to decrease the constraint on strategic active-site residues. The process gives the residues lining the catalytic cavity the

capability to change their conformation during the substrate binding process, thus allowing more space to accommodate larger substrates. This explains how residues that have no contact with the substrate can influence the substrate specificity by modulating an induced-fit process to accommodate larger substrates. This mechanism was proposed to explain the expanded substrate range of the mutant BphAE_{p4} compared to its parent BphAE_{LB400} (165).

BphAE_{p4}, a variant created from BphAE_{LB400} by substitution Thr335Phe336 to Ala335Met336, transforms several PCBs, including 2,6-dichlorobiphenyl, more efficiently than BphAE_{LB400} (21). The authors compared the structures of BphAE_{LB400} (Thr335Phe336) and that of BphAE_{p4} (Ala335Met336) and also investigated the biochemical properties of two other variants BphAE_{p401} (Ala335Phe336) and BphAE_{p402} (Thr335Met336) obtained by a single substitution of BphAE_{LB400}. Data showed that residue 336 is very close to the substrate and influences the regiospecificity toward *ortho*-substituted congeners. Unlike residue 336, residue 335 does not have contact with the substrate but has significant influence on expanding the substrate range. This is well explained by the examination of the crystal structure. The hydroxyl group of Thr335 forms several hydrogen bonds with the Val320-Gln322 segment (**Figure 2.12a**). Through these hydrogen bonds plus nonbonded contacts, Thr335 imposes constraints to the Val320-Gln322 segment. Most of these contacts disappear when Thr335 is exchanged by Ala (**Figure 2.12b**), allowing for significant movement of this segment during the binding process of 2,6-dichlorobiphenyl and increasing the space available to accommodate the substrate.

In addition, a study (303) based on a homology model of BphA1_{KF707} and a Thr376Asn mutant suggested that the disappearance of a hydrogen bond between Thr376 and Asn373 could be the reason for the difference in the regiospecificities of these two enzymes. However, in the absence of crystal structure of the enzymes, the authors were unable to confirm the loss of this hydrogen bond and its influence on the catalytic properties of the enzymes.

The results obtained increase our understanding about how BPDOs metabolize PCBs, and other xenobiotic compounds. Besides being useful for environmental applications, BPDOs were recently proposed as useful biocatalysts for the biosynthesis of highly valuable organic compounds. Notably, BPDOs are promising enzymes for the biocatalytic transformation of flavonoids which have numerous pharmaceutical and agricultural applications.

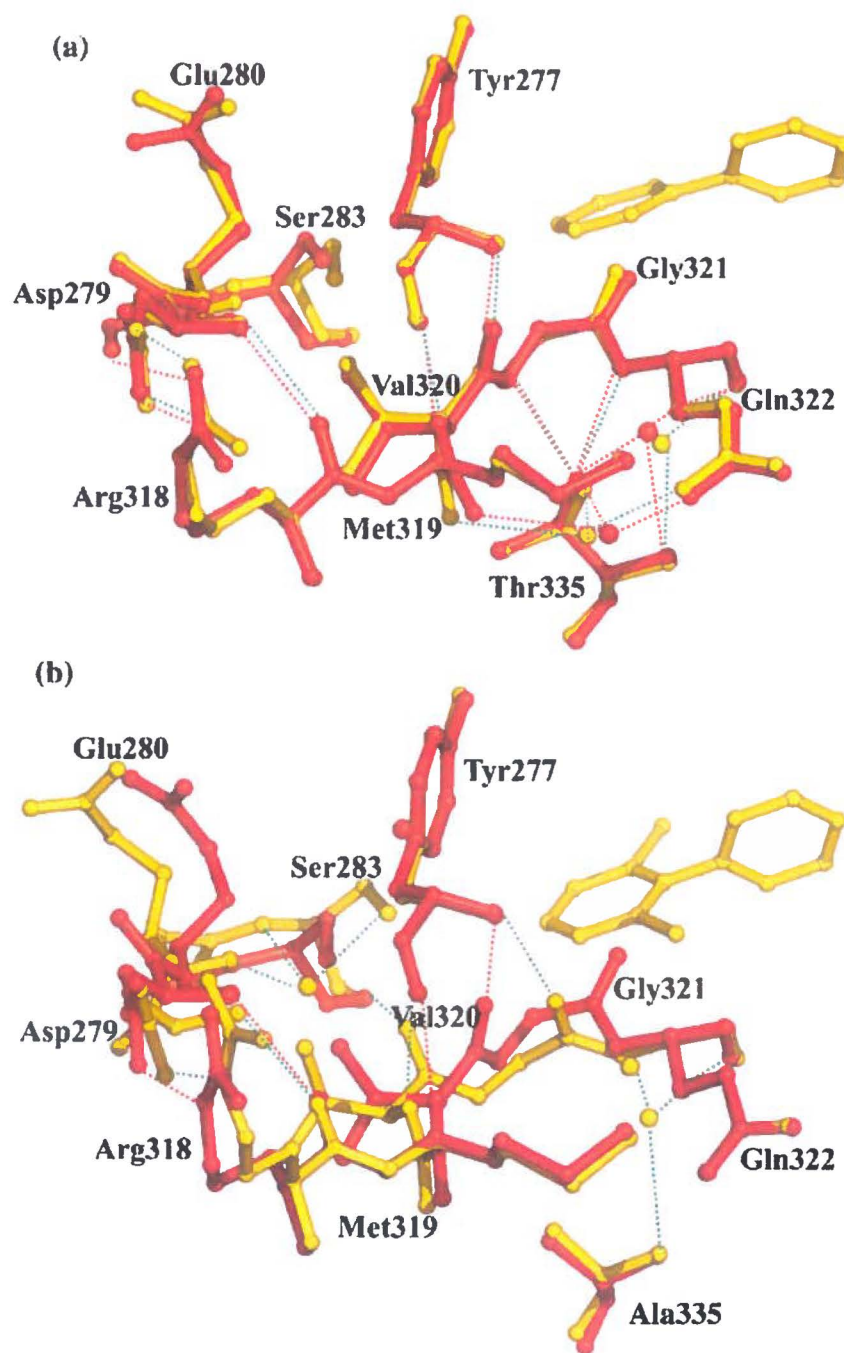


Figure 2.12: Superposition of segments of the crystal structure of BphAELB400 (red) with its biphenyl-bound form (yellow) (a) and of BphAEP4 (red) with its 2,6-dichlorobiphenyl-bound form (yellow) (b). The figures show how changing Thr335 to Ala has altered the hydrogen bond network around the Val320-Gln322 segment of the protein allowing conformational change of BphAEP4 to accommodate larger substrate. Image was taken from Kumar et al. (2011) (165).

2.2. Polychlorinated biphenyls: Environmental issues and methods of destruction

2.2.1. Polychlorinated biphenyls (PCBs)

2.2.1.1. Structure, properties and usage of PCBs

PCBs belong to a family of 209 biphenyl analogs containing one or more atoms of chlorine, and two aromatic rings (**Figure 1.2**).

They were massively manufactured from 1930s to 1970s for industrial purposes. PCBs were used as coolants and insulating fluids for transformers and capacitors; as plasticizers in paints and cements; as pesticide extenders and many other applications, because of their desirable physical and chemical properties, such as thermal and chemical stability, dielectric properties and fire resistance (252). As complex mixtures differing according to the level of chlorination, PCBs were sold worldwide under various trade names: “Aroclor” (United States); Clophen (Germany), Phenclor (Italy), Kanechlor (Japan), et Phenoclor (France) (52).

Although the production of PCBs has been prohibited since 1977 in most of industrial countries, because of their serious health and environment risks, they are still present in the environment. It was estimated that in 2006, 750,000 tons of the 1.5 million tons of PCBs produced worldwide, from 1930 to 1980, still remained in the environment (4). The major part of remaining PCBs is contained in soil and aquatic sediments with concentrations that may vary from 10^{-10} to 10^4 mg/kg whereas the permissible level range is from 0.01 to 50 mg/kg, depending on country (131).

2.2.1.2. Effects of PCBs on health

The toxicity of PCBs to humans and animals has been investigated since 1970s. It was concluded that the biological and toxic effects of PCBs vary depending on the number and position of the chlorine atoms (66). The highly chlorinated PCBs were demonstrated to cause cancer for animals (154) and to be probable carcinogens for humans (2). PCBs have also been shown to cause a number of serious non-cancer health effects in living organisms such as effects on the immune system, reproductive system, nervous system, and endocrine system in

animals. In humans, they may cause skin irritations, liver damage and other symptoms including ocular lesions, irregular menstrual cycles and lowered immune responses (2).

2.2.1.3. Polychlorinated biphenyls destruction technologies

Several technologies are available for the destruction of PCBs. They may be separated into two distinct categories: non-biological (including physical and chemical) processes and biological processes. Each has advantages and disadvantages.

2.2.1.3.1. Non-biological processes

- Incineration: PCBs can be incinerated at a temperature of 1,200 °C, under extremely controlled conditions since the process can result in the creation of chlorofurans and chlorodioxins, which are more toxic than PCBs (3). Although 99.9% of PCBs can be destroyed by this method (246), the destruction is exceedingly expensive. For this reason, incineration is not a suitable method for the decontamination of PCB-contaminated soil.

- Chemical and thermal-chemical processes: Under these processes, chlorine atoms of organochlorine pollutants are exchanged with hydrogen atoms at high temperature (700-925 °C) or at lower temperature with a metal catalyst (1). Chlorine atoms can also be reduced by a strong reducing agent such as highly electropositive metals. The advantage of these methods is that they proceed via a reductive process, and thus there is no production of chlorodioxins or other toxic compounds. However, again, these methods are prohibitively expensive.

2.2.1.3.2. Biological processes

Biological processes can potentially restore polluted sites with minimal adverse effects. However, many studies are needed to optimize these promising technologies.

Bioremediation is the use of microorganisms or plants and their associated microorganisms to transform toxic contaminants in the environment into less toxic or non-

toxic substances. This technology is considered a “green model” and less expensive in comparison to other methods. It is estimated that, by non-biological methods, it would take about \$6-8 billion annually to cleanup contaminated sites in the United States and the amount per year worldwide would be around \$25-50 billion (333). Recent estimations suggested that \$700 billion would be required to cleanup the 1,200 most heavily contaminated sites in US (104). However, the cost of bioremediation is on average ten times cheaper than non-biological methods (239).

2.2.1.3.2.1. Factors affecting the microbial degradation of PCBs

Bioremediation has many advantages, but it also has limitations. Microbes involved in the process need to be in close proximity with the contaminants and must be able to act on them. Therefore, many factors may influence the effectiveness of the process.

The first factor is the structure of pollutant. The number and the position of chlorine atoms of PCB molecules affect the efficiency of biodegradation process because: 1) it influences the resonance properties of the aromatic ring, the electronic density, and the energy necessary to cleave the carbon-carbon bonds. 2) it changes the stereo chemistry as well as enzyme-substrate affinity (93).

The second factor which influences the biodegradation capacity is the solubility of the pollutants in water. Water solubility influences bioavailability to microorganisms. The most chlorinated PCBs congeners are highly resistant to biodegradation because of their insolubility in water (28).

The concentration of the pollutants is the third factor. In general, a low concentration of pollutants may be insufficient to initiate the degradation process by enzymes, or to support the growth of the degrading microorganisms. By contrast, a too high concentration may be toxic to the microbes (315).

Other environmental factors may also influence biodegradation such as the pH, the temperature, the presence of toxic substances, the inhibitors, and the interaction between microorganisms.

2.2.1.3.2.2. Microbial processes for the degradation of PCBs

PCBs are metabolized differently by aerobic and anaerobic bacteria. Under anaerobic conditions, PCBs are reductively dehalogenated. Under aerobic condition, they are oxidativized by the biphenyl catabolic pathway enzymes.

Reductive dehalogenation:

It has been known for more than two decades that chlorinated organic compounds may act as electron acceptor in the anaerobic respiration process, in which the chlorine atoms are replaced by hydrogen (210).



Under anaerobic condition, the selective removal of *meta*- and *para*-chlorines are the most favored mechanisms, resulting in the decrease of highly chlorinated PCBs congeners with a corresponding increases in lower chlorinated (primarily *ortho*-substituted) congeners (241, 242). However *ortho*-dechlorination of certain PCBs has also been reported (355). One potential degradation pathway for PCBs that contain several chlorine atoms, demonstrating the *meta*- and *para*-dechlorination (77), is illustrated in **Figure 2.13**.

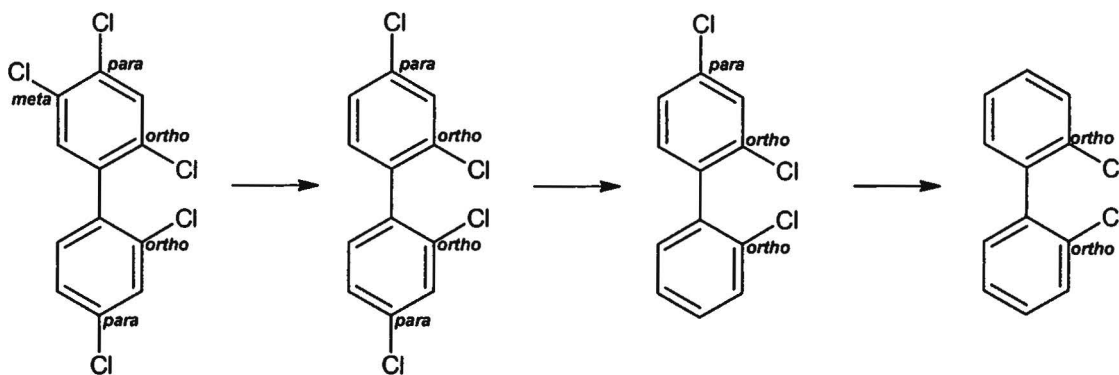


Figure 2.13: Potential reductive dechlorination pathway of 2,2',4,4',5-pentachlorobiphenyl.

A number of anaerobic bacteria that use chlorine as an electron acceptor have been described. They include, the proteobacteria *Desulfomonile tiedjei* (55), the low GC Gram-positive *Desulfitobacterium* (262), *Dehalobacter restrictus* (123), *Desulforomonas chloroethenica* (159), *Dehalococcoides ethenogenes* (193), and *Enterobacter agglomerans* (123). The presence of these bacteria in low redox polluted sites may reduce the proportion of high chlorinated pollutants (PCBs, chlorinated phenols, benzoates etc.) but will increase the concentration of low chlorinated ones as well.

Microbial degradation by oxidative pathways:

PCBs can be oxidatively degraded by various Gram-negative and Gram-positive bacteria. Examples of bacteria exhibiting the ability to metabolize PCBs include *Pseudomonas*, *Alcaligenes*, *Achromobacter*, *Burkholderia*, *Comamonas*, *Sphingomonas*, *Ralstonia*, and *Acinetobacter* (Gram-negative), *Rhodococcus*, *Corynebacterium*, and *Bacillus* (Gram-positive) (336). These bacteria utilize biphenyl as carbon source and cometabolize PCBs via the biphenyl catabolic pathway. Among them, some of the most studied ones are described in section 2.1.1.3 of this work. The biphenyl catabolic pathway is also presented in section 2.1.1.1.

The ability of these bacteria to degrade PCBs varies from strain to strain as is discussed in section 2.1.1.3. On the other hand, the structure of PCB congeners affects the degradation effectiveness as well. Higher chlorinated congeners are more resistant to the biodegradation; PCB congeners containing chlorine atoms on only one biphenyl ring are metabolized more easily than the ones containing chlorines on both rings; and doubly *ortho*-substituted PCBs (2,6- or 2,2'-) are more difficult to be degraded (5, 94).

Some fungi and yeasts have also been reported to degrade PCBs. *Aspergillus niger* is a fungus that metabolizes low level-chlorinated biphenyls (60). *Pleurotus ostreatus* and *Phanerochaete chrysosporium* are two fungi that can not only efficiently degrade monochlorobiphenyls but also transform certain high chlorinated biphenyls (51, 58, 143, 160). The yeast *Trichosporon mucoides* was reported by Sietman et al. to degrade low chlorinated biphenyls, generating chlorinated lactone derivatives (292). In all these processes, PCBs are metabolized by fungal oxidative enzymes involved in lignin degradation. Although

this process may reduce the toxic charge by reducing bioavailability, it does not destroy PCBs (316).

2.2.1.3.2.3. Phyto- and rhizoremediation processes for the degradation of PCBs

Phytoremediation is a process that uses plants to cleanup soil and ground water contaminated with xenobiotics including PCBs (259). Plant can help to cleanup PCBs via a range of mechanisms.

- Phytoextraction: plants uptake and concentrate the pollutants from the environment into their biomass.
- Rhizofiltration: Toxic substances are filtered and absorbed by the plant root system.
- Phytotransformation: Pollutants are transformed by plant enzymes such as cytochrome P450 or peroxidases.
- Phytovolatilization: Pollutants are released from plants into the atmosphere by the translocation process.
- Rhizoremediation: Pollutants are degraded by rhizosphere microorganisms in root zone. Among all phytoremediation processes, rhizoremediation is the most promising one. For this reason, this process will be described in details in section 2.2.2.

Several advantages of rhizoremediation as compared to other technologies have been invoked and they are listed below. Firstly, it is estimated that the cost is 50-90% less than alternative technologies (<http://www.epa.gov/>). Secondly, this process is less harmful because of the use of natural organisms and plants, thereby preserving the natural state of the soil. Thirdly, there is no restriction of which polluted sites this technology may be applied. Any contaminated site that supports the plant growth can be treated by this technology.

However, there are some disadvantages, such as: 1) the time required for the growth of plants, 2) the depth that the roots can reach into the soil, 3) the influence of the climate and

other pollutants in soil 4) the risk that plants which accumulate the contaminants will enter into the food chain.

Since the importance of the combined plants and microbes interaction in the rhizosphere for soil decontamination has been appreciated, the complexity of this relationship has been an attractive challenge for microbiologists. Despite the advances in this area, many details in the mechanism during the rhizoremediation of organic compounds are still unknown.

2.2.2. Rhizoremediation of PCBs

2.2.2.1. Plant-rhizobacteria relationship

2.2.2.1.1. Role of rhizobacteria

Plant growth-promoting rhizobacteria (PGPR) can promote plant growth by direct and indirect ways. By the direct way, plant growth is stimulated due to the ability of PGPR to fix and solubilize mineral nutrients for plants.

The enzyme nitrogenase presents in some PGPRs can catalyze the reduction of atmospheric dinitrogen (N_2) into ammonia so that plants can uptake and use it for their growth. These diazotrophic bacteria may live either closely to plants, forming nodules on roots, or loosely associated with plants (associated interactions). The efficiency of diazotrophic bacteria has been reported in several studies, on different plant species, such as sugarcane, soybean, wheat, and rice (135, 184, 354).

Another important mineral nutrient for plant is phosphorus. To be taken by plant, phosphorus must exist in monobasic ($H_2PO_4^-$) or dibasic (HPO_4^{2-}) soluble forms (354). However, phosphorus in soil is mostly insoluble with only about 0.1% available for plant, and fertilizer phosphorus applied to soil is rapidly immobilized and thus is unavailable in term of plant nutrient (247). Some bacteria in rhizosphere, such as *Azotobacter chroococcum*, *Bacillus* spp., *Enterobacter agglomerans*, *Pseudomonas chlororaphis*, *Pseudomonas putida* and *Rhizobium* spp. can either solubilize inorganic phosphates by secreting organic acids

(gluconic acid, 2-ketogluconic acid) or transform organic phosphates by releasing extracellular phosphatases (354).

Iron is also an important mineral nutrient for plant. Many bacteria can produce siderophores, iron-carrying organic compounds, which can bind with Fe^{3+} and reduce it to Fe^{2+} to facilitate the iron uptake process in plant. The Fe^{3+} -siderophore complex itself can be uptaken by several plant species as well (282, 283).

Beside the ability of facilitating mineral uptake by plants, PGPRs produce some phytohormones such as auxins, cytokinins, gibberellins and also affect the ethylene level, which play an important role in plant growth and development. Auxin indole-3-acetic acid can increase root growth and root length and is also involved in the elongation of the root hairs (317). In certain plant parts, cytokinins are reported to stimulate cell division, cell enlargement and tissue expansion. Gibberellins are known to modify plant morphology by plant tissue extension (354). Ethylene has multiple effects on plant development, including inhibition of root elongation, root growth and root hair formation (192). PGPRs can help to decrease ethylene levels via the activity of the bacterial 1-aminocyclopropane-1-carboxylate deaminase, and therefore promote root development (191).

Indirectly, many PGPRs can promote growth of plant via the production of antibiotics, hydrolytic enzymes, biosurfactants or siderophores. By producing antibiotics, that either kill or inhibit target pathogens, bacteria can help to control plant diseases (47). Siderophores, as mentioned above, excreted by many PGPRs can bind with iron under Fe-limiting conditions, therefore preventing pathogenic bacteria and fungi from accessing to iron (47). Some PGPRs release hydrolytic enzymes that cause cell wall lysis, useful in controlling fungal pathogens (158). Furthermore, by producing cyclic lipopeptides surfactants, *Pseudomonas fluorescens* can prevent the formation of biofilm on the root surface by pathogens and thence protect plant against pathogens (329).

2.2.2.1.2. Role of plants

Vegetation plays a significant role in modeling soil structure and composition via many processes in which it stimulates microbial activities in the rhizosphere and promotes microbial growth. The ability of plant to promote microbial growth and microbial activity in

soil is attributed to the release of plant metabolites such as sugars, amino acids, organic acids, nucleotides, enzymes, and PSMs into the root exudates (39). The main components of root exudates are sugars with a concentration of 90 mM. Organic acids and amino acids are present at concentrations varying between 10-20 mM for each class (259).

PSMs are traditionally regarded to be not essential for the survival of plants but play a pinnacle role in keeping plants stay healthy (59). There are more than 100,000 PSMs, among them the most widespread are isoprenes, the building block for the more complex terpenoids which include more than 15,000 compounds (59, 234). Terpenoids comprise several families including monoterpenes (more than thousands compounds), sesquiterpenes (with more than hundred skeletons). A few thousand of terpenoids structures have been elucidated (294). Another common class of PSMs comprises the flavonoids which have many interesting biological features for pharmaceutical application. These characteristics will be discussed in section 2.3 of this work. According to IUPAC (International Union of Pure and Applied Chemistry), flavonoids include three classes: flavones, isoflavans and neoflavonoids (198).

There are several mechanisms (listed below) by which plants consolidate the plants-microbes relationship as well as promote microbial activities such as the rhizoremediation of contaminants in rhizosphere.

- Organic acids such as citrate, acetate, malate, oxalate, succinate, butyrate etc. (180, 256) can help to solubilize high hydrophobic compounds such as PCBs and therefore increasing their bioavailability to be transformed by microbes or plants (36).
- Extracellular enzymes such as peroxidases in root exudates can initiate the transformation of pollutants and support the further microbial metabolism (339).
- Root exudates may act as carbon source to support the growth of biphenyl-degrading rhizobacteria. This conclusion was made based on several studies on microbial populations associated to plant-contaminated sites (173).
- Plants improve soil permeability, facilitate oxygen exchange in the rhizosphere thus enhancing aerobic transformation of the contaminants (39).

- An important contribution of plants in the rhizoremediation process aiming PCBs degradation is the production of PSMs, especially terpenoids and flavonoids, that may act as cometabolites or inducers to promote PCB catabolism (285) (311).

2.2.2.1.3. Rhizoremediation studies

To date, a number of studies have successfully utilized plants-associated rhizobacteria to degrade PCBs. Selected studies were cited in the **Introduction** section. Here we describe those studies with more detail in **Table 2.1**. Some of the studies highlighting the importance of PSMs, including terpenoids and flavonoids, in PCBs rhizoremediation are listed in **Table 2.2**.

Table 2.1: Recorded rhizoremediation attempts for PCBs degradation

Microbes used	Plants used	Results	References
Indigenous rhizobacteria	Orange peels, Eucalyptus leaves, Pine needles Ivy leaves	PCBs disappeared in all amended soils, but not in unamended soils (after 6 months). Level of biphenyl-utilizing bacteria in amended soils (10^8 /g) is higher than in unamended control (10^3 /g).	Hernandez et al. 1997 (119)
<i>Burkholderia sp.</i> LB400	Mulberry (<i>Morus sp.</i>)	Upon death, fine roots of mulberry served as a source of substrate for <i>Burkholderia sp.</i> LB400.	Leigh et al. 2002 (172)
Indigenous degraders	Alfalfa Flatpea Sericea lespedeza Deertongue Reed canarygrass Switchgrass Tall fescue	7 plant species treatments showed significantly greater PCB biodegradation (38% PCBs remained) compared to the unplanted controls (82%). Greater bacterial counts and soil enzyme activity were closely related to higher levels of PCB biodegradation.	Chekol et al. 2004 (41)
<i>Pseudomonas fluorescens</i> F113	Alfalfa (<i>Medicago sativa</i>)	<i>bph</i> operon from <i>Burkholderia sp.</i> strain LB400 was cloned in <i>P. fluorescens</i> F113, an excellent plant root colonizer. The modified strain grew better on biphenyl and cometabolized PCBs in alfalfa's rhizosphere better than LB400.	Villacieros et al. 2005 (347)
Indigenous rhizobacteria	5 indigenous trees including Austrian pine (<i>Pinus nigra</i>), Goat willow (<i>Salix caprea</i>) and three others	PCBs were degraded more significantly (2.7- to 56.7-fold-higher means) in the root zones of Austrian pine (<i>P. nigra</i>) and goat willow (<i>S. caprea</i>) than in the root zones of other plants or in bulk soil.	Leigh et al. 2006 (173)
<i>Rhizobium meliloti</i>	Alfalfa (<i>M. sativa</i>)	PCB levels decreased by 36% in rhizosphere (after 90 days), and by 43% in rhizosphere of <i>Rhizobium</i> inoculated plant, compared to 5.4% in the unplanted soil. Plant biomass production and CFUs of total microorganisms was higher in the inoculated treatment.	Xu et al. 2010 (358)
<i>Cupriavidus</i> spp.	Felt-leaf willow (<i>Salix alaxensis</i>)	Soil treated with willow root crushates (180 days) showed a significantly greater loss of some PCB congeners, than untreated soils.	Slater et al. 2011 (295)

Table 2.2: Studies using PSMs to enhance PCBs removal

Microbes used	PSMs or plants used	Results	References
<i>Alcaligenes eutrophus</i> H850 <i>Corynebacterium sp.</i> MB1 <i>Pseudomonas putida</i> LB400	16 flavonoids	Several flavonoids, including naringin, catechin, chrysin and other flavonoids supported the growth and enhanced the ability of of 3 bacterial strains to degrade PCBs.	Donnelly et al. 1994 (62)
<i>Arthrobacter sp.</i> strain B1B	Spearmint Basil Dill, Barley Green bean Pennyroyal	l-carvone and several structurally similar compounds including limonene, <i>p</i> -cymene, and isoprene, induced the cometabolism of PCBs (including tetra- and pentachlorobiphenyls) by <i>Arthrobacter sp.</i> strain B1B	Gilbert et al. 1997 (103)
<i>Pseudomonas stutzeri</i>	Carvone Limonene	In experiments using xylose as carbon source and carvone as inducer, 30–70% of the added PCBs congeners were removed, compared to 7–37% removal from the cultures without terpene addition.	Tandlich et al. 2001 (325)
<i>P. putida</i> Flav1-1 <i>P. putida</i> PML2	Rockcress (<i>Arabidopsis</i>)	PCBs in rhizosphere of wild-type <i>A. thaliana</i> were removed more efficiently than in its mutant that excretes less flavonoids.	Narasimhan et al. 2003 (216)
Indigenous bacteria	Naringin Limonene Caffeic acid	Bacterial populations were higher, and residual content of PCBs was lower, in treated soil than in non-amended soil.	Uhlik et al. 2012 (334)

2.2.3. Engineering the biphenyl catabolic pathway and plants to degrade PCBs

Rhizoremediation using combined bacterial enzymes and plant systems is a very promising process to degrade PCBs and other xenobiotics in soil. However, rhizoremediation based on natural biphenyl-degrading bacteria and natural plants will be very slow due to the limitation in the ability of bacterial enzymes to transform PCBs as well as the difficulty of plants to survive in soil contaminated with high concentration of PCBs and of hydroxyl metabolites derived from them. These bottlenecks can be overcome by modifying bacterial enzymes and plants. This objective may be achieved by exploiting recent advancements

regarding the engineering of the biphenyl catabolic pathway enzymes and our understanding of the plants-microbes interactions.

2.2.3.1. Engineering biphenyl catabolic pathway enzymes

The catalytic component (BphAE) of the first enzyme of the biphenyl catabolic pathway has been thoroughly investigated since it is responsible for the substrate range of the pathway. Using directed evolution, Barriault et al. (2002) created BphAE_{p4} (21) and Mohammadi et al. (2005) created BphAE_{RR41} (205), two variants of *B. xenovorans* LB400. These two variants metabolized a much broader range of PCBs than BphAE_{LB400} did (346). BphAE_{RR41} was able to transform 17 of 18 PCBs tested containing 2 to 5 chlorine atoms, including 3,3',4,4'-tetrachlorobiphenyl, one of the most persistent congeners that wild-type oxygenases transformed poorly (346). Several new variants obtained by shuffling *bphA*_{LB400}, *bphA*_{B356} and *bphA*_{P6} that were able to oxygenate PCBs more efficiently than any of the three parents, were obtained by Barriault et al. (2002) (20). Furthermore, several variants of *P. pseudoalcaligenes* KF707 generated by site-directed mutagenesis, random-priming recombination or by DNA shuffling, which have expanded degradation capabilities toward PCBs and other aromatic hydrocarbon xenobiotics (303-307), are also interesting candidates for PCBs degradation. Some of these engineered enzymes are likely to be useful if they are cloned into rhizobacteria.

The second enzyme of the pathway is 2,3-DDHBD (BphB) has no need to be modified since this enzyme has a very wide substrates range including metabolites generated from the dioxygenation of PCBs, naphthalene, dibenzofuran and flavonoids (22, 202, 205). Its versatility was explained by its highly flexible substrate-binding loop as mentioned in section 2.1.1.2 (57).

The third enzyme, the 2,3-DHBD (BphC) has two limitations that can cause an incomplete PCB degradation as mentioned in section 2.1.1.2. The first limitation is its inability to metabolize *meta*-, *para*-dihydroxybiphenyl. This bottleneck may be overcome by using 1,2-dihydroxynaphthalene dioxygenase of *Pseudomonas* sp. C18 (17) and its variants obtained by directed evolution (85) that exhibit higher ability to cleave *meta*-, *para*-hydroxybiphenyls. The second limitation of this enzyme is its high sensitivity toward 3-

chlorocatechol, which can prevent the metabolization of PCBs. For this bottleneck, engineered bacteria that can metabolize efficiently chlorobenzoate like the one obtained by incorporating *bph* locus of LB400 into the genome of the chlorobenzoate-degrading bacterium *Cupriavidus necator* JMP 134-X3 (257) is a good approach.

The last enzyme of the biphenyl catabolic pathway, the HODA hydrolase (BphD), has been well characterized. Depending on the organism from which it originates, the enzyme responds differently to chloroHODAs (269) (see section 2.1.1.2). Furthermore, it has been shown that the homologous enzyme, DxnB2, from the dibenzofuran-degrading pathway of *Sphingomonas wittichii* RW1, is able to catalyze the chloroHODAs that BphD does not metabolize (268). On the other hand, some non-biphenyl-degrading enzymes can also hydrolyze the aliphatic side-chain of chloroHODAs (189, 359). Therefore this enzyme of the biphenyl catabolic pathway need only minor adjustments through enzymatic engineering to optimize its PCB-degradation ability.

2.2.3.2. Engineering plants

Since PSMs, especially flavonoids, play an important role in the rhizoremediation process, flavonoid-overproducing plants should therefore help improve this process. Many plants were successfully engineered to increase the amount of flavonoids produced (343), for example, *Saussurea involucre* overproduced apigenin (174); naringenin, kamferol, rutin and quercetin were over produced in *Lycopersicon esculentum* (265, 342); genistein in *A. thaliana* (141, 177), *Nicotiana tabacum* and *Lectuca sativa* (178); and neohesperidin in *N. tabacum* (89). More details about flavonoids-overproducing transgenic plants are discussed in the review of Ververidis et al. (2007) (343). On the other hand, transgenic plants expressing PCB-degrading enzymes are also interesting since these enzymes may help improving plants resistance toward PCBs toxicity in soil (225, 313). *B. xenovorans* LB400 genes encoding BPDO components were successfully cloned and active individual proteins were expressed in tobacco, according to the work of Mohammadi et al. (2007) (204). 2,3-DHBD (*bphC*) of *P. pnomenus* B356 was also cloned in *N. tabacum* (225). These studies suggest that transgenic plants to overproduce flavonoids or to express PCB-degrading enzymes are promising and feasible.

2.2.3.3. *Other processes that can be combined with biphenyl catabolic pathway to better degrade PCBs*

Exploiting plants and biphenyl-degrading rhizobacteria is a process that enhances the degradation of PCBs in soil through natural bacterial catabolic pathways. However, the rate of this natural catabolic process is low and even ineffective in the case of highly halogenated compounds. Recently, several chemical processes have been introduced to assist the microbial catabolic activity in removing recalcitrant pollutants and thus enhancing the effectiveness of the PCBs degradation processes. Two processes, reductive dehalogenation (151), and hydroxyl radical-based production (42), are worth to mention as promising candidates to be combined with biphenyl catabolic pathway for PCBs degradation.

Reductive dehalogenation is a process using zero-valent iron or bimetallic zero-valent iron (48, 151) to reductively dehalogenate halogenated pollutants and generate lower halogenated compounds. The processes are based on electron transfer from zero-valent iron centers to organic contaminant. An example of this approach, we may cite, is the work of He et al. (2009) (116) who used Pd/Fe bimetal to dechlorinate 2,2',4,5,5'-pentachlorobiphenyl, a compound that is hardly transformed by bacterial strains. The resulting 2,2',4-trichlorobiphenyl may, then, readily be further degraded by aerobic bacterial strain.

As mentioned above, PCBs biodegradation is limited due to the hydrophobicity of PCBs. Physicochemical processes that generate hydroxyl radicals may help solve this problem by introducing hydrophilic functions such as aldehydes or carboxylic acids onto the substrates and therefore increasing their hydrophilicity. Hydroxyl radicals may be generated by ozonation, Fenton chemistry (using hydrogen peroxide) and photocatalysis (43, 72, 140, 229). Dehalogenation reactions may also occur during these processes. The substrates are then more readily degraded by microbial catabolic reactions. There have been many such studies using either one of these chemical approaches together with biocatalysis to degrade persistent pollutants (43, 72, 107, 110, 254, 363).

2.3. Manufacturing flavonoids via BPDOs

2.3.1. Green way to manufacture molecules

“Green chemistry” is defined as the design, development and application of chemical processes and products, to reduce or eliminate the use and production of substances hazardous to human health and the environment (9). Using biocatalytic processes is a greener way compared to traditional organic syntheses that may require multi-step reactions, with expensive starting materials, complicate equipments, and that may also require a cleanup process due to the formation of undesirable side-products (15).

Biocatalysts provide appropriate tools to transform natural or synthetic materials under mild conditions. The enzymatic reactions require low energy and the products isomerization and rearrangement are minimized during the reaction (15, 267). In addition, enzymes can display chemo-, regio-, and stereo- selectivity, resulting in reducing by-products and avoiding the need for activation, protection and deprotection of the functional groups. Thus, biocatalysts have become an important technology in syntheses of fine chemicals and pharmaceutical products. It is projected that biocatalytic processes and biotransformation will account for 30% of the chemical industry, by the year 2050 (340).

Recently, metabolic engineering has overcome many challenges and started to be successful for many applications. Metabolic engineering is a process to convert raw materials into expected molecules by using serially biochemical reactions. The main difficulties of this process are the choice of appropriate microbial host; the expression of enzymes in the pathway to produce desired compounds; and the maximization of yields and effectiveness (148). Fortunately, since 1990s, various technologies required to promote metabolic engineering such as the DNA sequencing, gene expression profiling, enzyme structure determination, and bioinformatics creating database of metabolic reactions, have evolved very rapidly, therefore stimulating the development of this field (148).

Metabolic engineering mainly focuses on active pharmaceutical ingredients and fine chemicals. Its success includes the microbial formation of carotenoids, and many other natural terpenes in *E. coli* and yeast (186, 245), as well as the production of artemisinin, an antimalaria drug, by semi-microbial synthesis using the engineered *Saccharomyces cerevisiae* (38, 245). The application of metabolic engineering in the production of fuels has also

obtained many advances. For example, linear hydrocarbon, typical of diesel and jet fuel may be synthesized inexpensively from fatty acids by modifying or extending their biosynthetic pathway (266, 302).

Dioxygenases including BPDOs are ubiquitous in nature and play an important role in the transformation of a broad range of compounds (34). They have the ability to regiospecifically hydroxylate aromatic rings or sidechain substituents of aromatic substrates, one of the most challenging and fundamental reactions in organic synthesis (224). This ability offers opportunities to synthesize compounds that are difficult to synthesize using chemical synthesis (335). Over the past few years, numerous papers and books have described applications of these enzymes in green biocatalytic syntheses (15, 65, 71, 267, 349).

Dioxygenases transform aromatic substrates to *cis*-dihydrodihydroxyls, catechols, and hydroxylated-compounds (102). More than three hundred 2,3-*cis*-dihydrodihydroxy derivatives have been synthesized by the toluene dioxygenase with a high enantiomeric purity (31). Among them, certain compounds such as 2,3-*cis*-dihydrodihydroxy derivatives of chlorobenzenes, bromobenzenes and toluene, are used in the synthesis of natural target molecules, e.g. (-)-cladospolide A, (-)-*ent*-bengamide E and 6C-methyl-D-mannoses (30). In addition, naphthalene *cis*-1,2-dihydrodihydroxy produced from naphthalene by NDO, have been used for the production of (+)-goniodiol (30).

Substituted catechols are important and widely used in industrial processes including the manufacture of plastics, polymers, drugs and dyes (10, 326). Furthermore, 3,4-substituted catechols themselves, such as 3,4-dihydroxyphenylalanine, adrenaline and noradrenaline, were shown to also have high biological activities (224).

There are some typical examples of the application of dioxygenases in synthesis. Cortisone, an important anti-inflammatory agent, was recently synthesized through a six-step mixed biotransformation and chemical synthesis process instead of a 37-step chemical synthetic process (348). Indigo dye, a significant commercial product, is synthesized by the oxidation of indole using NDO. The biological indigo production is cost-competitive with the chemical process (348).

2.3.2. Flavonoids

Flavonoids are 15-carbon PSMs and are “the most common group of polyphenolic compounds in the human diet” (299). These natural products are known for their beneficial effects on human health, with diverse physiological and pharmacological activities such as anti-oxidative, anti-cancer, anti-allergic, anti-inflammatory, antiplatelet, antiviral, antifungal, antihemolytic, anti-ischemic, estrogenic etc. (84, 219, 253). Due to their potential effects, flavonoids have recently attracted considerable attention in the disciplines of nutrition and food sciences, environmental science and pharmacology.

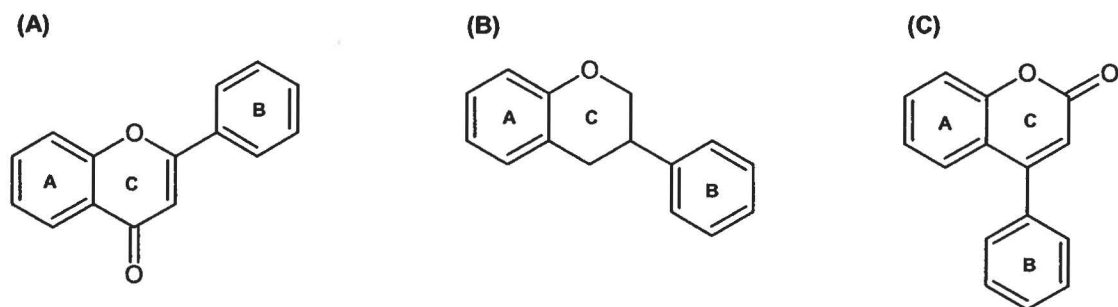


Figure 2.14: Molecular structures of three classes of flavonoids: flavones (A); isoflavans (B); and neoflavonoids (C).

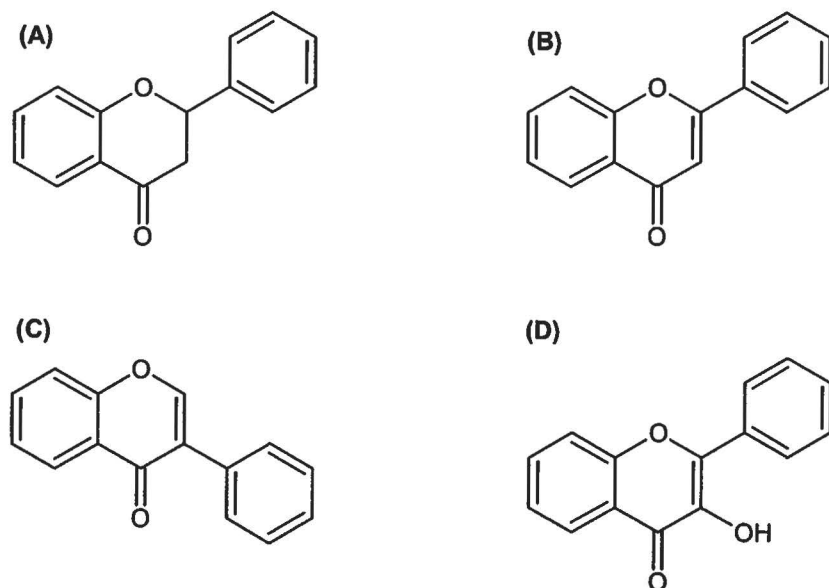


Figure 2.15: Skeleton of some common flavonoids: (A)- Flavanone; (B)- Flavone; (C)- Isoflavone and (D)- Flavonol or 3-hydroxyflavone

More than 10,000 natural flavonoids from various plants have been identified (318). According to IUPAC, these compounds can be classified into three classes (flavones, isoflavans, and neoflavonoids) (**Figure 2.14**). The skeleton of some common flavonoids such as flavanone, flavone, isoflavone and flavonol are shown in **Figure 2.15**.

2.3.3. Transformations of some common flavonoids

As mentioned above, flavonoids have many potential applications, therefore many works have focused on the biological transformation of these compounds in order to obtain some novel better performing derivatives. We will discuss here microbial and enzymatic transformations of some common flavonoids.

2.3.3.1. Flavonoids transformation by fungi and streptomycetes

Many fungi and streptomycetes can transform flavonoids. The reactions are diverse, including dehydrogenation, hydration, hydroxylation, oxidation, reduction and bond cleavage. Some fungi attack ring A of flavonoids, others prefer ring C especially for the cleavage reactions, while many of them attack ring B. The lack of information about the catabolic pathway and enzymes involved, unfortunately, makes the biotransformation of flavonoids to be arbitrary and unpredictable, preventing their applications for metabolic engineering purposes. However, because of their complexity and diversity, these reactions may produce unnatural flavonoids that are more interesting than their natural counterparts. In this section, we summarize some of the flavonoids transformations that fungi and streptomycetes can catalyze.

Isoflavanone was shown to be converted to 4'-hydroxyisoflavanone and 2',4'-dihydroxyisoflavanone by *Absidia blakesleeana* NRRL 1306 (132). *Aspergillus niger* X172 also can convert this substrate to 2-hydroxyisoflavanone and 3',4'-dihydroxyisoflavanone and *A. niger* NRRL 599 transforms it to isoflavone which may be further transformed to 4'-hydroxyisoflavone and 3',4'-dihydroxyisoflavone by several organisms such as *Cunninghamella blakesleeana* ATCC 8688A, *Helicostylum piriformi* QM6945 and *Penicillium purpurogenum* U-193 (133) (**Figure 2.16**).

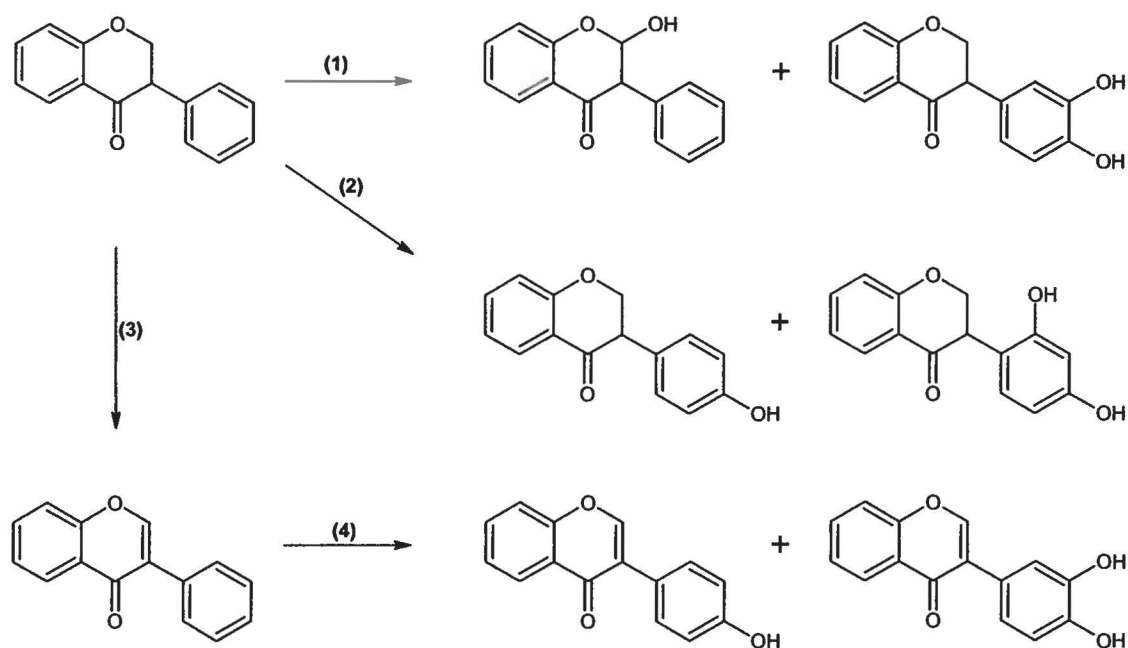


Figure 2.16: Microbial transformation of isoflavanone and isoflavone (132, 133). Microbes involved: (1): *A. blakesleeana* NRRL 1306; (2): *A. niger* X172; (3): *A. niger* NRRL 599 and (4): *C. blakesleeana* ATCC 8688A, *H. piriformis* QM6945 and *P. purpurogenum* U-193.

Fungi may also oxidize flavanone onto ring A or B or C, resulting in the formation of many metabolites (133) (**Figure 2.17**). *A. niger* NRRL 599 attacks ring C of flavanone by dehydrogenation or hydroxylation reactions to form flavone and flavanol, respectively. *A. blakesleeana* can simultaneously perform a hydrogenation reaction at ring C and a hydroxylation at ring B of the substrate, forming 4'-hydroxyflavan-4-ol. C2-O1 bond may then be cleaved by four fungi including *A. niger* NRRL 599, *A. blakesleeana*, *Penicillium chrysogenum* and *A. niger* X172. Unlike *P. chrysogenum* that only cleaves the C2-O1 bond, the other ones may cleave this bond and simultaneously introduce one or two atoms of oxygen, resulting in the formation of hydroxychalcone. *Streptomyces fulvissimus* can also add one or two oxygen atoms into ring B of flavanone at position 3' and 4' to create hydroxyflavanone (**Figure 2.17**).

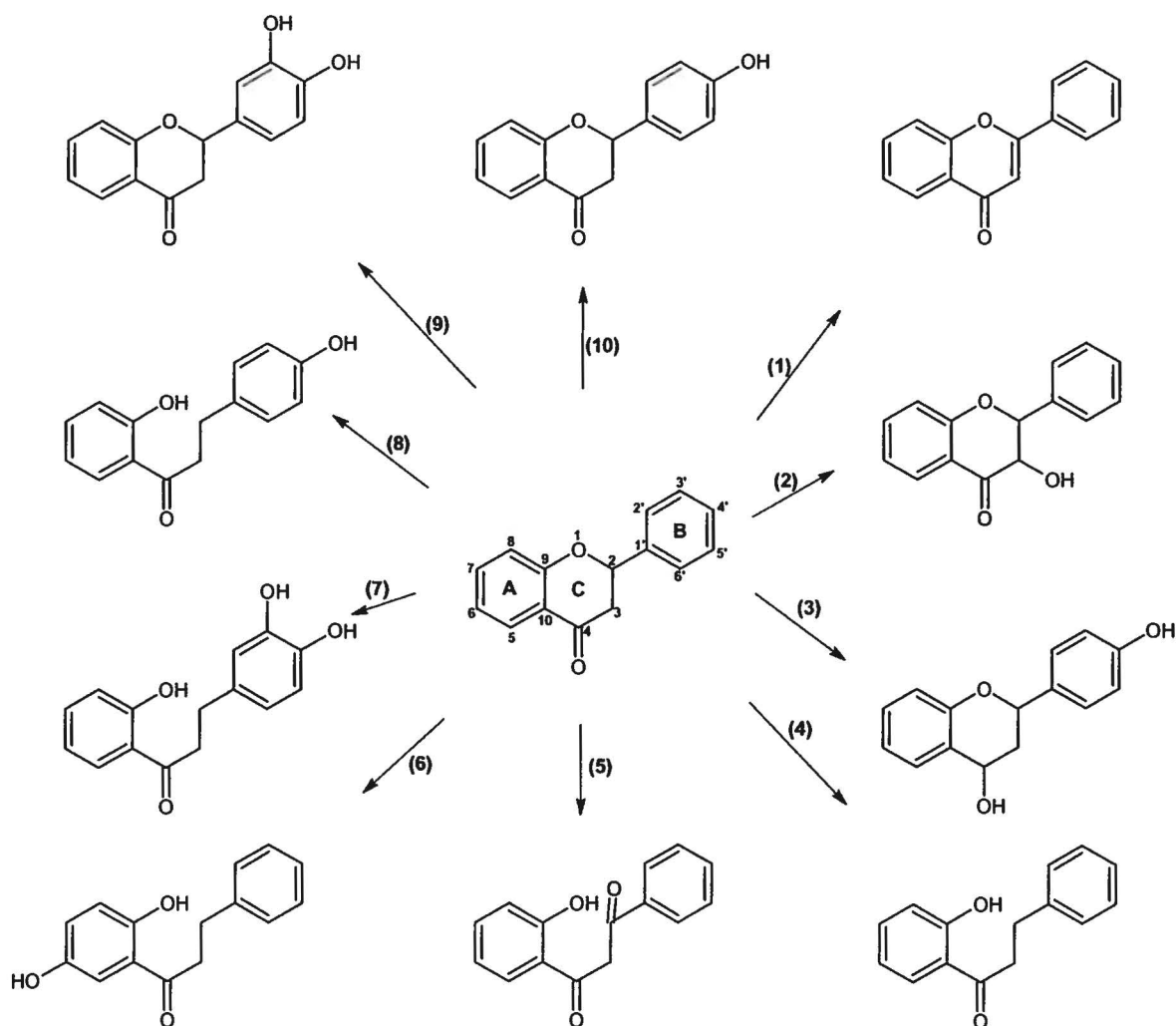


Figure 2.17: Microbial transformation of flavanone. Microbes involved: (1), (2) and (6): *A. niger* NRRL 599; (3): *A. blakesleeana*; (4): *P. chrysogenum*; (5), (7): *A. niger* X172; (8-10): *S. fulvissimus*.

Recently, Niraula and colleagues have investigated the ability of *Streptomyces peucetius* to transform flavone (220). They showed that, this organism produced a cytochrome P450 (CYP102P2), which was able to hydroxylate ring B of flavone (220) to generate 3'-hydroxyflavone (**Figure 2.18**). 3',4'-dihydroxyflavone was identified as the major flavone metabolite produced by many fungi such as *Aspergillus*, *Cunninghamella*, *Helicostylum*, *Penicillium* and *Linderina*. The cleavage of ring C was observed when flavone

was used as substrate for several fungi including *Absidia*, *Gongronella*, *Rhizopus* and *Manascus* (133) (**Figure 2.18**).

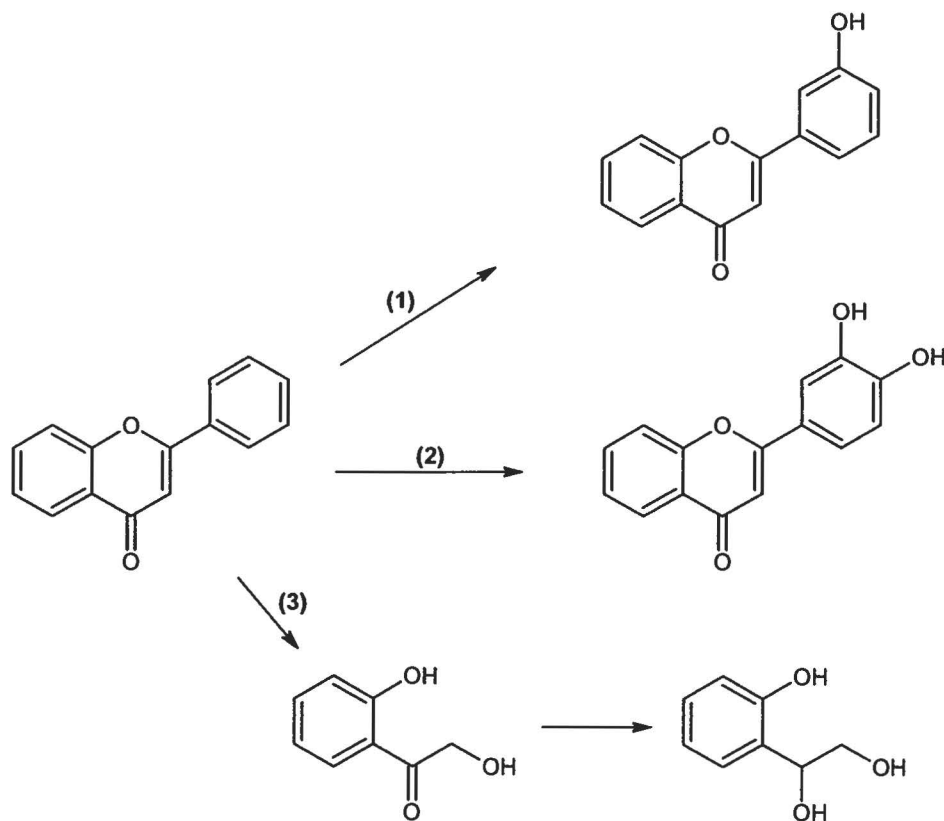


Figure 2.18: Biotransformation of flavone. Microbes involved: (1): *S. peucetius* (220); (2): *Aspergillus*, *Cunninghamella*, *Helicostylum*, *Penicillium*, and *Linderina* (133); (3): *Absidia*, *Gongronella*, *Rhizopus*, and *Manascus* (133).

2.3.3.2. Flavonoids transformations by BPDOs

Flavonoids may be considered as a biphenyl analog and thus likely to serve as substrate for BPDOs. The ability of BPDOs to metabolize flavonoids was reported in several recent researches (44, 112, 142, 152, 271, 278, 289, 290). Most of metabolites were shown to have a markedly higher antioxidative activity than that of the parent substrates (142), others had free radical-scavenging activity while the parent compounds did not show any activity (44).

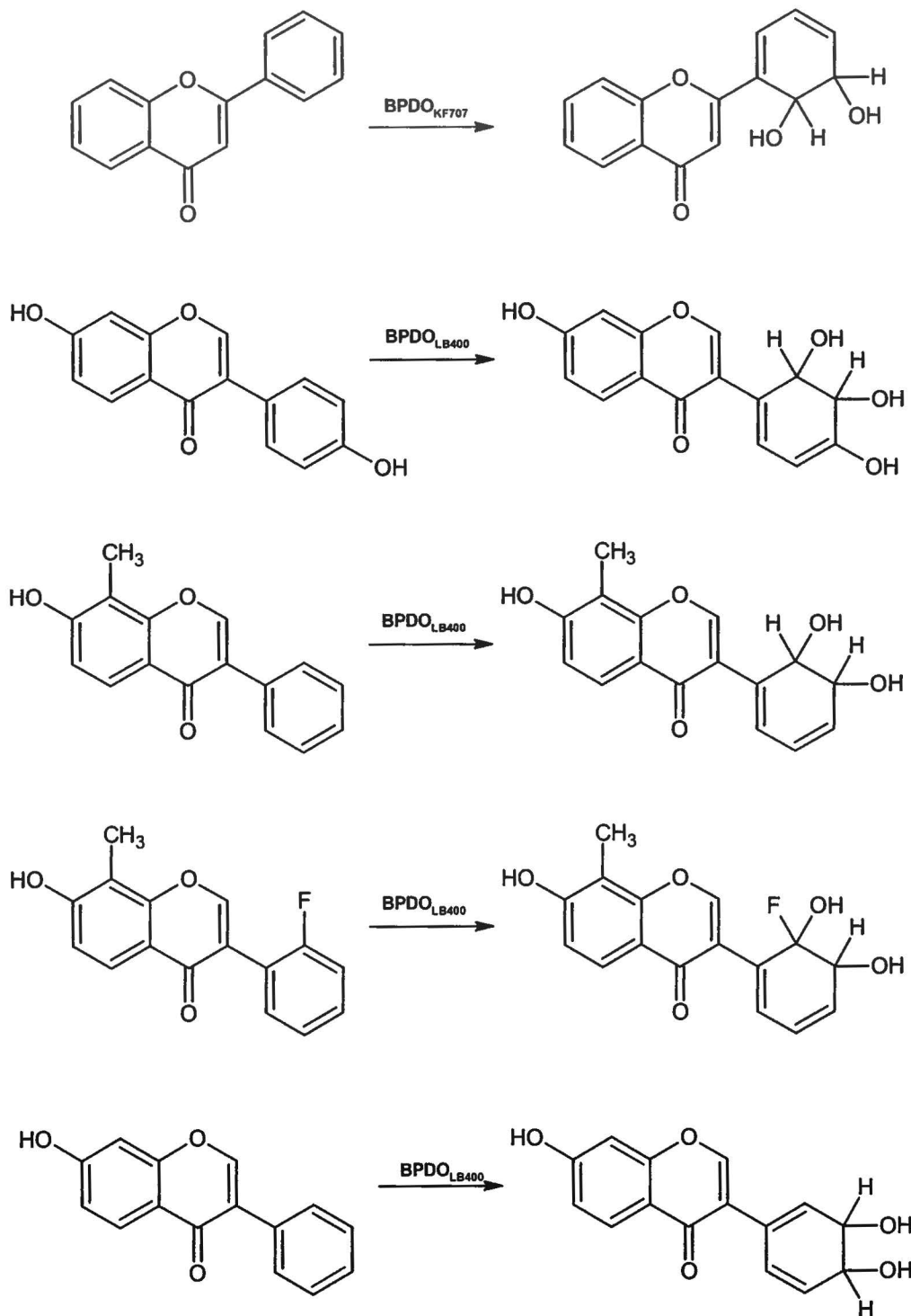


Figure 2.19: Biotransformation of certain flavonoids by $\text{BPDO}_{\text{LB400}}$ (271) and by $\text{BPDO}_{\text{KF707}}$ (152).

Several flavonoids including flavone (152), 7-hydroxyisoflavone, 7,4'-dihydroxyisoflavone (daidzein), 7-hydroxy-8-methylisoflavone, and 2'-fluoro-7-hydroxy-8-methylisoflavone (271) were shown to be metabolized by *P. pseudoalcaligenes* KF707 BPDO (BPDO_{KF707}) and *B. xenovorans* LB400 BPDO (BPDO_{LB400}). Based on mass spectral and nuclear magnetic resonance analyses, it was determined that four of five compounds tested (**Figure 2.19**), were oxidized at *ortho* and *meta* positions of ring B, resulting in the formation of *cis*-2'-3'-dihydrodihydroxyflavonoids. However, in the case of 7-hydroxyisoflavone, BPDO_{LB400} oxidized ring B at positions *meta* and *para*, yielding 3',4'-dihydro-7,3',4'-trihydroxyisoflavone (**Figure 2.19**).

Some studies investigated the ability of engineered BPDOs to metabolize flavonoids. These studies are summarized in **Table 2.3**. In general, the oxygenation occurs onto the *ortho* and *meta* carbons of ring B of the substrates. However in most cases, the dihydroxy- rather than the dihydrodihydroxy metabolites were detected. Furthermore, in several instances, the monohydroxylated metabolite was produced. This was explained by a spontaneous conversion of the dihydrodihydroxy metabolites to a more stable form.

Table 2.3: The transformation of some flavonoids by engineered BPDOs

Genes	Host strains	Substrates	Metabolites
<p><i>bphA1(2072)A2A3A4</i>:</p> <p>- <i>bphA1(2072)</i> generated by DNA shuffling using <i>bphA1_{KF707}</i> and <i>bphA1_{LB400}</i></p> <p>- <i>bphA2A3A4_{KF707}</i></p>	<p>(44)</p> <p><i>Streptomyces lividans</i> TK21</p>	<p>- Flavone</p> <p>- Flavanone</p> <p>- 6-hydroxyflavone</p> <p>- 6-hydroxyflavanone</p>	<p>- 2',3'-dihydroxyflavone (major); 3'-hydroxyflavone (minor)</p> <p>- 2',3'-dihydroxyflavanone (major); 2'-hydroxyflavanone and 3'-hydroxyflavanone (minor)</p> <p>- 3',6-dihydroxyflavone</p> <p>- 2',6-dihydroxyflavanone</p>
<p><i>bphA1(2072)A2A3A4</i>:</p> <p>- <i>bphA1(2072)</i> generated by DNA shuffling using <i>bphA1_{KF707}</i> and <i>bphA1_{LB400}</i></p> <p>- <i>bphA2A3A4_{KF707}</i></p>	<p>(287)</p> <p><i>E.coli</i> JM109</p>	<p>- Flavone</p> <p>- Flavanone</p> <p>- 6-hydroxyflavone</p> <p>- 6-hydroxyflavanone</p> <p>- 7-hydroxyisoflavone</p>	<p>- 2',3'-dihydroxyflavone (major); 3'-hydroxyflavone (minor)</p> <p>- 2',3'-dihydroxyflavanone (major); 2'-hydroxyflavanone and 3'-hydroxyflavanone (minor)</p> <p>- 3',6-dihydroxyflavone</p> <p>- 2',6-dihydroxyflavanone</p> <p>- 2',3'-dihydro-7,2',3'-trihydroxyisoflavone</p>
<p><i>bphA1A2A3A4B</i>:</p> <p>- <i>bphA1_{KF707}</i> with central fragment (coding amino acids 268-397) replaced by corresponding fragment of <i>bphA1_{KF715}</i> (<i>Pseudomonas putida</i> 715)</p> <p>- <i>bphA2A3A4B_{KF707}</i></p>	<p>(142)</p> <p><i>E.coli</i> JM109</p>	<p>- 7-hydroxyflavone</p> <p>- 5,7-dihydroxyflavone (chrysine)</p>	<p>- 7,2',3'-trihydroxyflavone</p> <p>- 5,7,2',3'-tetrahydroxyflavone</p>

Aside from its typical mechanism that adds two atoms of oxygen onto the aromatic ring of substrates, to form *cis*-dihydrodihydroxy metabolites, under certain conditions, BPDOs reaction alone or sometimes in combination with other enzymes may also generate unusual products that may have high pharmaceutical, agrochemical or industrial value.

Shindo et al. (2004) (289) constructed a recombinant *E. coli* strain expressing *bphA1*(2072)*A2A3A4*, *bphB* and *bphC* genes from *P. pseudoalcaligenes* KF707. The *bphA1*(2072) was obtained from shuffling *bphA1*_{KF707} and *bphA1*_{L.B400}. Six flavonoids (flavanone, flavone, 6-hydroxyflavanone, 6-hydroxyflavone, 7-hydroxyflavanone and *trans*-chalcone) were chosen as substrates for the biotransformation. Unexpectedly, aromatic compounds containing picolinic acid, instead of hydroxyflavonoids were identified as products. The ammoniacal nitrogen was suggested to derive from NH₄Cl present as a component of M9 medium, which was used as buffer for the catalytic reaction. These organic chemicals are very difficult or impractical to synthesize chemically, thus this catabolic reaction may serve as a novel synthetic process to produce these compounds. **Figure 2.20** shows an example of the transformation a flavonoid by BphA1(2072)*A2A3A4BC* to a picolinic acid.

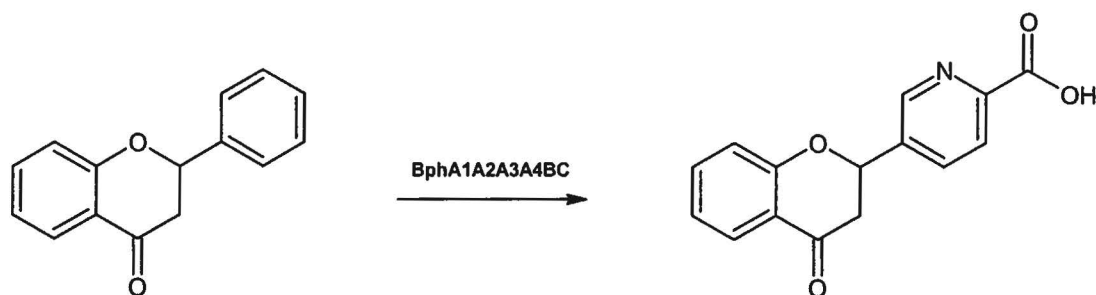


Figure 2.20: Transformation of flavonoid by cells of *E. coli* carrying *bphA1*(2072), *bphA2*, *bphA3*, *bphA4*, *bphB*, and *bphC* genes (289).

Recently, Seo et al. (2011) (278) reported the biotransformation of isoflavan-4-ol to the corresponding epoxides by *P. pseudoalcaligenes* KF707 BPDO. Interestingly, the epoxide metabolites were further abiotically transformed into pterocarpan, the structural

backbone of antimicrobial natural products from plants. Although it needs to be further investigated, the result provides a new, effective way to synthesis pterocarpan (**Figure 2.21**).

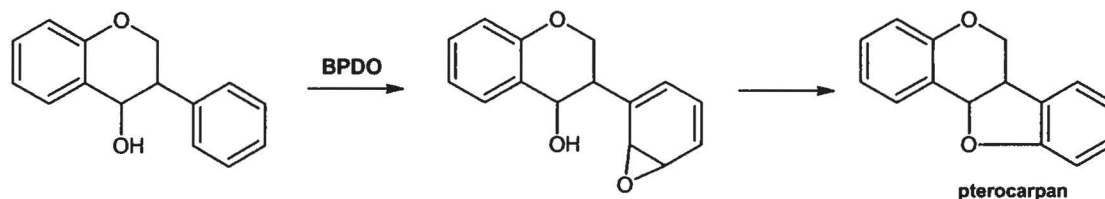


Figure 2.21 : Biotransformation of isoflavan-4-ol by BPDO of *P. pseudoalcaligenes* KF707 (278).

2.3.4. Engineering BPDOs for manufacturing flavonoids

The most desirable features of engineered enzymes for biocatalysis are high chemo-, regio-, and enantioselectivity. However, these features are not easy to improve (243). Fortunately, BPDOs catalyze the formation of chiral *cis*-dihydrodihydroxy metabolites that may be very useful for biosynthetic purposes (124). Furthermore, their broad substrate specificity is also a useful property that makes the enzymes very promising as biocatalyst.

Despite this advantage, BPDOs applications are much less widespread in biocatalytic processes compared with other enzymes such as hydrolases, lyases and isomerases. The limitation is explained by many factors. BPDOs are poorly stable. In addition, their function depends on reduced nicotiamide adenine dinucleotide (NADH). This is one of the main limitations for using BPDOs in industrial applications as the use of NADH increases the cost. A whole-cell system is an alternative solution to overcome these problems (124). However, using whole-cell system will increase the formation of by-products, and limit substrate uptake as well. Furthermore, substrates and products toxicity is also a problem for the whole-cell system (124).

In order to overcome the limitations mentioned above, some modifications should be made, firstly to make enzyme suitable to perform under chemical manufacturing conditions, and secondly to improve the catalytic features, such as product chirality, catalytic rate,

production yield, substrate specificity. Recently, several studies have been carried out to modify BPDOs as well as to investigate the ability of engineered variants to transform flavonoids (44, 142, 287) (see section 2.3.3.2). Although results obtained are promising, more studies are needed in order to use BPDOs for the manufacturing of flavonoids or their analogs.

3. Presentation of article 1

3.1. The context of the article

Biphenyl-degrading bacteria are promising tools to restore PCB-contaminated sites. However, the fact that biphenyl is needed to induce the bacterial biphenyl catabolic pathway is a disadvantage. Since many PSMs are structurally similar to biphenyl, it has been suggested that they could be suitable candidates to act as inducers for the pathway. This hypothesis was supported by several studies reporting that PSMs could support the growth of biphenyl-degrading bacteria and also induce their biphenyl catabolic pathway. On the other hand, Gram-positive rhodococcal rhizobacteria were recently shown to represent the dominant population in the rhizosphere of plant that grown in PCBs-contaminated soil.

On the basis of these premises, the purpose of article 1 was to investigate the mechanistic interactions between PSMs and the biphenyl catabolic pathway of a PCB-degrading rhodococcal rhizobacteria.

The results are presented in **Article 1**, which was published in *Applied Microbiology and Biotechnology*.

3. 2. Contribution of the student to article 1

The student is a coauthor of this article. Jean-Patrick Toussaint has initiated this investigation. He isolated and characterized *R. erythropolis* U23A, the PCB-degrading rhizobacteria. He set up the hydroponic culture to produce root exudates of *A. thaliana* and he examined the ability of these exudates to support the growth of strain U23A and to trigger its PCB-degrading ability. J.-P. Toussaint has also set up the chromatographic conditions to analyze and identify the PSMs present in *A. thaliana* root exudates. The student has contributed to the identification of the PSMs found in *A. thaliana* root exudates. She found that flavanone was the major PSM-component of the exudates and discovered that it was metabolized by strain U23A, and that it induced biphenyl catabolic pathway of strain U23A. The article was prepared by Michel Sylvestre, Jean-Patrick Toussaint and the student. The final version was written by Michel Sylvestre.

3.3. Article 1

Plant exudates promote PCB degradation by a rhodococcal rhizobacteria

Jean-Patrick Toussaint¹, Thi Thanh My Pham, Diane Barriault and Michel Sylvestre*

Institut National de la Recherche Scientifique, INRS-Institut Armand-Frappier, 531 Boul. des Prairies, Laval, QC, Canada, H7V 1B7

* Corresponding author: phone: 450-687-5010
 fax: 450-686-5001
 E-mail: michel.sylvestre@iaf.inrs.ca

¹ JPT present address: Fondation David Suzuki, 50 rue Sainte-Catherine Ouest, Montréal QC, H2X 3V4

References: Toussaint, J. P., Pham, T. T., Barriault, D., and Sylvestre, M. 2012. Plant exudates promote PCB degradation by a rhodococcal rhizobacteria. *Appl Microbiol Biotechnol* **95**:1589-1603.

Keywords

Rhodococcus erythropolis, polychlorinated biphenyl (PCB), rhizoremediation, root exudates, plant secondary metabolites (PSMs), flavonoids, flavanone

3.4. Résumé

Rhodococcus erythropolis U23A est une bactérie capable de dégrader les biphényles polychlorés (BCPs). Cette bactérie a été isolée à partir de la rhizosphère de plantes cultivées sur un sol contaminé artificiellement aux BPCs. Le gène *bphA* de la souche U23A est homologue à 99% avec le gène *bphA1* de *Rhodococcus globerulus* P6. Nous avons cultivé *Arabidopsis thaliana* dans un système hydroponique axénique. Nous avons ensuite recueilli et concentré l'exsudat des racines contenant les métabolites secondaires de la plante. La souche U23A montrait une réponse chimiotactique envers ces exsudats racinaires. Dans un essai de colonisation de racines de *Medicago sativa*, le nombre d'unités formatrices de colonie de la souche U23A associées aux racines ($5,7 \times 10^5$ UFC g⁻¹) était supérieur à celui présent dans le sable les entourant ($4,5 \times 10^4$ UFC g⁻¹). Par ailleurs, les exsudats pouvaient soutenir la croissance de la souche U23A et induire la voie catabolique du biphényle. En effet des cellules au repos de la souche U23A, préalablement cultivées sur un milieu minimal contenant l'exsudat racinaire d'*Arabidopsis* comme seul substrat de croissance étaient capables de métaboliser le 2,3,4'- et le 2,3',4-trichlorobiphényle. Cependant, lorsque les cellules étaient préalablement cultivées sur le milieu Luria-Bertani, aucune dégradation significative de l'un des congénères n'a été observée. Bien qu'aucun des flavonoïdes identifiés dans l'exsudat de racine ne pouvait supporter la croissance de la souche U23A, les cellules induites par le biphényle pouvait métaboliser la flavanone, l'un des principaux composants de l'exsudat racinaire. En outre, lorsqu'utilisée comme cosubstrat avec de l'acétate de sodium, la flavanone était aussi efficace que le biphényle pour induire la voie catabolique du biphényle.

3.5. Abstract

Rhodococcus erythropolis U23A is a PCB-degrading bacterium isolated from the rhizosphere of plants grown on a PCB-contaminated soil. Strain U23A *bphA* exhibited 99% identity with *bphA1* of *Rhodococcus globerulus* P6. We grew *Arabidopsis thaliana* in a hydroponic axenic system, collected and concentrated the PSM-containing root exudates. Strain U23A exhibited a chemotactic response toward these root exudates. In a root colonizing assay, the number of cells of strain U23A associated to the plant roots (5.7×10^5 CFU g⁻¹) was greater than the number remaining in the surrounding sand (4.5×10^4 CFU g⁻¹). Furthermore, the exudates could support the growth of strain U23A. In a resting cells suspension assay, cells grown in a minimal medium containing *Arabidopsis* root exudates as sole growth substrate were able to metabolize 2,3,4'- and 2,3',4-trichlorobiphenyl. However, no significant degradation of any of congeners was observed for control cells grown on Luria-Bertani (LB) medium. Although strain U23A was unable to grow on any of the flavonoids identified in root exudates, biphenyl-induced cells metabolized flavanone, one of the major root exudates component. In addition, when used as cosubstrate with sodium acetate, flavanone was as efficient as biphenyl to induce the biphenyl catabolic pathway of strain U23A. Together these data provide supporting evidence that some rhodococci can live in soil in close association with plant roots and that root exudates can support their growth and trigger their PCB-degrading ability. This suggests that, like the flagellated Gram-negative bacteria, non-flagellated rhodococci may also play a key role in the degradation of persistent pollutants.

3.6. Introduction

Although the use of PCBs has been banned in many countries since the late 1970s (339, 341), they still persist in the environment due to their chemical and physical properties for which they were appreciated in the first place. PCBs mainly accumulate in soils, sediments, but also in animal and human adipose tissues (28), which provided the incentive to find ways of eradicating these compounds from the environment. Because of the relatively high cost associated with landfilling or incineration, biological degradation of PCBs has received increasing interest over the years. Many studies have now shown that a wide range of bacteria that can utilize or cometabolize PCBs through the biphenyl catabolic pathway, are promising tools to remediate these compounds (see review by Vasilyeva et al. (2007) (341)).

Generally, the bacteria capable of aerobically degrading PCB congeners do so via the 2,3-dioxygenase pathway (6). Although analog enrichment with biphenyl can increase bacterial PCB degradation rates (73, 182), the use of biphenyl to enrich PCB-contaminated soils is not a viable idea. Because of the similarity between xenobiotics (e.g. PCBs) and natural occurring compounds in the soil (e.g. PSMs), it has been suggested that PSMs could be suitable candidates to be exploited in order to stimulate bacterial degradation of PCBs and other persistent organic pollutants such as polycyclic aromatic hydrocarbons (203, 294). This is supported by several studies showing that PSMs such as flavonoids and terpenes can support the growth of PCB-degrading bacteria and trigger their PCB-degrading abilities (62, 119, 172, 173, 216). For example, PCB degradation was stimulated in soils containing natural sources of terpenes (e.g. orange peels, eucalyptus leaves, pine needles, spearmint leaves and ivy leaves) (103, 119); or in liquid culture, when biphenyl-degrading bacteria were grown in the presence of flavonoids (62). Furthermore, PCB depletion was significantly higher in soil sown with an *Arabidopsis* mutant overproducing root PSMs and inoculated with the PCB-degrading and flavonoid-degrading rhizobacteria *Pseudomonas putida* PML2, than in soil sown with the wild-type plants (216). These experiments provide evidence that plant chemicals can trigger bacterial, and notably rhizobacterial PCB degradation in soil.

These observations encourage the development of processes exploiting plants and their associated rhizobacteria to degrade PCBs (316). However the mechanism by which PSMs trigger the PCB-degrading ability of rhizobacteria is still unclear since no study has yet demonstrated that these chemicals can act as non-specific inducers of the bacterial biphenyl

degradation enzymes when they are used as growth substrate (285). It is also unclear whether these chemicals act at low concentrations, as signals to induce PCB degradation (294), or if they act as substrates in a cometabolism process as suggested by Hernandez et al (119). Answers to these questions will help in designing new enrichment strategies based on plant-microbe interactions to increase PCB degradation in the rhizosphere.

On the other hand, although Gram negative bacteria are traditionally believed to play a major role in pollutant removal in soil and in the rhizosphere, many rhodococcal bacteria capable of degrading PCBs have been described (40, 136, 150, 195). In addition, rhodococci were recently found to represent the dominant population in the rhizosphere of plants grown in a PCB-contaminated site (173). However a very limited number of studies examining plant-rhodococcal bacteria interactions and their impact on PCB degradation have been reported (86).

In this work, we have isolated a PCB-degrading rhodococcal strain. We provide evidence that this strain is able to colonize plant roots and exhibits a chemotactic response toward root exudates. We have examined the ability of *A. thaliana* PSMs to promote growth and PCB degrading ability of this bacterium and we have assessed the ability of flavanone, one of the major root exudates components to induce its biphenyl catabolic pathway. Data provide more insights into how plant flavonoids might interact with rhodococcal rhizobacteria to trigger their PCB-degrading ability.

3.7 Materials and methods

3.7.1. Bacterial strains, culture media and chemicals

The bacterial strains used in this study were isolate U23A identified based on 16S rRNA gene sequencing as *R. erythropolis* (see below) and *Pseudomonas fluorescens* F113 (32) (obtained from Prof. David Dowling–Institute of Technology, Carlow, Ireland). The culture media used were LB broth (260), basal medium M9 (260), or minimal mineral medium no. 30 (MM30) (310) amended with various sources of carbon depending on the experiment (see below). All strains were maintained on LB agar medium at 28 °C for experimental purposes. The flavonoids and other chemical standards used in this study were obtained from Sigma-Aldrich and the PCB congeners were purchased from UltraScientific.

R. erythropolis U23A was isolated by enrichment on biphenyl from the rhizosphere of a PCB-contaminated microcosm set in the laboratory. To prepare the microcosm, a beaker (250 ml) was filled to approximately 10-cm height with a PCB-contaminated soil obtained from Netolice, Czech Republic and this soil was covered with the 2-cm top portion of a vegetated soil from St-Hippolyte, QC, Canada which contained a mixture of monocotyledon plants and their roots. The microcosm was kept under laboratory conditions for 6 months at 20°C under a fluorescent light with a 16/8-h day/night cycle so that the plant could grow. Then, the rhizosphere (*i.e.* the remaining soil adhering to plant roots after vigorous shaking) of this mixture of monocotyledon plants was collected. One gram of freshly collected rhizosphere material was then transferred in 10 ml sterile NaCl (0.85% w/v). The suspension was vigorously shaken by vortexing, diluted serially and inoculated onto solid MM30 agar plates exposed to biphenyl vapour as sole growth substrate. The cultures were grown at 25 °C for 48 to 72 hours. The colonies able to degrade chlorobiphenyls were identified using the 4-chlorobiphenyl sprayed-plate assay described previously (310). From this screening step, seven bacterial strains were retained based on colony morphology (size, color and colony surface roughness) and were further purified by streaking on MM30 agar plates exposed to biphenyl vapour. Based on their ability to use root exudates as sole growth substrate (see below) three of these isolates U22, U23A and U24 were selected. Because of their inability to grow on root exudates, the other isolates were not considered for this study and discarded.

3.7.2. Identification of strain U22, U23A and U24 and amplification of *bphA* gene

Strains U22, U23A, and U24 were identified based on their 16S rRNA gene sequence and, strain U23A was further characterized on the basis of morphological examination and biochemical tests. Genomic DNA was isolated using the QIAGEN QIAamp DNA Mini kit according to the protocol suggested by the manufacturer. The 16S rRNA gene was amplified from total genomic DNA using primers pA (AGAGTTTGATCCTGGCTCAG) and pH (AAGGAGGTGATCCAGCCGCA) (67). Genomic DNA was also probed for the presence of *bphA* gene using a previously described set of three pairs of degenerated primers that amplify the C-terminal portion of *bphA* gene (345), and specific primers designed to amplify the complete *bphA* genes from *B. xenovorans* LB400 (130), from *P. pnomenusa* B356 (129) and from *R. globerulus* P6 (40). The PCR conditions used to amplify the genes were as recommended by QIAGEN for the HotStart High Fidelity polymerase kit (QIAGEN), with the following modifications of the program: 15 min at 95 °C to activate the polymerase, then for 30 cycles, 94 °C for 1 min, 56 °C for 1 min and 72 °C for 2.5 min and 1 cycle at 72 °C for 10 min. The amplicons from the PCR were sequenced at the Génome Québec Innovation Center (Montreal, Quebec, Canada). BLASTn from NCBI data bank was used to analyze the 16S rRNA gene sequence and BLASTp for the deduced sequence of BphA.

3.7.3. Axenic culture for the production of root exudates

A. thaliana was grown in a hydroponic axenic culture system containing 100 ml of a tenth-strength Hoagland's solution (Hoagland's No. 2 Basal Salt Mixture from Sigma-Aldrich; see **Figure 3.1**). The system in which the plants were grown was made out of a pipette tip support and 0.5 ml Eppendorf tubes without lids. Holes were punched at the bottom of the Eppendorf tubes in order to let *A. thaliana* roots grow through. The tubes were then fitted in a pipette tip support rack, which was sterilized by autoclaving for 1 h at 121 °C, and put in sterile transparent plastic Magenta containers. Each Eppendorf tube was filled with a tenth-strength Hoagland's solution containing 1% agar. Once the medium was solidified, sterilized seeds of *A. thaliana* were deposited on the top of the solidified medium. The seeds were sterilized by soaking into a 2% hypochloric solution for 5 min and rinsing with deionized sterile water for 5 min. There was one seed per Eppendorf tube, and the whole system comprised approx. 30 tubes (plants). The plants were grown for 18 weeks under a

fluorescent light with a 16/8-h day/night cycle. Root exudates were collected under sterile conditions periodically starting the eighth week after seed germination. Preliminary experiments allowed us to determine that out of all the exudates harvested and tested, the ones collected after 16 weeks of *A. thaliana* growth were the ones that allowed optimal bacterial growth. Hence, those exudates were used for all of the experiments described thereafter.

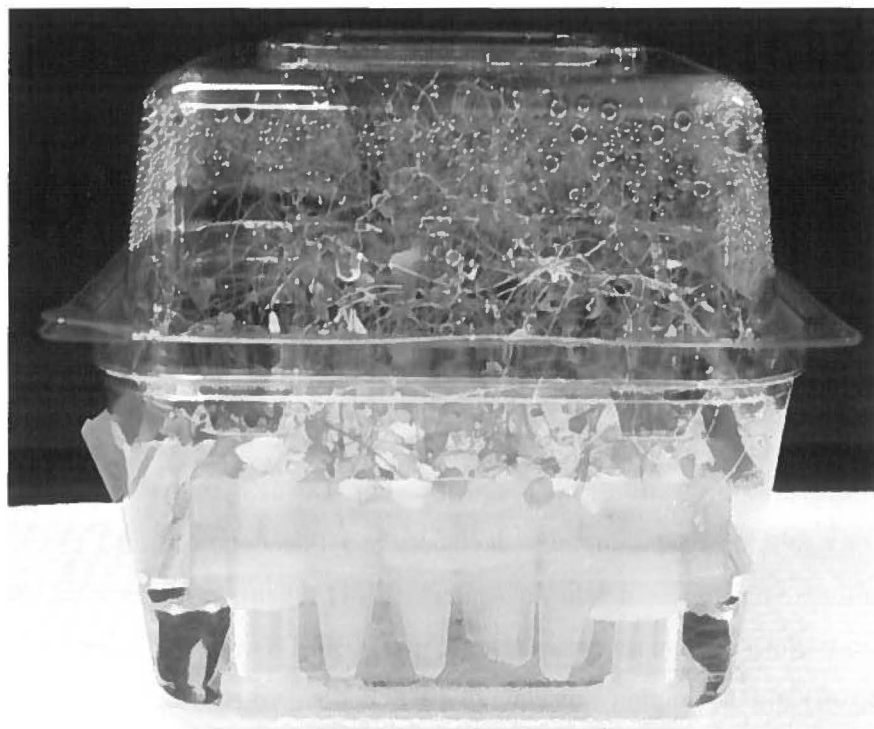


Figure 3.1: Axenic culture system for the growth of *A. thaliana* and the collection of root exudates. Sterile plastic Magenta containing approx. 30 Eppendorf tubes punched with holes at the bottom that were mounted on a pipette rack and filled with a tenth strength Hoagland's solution containing 1% agar. Sterilized seeds of *A. thaliana* were grown for several weeks in 100 ml of a tenth strength Hoagland solution, under a fluorescent lamp with a 16/8-h day/night cycle.

3.7.4. *Flavonoids detection and identification from root exudates by HPLC, LC-MS and GC-MS*

For root exudates fractionation, 10 ml of root exudates from *A. thaliana* were collected and concentrated approx. 15 times using a Büchi roto-evaporator prior injection to HPLC. The HPLC apparatus was an Agilent 1100 Series liquid chromatography system comprising a UV lamp detector. The analysis was performed on a reverse-phase Eclipse XBD-C8 column (Agilent 4.6 X 150 mm, 5- μ m pore size). The column was eluted with a non-linear gradient starting from 80% A (HPLC-grade water with 0.085% ortho-phosphoric acid) and 20% B (acetonitrile) to 50% B in 12 min, 70% B at 17 min, 80% at 21 min, 100% B at 25 min, then back to 80% A at 29 min. Fifty microliters of the root exudates were injected and the column was eluted at a flow rate of one ml min⁻¹ and detected at 280 nm.

For further detection of the compounds, root exudates were hydrolyzed for one hour at 90 °C with 1 M HCl to hydrolyze the conjugated plant metabolites. The hydrolysate was then neutralized (pH=7-8) before extracting the metabolites twice with ethyl acetate. The extract was dried over ammonium sulphate and evaporated to dryness under N₂. This hydrolyzed extract was analyzed by liquid chromatography-mass spectrometry (LC-MS) and by gas chromatography-mass spectrometry (GC-MS). For LC-MS analysis, the residues were dissolved in a solution containing 30% methanol and 1% acetic acid in HPLC-grade water. Fifty microliters were injected into an Agilent HP111/Quatro Micromass LC-MS. The LC analysis was performed on a reverse-phase Eclipse XBD-C8 column (Agilent 4.6 X 150 mm, 5- μ m pore size) and the column was eluted with a gradient consisting of solvent A, water and solvent B, 1% acetic acid in acetonitrile (0-1 min 0% solvent B; 1-5 min 50% B; 5-10 min 50% B; 10-19 min 100% B; 19-24 min 100% B; and 24-29 min 0% B). The mass spectrometry detection was done using a positive mode (ESP+) with a capillary value of 3.50, cone value of 28 and extractor value of 5.

For GC-MS analysis, the dried residues from the ethyl acetate extract of the hydrolyzed exudates were dissolved in N,O-bis(trimethylsilyl)trifluoroacetamide (BSTFA) (Supelco, Sigma–Aldrich) and the solution was heated for 30 min at 70 °C (189). The trimethylsilyl (TMS) derivatized extract was then injected in a Hewlett Packard HP6890 gas chromatograph equipped with a SPB-5 capillary column (30 m x 0.2 mm i.d.) (Sigma-Aldrich Biotechnology LP) and a HP5973 mass selective detector. The initial oven temperature (100

°C) was held for 2 min and programmed at 15 °C per min to 200 °C and at 10 °C per min to 300 °C. The injector and the detector were maintained at 250 °C and 300 °C respectively. The mass spectrometer was operated in the electron impact (EI) ionization mode.

3.7.5. Growth of *R. erythropolis* U23A and other isolates on root exudates

To test for the ability of isolates to grow on root exudates, the exudates from a 16-week-old *A. thaliana* hydroponic culture were concentrated 15 times using a Büchi roto-evaporator. The concentrated preparation was filter-sterilized, aliquoted and frozen at -20 °C until used. Cells grown overnight in LB broth were washed twice in 0.85% NaCl, suspended in 0.85% NaCl to an optical density at 600 nm (OD_{600nm}) of 0.5. Ten milliliter screw-capped tubes containing 2 ml of MM30 were supplemented with 1% (v/v) (20 µl) of the 15 times concentrated exudates. Concentrated exudates were used in order to avoid diluting the culture medium, but the final medium contained the equivalent of 15 parts of exudates per 100 parts of culture medium. These media were inoculated with 100 µl of the above cell suspension. The cultures were incubated at 28 °C at 100 rpm. Cell growth was monitored at OD_{600nm} .

3.7.6. PCB congener degradation

R. erythropolis U23A was grown overnight at 28 °C on MM30 containing 0.1% (w/v) sodium acetate, in LB or in MM30 amended with either 3.4 mM biphenyl or with 1% (v/v) of the 15 times concentrated root exudates described above. Cultures growing on biphenyl were filtered through packed glass wool to remove crystals of the substrate. Cells from overnight cultures were centrifuged, washed with MM30 medium, and suspended in a final volume of 1 ml. The bacterial suspensions were adjusted to OD_{600nm} of 1 with MM30 and distributed in 2 ml Teflon-lined screw-cap tubes by portions of 200 µl containing one µl of a mixture of 18 PCB congeners prepared in ethanol such as to give the final concentration of each congener which is indicated in **Table 3.1**. Tubes were incubated overnight at 28 °C and shaken at 100 rpm. The cultures were then extracted twice with hexane and the extracts were analyzed by gas chromatography using an electron capture detector to quantify PCB depletion using previously published protocols (18).

Table 3.1: List of PCBs and their concentrations in a mixture of 18 congeners

Congener	Final concentration in the reaction (μM)
2,6-Dichlorobiphenyl	1
3,3'-Dichlorobiphenyl	5
4,4'-Dichlorobiphenyl	5
2,3,4'-Trichlorobiphenyl	1
2,3',4-Trichlorobiphenyl	1
2,4,4'-Trichlorobiphenyl	1
2,2',3,3'-Tetrachlorobiphenyl	1
2,2',4,4'-Tetrachlorobiphenyl	1
2,2',5,5'-Tetrachlorobiphenyl	1
2,2',6,6'-Tetrachlorobiphenyl	1
2,3',4,4'-Tetrachlorobiphenyl	1
3,3',4,4'-Tetrachlorobiphenyl	1
3,3',4,5'-Tetrachlorobiphenyl	1
2,2',3,4,5'-Pentachlorobiphenyl	1
2,3',4,4',5-Pentachlorobiphenyl	1
2,2',3,4,5,5'-Hexachlorobiphenyl	1
2,2',4,4',5,5'-Hexachlorobiphenyl	1
2,2',3,3',4,5,5',6,6'-Nonachlorobiphenyl	0.5
(internal standard)	

3.7.7. Metabolism of flavanone by biphenyl-induced cells of strain U23A

R. erythropolis U23A was grown at 28 °C on MM30 containing 3.4 mM biphenyl. Cells from overnight cultures were harvested by centrifugation and washed with M9 medium. The cells were suspended in M9 to an OD_{600nm} of 5. This cell suspension was proportionally distributed (5 ml) among 50 ml glass tubes covered with Teflon-lined screw caps. Flavanone was added to a final concentration of 200 µM and the cell suspensions were incubated at 28 °C. After 30 min, or periodically between 3 h to 18 h, the cell suspensions were extracted twice with 5 ml of ethyl acetate, and the solvent phases were combined, dehydrated over ammonium sulphate, and evaporated to dryness under a stream of nitrogen. The residues were dissolved in 250 µl of anhydrous acetone plus 5 µl of a 25 mM solution of *n*-butylboronate (*n*BuB). The mixture was incubated at 20 °C for 30 min, it was then evaporated and the residues were dissolved in 50 µl hexane for GC-MS analysis. Alternatively, the extracts were treated with BSTFA as above to generate the TMS derivatives. The GC-MS conditions were identical to those described above.

As a control to facilitate the identification of the metabolites produced from flavanone by U23A cells, we also examined the ability of a reconstituted purified preparation of *P. pnomenus* B356 biphenyl dioxygenase (BPDO) to metabolize flavanone. In this case, each of the three purified enzyme components was produced as His-tagged proteins by recombinant *E. coli* cells and they were purified by affinity chromatography using previously described protocols (169). The enzyme assays were performed in a volume of 200 µl in 50 mM morpholinethanesulfonic (MES) buffer pH 5.5, at 37 °C as described previously (129). The metabolites generated after 10 min of incubation were extracted with ethyl acetate and treated with *n*BuB or BSTFA for GC-MS analysis.

3.7.8. 4-Chlorobiphenyl degradation assay

A resting cell assay using 4-chlorobiphenyl as substrate was performed to assess the ability of root exudates to induce the biphenyl catabolic pathway of *R. erythropolis* U23A. 4-Chlorobiphenyl metabolism was determined by monitoring 4-chlorobenzoate which accumulates as end metabolite of the biphenyl catabolic pathway. Cells of *R. erythropolis* U23A were grown overnight at 28 °C on LB medium or M9 medium amended with biphenyl

(3.4 mM) or with 1% (v/v) of the 15 times concentrated root exudates described above. The bacterial cultures were centrifuged at 7000 rpm for 10 min and washed twice in M9. The suspensions were adjusted to OD_{600nm} of 1 with M9 and distributed by portions of 200 µl into 1.5 ml Eppendorf tubes. The tubes were vortexed quickly and incubated at 28 °C in an Eppendorf Thermomixer 5436 for 5 min. Five microliters of 4-chlorobiphenyl in acetone (final concentration of 1.25 mM) or acetone (negative control) was added and the reaction vials were further incubated for 120 min. The suspensions were then acidified with HCl before extracting the metabolites twice with ethyl acetate. The extracts were dried over ammonium sulphate, evaporated to dryness under N₂ and derivatized with BSFTA for GC-MS analysis according to published protocols (189).

A similar experiment was set up to examine the ability of flavanone to induce the biphenyl catabolic pathway of strain U23A when it was used as cosubstrate. In this case, cells were grown overnight in MM30 containing 30 mM sodium acetate as sole growth substrate or in MM30 containing 30 mM sodium acetate plus variable amounts (1 mM, 0.01 mM or 0.001 mM) of flavanone or of biphenyl. The latter two concentrations were in the range of those estimated to be present in the culture media containing 15 times concentrated root exudates described above. Cells from each of the overnight grown cultures were then prepared to evaluate their ability to metabolize 4-chlorobiphenyl to 4-chlorobenzoate using the 4-chlorobiphenyl assay described above.

3.7.9. Motility assays

Although *R. erythropolis* U23A is a Gram-positive bacterium, it can likely be motile by gliding (139). Therefore, it was tested for its capacity to exhibit phenotypic traits that are likely to contribute in the root colonization process. Hence, mobility, chemotaxis, cell hydrophobicity, cell adhesion, and root colonization capacities were tested as described below.

3.7.10. Chemotaxis assay

The chemotaxis assay was based on a protocol described by Gordillo et al. (2007) (108). Tryptone 1% (positive control), sterile water (negative control), and a sterile concentrated root exudates were tested for their capacity to induce a chemotaxis response. *R. erythropolis* U23A was grown overnight at 28 °C in Petri dishes on solid LB medium. Cells were then collected and suspended in a 0.5 M phosphate buffer solution (PBS), pH 7.3 containing 0.1% agar and the suspension was adjusted to an OD_{600nm} of 5. The suspension was poured into 50 mm Petri dishes and let to settle for a few minutes before transferring the disk soaked with the substrates to be tested. Sterile filter paper discs were soaked individually with twenty µl of each preparation to be tested, the filters were air-dried in a sterile laminar-flow cabinet, and then gently deposited on the surface of the soft agar medium containing the bacterial suspension. The formation of a turbidity ring around the disc, reflecting the movement of the bacterial suspension towards the chemo-attractant, was observed regularly for 2 h and pictures were taken to document the assay.

3.7.11. Binding assays: microbial adhesion test on hydrocarbons/sand

Microbial adhesion to hydrocarbons (MATH) (251) and microbial adhesion to silica sand (MATS) (56) assays were performed according to previously described protocols (56, 251). *R. erythropolis* U23A and *P. fluorescens* F113 (a positive control) were grown on liquid LB medium overnight at 28 °C, centrifuged at 7000 rpm and washed twice in 0.85% NaCl, suspended in 3 ml of 0.5 M PBS, pH 7.3, and OD_{600nm} was adjusted to 0.5. For the MATH assay, 500 µl of the bacterial suspension were mixed with 500 µl mineral oil in 2 ml glass vials, vortexed for 1 min at maximum speed and let to settle for 30 min at room temperature. Two hundred microliters of the aqueous phase were transferred into the wells of a 96-well plate and OD_{600nm} was recorded. For the MATS assay, 500 µl of the bacterial suspension was mixed in 500 mg of washed sand in an Eppendorf tube and mixed on a rotation shaker for 30 min at room temperature. The tubes were then put aside to let the sand settle at the bottom, and the supernatant was transferred in a spectrophotometer tube to read OD_{600nm} against a blank of PBS. For both assays, OD_{600nm} was measured prior and after

completing the test in order to compare and calculate the absorption percentage on either mineral oil or sand. Comparisons were also made between the two strains for each assay.

3.7.12. Root colonization assay

The root colonization assay was partly adapted from that of Scher et al. (1984) (264) and Villaceros et al. (2005) (347). For this assay, alfalfa (*Medicago sativa* L. var. Geneva) seeds were used as their root system is bigger and easier to handle than that of *A. thaliana*. Seeds were surface-sterilized by soaking in a 50% hypochlorite solution (commercial bleach 4%) for 5 min and rinsed with sterile distilled water. Bacterial cultures of *R. erythropolis* U23A and *P. fluorescens* F113 were grown at 28 °C overnight in 2 ml LB medium, and OD_{600nm} was adjusted to 1 in sterile NaCl (0.85%). The sterilized seeds were soaked in the bacterial suspension for 30 min on a horizontal agitator, after which they were inoculated in 50 ml test tubes filled with 40 g sterilized Ottawa sand. Prior seed inoculation, the sand was watered with 7 ml of half-strength Hoagland's solution. Triplicate tubes were seeded for each treatment. Triplicate control tubes seeded with uninoculated seeds were also included in the experiment to confirm the sterility of the plant cultures. The seeds were allowed to germinate and grow for four weeks before harvesting. For each treatment, 3 replicated seeds that had been soaked in the bacterial suspensions were washed in sterile 0.85% NaCl and vortexed for 10 s. Serial tenfold dilutions were made in sterile 0.85% NaCl from which 0.1 ml were inoculated on LB agar plates in triplicate. Colonies were counted following incubation for 24 h at 28 °C to determine the total number of colony-forming units (CFUs) per inoculated seed. The extent of root colonization was evaluated using a protocol similar to the one described by Sanchez-Contreras et al. (2002) (261). Four-weeks-old plants (including the roots) were carefully removed from the sands, their roots were excised, weighted, transferred in a tube containing 5 ml sterile 0.85% NaCl and vortexed vigorously. Similarly, the sand from each tube was collected, weighted and vortexed into 5 ml 0.85% NaCl to release the bacteria remaining in the sand fraction. Both bacterial suspensions (roots and sands) were diluted and plated on LB agar as above to count the CFUs from the roots or sand fractions. The CFUs were expressed per gram of roots or of sand.

3.8. Results

3.8.1. Isolation and identification

Based on 16S rRNA sequence analysis, strains U22 and U24 clustered with *R. globerulus*. Their PCB-degrading patterns, based on their ability to metabolize the mixture of 18 PCB congeners described in **Table 3.1** was very similar to the one obtained for strain U23A described below (data not shown). However, both of these strains exhibited a poor growth when root exudates were used as the sole carbon source. Therefore, these two strains were not further considered in the study. Strain U23A is an aerobic, non-sporulating, Gram-positive bacterium. It is catalase-positive and based on microscopic observation, it forms rods to extensively branched vegetative chains. On the basis of its morphological and biochemical features, it was identified as a *Rhodococcus*. The identity was confirmed as *R. erythropolis* based on 16S rRNA gene sequence. The 16S rRNA gene sequence of *R. erythropolis* U23A is available under the GenBank accession numbers HQ412801 and it is 99% identical to that of *R. erythropolis* strain LG12 and OUCZ211 16S rRNA gene (GenBank: AY785750.1 and EU852376.1). Strain U23A has been deposited at the American Type Culture Collection under the accession number ATCC BAA-2259.

Furthermore, using the primers to amplify the gene encoding for the large subunit of the BPDO's oxygenase component (*bphA*), we amplified a 1.2-kb fragment with the primers that are specific for *R. globerulus* P6 *bphA1*. Sequence analysis of the amplified 1.2-kb fragment confirmed the presence of *bphA* and its deduced amino acid sequence was closely related (99% identity) to BphA1 of *R. globerulus* strain P6 (20). The two proteins differ by only one amino acid residue, where the alanine at position 446 of P6 BphA1 is replaced by a glycine in U23A BphA. The presence of a single *bphA* in the genome of strain U23A was supported by the fact that the previously described sets of degenerated pairs of primers designed to amplify a broad range of *bphA* genes (345) did not amplify any amplicon other than the one corresponding to the sequence described above and the primers specific for *B. xenovorans* LB400 or *P. promoenusa* B356 *bphA* did not amplify any gene.

3.8.2. Bacterial growth on root exudates and flavonoids detection by HPLC

R. erythropolis U23A was able to grow in MM30 containing 1% (v/v) of the 15 times concentrated root exudates as sole growth substrate, reaching an OD_{600nm} of approximately 0.7 within 48 h at 28 °C. Under the same conditions, when grown on 3.4 mM biphenyl strain U23A reached an OD_{600nm} of 2.5 after 24 h of incubation. The root exudates were fractionated by HPLC according to the protocol described in the “Materials and methods” section. Approximately 40 HPLC chromatographic peaks were obtained from this separation. In order to facilitate identification of the components, the exudates were acid-hydrolyzed before separation by HPLC. On the basis of LC-MS, GC-MS analyses and with comparison to commercially available flavonoids and phenylpropanoids few peaks were identified, including coumarin, flavanone, hydroxybenzoic acid, hydroxytyrosol, naringenin, syringic acid, and vanillic acid (not shown). However, under our experimental conditions we were unable to identify the other peaks, many of which were very low, indicating they were minor components of the mixture or they were lost during acid hydrolysis.

3.8.3. PCB and 4CB degradation by cells grown on root exudates

Resting cells suspensions of biphenyl-induced *R. erythropolis* U23A were able to degrade seven congeners of the mix of 18 congeners described in **Table 3.1**, ranging from di- to tetra-chlorinated biphenyls (**Table 3.2**). More importantly, when cells were grown in a minimal medium containing 1% (v/v) of the 15 times concentrated root exudates as sole growth substrate, the resting cells were able to degrade 3 chlorobiphenyls more significantly than cells grown on MM30 containing sodium acetate as sole growth substrate or grown on LB medium (**Table 3.2**).

A resting cells assay described in the “Materials and methods” section was performed to determine the effect of root exudates on the ability of *R. erythropolis* U23A to convert 4-chlorobiphenyl to 4-chlorobenzoate. When cells were grown on MM30 containing biphenyl as growth substrate, the resting cell suspension converted approximately half (750 µM) of the 1.25 mM of 4-chlorobiphenyl added to the medium into 4-chlorobenzoate (**Figure 3.2**) which was detected as sole metabolite by GC-MS analysis (not shown). When cells were grown on LB medium, approximately 7 µM 4-chlorobenzoate were produced and no other intermediate

metabolites were detected in the medium, indicating that the biphenyl-degrading enzymes are constitutively expressed at a very low level in strain U23A. However, when cells were grown using root exudates as sole growth substrate, using identical conditions, resting cells of *R. erythropolis* produced 3.5 times more 4-chlorobenzoate than those grown on LB broth. This observation provides further evidence that U23A *bph* gene cluster responds to the *Arabidopsis* root exudates (although to a lesser extent than for biphenyl) by increasing the level of the biphenyl-catabolic enzymes above the basal level found in cells grown in LB broth.

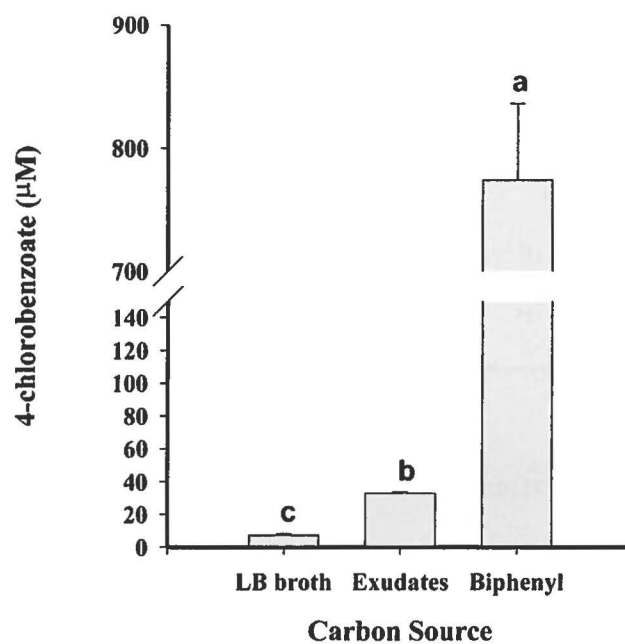


Figure 3.2: Amount (micromolar) of 4-chlorobenzoic acid produced when standardized resting cell suspensions of *R. erythropolis* U23A were incubated with 1,250 μM 4-chlorobiphenyl for 2 h. *R. erythropolis* was previously grown overnight at 28 °C in either LB Broth, MM30 amended with 3.4 mM biphenyl, or a 1% (v/v) of a 15 times concentrated root exudates. Bars represent mean (n=2) and SD are shown. Different letters indicate significant differences according to Tukey's test ($P \leq 0.05$). The protocol for the standardized 4-chlorobiphenyl assay is described in the Materials and methods.

Table 3.2: Effect of carbon source on the PCB-degrading ability of *R. erythropolis* U23A toward the PCB congeners found in a mixture of 18

Congener ^a	LB broth	Na acetate	Exudates	Biphenyl
% depletion of each congener ^{**}				
33'	0.0 ± 0.0 ^a	1.4 ± 2.5 ^a	17.6 ± 9.6^b	97.9 ± 3.6 ^c
44'	0.0 ± 0.0 ^a	0.0 ± 0.0 ^a	0.0 ± 0.0 ^a	30.8 ± 1.6 ^b
23'4	5.4 ± 4.8 ^a	2.5 ± 4.3 ^a	84.5 ± 2.9^b	100.0 ± 0.0 ^b
244'	3.0 ± 1.4 ^a	2.8 ± 4.9 ^a	5.0 ± 6.6 ^a	83.6 ± 4.1 ^b
234'	5.8 ± 2.7 ^a	3.0 ± 5.2 ^a	21.7 ± 10.1^b	94.4 ± 4.9 ^c
22'33'	0.0 ± 0.0 ^a	0.0 ± 0.0 ^a	0.0 ± 0.0 ^a	59.0 ± 13.6 ^b
23'44'	0.0 ± 0.0 ^a	0.0 ± 0.0 ^a	0.0 ± 0.0 ^a	25.7 ± 11.0 ^b

^a Only the congeners that are degraded by the biphenyl-grown cells are indicated

^b Cells were grown overnight at 28 °C on LB Broth or on MM30 amended with 0.1% sodium acetate (Na acetate), with 3.4 mM biphenyl (Biphenyl) or with 1% (v/v) 15 times concentrated root exudates (Exudates) and then used in the resting cell assay described in the Materials and Methods. Means (n=3) ± standard deviations are shown. Values in bold represent the congeners that were significantly degraded compared to the control cultures grown on Na acetate or in LB broth, and for each congener, different letters in superscript indicate significant differences according to Tukey's test ($P \leq 0.05$).

3.8.4. Metabolism of flavonoids by strain U23A

None of the compounds that were identified from root exudates (listed above) were able to sustain the growth of strain U23A when used as sole growth substrate. Since flavanone was among the most abundant chemicals detected in the root exudates (its concentration was estimated between 0.5 and 1 mM based on the peak area of HPLC and GC-MS chromatography), we have examined the ability of biphenyl-induced cells to metabolize this flavonoid. When a resting cell suspension was incubated for 30 min in the presence of 200 μ M flavanone under the conditions described in the “Materials and methods” section, two dihydrodiol metabolites were detected in the culture media (**Figure 3.3a**). The mass spectral features of the butylboronate derivatives of both metabolites were very similar and corresponded to the 2-(2,3-dihydro-2,3-dihydroxyphenyl)chromane-4-one and the 2-(3,4-dihydro-3,4-dihydroxyphenyl)chromane-4-one. Both metabolites were characterized by a high molecular ion at m/z 324 and diagnostically important ions at m/z 308 ($M^+ - O$), 267 ($M^+ - nBu$), 240 ($M^+ - nBuBO$), 224 ($M^+ - nBuBO_2$), 147 ($M^+ - nBuBO_2 - C_6H_5$), 120 ($M^+ - nBuBO_2 - C_6H_5 - CH - CH_2$). The identity of these two metabolites as dihydrodihydroxy compounds was confirmed by the fact that a reconstituted purified preparation of *P. pnomenus* B356 BPDO produced the same two metabolites from flavanone (**Figure 3.3a**). Although GC-MS analysis did not allow us to distinguish between the 2,3- and 3,4-dihydroxylated metabolites, the mass spectral fragmentation pattern (presence of ions at 147 and 120) was consistent with a dihydroxylation reaction occurring on the phenyl ring, at both positions. This ring was also the one that an engineered BPDO produced by *P. pseudoalcaligenes* KF707 was shown to hydroxylate (287).

When the cell suspensions were incubated from 3 to 18 h under the same conditions, a single metabolite was detected. This metabolite accumulated in the culture medium until the substrate was completely depleted and it was not further degraded by the cells. The TMS-derived metabolite was detected by GC-MS and its mass spectral features corresponded to the 4-oxo-2-chromanecarboxylic acid (**Figure 3.3b**). It was characterized by diagnostically important ions at m/z 264 (M^+), 249 ($M^+ - CH_3$), 219 ($M^+ - 3CH_3$), 205 ($M^+ - CH_3 - O - CO$), 174 ($M^+ - COOTMS$), 131 ($M^+ - COOTMS - O$).

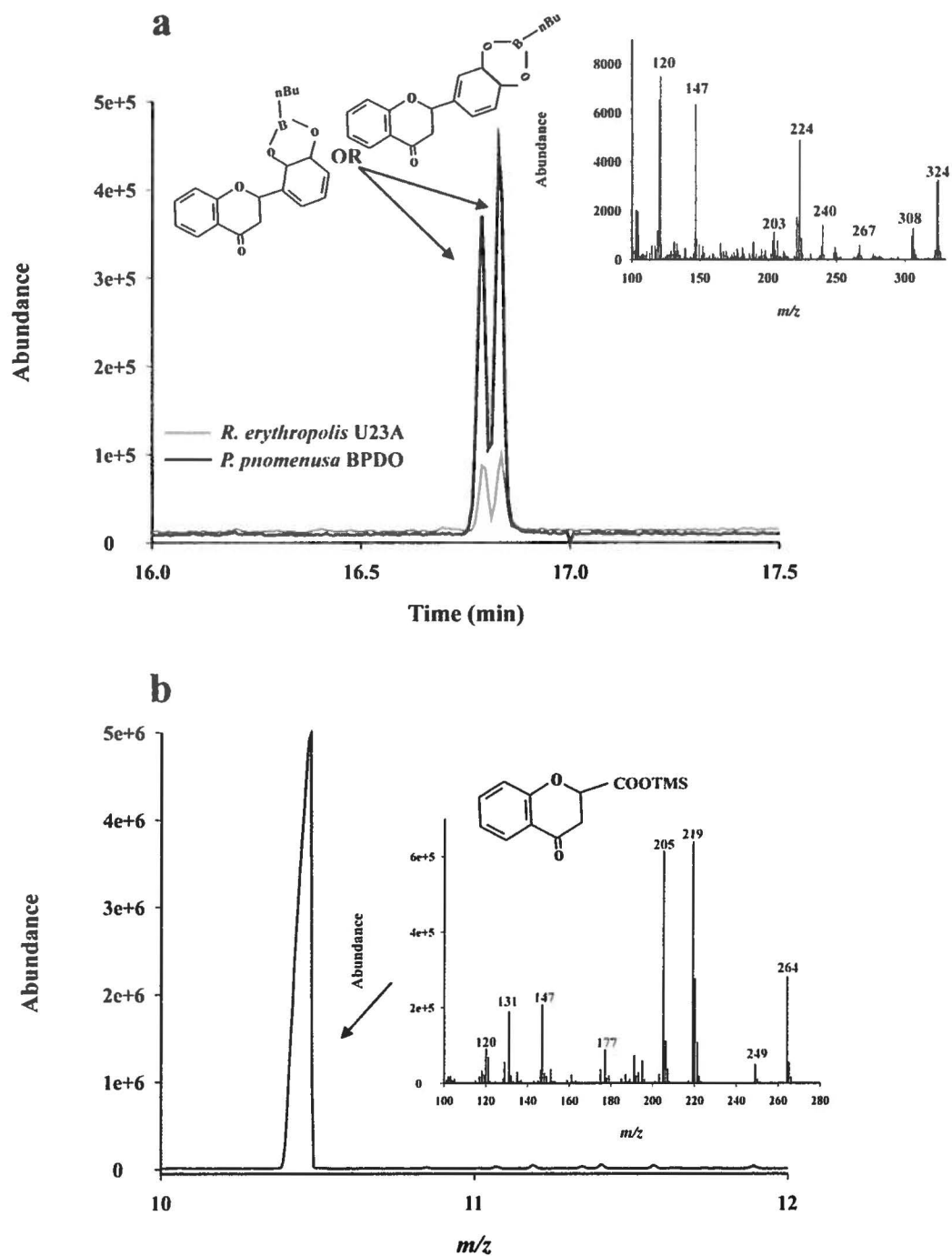


Figure 3.3: (a) Total ion chromatogram showing the peaks of the two metabolites produced from flavanone after 30 min by a resting cell suspension of *R. erythropolis* U23A (grey curve) or after 10 min by a purified preparation of *P. pnomenusa* BPDO (black curve). The inset shows the mass spectra of one of the two metabolites; the second mass spectrum is not shown but very similar. (b) Total ion chromatogram showing the single peak of metabolite produced after 18 h by a resting cell suspension of *R. erythropolis* U23A. The inset shows the mass spectra of the metabolite.

Together, the data show the unique BPDO of the biphenyl catabolic pathway of strain U23A oxidized flavanone on the phenyl ring and the ring is then cleaved to ultimately generate 4-oxo-2-chromanecarboxylic acid. However, since the hydroxylation occurs on carbons 2,3 and 3,4 of the phenyl ring and a single metabolite was detected as end product of this pathway, more work will be required to determine the exact steps involved in the metabolism of flavanone dihydrodiols. The BPDO, the 2,3-dihydro-2,3-dihydroxybiphenyl 2,3-dehydrogenase and the 2,3-dihydroxybiphenyl 2,3-dioxygenase of *P. alcaligenes* K707 were found to metabolize flavanone to the *meta*-cleavage metabolite (289) through an initial oxygenation on carbons 2 and 3 of the phenyl ring. Therefore it is likely that 2,3-dihydroxylated metabolite generated by U23A BPDO would be transformed to the 4-oxo-2-chromanecarboxylic acid using the four enzymatic steps of the biphenyl catabolic pathway. However, it is not clear how the 3,4-dihydroxylated metabolite was converted to this final metabolite. Trace amounts of a metabolite whose TMS derivative exhibited mass spectral features that were consistent with the 2-hydroxy(4-oxo-2-chromane) acetaldehyde or the 4-oxo-2-chromane acetic acid was detected. Diagnostically important ions were observed at m/z 278 (M^+), 263 (M^+-CH_3), 147 ($M^+-TMS-O-CH-CH$) (not shown). This metabolite is likely to be generated from the cleavage of the 3,4-dihydroxylated metabolite. However, it is not clear what are the enzymes involved in the ring cleavage and in the oxidation of the aliphatic chain to generate the 4-oxo-2-chromanecarboxylic acid.

3.8.5. Induction of U23A biphenyl catabolic enzymes by flavanone

Since flavanone alone was unable to serve as growth substrate for strain U23A, we verified if this chemical could induce the biphenyl catabolic enzymes when the cells were grown cometabolically on sodium acetate plus flavanone. The resting cells assay described in the “Materials and methods” section was performed to determine the effect of growing cells cometabolically on sodium acetate plus variable concentrations of flavanone on the ability of *R. erythropolis* U23A to convert 4-chlorobiphenyl to 4-chlorobenzoate. By growing the cells cometabolically on sodium acetate plus flavanone and collecting them after overnight growth (late log phase) we were reproducing the conditions that were used to prepare the cells grown on root exudates. Under these conditions flavanone was metabolized during growth on sodium acetate to generate principally 4-oxo-2-chromanecarboxylic acid (not shown). When

cells were grown overnight on MM30 containing sodium acetate alone and tested for their ability to metabolize 4-chlorobiphenyl, only traces of 4-chlorobenzoate were detected in the assay medium after 2 h of incubation. However, cells grown cometabolically on sodium acetate plus flavanone metabolized 4-chlorobiphenyl to 4-chlorobenzoate and the amounts of 4-chlorobenzoate produced varied depending on the amount of flavanone added to the growth medium (**Figure 3.4**). Cells grown in the presence of 1 mM flavanone produced significantly more 4-chlorobenzoate than those grown on 0.01 mM. However, it is noteworthy that in spite of the fact that flavanone was metabolized and its concentration decreased during growth on sodium acetate, cells grown in medium containing as little as 10 or 1 μ M flavanone produced more chlorobenzoate than the control without flavanone. Cells grown on sodium acetate plus biphenyl responded similarly to those grown on sodium acetate plus flavanone, where the catabolic activity of overnight grown cells toward 4-chlorobiphenyl decreased as the level of biphenyl was lowered in the medium (**Figure 3.4**). However, the amount of 4-chlorobenzoate produced by the cells grown in the presence of flavanone was in the same range and even higher than for those grown in the presence of biphenyl.

Together, the data provided strong evidence for the ability of the root exudates to promote PCB degradation, which can be attributed to the capacity of flavanone (and perhaps other unidentified phenylpropanoids) to serve as inducer of U23A biphenyl catabolic pathway. Flavanone was unable to serve as growth substrate, most likely because the chromane-4-one portion was not metabolized. However, the data show that the flavonoids, (especially flavanone found in the exudates) are metabolized by the enzymes of the biphenyl catabolic pathway and can serve as inducers of the biphenyl catabolic pathway. The exudates components supporting cell growth could not be identified but could be anyone of the many peaks, including glycosylated compounds, sugars and/or amino acids that are likely to be present in exudates.

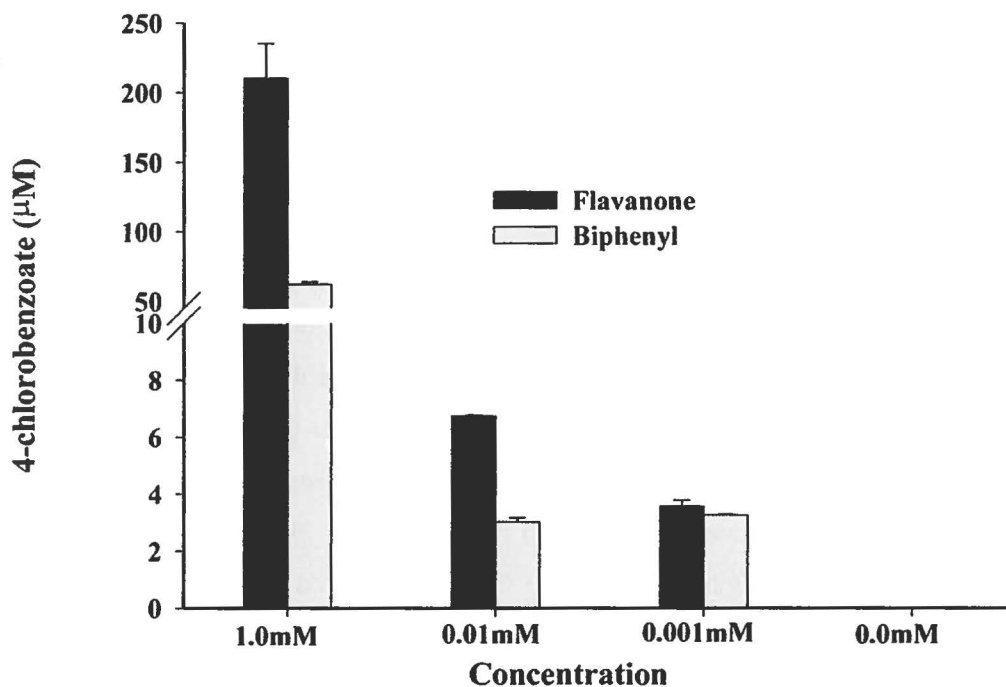


Figure 3.4: Amount (micromolar) of 4-chlorobenzoic acid produced when standardized resting cell suspensions of *R. erythropolis* U23A were incubated with 1,250 μ M 4-chlorobiphenyl for 2 h. *R. erythropolis* was previously grown overnight at 28 °C in MM30 amended with 30 mM acetate or with 30 mM acetate plus the indicated concentrations of flavanone or of biphenyl. Bars represent mean ($n=2$) and SD are shown. The protocol for the standardized 4-chlorobiphenyl assay is described in the Materials and methods.

3.8.6. Motility, binding, and colonization assays

In order to assess the ability of *R. erythropolis* U23A to colonize plant roots, we have examined some of the traits that are normally associated with bacterial adhesion to surface, formation of biofilm, and colonization of plant roots. In this respect, when 500 μ l of a cell suspension of strain U23A adjusted to 0.5 OD_{600 nm} was mixed with 500 mg of sand, $30 \pm 2\%$ of cells remained associated to the sand fraction which was much higher than the $8 \pm 1\%$ of *P. fluorescens* F113 cells. On the other hand, when the same cell suspensions of strain U23A

were mixed with an equal amount of mineral oil (MATH assay), $52 \pm 4\%$ cells remained associated to the oil fraction compared to $98 \pm 8\%$ of strain F113 cells that remained in the hydrocarbon fraction. The cell surface of strain U23A was quite hydrophobic in the MATH assay since 50% of the cells remained associated with the hydrocarbon fraction, although this was to a lesser extent than cells from strain F113, which is a well-characterized Gram-negative root colonizer (32).

Notably, *R. erythropolis* U23A exhibited a chemotactic response to root exudates, which was significantly stronger than that of the positive control using tryptone (**Figure 3.5**). No chemotaxis movement was observed in presence of water (negative control; results not shown). Finally, as shown on **Figure 3.6**, although *R. erythropolis* U23A did not colonize alfalfa roots as well as the well-characterized *P. fluorescens* F113 strain, the number of cells associated to the plant roots fraction (5.7×10^5 CFU g⁻¹) compared to the sand fraction (4.5×10^4 CFU g⁻¹) was high enough for strain U23A to conclude that this strain can either colonize the roots or adhere to them.

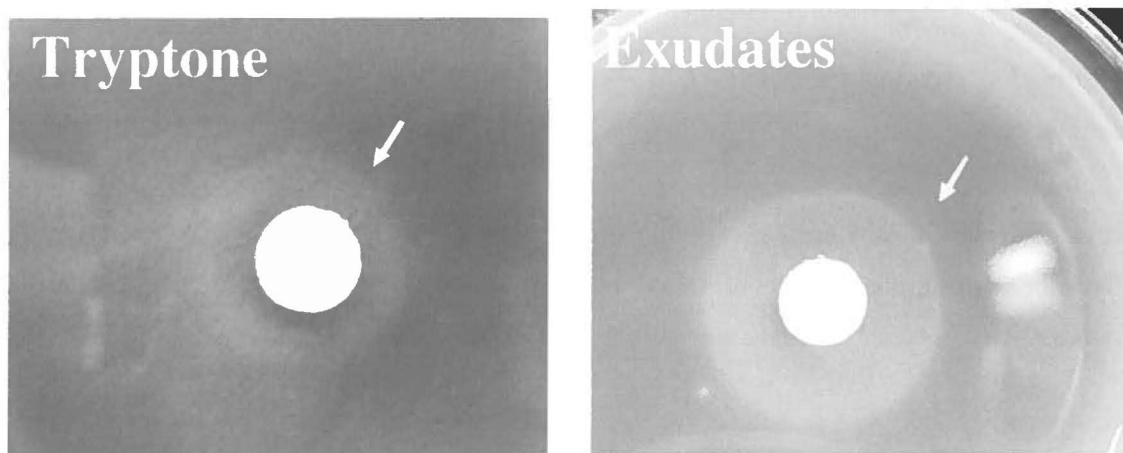


Figure 3.5: Chemotaxis movement of *R. erythropolis* U23A towards a filter paper soaked with 1% tryptone (positive control; left) or *A. thaliana* root exudates (concentrated 15 times; right) as indicated by the white arrows. The bacterial suspension was adjusted to OD_{600nm} of 5 in a phosphate buffered saline solution containing 0.1% agar.

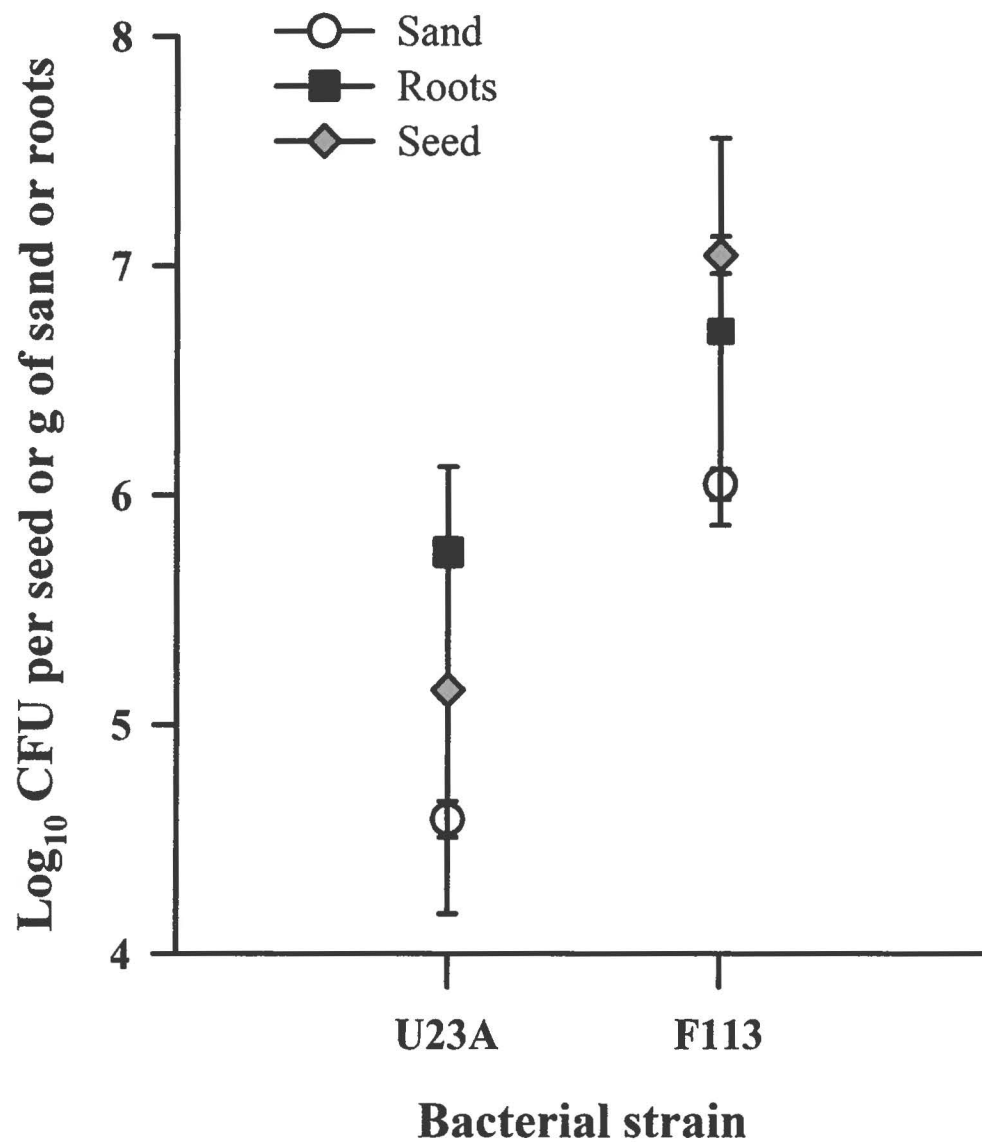


Figure 3.6: Number of CFUs of *R. erythropolis* U23A or *P. fluorescens* F113 remaining in sand or associated to roots of *M. sativa* (alfalfa) after 4 weeks growth in vitro. The experimental conditions are described in the Materials and methods; CFUs are expressed per unit of seed or per g of roots or sand. Mean (n=3) and SE are shown.

3.9. Discussion

Rhizoremediation is becoming increasingly popular as a means to treat soils contaminated with xenobiotics such as PCBs (49, 76, 313, 339). Several reports have provided evidence that plants promote the bacterial PCB degradation in soil (41, 54, 173, 216). However, the mechanism by which plants associate with rhizobacteria to remove the contaminants in the soil is poorly understood. Understanding how plants stimulate the bacterial degradation of pollutants in soil will help design novel approaches for soil remediation. Here we have isolated and characterized a rhodococcal rhizobacterium whose PCB-degrading pathway was shown to be triggered by root exudates components.

The presence of *bphA* encoding for the large subunit of BPDO's oxygenase component and its ability to transform 4-chlorobiphenyl into 4-chlorobenzoate are lines of evidence that *R. erythropolis* U23A metabolizes PCB congeners and flavanone through the biphenyl catabolic pathway. The detection of 2-(dihydro-dihydroxy-phenyl) chromane-4-ones and 4-oxo-2-chromanecarboxylic acid in resting cell assay performed with biphenyl-induced cells provided strong evidence that flavanone was metabolized by the unique BPDO found in strain U23A and most likely by the other three enzymes of the biphenyl catabolic pathway.

Other *R. erythropolis* strains have previously been shown to carry the *bph* gene cluster (237, 361, 362). However, sequence analysis of U23A *bphA* shows that the dioxygenase that initiates the catabolic pathway is closely related to that of *R. globerulus* P6, which is distinct from those of previously described *R. erythropolis* PCB-degrading strains. Because of the similarity between the BPDO of strains P6 and U23A, it was expected that both strains would degrade the same range of PCB congeners. This was confirmed since the pattern of PCB congeners degraded by biphenyl-induced *R. erythropolis* U23A cells (inability to metabolize 2,2'-dichlorobiphenyl or 2,2',5,5'-tetrachlorobiphenyl and ability to metabolize 3,3'-dichlorobiphenyl and 2,2',3,3'-tetrachlorobiphenyl) is identical to the one previously reported by Bedard et al. (1986) (25) for *Corynebacterium* strain MB1 (later reclassified and renamed as *R. globerulus* P6) (13).

Many species belonging to the *Rhodococcus* genus are known to degrade PCBs (12, 279, 351). Chlorobenzoate degradation by *R. erythropolis* strain S-7 and *Rhodococcus* sp. R04 has also been reported previously (45, 362, 366, 367). However, unlike these strains,

U23A was unable to metabolize 4-chlorobenzoate produced from 4-chlorobiphenyl and it was unable to metabolize 4-oxo-2-chromanecarboxylic acid derived from flavanone.

Being non-flagellated, *R. erythropolis* U23A is not expected to be motile, which is an important trait for root colonization (181). However, our data show that the strain was able to colonize (or at least to adhere) the roots of alfalfa, as well as to move towards a disk soaked with a solution containing root exudates in a chemotaxis assay. Motility is traditionally associated with bacteria that possess flagella and/or pili that confer them the ability to swarm (147) or to move by swimming or twitching (226), thus giving them the potential to colonize plant roots. Rhodococci are not flagellated and there is no evidence indicating that they possess pili on their surface. However, we cannot exclude the possibility that *R. erythropolis* U23A is able to move by gliding, as reported for other bacteria that lack flagella (139), or by sliding, as reported for a *Pseudomonas aeruginosa* mutant lacking both pili and flagella (212).

On the other hand, the binding capacity of *R. erythropolis* in the MATH test indicated that the hydrophobicity of this strain is in the same range as found for *R. erythropolis* strain CCM 2595 in a similar assay (188). Although the role of cell surface properties on microbial adhesion to surface is not clearly understood, surface hydrophobicity appears as an important factor (250). In the case of strain U23A, hydrophobicity might facilitate aggregation on or around plant roots.

An important finding in this work is that cells of strain U23A grown in a medium containing *Arabidopsis* root exudates as sole growth substrate could metabolize 3,3'-dichlorobiphenyl, 2,3,4'-trichlorobiphenyl and 2,3',4-trichlorobiphenyl more efficiently than cells grown on LB medium or on MM30 with sodium acetate as sole growth substrate (see **Table 3.2**). This suggests that root exudates contain components not present in LB medium that can trigger (or induce) the expression of *bph* genes. The inability of cells grown on root exudates to degrade all the congeners that are degraded by biphenyl-induced cells is most likely due to the very low expression of the biphenyl catabolic genes in the PSM-induced cells. The first enzyme of the *bph* pathway, the three-component BPDO, determines which PCBs are at least partially transformed by the microorganism (206). In a previous investigation with a reconstituted purified BPDO preparation, dihydroxylation of the more resistant congeners, such as 2,2'-dichlorobiphenyl, was only detected when the levels of

enzyme components were high and optimized, i.e., when the proportions of the ferredoxin and ferredoxin-reductase were much higher than the oxygenase component (134). Although no explanation has yet been provided for this observation, it would explain why cells grown on root exudates only degraded the low and most labile congeners (4-chlorobiphenyl and 2,3',4-trichlorobiphenyl).

Our results indicated that flavanone, one of the major components of *A. thaliana* exudates, is an inducer of the biphenyl catabolic pathway. It is noteworthy to say that flavanone is not only an inducer of the biphenyl catabolic pathway, but is also metabolized by the biphenyl catabolic pathway. However, despite the ability of the biphenyl catabolic enzymes to metabolize flavanone, this compound could not support growth of strain U23A, most likely because of the inability of the cells to metabolize the 4-oxo-2-chromanecarboxylic acid. However, we cannot exclude an inhibitory effect of flavanone on one or more of the steps of the biphenyl assimilatory process since strain U23A was unable to grow in a culture medium containing biphenyl plus flavanone (results not shown). A similar inhibitory effect of phenylterpenoids was made by Gilbert and Crowley (103) where carvone, a terpenoid present in spearmint (*Mentha spicata*), was shown to promote the PCB-degrading ability of an *Arthrobacter* isolate. However, this terpene was toxic to this organism and it was unable to support its growth.

It has long been suspected that PSMs may allow the growth of bacteria in the rhizosphere as well as triggering their biphenyl pathway, resulting in enhanced PCB degradation (16, 62, 78, 172, 285). Recently, Leigh et al. (2006) (173) demonstrated that rhodococci isolates were associated with the roots of certain tree species (e.g. pine and willow) in a contaminated site, and that some of these isolates had strong PCB degradation potential. As highlighted by the authors, rhodococci seem to be able to use PSMs as growth substrate in soil (62, 119) and this feature might explain why they are well adapted to degrade PCBs. However, this hypothesis has not yet been demonstrated.

Although the interactions between *Actinobacteria* and plants and their effect on plant growth and bacterial metabolism has been much less documented than the interaction involving other bacterial groups (86), it is clear that many members of the *Actinobacteria* including members of the non-mobile genus *Streptomyces* have been associated to plant diseases or been used to control plant diseases. Our observation with strain U23A is

corroborated by the recent observation whereby *R. erythropolis* (MtCC 7905) (331) was shown to exhibit plant growth promoting activity. In addition to its plant growth promoting ability, strain MtCC 7905 was also shown to be a useful chromate-reducing bacterium in soil. Therefore, our data strongly support the idea that Gram-positive rhodococci may play an active role in the rhizosphere microbiota.

This is strengthened by the fact that flavanone induces the biphenyl catabolic enzymes of *R. erythropolis* U23A and is metabolized by this pathway. In a previous metabolomic analysis of *A. thaliana* exudates, 125 PSMs were identified (216), 76% of which belonged to the phenylpropanoid class of compounds. Therefore, flavanone might not be the sole exudate component to exert an inducing effect on the biphenyl catabolic enzymes. However, by singling out flavanone, our study clearly shows that although each single component of root exudates cannot support growth, individually, some of the exudates components can serve as inducer of this pathway. de Lorenzo and Pérez-Martin (50) have introduced the notion of fortuitous inducers to explain why several substrate analogs can induce catabolic pathway enzymes. Traditionally, the level of induction obtained from fortuitous inducers is significantly lower than for the natural substrate of the pathway. However, it is quite intriguing that during cometabolic growth, flavanone was found to be as efficient as biphenyl to induce the biphenyl catabolic pathway enzymes and that flavanone phenyl ring was metabolized completely by this pathway.

The ability of the biphenyl catabolic enzymes to metabolize flavanone and other flavonoids has been reported by several investigators (271, 276, 287, 289). Until now, these reactions were believed to be fortuitous and explained on the basis of the ability of the pathway enzymes to bind biphenyl analogs productively. However, on the basis of our investigation and others that provided evidence that PSMs act as inducers of the biphenyl catabolic enzymes (54, 62, 103, 119, 203, 294), the question can be raised whether this pathway plays a role in the maintenance or recycling of phenylpropanoids and phenylterpenoids in the rhizosphere.

Altogether, our results highlight the fact that even though *R. erythropolis* is considered a non-mobile bacterium, it still possesses several traits conferring the capacity to colonize (or grow on) plant roots surface (or in the rhizosphere). Our data do not allow us to distinguish between the increase in bacterial density in the rhizosphere that would be

associated to root colonization and growth promotion due to the presence of PSMs that promote growth of bacteria adhering to root surfaces. Further work will be required to clearly show that rhodococci can colonize plant roots. However, our data clearly show that strain U23A exhibits a chemotactic response to root exudates and that flavanone and perhaps other chemicals present in the root exudates can trigger the biphenyl catabolic enzymes. We can thereby propose a model for explaining how plants promote PCB degradation in soil. In the rhizosphere, labile chemicals such as the sugar moiety of the conjugated PSMs might provide a substrate on which to grow, whereas the flavonoids or other phenylpropanoids would then induce the biphenyl pathway of strain U23A. The ability of flavanone to act as strong inducer of the biphenyl pathway raises the question of whether this pathway plays a role in phenylpropanoid metabolism in soil. However, an important contribution of this process is the finding that flavanone triggers the metabolism of PCBs in soil.

3.10. Acknowledgements

This work was supported by grant STPSC 356996-07 from the Natural Sciences and Engineering Research Council of Canada. We thank Prof. David Dowling–Institute of Technology, Carlow, Ireland, who generously provided *Pseudomonas fluorescens* F113. We thank Prof. Martina Mackova–Prague Institute of Chemical Technology, Prague, Czech Republic for providing the PCB-contaminated soil used in this investigation. We also thank Inspec-Sol Inc., Montreal, Quebec, Canada, for providing an in-kind contribution to this work.

4. Presentation of article 2

4.1. The context of article 2

Article 1 showed that the root exudates of *A. thaliana* could support the growth of strain U23A and trigger its PCB-degrading ability. Several PSMs were found in the exudates, most of them are flavonoids, including flavanone, coumarin, naringenin, and others. Further investigations (not yet published) using commercially available flavonoids showed that flavanone and several other flavonoids which are present in *A.thaliana* root exudates induced the biphenyl catabolic pathway of strain U23A.

Strain U23A belongs to one of the three genetically distinct clusters of the biphenyl-degrading bacteria. It belongs to the group composed of the Gram-positive rhodococci. We pursue our study by verifying the hypothesis whereby each of these three clusters may respond differently to individual PSMs. To test this hypothesis, we further investigated the response of two other biphenyl-degrading bacteria to PSMs. Each of the selected bacterial strains *P. pnomenusa* B356 and *B. xenovorans* LB400 belongs to one of the other two phylogenetic groups of PCB-degrading bacteria, the Gram-negative group I and the Gram-negative group II.

On the other hand, flavonoids are known for their beneficial effects on human health with diverse physiological and pharmacological activities. Studies have shown that hydroxy-flavonoids have stronger activities than simple flavonoids. Hydroxy-flavonoids may be produced by chemical synthesis, but in some cases, the synthetic process requires many steps and it generates environmental contaminants. In this regard, biocatalysis is a promising way to overcome these drawbacks. BPDs are known to hydroxylate certain flavonoids and therefore they are interesting candidates.

In this study, we investigated the response of *P. pnomenusa* B356 and *B. xenovorans* LB400 toward certain commercially available flavonoids. The study also investigated the ability of BPD_{B356} and BPD_{LB400} to transform these flavonoids. We identified the metabolites generated from these flavonoids and we determined the kinetic parameters of the enzymatic reactions. The fact that each strain responded differently to the tested flavonoids supported our hypothesis whereby each of the genetically distinct PCB-degrading bacterial cluster may have evolved divergently to play distinct ecophysiological role with respect to the metabolism of PSMs in soil. The results were presented in **Article 2**, which was published in **Applied and Environmental Microbiology**.

4.2. Contribution of the student to article 2

Results presented in this article were obtained principally by the student. She has planned and performed the following experimental works: 1- the whole-cell assays to determine the ability of the two bacterial strains to metabolize flavanone and the assay to examine the potential of each flavonoid to induce the biphenyl catabolic pathway; 2- the production of the purified BPDOs preparation; 3- the identification of the metabolites produced from the tested PSMs by GC-MS analysis; 4- the experiment to determine the kinetic parameters. The major discovery is that strain B356 BPDO metabolizes flavanone very efficiently and this PSM is a very good inducer of the biphenyl catabolic pathway of strain B356. The docking experiments, in this work, were done by Youbin Tu (postdoct) and the structural analyses were done by Michel Sylvestre. The article was prepared by the student and Michel Sylvestre. Youbin Tu verified the portion of the manuscript related to the docking experiment.

4.3. Article 2

Remarkable ability of *Pandoraea pnomenusa* B356 biphenyl dioxygenase to metabolize simple flavonoids

Thi Thanh My Pham, Youbin Tu and Michel Sylvestre[#]

Institut National de la Recherche Scientifique

INRS-Institut Armand-Frappier, Laval, QC H7V 1B7, Canada

Running title: Flavonoids metabolism by *Pandoraea pnomenusa* B356

[#]Corresponding author: Michel Sylvestre, Institut National de la Recherche Scientifique

(INRS-Institut Armand-Frappier), Laval, Québec, H7V 1B7, Canada.

450-687-5010; FAX: 450-686-5501; E-mail: Michel.Sylvestre@iaf.inrs.ca

References : **Pham, T. T. M., Tu, Y. B., and Sylvestre, M.** 2012. Remarkable ability of *Pandoraea pnomenusa* B356 biphenyl dioxygenase to metabolize simple flavonoids. Appl Environ Microb **78**:3560-3570.

4.4. Résumé

Plusieurs investigations ont fourni la preuve que les métabolites secondaires des plantes, particulièrement les flavonoïdes, peuvent servir de molécules de signalisation pour promouvoir la capacité des bactéries à dégrader les biphényles chlorés dans le sol. Cependant, les mécanismes responsables de cette action sont largement inconnus. Dans ce travail, nous avons découvert que BphAE_{B356}, la dioxygénase du biphényle/chlorobiphényle de *Pandoraea pnomenusa* B356, est significativement mieux adaptée pour métaboliser la flavone, l'isoflavone, et la flavanone que BphAE_{LB400} de *Burkholderia xenovorans* LB400. Contrairement à BphAE_{LB400}, les paramètres cinétiques de BphAE_{B356} envers ces flavonoïdes sont comparables à ceux du biphényle. En outre, de façon notable, l'isoflavone s'est avérée être un inducteur efficace de la voie catabolique du biphényle de la souche B356, tandis qu'aucun des trois flavonoïdes n'a induit la voie catabolique de la souche LB400. Des expériences de modélisation réalisées en remplaçant le biphényle par l'un ou l'autre de ces flavonoïdes dans la structure tridimensionnelle de BphAE_{B356} liée au substrat, ont montré que la capacité supérieure de BphAE_{B356} comparé à BphAE_{LB400} est principalement attribuable au remplacement de Phe336 de BphAE_{LB400} par Ile334 et de Thr335 de BphAE_{LB400} par Gly333 de BphAE_{B356}. Cependant, une comparaison des caractéristiques biochimiques et structurales de BphAE_{B356} avec celles de BphAE_{p4}, un double mutant Phe336Met et Thr335Ala de BphAE_{LB400}, qui a été obtenu dans un travail précédent, indique que d'autres résidus ou caractéristiques structurales de BphAE_{B356} dont l'identification n'a pu être établie de façon précise par les expériences de modélisation, sont également responsables des capacités catalytiques supérieures de BphAE_{B356}. Ensemble, ces données fournissent des preuves appuyant l'hypothèse selon laquelle les voies cataboliques du biphényle ont évolué de manière divergente chez les protéobactéries, où certaines d'entre elles ont acquis la possibilité de remplir des fonctions écologiques liées au métabolisme des métabolites secondaires des plantes dans le sol.

4.5. Abstract

Many investigations have provided evidence that plants secondary metabolites, especially flavonoids, may serve as signal molecules to trigger the abilities of bacteria to degrade chlorobiphenyls in soil. However, the bases for this interaction are largely unknown. In this work, we found that BphAE_{B356}, the biphenyl/chlorobiphenyl dioxygenase from *Pandoraea pnomenusa* B356, is significantly better fitted to metabolize flavone, isoflavone, and flavanone than BphAE_{LB400} from *Burkholderia xenovorans* LB400. Unlike those of BphAE_{LB400}, the kinetic parameters of BphAE_{B356} toward these flavonoids were in the same range as for biphenyl. In addition, remarkably, the biphenyl catabolic pathway of strain B356 was strongly induced by isoflavone, whereas none of the three flavonoids induced the catabolic pathway of strain LB400. Docking experiments that replaced biphenyl in the biphenyl-bound form of the enzymes with flavone, isoflavone or flavanone showed that the superior ability of BphAE_{B356} over BphAE_{LB400} is principally attributable to the replacement of Phe336 of BphAE_{LB400} by Ile334 and of Thr335 of BphAE_{LB400} by Gly333 of BphAE_{B356}. However, biochemical and structural comparison of BphAE_{B356} with BphAE_{p4}, a mutant of BphAE_{LB400} which was obtained in a previous work by the double substitution Phe336Met Thr335Ala of BphAE_{LB400}, provided evidence that other residues or structural features of BphAE_{B356} whose precise identification the docking experiment did not allow are also responsible for the superior catalytic abilities of BphAE_{B356}. Together, these data provide supporting evidence that the biphenyl catabolic pathways have evolved divergently among proteobacteria, where some of them may serve ecological functions related to the metabolism of plants secondary metabolites in soil.

4.6. Introduction

Aryl hydroxylating Rieske-type dioxygenases (ROs) catalyze a *cis*-dioxygenation of aryl compounds to generate a *cis*-dihydrodiol metabolite. ROs are promising biocatalysts that metabolize many substituted benzene or diphenyl rings as well as bicyclic- or tricyclic-fused heterocyclic aromatics such as quinoline, dibenzofuran, phenanthridine and flavonoids (29, 44, 142, 201, 271, 277, 288). The biphenyl dioxygenase (BPDO) which catalyzes the first reaction of the bacterial biphenyl catabolic pathway is a RO that has been extensively studied because of its ability to metabolize several PCB congeners. BPDO reaction (**Figure 4.1**) requires three components (111, 128, 129). The catalytic component (BphAE) is a RO protein which is a hetero hexamer made up of three α (BphA) and three β subunits (BphE). The ferredoxin (BphF) and the ferredoxin reductase (BphG) are involved in electron transfer from NADH to BphAE. The encoding genes for both *Burkholderia xenovorans* LB400 and *Pandoraea pnomenusa* B356 are *bphA* (BphAE α subunit), *bphE* (BphAE β subunit), *bphF* (BphF) and *bphG* (BphG) (70, 314). The α subunit is the one involved in the catalytic activity. It comprises two domains; the Rieske domain containing a 2Fe-2S Rieske cluster receives the electrons from BphF and transfers them to the catalytic mononuclear iron center of the catalytic domain (75).

Several investigations have shown that BPDO can metabolize flavonoids (44, 142, 271, 277). These PSMs are regarded as very promising for the prevention and treatment of cancers (218) and cardio-vascular diseases (301). Plants are currently the major source for these chemicals, but the synthesis of novel derivatives exhibiting improved biological properties is often difficult or impractical (201). Furthermore, in the context of the green chemistry concept, new, more selective and more environmentally friendly approaches to manufacture these biologically specific fine chemicals will be required.

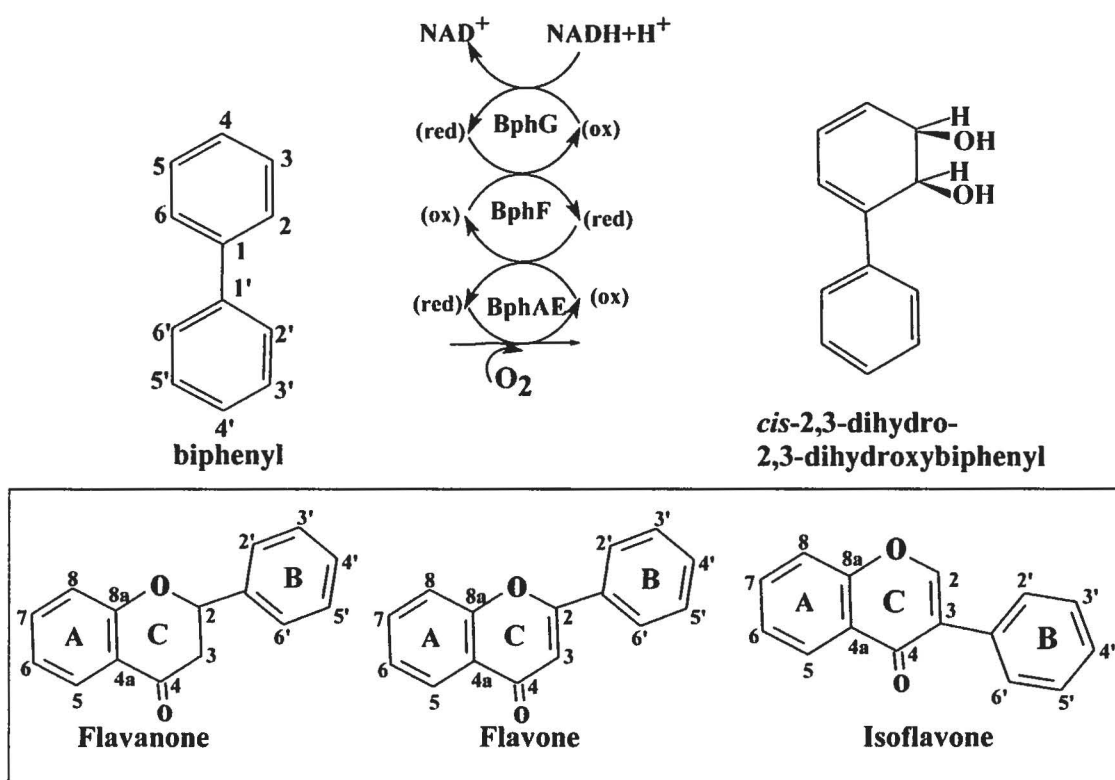


Figure 4.1: BPDO reaction (upper) and structures of flavanone, flavone and isoflavone (lower).

Seeger et al. (2003) (271) have shown that *B. xenovorans* LB400 BPDO (BphAE_{LB400}) is able to dihydroxylate several isoflavonoids on ring B. BphAE_{LB400} has been extensively investigated because it is regarded as one of the most efficient dioxygenase of natural origin for the degradation of a wide range of chlorobiphenyls. However, in recent years, *P. pnomenusa* B356 BPDO (BphAE_{B356}) was shown to exhibit superior abilities to degrade several biphenyl analogs, including 2,6-dichlorobiphenyl, 2,4,4'-trichlorobiphenyl and DDT, that BphAE_{LB400} metabolizes poorly (106, 169). Furthermore, preliminary unpublished experiments have suggested that BphAE_{B356} metabolizes flavonoids more efficiently than BphAE_{LB400}. On the other hand, a mutant of BphAE_{LB400}, BphAE_{p4} an evolved BPDO derived from BphAE_{LB400} by the substitutions Thr335Ala Phe336Met was

shown to metabolize a broader range of chlorobiphenyls and dibenzofurans than the parent BphAE_{LB400} (21). The new catalytic properties of this mutant were attributed to the single Thr335Ala substitution. Thr335 exerts constraints on a segment comprised of Val320-Gln322 that lines the catalytic pocket. Replacing Thr335 with Ala releases the constraints on this segment allowing for more movement during substrate binding (165, 206).

The bacterial metabolism of flavonoids may also impact on soil microbiology and on plant-microbe interactions. Many investigations have provided evidence that PSMs may act as signal molecules to trigger the PCB degrading abilities of soil bacteria (for a review, see reference (293)). These signal molecules may have a major impact on the success of the rhizoremediation processes aiming at the destruction of PCBs in soil. However, the bases for the PCB-degrading bacteria-PSM interactions are largely unknown. In a recent work (330) we showed that *A. thaliana* root exudates trigger the PCBs catabolic abilities of *R. erythropolis* U23A, a rhodococcal rhizobacteria isolated from the rhizosphere of PCB-contaminated plants roots. Flavanone, one of the major component of these root exudates was unable to support the growth of strain U23A, but it was metabolized by this strain through its biphenyl catabolic pathway (330). In addition, when used as a cosubstrate with sodium acetate, flavanone was as efficient as biphenyl to induce the biphenyl catabolic pathway of strain U23A (330). These observations are consistent with the proposed hypothesis whereby flavonoids would act as a signal molecule in soil to modulate the quantity and quality of phenylpropanoids in the rhizosphere (285).

Given the significant impacts the bacterial metabolism of flavonoids may have on green chemistry and on PCB-remediation processes and given the preliminary data showing that the two well-characterized *P. pnomenusa* B356 and *B. xenovorans* LB400 BPDOs metabolized flavonoids differently, we compared the catalytic properties of BphAE_{LB400} and BphAE_{B356} toward the simple flavonoids flavone, isoflavone and flavanone and we assessed the ability of these flavonoids to induce the biphenyl catabolic pathway of these two organisms. In order to get more insights about structural features of BphAE conferring the ability to metabolize these flavonoids, we also docked these chemicals in these protein structures and compared the structure of the docked enzymes with that of BphAE_{p4}.

4.7. Materials and methods

4.7.1. Bacterial strains, plasmids, and chemicals

Wild-type strains *P. pnomenusa* B356 and *B. xenovorans* LB400 were described previously (19, 70). All plasmids used in this study were described previously. pET14b[LB400-*bphAE*] and pET14b[*p4-bphAE*] carry the genes encoding the wild-type BphAE_{LB400} and its mutant BphAE_{p4} (Thr335Ala/Phe336Met) (21, 163), plasmid pET14b[B356-*bphAE*] carries the genes encoding BphAE_{B356} (169) and plasmid pET14b[LB400-*bphF*] and pET14b[LB400-*bphG*] carry the genes encoding strain LB400 BphF and BphG (206). Flavone and flavanone were from Sigma-Aldrich and isoflavone from Indofine Chemical Company Inc. They were all 99% pure.

4.7.2. Whole-cell assays to determine the ability of *P. pnomenusa* B356 and *B. xenovorans* LB400 to metabolize flavanone

The metabolism of flavanone by resting-cell suspensions of biphenyl-induced cells of *P. pnomenusa* B356 and *B. xenovorans* LB400 was examined according to a protocol described previously to investigate the metabolism of flavanone by *R. erythropolis* U23A (330). Briefly, each strain was grown overnight on medium MM30 (330) containing 3.4 mM biphenyl, the cells were harvested, washed and suspended in M9 medium (330) with no carbon source to an OD_{600nm} of 5. This cell suspension was distributed (5-ml amounts) among 50-ml glass tubes and flavanone was added to a final concentration of 200 µM. The resting-cell suspensions were incubated at either 28 °C or 15 °C for periods of between 5 min and 18 h. They were then extracted with ethyl acetate, the organic phase was evaporated and the residues were treated with *n*-Butylboronate (*n*BuB) or *N,O*-bis(trimethylsilyl)trifluoroacetamide (BSTFA) as described previously for gas chromatography-mass spectrometry (GC-MS) analyses (330).

4.7.3. Assays to identify the metabolites produced from flavone, flavanone, and isoflavone by *BphAE*_{B356}, *BphAE*_{LB400} and *BphAE*_{p4}, and to determine their kinetics parameters

Reconstituted His-tagged BPDO preparations were used in the experiments to identify the metabolites and kinetics of the enzymes and substrates. His-tagged purified enzyme components were produced in recombinant *Escherichia coli* strains and purified according to published protocols (206). The enzyme assays were performed at 37 °C as described previously in a volume of 200 µl in 50 mM MES buffer, pH 6.0, containing 100 nmol of substrate (129). The metabolites were extracted at pH 6.0 with ethyl acetate and treated with *n*BuB or BSTFA for GC-MS analyses.

Catalytic activities were determined by monitoring substrate depletion and metabolite production after 10 min incubation under the conditions described above. GC-MS peak areas were used to quantify substrate depletion and metabolite production. GC-MS analyses were performed using a Hewlett Packard HP6980 series gas chromatograph interfaced with an HP5973 mass selective detector (Agilent Technologies). The mass selective detector was operated in EI ionization mode and used a quadrupole mass analyzer. The steady-state kinetic parameters of all *BphAE*s were determined by recording oxygen consumption rates using a Clarke-type Hansatech model DW1 oxygraph (134) for various concentrations of flavonoids varying between 5 and 150 µM. The kinetic parameters reported in this work were obtained from the analysis of at least two independently produced preparations tested in triplicate.

4.7.4. Assays to assess the ability of flavone, flavanone, and isoflavone to induce the biphenyl catabolic pathway of strains *B356* and *LB400*

The induction of the biphenyl catabolic pathway of strains *B356* and *LB400* was assessed on the basis of the amount of 4-chlorobenzoate produced from 4-chlorobiphenyl by resting cell suspensions previously grown on sodium acetate plus variable concentrations of flavonoids or biphenyl. This assay was performed according to the same method as the previously described assay to assess the ability of flavanone to induce the biphenyl catabolic pathway of *R. erythropolis* U23A (330). Briefly, cells were grown overnight in medium MM30 amended with 30 mM sodium acetate or with 30 mM sodium acetate plus variable amounts (6 mM, 1 mM, 0.01 mM or 0.001 mM) of flavone, isoflavone, flavanone, or

biphenyl. Cells were harvested and washed in M9 medium without carbon source. The suspensions were adjusted to OD_{600nm} of 1 with M9 medium and distributed in portions of 200 µl into 1.5-ml Eppendorf tubes. 4-Chlorobiphenyl was added to a final concentration of 1.25 mM and the reaction vials were incubated for 120 min at 28 °C in an Eppendorf thermomixer 5436. The suspensions were then acidified with HCl before the metabolites were extracted with ethyl acetate. The extracts were evaporated, and the residues were derivatized with BSFTA for GC-MS analysis (330).

4.7.5. Docking and structure analysis

BphAE_{LB400} (RCBS Protein Data Bank PDB entry 2XRX), BphAE_{B356} (RCBS Protein Data Bank PDB entry 3GZX) and BphAE_{p4} (RCBS Protein Data Bank PDB entry 2XSH) were used as protein targets, and they were prepared as previously described (169). In the case of BphAE_{LB400} and BphAE_{p4}, we used the structural coordinates of dimer AB for the docking. Ligands were all downloaded as sdf files from pubchem (<http://pubchem.ncbi.nlm.nih.gov>) and converted into pdb format in Discover Studio Visualizer 2.5. Both proteins and ligands were processed with AutoDockTools to obtain their proper pdbqt format. The searching space for the ligand was centered on the mononuclear iron and contained 20 Å in each x, y, and z direction. Autodock Vina 1.1.2 (209) with the default parameters was used to perform the automatic docking.

4.8. Results

4.8.1. Metabolism of flavanone by biphenyl-induced resting cells of strains B356 and LB400

In a previous report, we showed that although flavanone could not support the growth of *R. erythropolis* U23A, biphenyl-induced cells of strain U23A metabolized this plant metabolite (330). The induced cells of strain U23A produced small amount of 2-(2,3-dihydro-2,3-dihydroxyphenyl)chromane-4-one and 2-(3,4-dihydro-3,4-dihydroxyphenyl)chromane-4-one when they were incubated in the presence of flavanone, but the major and ultimate metabolite exhibited mass spectral features corresponding to those of 4-oxo-2-chromanecarboxylic acid (330). Neither strain B356 nor strain LB400 could grow on flavone, isoflavone, or flavanone but biphenyl-induced cells of both converted flavanone to 4-oxo-2-chromanecarboxylic acid as a dead-end metabolite. 4-Oxo-2-chromanecarboxylic acid was identified from the mass spectral features of its TMS derivative which exhibited diagnostically important ions at m/z 264 (M^+), 249 ($M^+ - CH_3$), 219 ($M^+ - 3CH_3$), 205 ($M^+ - CH_3 - O - CO$), 174 ($M^+ - COOTMS$), 131 ($M^+ - COOTMS - O$).

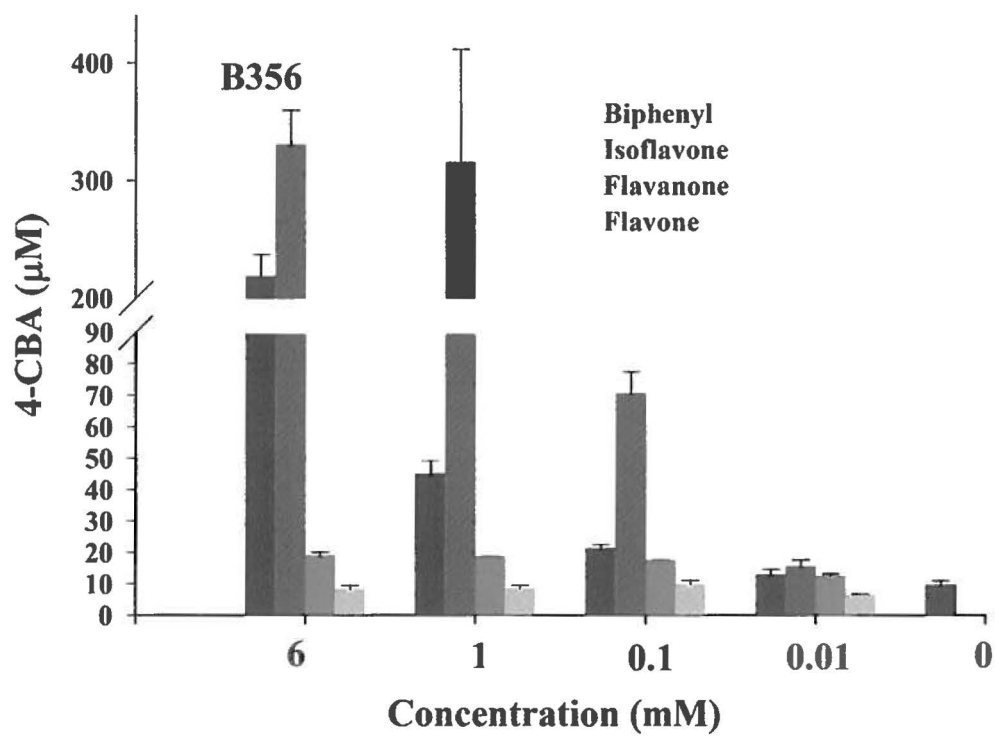
When the resting cell suspensions of strain B356 were incubated at 15°C and for less than 5 min, in addition to 4-oxo-2-chromanecarboxylic acid, small amounts of 2-(2,3-dihydro-2,3-dihydroxyphenyl)chromane-4-one and 2-(3,4-dihydro-3,4-dihydroxyphenyl)chromane-4-one were detected. These two metabolites were identified on the basis of their GC-MS spectral features as described below for the purified enzyme preparation. When the resting cells were incubated at higher temperature, and for longer incubation periods, 4-oxo-2-chromanecarboxylic acid was the only metabolite detected in the culture. This shows that the biphenyl catabolic enzymes of this organism were very efficient in transforming flavanone to 4-oxo-2-chromanecarboxylic acid. In addition, while cells of strain B356 metabolized more than 80% of the added substrate within 5 min at 15 °C, cells of strain LB400 metabolized less than 20% of the substrate when they were incubated for 1 h at 28 °C. This shows the superiority of strain B356 over strain LB400 in metabolizing flavanone.

4.8.2. Induction of the biphenyl catabolic pathway of strain B356 and LB400 by flavonoids

Flavanone induction was assessed by monitoring the 4-chlorobenzoate produced from 4-chlorobiphenyl which, in both strains B356 and LB400, accumulates as dead-end metabolite of the biphenyl catabolic pathway. In a recent report, it was shown that the biphenyl catabolic genes are expressed constitutively at low level during growth of *B. xenovorans* LB400 on succinate (232). Furthermore, the level of expression of the pathway enzymes appeared to be influenced by post-transcriptional regulation factors and by the physiological state of the cells which may significantly influence the chlorobiphenyl degradation abilities of cells (232). In spite of these difficulties, we reasoned that the assay monitoring 4-chlorobenzoate should allow us to determine if strains B356 and LB400 respond similarly to the presence of simple flavonoids during growth on sodium acetate and if the enzymes of the upper biphenyl catabolic pathway are induced by flavonoids.

When cells of strain B356 were grown on sodium acetate alone, small amounts of chlorobenzoate were produced in the growth medium (**Figure 4.2A**). However, when cells were grown in the presence of sodium acetate plus variable amounts of biphenyl, the amount of 4-chlorobenzoate varied depending on the amount of biphenyl added to the culture medium (**Figure 4.2A**). This response was similar to that observed for strain U23A grown in the presence of sodium acetate plus biphenyl (330). Cells of strain LB400 grown on sodium acetate alone produced slightly larger amounts of 4-chlorobenzoate than cells of strain B356 and the addition of biphenyl in the growth medium did not induce the biphenyl catabolic enzymes as strongly as for strain B356 (**Figure 4.2B**).

A



B

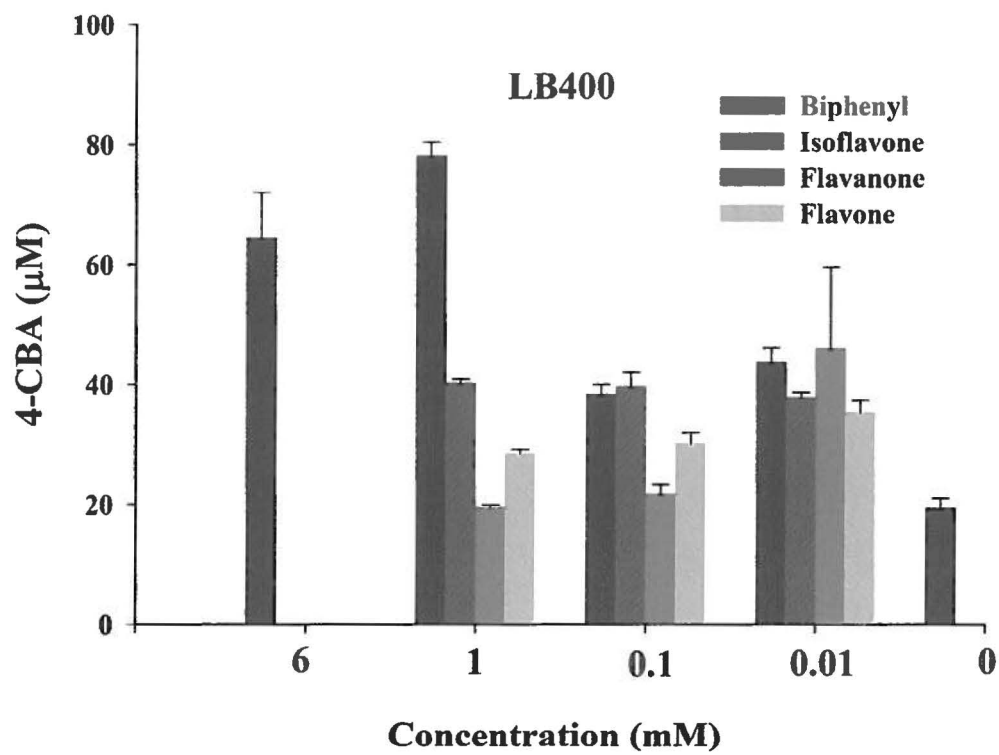


Figure 4.2: (A) Amounts (μM) of 4-chlorobenzoic acid (4-CBA) produced when standardized resting cell suspensions of strain B356 were incubated with 1,250 μM 4-chlorobiphenyl for 2 h. (B) Amounts (μM) of 4-CBA produced when standardized resting cell suspensions of strain LB400 were incubated with 1,250 μM 4-chlorobiphenyl for 2 h. Each strain was previously grown overnight at 28 °C in MM30 medium amended with 30 mM sodium acetate or with 30 mM sodium acetate plus the indicated concentrations of the indicated flavonoid or of biphenyl. Bars represent mean ($n=2$) and standard deviations. The protocol for the standardized 4-chlorobiphenyl assay is described in the Materials and Methods.

When strain B356 was grown on sodium acetate plus flavanone, for concentrations ranging between 1 mM and 0.01mM, the amount of 4-chlorobenzoate produced during the assay was not significantly higher than for cells grown on sodium acetate alone (**Figure 4.2A**). Similar results were obtained when cells were grown on sodium acetate plus flavone. However, remarkably, the amounts of 4-chlorobenzoate produced from 4-chlorobiphenyl by resting cells grown on sodium acetate plus isoflavone were significantly higher than those produced for cells grown on sodium acetate plus biphenyl (**Figure 4.2A**). We cannot exclude the possibility that post-transcriptional regulation mechanisms exerted by biphenyl metabolites be responsible for the lower enzyme activity found in cells grown on sodium acetate plus biphenyl. Furthermore, since all three flavonoids are metabolized by whole cells of strain B356, we must exclude the possibility that permeation of flavonoids across the cell membrane/wall had affected the cell activity for substrate. Therefore, data show that isoflavone is a good inducer of the biphenyl catabolic enzymes of strain B356. In the case of strain LB400, there was no clear-cut effect for any of the three tested flavonoids that would demonstrate the ability of these flavonoids to induce the biphenyl catabolic pathway. The amounts of 4-chlorobenzoate produced varied slightly in presence of flavonoids (**Figure 4.2B**), but the amounts produced were not statistically significantly different from those observed in absence of flavonoids. Therefore, none of the three flavonoids tested influenced significantly the activity of the biphenyl catabolic enzymes of strain LB400, whereas isoflavone was found to act as an inducer of the biphenyl catabolic pathway of strain B356 when it was added as cosubstrate with sodium acetate.

4.8.3. Metabolites produced from flavonoids by purified BphAE_{B356}, BphAE_{LB400}, and BphAE_{p4}

Since whole cells of strains B356 and LB400 metabolized flavanone differently, and since they responded differently to the presence of flavone, flavanone, and isoflavone in the growth medium, we have compared the ability of purified preparations of their BPDO to metabolize these three plant metabolites. The purified enzymes were prepared from recombinant *E. coli* cells as described in Materials and Methods. We have also included BphAE_{p4}, a Thr335Ala Phe336Met mutant of BphAE_{LB400} exhibiting an expanded substrate range compared to its parent enzyme (21, 165). In a previous report, we showed that replacing Phe336 of BphAE_{LB400}, which lines the catalytic pocket, with a residue with a smaller side chain (Met336) increases the space inside the catalytic pocket. In a similar manner, the corresponding Ile334 of BphAE_{B356} that lines the catalytic pocket is smaller than Phe336 of BphAE_{LB400} and, thus, allows the enzyme to metabolize bulkier substrates such as DDT (169). Thr335 is far from the substrate; however, changing this residue to the smaller Ala335 relieves intramolecular constraints on Gly321 allowing for significant movement of this residue during substrate binding and thereby increasing the space available to accommodate bulkier substrates (169). In a manner similar to Ala335 of BphAE_{p4}, Gly333 (corresponding to Thr335 of BphAE_{LB400}) does not interact with Gly319 (corresponding to Gly321 of BphAE_{LB400}). Therefore, although the side chain of Ala335 and Gly333 differs, their effect on the enzyme's structure is likely to be comparable (165).

Based on GC-MS peak area of the remaining substrate, purified preparations of BphAE_{B356} incubated with 100 nmol flavanone oxidized more than 90 nmol of this substrate within 10 min. Under identical conditions, BphAE_{p4} metabolized approximately 20 nmol flavanone, and BphAE_{LB400} metabolized less than 10 nmol of this substrate (**Figure 4.3A**). Consistent with these results, the amount of metabolites generated by BphAE_{B356} after 10 min of incubation was significantly higher than for the two other enzymes (**Figure 4.3A**). In addition, the pattern of metabolites generated by the three enzymes differed significantly. BphAE_{B356} produced two metabolites in approximately equal amounts. They both exhibited a very similar mass spectral fragmentation pattern (**Table 4.1**). The presence of ions at m/z 147 ($M^+ - n\text{BuBO}_2 - \text{C}_6\text{H}_5$) and 120 ($M^+ - n\text{BuBO}_2 - \text{C}_6\text{H}_5 - \text{CH} - \text{CH}_2$) was consistent with a dihydroxylation occurring on ring B. BphAE_{LB400} generated only one of the two dihydrodiol metabolites whereas BphAE_{p4} produced four dihydrodiol metabolites from flavanone. It

produced the two metabolites resulting from the oxidation of ring B, but in addition, it produced two other dihydrodiols that could only result from a hydroxylation of ring A. The mass spectral fragmentation patterns of their butylboronate derivatives are shown in **Table 4.1**. The ions at m/z 192 ($M^+ - C_6H_5 - C_3H_3 - O$), 176 ($M^+ - C_6H_5 - C_3H_3 - O_2$) resulting from the loss of the non-hydroxylated ring B (C_6H_5), provide evidence that the hydroxylation occurred on ring A. These data were confirmed by the GC-MS analysis of the trimethylsilyl derivatives of the metabolites, which evidenced the formation of two dihydrodiol metabolites from BphAE_{B356}, a single one from BphAE_{LB400}, and four dihydrodiol metabolites from BphAE_{p4} (not shown).

BphAE_{B356} and BphAE_{p4} metabolized, respectively, 70 nmol and 50 nmol of flavone when they were incubated with 100 nmol of this substrate for 10 min. However, BphAE_{LB400} performed very poorly on flavone, where less than 5% of the added substrate was degraded. As with flavanone, the pattern of metabolites produced from flavone differed significantly among the enzymes (**Figure 4.3B**). Two metabolites were produced when the reaction was catalyzed by BphAE_{B356}, but their proportion differed considerably. Based on the mass spectral fragmentation features of their butylboronate derivatives shown in **Table 4.1**, they were identified as 2-(2,3-dihydro-2,3-dihydroxyphenyl) chromene-4-one and 2-(3,4-dihydro-3,4-dihydroxyphenyl)chromene-4-one. On the basis of docking experiments described below, the major metabolite would result from a hydroxylation of carbons 2'-3' to generate the 2-(2,3-dihydro-2,3-dihydroxyphenyl) chromene-4-one. BphAE_{p4} produced three metabolites from flavone (**Figure 4.3B**). The GC-MS features of their butyl boronate derivatives are shown in **Table 4.1**. Two of the metabolites are identical to those produced by BphAE_{B356}. The mass spectral features of the third one, which is a major metabolite, comprise ions at m/z 192 ($M^+ - C_6H_5 - C_3H - O$) and 163 ($M^+ - n-Bu - C_6H_5 - C_2H$) which are consistent with a hydroxylation on ring A. On the basis of the docking experiments described below, this metabolite would be 4a,5-dihydro-4a,5-dihydroxy-2-phenyl chromene-4-one. BphAE_{LB400} produced trace amounts only of the metabolite corresponding to the peak of 2-(3,4-dihydro-3,4-dihydroxyphenyl)chromene-4-one.

Table 4.1: Mass spectral features of the butylboronate-derived metabolites produced from flavanone and flavone by BphAE_{B356}, BphAE_{LB400} and BphAE_{p4}

Substrat	Enzyme			Metabolite structure ^a	Oxidized ring	M ⁻	Other ions
	BphAE _{B356}	BphAE _{LB400}	BphAE _{p4}				
	Number of metabolites						
Flavanone							
	2	1	2	2-(2,3-dihydro-2,3-dihydroxyphenyl) chromane-4-one or 2-(3,4-dihydro-3,4-dihydroxyphenyl) chromane-4-one.	B	324	308, 267, 240, 224, 147, 120
			2	4a,5-dihydro-4a,5-dihydroxy-2-phenyl chromane-4one	A	324	308, 267, 240, 224, 192, 176, 131
Flavone							
	2	1	2	2-(2,3-dihydro-2,3-dihydroxyphenyl) chromene-4-one or 2-(3,4-dihydro-3,4-dihydroxyphenyl)chromene-4-one	B	322	306, 265, 238, 222, 210, 181, 120
			1	4a,5-dihydro-4a,5-dihydroxy-2-phenyl chromene-4one	A	322	306, 265, 238, 222, 192, 163, 129

^a Structures were tentatively identified on the basis of their mass spectral fragmentation features and on the orientation of the docked substrates in the enzyme catalytic pocket.

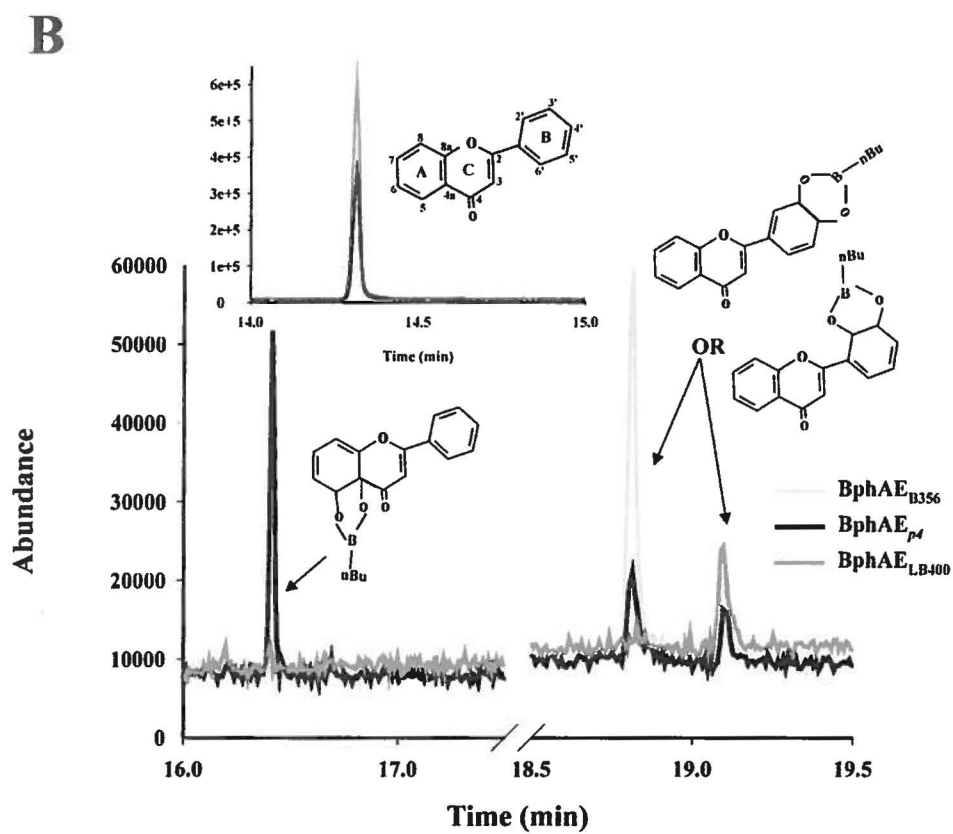
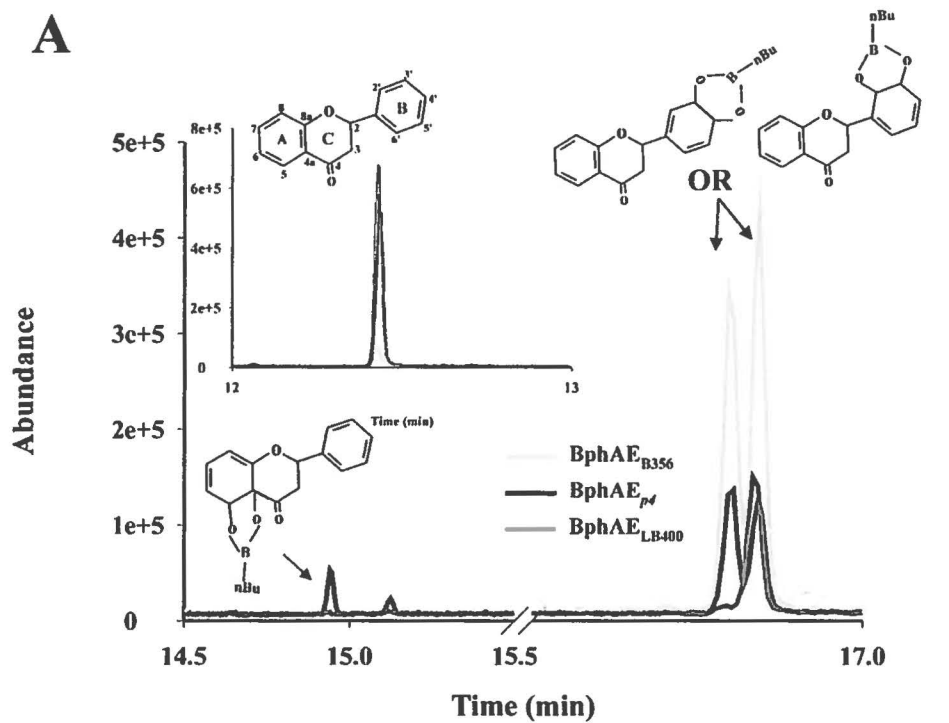


Figure 4.3: (A) Total ion chromatogram showing the peaks of metabolites produced from flavanone after 10 min by reconstituted His-tagged BphAE_{B356} (grey curve), BphAE_{L.B400} (dark grey curve) and BphAE_{p4} (black curve). The inset shows the peak of the substrate remaining in the reaction vial. (B) Total ion chromatogram showing the peaks of metabolites produced from flavone after 10 min by reconstituted His-tagged BphAE_{B356} (grey curve), BphAE_{L.B400} (dark grey curve) and BphAE_{p4} (black curve). The inset shows the peak of the substrate remaining in the reaction vial.

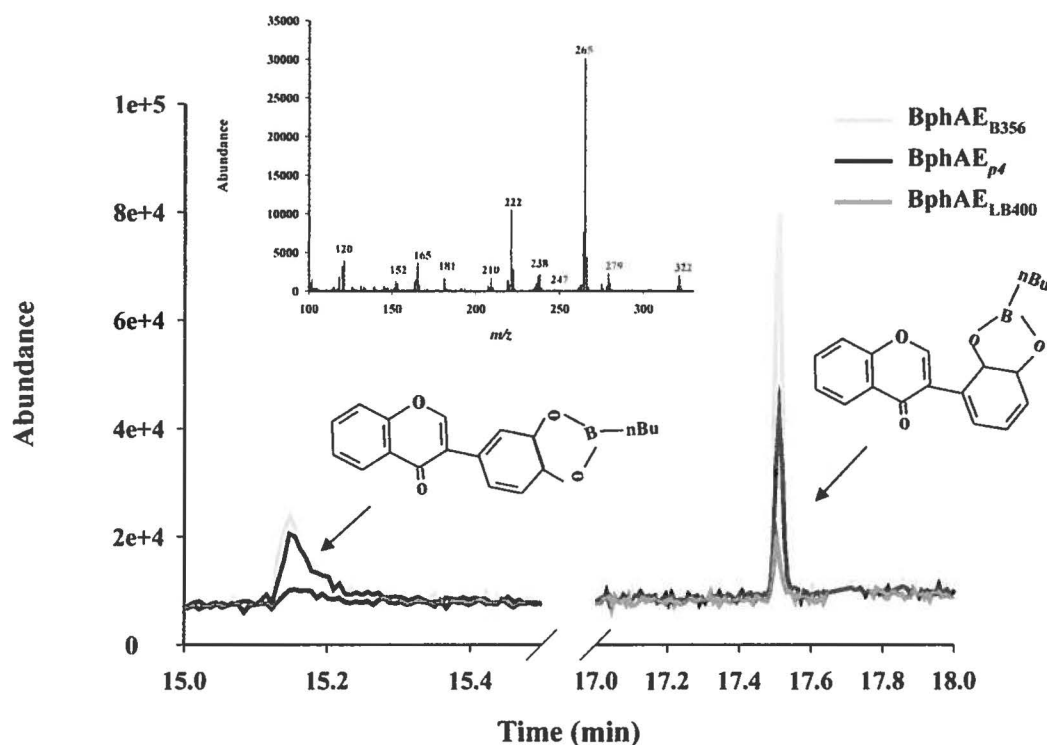


Figure 4.4: Total ion chromatogram showing the peaks of metabolites produced from isoflavone after 10 min by reconstituted His-tagged BphAE_{B356} (grey curve), BphAE_{LB400} (dark grey curve) and BphAE_{p4} (black curve). The inset shows the mass spectrum of the metabolite exhibiting a retention time of 17.5 min. The mass spectrum for the second metabolite is almost identical (not shown).

As was the case for the previous two substrates, BphAE_{B356} performed better than the other two enzymes towards isoflavone. However, in this case, all three enzymes produced the same two metabolites from this flavonoid (**Figure 4.4**). Both of them exhibited a fragmentation pattern comprising ions at m/z 181 ($M^+ - n\text{BuBO}_2 - \text{CO} - \text{CH}$), 165 ($M^+ - n\text{BuBO}_2 - \text{CO} - \text{CH} - \text{O}$), 120 ($M^+ - n\text{BuBO}_2 - \text{C}_6\text{H}_5 - \text{C}_2\text{H}$) that was consistent with a dihydroxylation of ring B.

4.8.4. Kinetic parameters of purified BphAE_{B356}, BphAE_{LB400}, and BphAE_{p4} toward flavone, flavanone, and isoflavone

The steady-state kinetic parameters of purified preparations of BphAE_{B356} and BphAE_{p4}, and BphAE_{LB400} toward each of the three flavonoids were calculated from the initial oxygen consumption using a Clark-type oxygraph. Notably, for the three substrates, the k_{cat} and k_{cat}/K_m values for BphAE_{B356} were in the range reported (169) for biphenyl (respectively 4.3 s^{-1} and $63 \times 10^3 \text{ M}^{-1}\text{s}^{-1}$) when this enzyme was used under the same reaction conditions (**Table 4.2**). Consistent with the whole-cell assays described above, flavanone was the best substrate, exhibiting k_{cat} and k_{cat}/K_m values that were significantly higher than those previously reported for biphenyl (**Table 4.2**). However, flavone and isoflavone were also good substrates for the enzyme since their kinetic parameters were in same range as those reported for biphenyl. Furthermore, for all substrates, the steady-state kinetic parameters of BphAE_{B356} were significantly higher than those for BphAE_{p4}. The reported k_{cat} and k_{cat}/K_m values of BphAE_{p4} toward biphenyl (1.0 sec^{-1} and $31 \times 10^3 \text{ M}^{-1}\text{s}^{-1}$) (206) were higher than those for all three flavonoids. Therefore, although BphAE_{p4} performed well on these substrates, unlike BphAE_{B356}, biphenyl remains a better substrate than the flavonoids. Consistent with the time point measurement experiments, BphAE_{LB400} was poorly active toward the three flavonoids. The steady-state kinetic parameters obtained with flavone and isoflavone were too low to be determined accurately and therefore are not reported here. Flavanone was the best substrate, the k_{cat} and k_{cat}/K_m values obtained with this substrate were significantly lower than the values reported when BphAE_{LB400} was used to metabolize biphenyl under identical conditions (respectively 0.9 sec^{-1} and $41 \times 10^3 \text{ M}^{-1} \text{ sec}^{-1}$) (206). Together, these data shows that in comparison to the activity of BphAE_{LB400}, the double Thr335Ala Phe336Met substitution in BphAE_{p4} contributed to enhancement of the catalytic

activity towards the simple flavonoids. However, these mutations did not allow the enzyme to reach the level of activity of the naturally occurring BphAE_{B356}.

Table 4.2: Steady-state kinetic parameters of BphAE_{B356}, BphAE_{L.B400}, and BphAE_{P4} toward flavanone, flavone, and isoflavone^a

Substrate/Enzyme	K_m (μM)	k_{cat} (s^{-1})	k_{cat}/K_m ($10^3 \text{ M}^{-1}\text{s}^{-1}$)
Flavanone			
BphAE _{B356}	77.5 ± 4.8	9.0 ± 0.4	116.1 ± 8.9
BphAE _{P4}	27.5 ± 5.7	0.60 ± 0.1	21.8 ± 4.0
BphAE _{LB400}	32.1 ± 3.9	0.36 ± 0.0	11.1 ± 1.3
Flavone			
BphAE _{B356}	121.4 ± 7.2	4.0 ± 1.3	32.9 ± 11.2
BphAE _{P4}	21.4 ± 1.4	0.08 ± 0.0	3.8 ± 0.1
Isoflavone			
BphAE _{B356}	15.8 ± 1.0	1.2 ± 0.0	75.9 ± 4.7
BphAE _{P4}	27.6 ± 0.3	0.59 ± 0.0	21.3 ± 0.0

^a The \pm standard deviations of the results for two independently produced enzyme preparations are shown.

4.8.5. Structural analysis of docked flavonoids at active sites of BphAE_{B356}, BphAE_{LB400}, and BphAE_{p4}

In order to identify the structural features of BphAE_{B356} and BphAE_{LB400} that explain why the two enzymes catalyze flavone, isoflavone, and flavanone oxidation differently, we have docked these flavonoids at their active site. Since previous reports showed that an induced-fit mechanism was required to bind the substrate productively inside the BPDO catalytic pocket (206), we have docked the flavonoids in the substrate-bound form of the enzymes after removing biphenyl (or 2,6-dichlorobiphenyl in the case of BphAE_{p4}). When flavone was docked into BphAE_{B356}, consistent with the biochemical data, the conformation of the top-ranked docked molecule exhibited an orientation that would enable an oxygenation of ring B. Carbons 2' and 3' of ring B closely aligned with carbons 2 and 3 of the oxidized ring of biphenyl in the complexed form (**Figure 4.5A**). This suggested that the major metabolite produced from flavone when BphAE_{B356} catalyzed the reaction, would be 2-(2,3-dihydro-2,3-dihydroxyphenyl)chromene-4-one. Therefore, the regiospecificity of BphAE_{B356} toward flavone would be similar to that of the previously reported BphA1A2(2072) which was obtained by shuffling *bphA1* from *Pseudomonas alcaligenes* with *bphA* from *B. xenovorans* LB400 (287). In the case of BphAE_{LB400}, none of the docked substrate conformations exhibits a productive orientation toward the catalytic iron. This is consistent with the fact that the catalytic activity of BphAE_{LB400} toward this flavonoid was very low. When BphAE_{B356} docked with flavone was superposed to the biphenyl-bound form of BphAE_{LB400} (without biphenyl), the chromene oxo group of the docked molecule was at less than 3 Å from both Phe336 and Gly321 of BphAE_{LB400} (not shown). Therefore, the proximity of the chromene oxo group to these two residues probably prevents productive binding to BphAE_{LB400}.

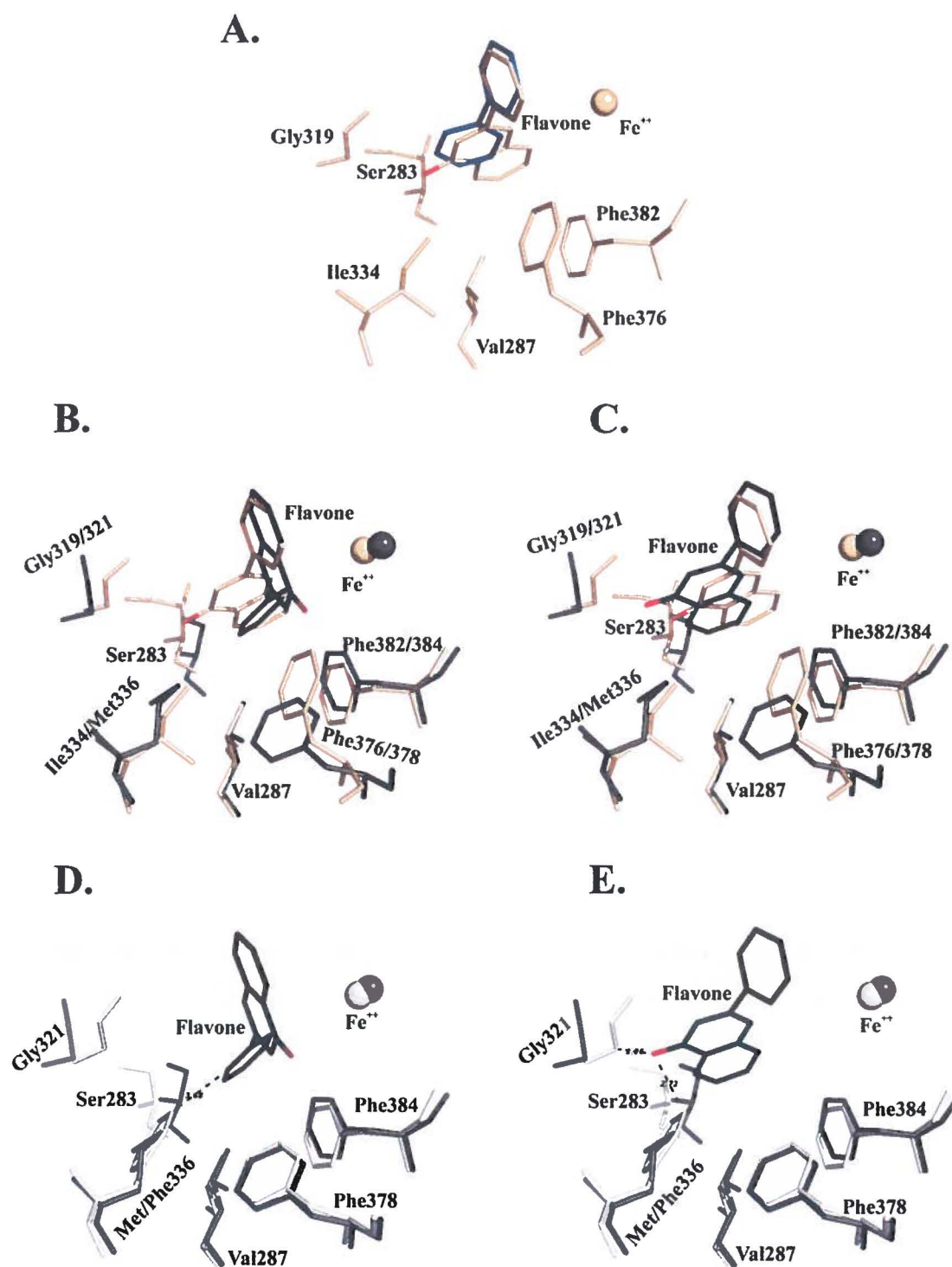


Figure 4.5: (A) Superposition of catalytic center residues of the flavone-docked (wheat) and biphenyl-bounded (blue) forms of BphAE_{B356}. (B and C) Superposition of catalytic center residues of two flavone-docked forms of BphAE_{p4} (black) and the top-ranked flavone-docked form of BphAE_{B356} (wheat). (D and E) Superposition of catalytic center residues of two flavone-docked forms of BphAE_{p4} (black) and the biphenyl-bound form of BphAE_{LB400} (white) after removal of biphenyl. The oxygen of the flavone oxo group is in red.

Unlike the result for BphAE_{B356}, the conformation of the top ranked docked flavone molecule in BphAE_{p4} was consistent with the observation that its major metabolite resulted from a dihydroxylation on ring A. On the basis of the orientation of ring A toward the catalytic Fe⁺⁺ in the docked form of BphAE_{p4}, the hydroxylation should occur onto carbon 4a and 5 to produce 4a,5-dihydro-4a,5-dihydroxy-2-phenyl chromene-4-one (**Figure 4.5B**). Another of the 10 top-ranked conformations of flavone in BphAE_{p4}'s catalytic pocket was similar to, but did not superpose exactly with the molecule docked in BphAE_{B356} (**Figure 4.5C**). In a previous report, the ability of BphAE_{p4} to oxidized 2,6-dichlorobiphenyl on the *meta-para* and *ortho-meta* carbons of biphenyl was attributed to the fact that none of the C2'-C3' or C3'-C4' pairs of carbons were equidistant from the catalytic Fe⁺⁺ and they all were within 4.5 Å from it (165). A similar situation was obtained when flavone was docked in BphAE_{p4}. Carbons C2' and C3' of ring B were not equidistant from the catalytic Fe⁺⁺, and they were more distant from it than the corresponding atoms of flavone docked in BphAE_{B356} (**Figure 4.5C**). This may explain why both 2-(2,3-dihydro-2,3-dihydroxyphenyl)chromene-4-one and 2-(3,4-dihydro-3,4-dihydroxyphenyl)chromene-4-one were produced and why these metabolites were produced in lesser amounts than when BphAE_{B356} catalyzed the reaction.

As shown in **Figure 4.5B**, when flavone takes an orientation enabling an oxidation of ring A (in black), Phe376 of BphAE_{B356} is too close (1.5 Å) to the chromene oxo group to allow productive binding of this substrate. Therefore, this residue or others that modulate its conformation exert a strong influence on the regiospecificity of the enzyme toward flavone. In order to confirm that Phe336 and Gly321 prevent the binding of flavone to BphAE_{LB400}, we superposed both docked conformations of flavone in BphAE_{p4} with the biphenyl-bound form of BphAE_{LB400} after biphenyl removal. This is shown in **Figure 4.5D** and **E**, where it is clear that for both conformations of the docked substrate in BphAE_{p4}, residues Gly321 and Phe336 of BphAE_{LB400} are both too close to the substrate to allow productive binding. Therefore, the Phe336Met and the Thr335Ala substitutions are both required to facilitate flavone binding to BphAE_{p4}. However, as shown from the steady-state kinetic parameters of the enzymes, although BphAE_{p4} can metabolize flavone, its turnover rate of reaction is significantly lower than that of BphAE_{B356}. Therefore, although the two mutations that occurred in BphAE_{p4} have enhanced its catalytic activity toward flavone, other structural features of BphAE_{B356}, not present in BphAE_{p4} are required to facilitate the chemical steps in the catalytic oxygenation reaction. A structural comparison of the catalytic pocket of

BphA_{B356} and BphAE_{p4} identified Phe376/Phe378 and Ser283/Ile283 as likely candidates to explain the different catalytic properties of the two enzymes (Figure 4.5).

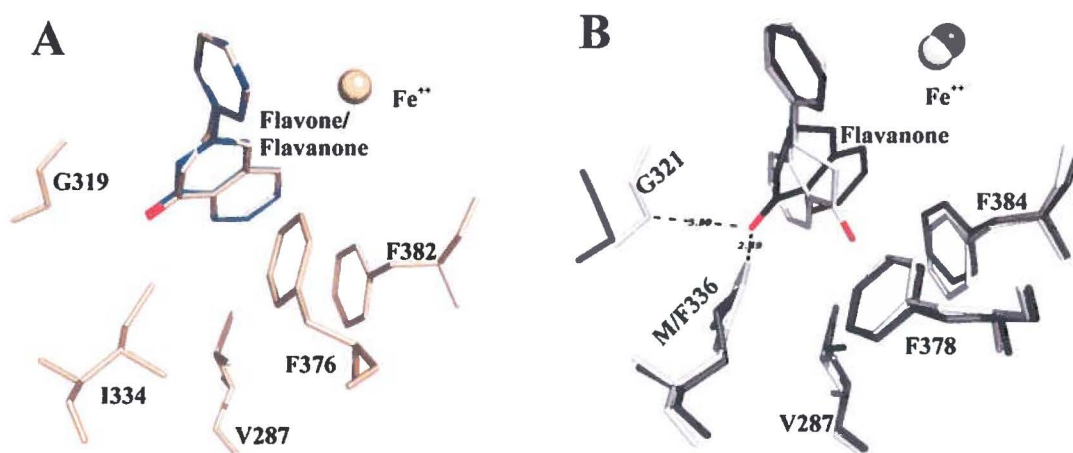


Figure 4.6: (A) Superposition of catalytic center residues of the flavanone-docked (wheat) and flavone-docked (blue) forms of BphAE_{B356}. (B) Superposition of catalytic center residues of the top-ranked flavanone-docked form of BphAE_{p4} (black) enabling the oxidation of ring B and the top-ranked flavanone-docked form of BphAE_{LB400} (white). The oxygen of the flavanone oxo group is in red.

In the flavanone docking experiment, both flavanone and flavone are placed at the same position in BphAE_{B356} where carbon 2' and 3' of ring B superposed almost perfectly with the reactive carbons of biphenyl (Figure 4.6A). Biochemical analysis showed that BphAE_{B356} oxidized both the 2',3' and 3',4' carbons of ring B (Figure 4.3A). Therefore, the binding of BphAE_{B356} to flavanone can induce other conformations of the substrate that the docking experiment could not reproduce. The docking experiment in BphAE_{p4} showed that flavanone can take an orientation where ring B superpose exactly with ring B of the docked molecule in BphAE_{B356} (not shown). However, similar to flavone docking, and consistent with the biochemical data, flavanone can also be docked in BphAE_{p4} in an orientation that would enable a hydroxylation of ring A (not shown). As seen by the observations described above, although BphAE_{LB400} is not as efficient as BphAE_{p4} in oxidizing flavanone, its activity toward this substrate is more efficient than toward flavone. Consistent with the biochemical

data, automatic docking placed flavanone in an orientation that would allow an oxygenation of ring B by BphAE_{LB400}. Structural analysis shows that, unlike the results of the docking experiment done with BphAE_{p4}, in the case of BphAE_{LB400}, the chromane moiety of flavanone is oriented such that the oxo group of ring C is distanced from Phe336 and pulled toward Phe378 and Phe384 (**Figure 4.6B**). This shows that the chromane moiety of the molecule reacts differently than the chromene moiety of flavone with the surrounding atoms of the catalytic pocket of BphAE_{LB400}. However, the docking experiment has limitations since it did not allow identification of the protein atoms of BphAE_{LB400} that interact with the chromane moiety of flavanone.

The isoflavone docking experiments are also in agreement with the biochemical data. Ring B of isoflavone superposes well with ring B of flavone in the top-ranked isoflavone-docked form of BphAE_{B356}. The docking experiment suggests the major metabolite generated by the oxygenation of isoflavone would be 3-(2,3-dihydro-2,3-dihydroxyphenyl) chromene-4-one (**Figure 4.7A**). In the case of BphAE_{p4}, it is not clear why the oxo group is flipped in the opposite orientation for the top-ranked form of isoflavone-docked BphAE_{p4} (**Figure 4.7B**). There are no apparent constraints that would prevent isoflavone from taking the same conformation as in BphAE_{B356}. This shows that as for flavanone, other structural features that the docking experiment could not identify are likely to be involved in the binding process for this flavonoid. It is also interesting that automatic docking has placed isoflavone in a productive orientation for BphAE_{LB400} (**Figure 4.7C**). However, in this case, unlike BphAE_{p4}, the oxo group is in an orientation similar to that found in the isoflavone-docked BphAE_{B356}. Since isoflavone was a poor substrate for BphAE_{LB400} it is likely that unidentified structural features that place isoflavone in the opposite orientation in BphAE_{p4} are required to enable the chemical reactions to proceed. Since in the docked form of BphAE_{B356}, the oxo group is at a distance of approximately 4 Å from Fe⁺⁺ and from the two His that coordinate it, the proximity of the oxo group to the iron may hinder the catalytic activity in BphAE_{LB400}. The iron is at the interface between two α subunits and it was shown in a previous work that protein structures surrounding the catalytic iron move during binding and that these structures appeared to be involved in maintaining the integrity of the $\alpha_3\beta_3$ conformation of the enzyme (206). However, more structural analyses of the substrate-bound enzymes will be required to determine more precisely why BphAE_{LB400} has poor activity on isoflavone.

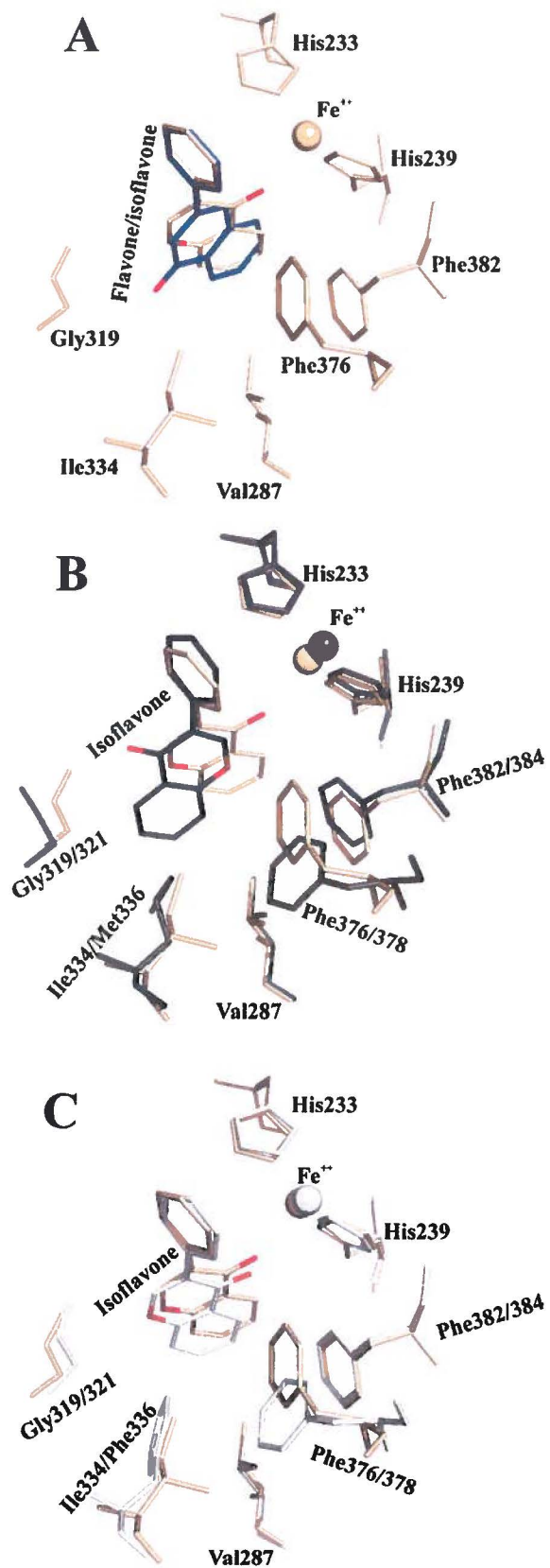


Figure 4.7: (A) Superposition of catalytic center residues of the top-ranked isoflavone-docked (wheat) and flavone-docked (blue) forms of BphAE_{B356}. (B) Superposition of catalytic center residues of the top-ranked isoflavone-docked forms of BphAE_{p4} (black) and of BphAE_{B356} (wheat). (C) Superposition of catalytic center residues of the top-ranked isoflavone-docked forms of BphAE_{LB400} (white) and of BphAE_{B356} (wheat). The oxygen of the flavanone oxo group is in red.

4.9. Discussion

The perception of flavonoids by plant pathogen and their function as signals in the initiation of legume-rhizobia symbiosis have been well characterized (285). However, the potential impacts of flavonoids on soil and rhizosphere bacteria that do not interact with plant directly in a host-pathogen or in a symbiotic interaction remain largely unknown. Better insight into this mechanism will help in understanding how plants promote PCB degradation in soil. Many investigations have identified plants secondary metabolites (flavonoids or terpenes) as likely candidates to trigger microbial degradation of PCBs in soil (293). Shaw et al. (2006) (285) have hypothesized that PSMs act to shape rhizosphere microbial community structure and, thus, they may have an impact on the rhizosphere function by triggering microbial pathways that can influence the quality and quantity of PSMs in soil. However this hypothesis remains to be demonstrated.

In a previous report, we showed *R. erythropolis* U23A biphenyl catabolic pathway was induced by flavanone (330). In this work we showed isoflavone instead of flavanone was an inducer for the biphenyl catabolic pathway of *P. pnomenusa* strain B356 whereas none of the three flavonoids induced the biphenyl catabolic pathway of strain LB400. The observation that strains U23A, B356, and LB400 responded differently to simple flavonoids is consistent with divergent regulation mechanisms for their respective biphenyl catabolic operons. Strain LB400's *bph* operon is controlled by *orf0* producing a positive regulator belonging to the GntR family, and by *bphR2* a LysR-type regulator (53), whereas the biphenyl operon of *R. globerulus* P6 and *R. jostii* RHA1 are regulated through a two-component regulatory system (14, 187). The regulation of strain U23A's *bph* operon is likely to be very similar to that of other Rhodococci. The regulatory system of strain B356's *bph* operon has not yet been elucidated. However, a gene (*orf0*B356, Genebank accession number JQ322530) coding for a protein exhibiting 48% homology with BphS of *Cupriavidus oxalaticus* A5 (previously called *C. necator* A5, *Alcaligenes eutrophus* or *Ralstonia eutropha* A5) (211) and exhibiting homology with other members of GntR family was found in the genome of strain B356 just upstream of *bphG*. Sequence alignment of this protein with other members of GntR family proteins showed it clustering with BphS of strain A5 and of *Pseudomonas* sp. strain KKS102 (not shown) which, unlike ORF0 of strain LB400, were found to be negative regulators (53, 227). The phylogenetic tree obtained when sequences of known BphAs from cultured and uncultured bacteria are aligned (344), shows three branches;

two comprise principally Gram-negative proteobacteria, and one comprises exclusively high-GC-content Gram-positive bacteria of the rhodococcal group. It is noteworthy that BphAE_{B356} clusters with BphA1A2 of strain A5 and of strain KKS102, whereas BphAE_{LB400} belongs to a separate branch. The fact that a similar clustering of the phylogenetic tree is obtained for the deduced amino acid sequences of the regulatory protein and of the first enzyme of the biphenyl catabolic pathway of these strains highlights the possibility that the three biphenyl catabolic pathway clusters may have evolved to serve distinct functions in the environment.

In this work, in order to get more insight about how these pathways interact with simple flavonoids, we compared the metabolism of flavanone, flavone and isoflavone by BphAE_{B356} and BphAE_{LB400}. Biochemical data showed that, unlike BphAE_{LB400}, BphAE_{B356} is well fitted to metabolize these PSMs. Structural analysis identified two features of BphAE_{LB400} that are responsible for the poor ability of the enzyme to metabolize these flavonoids. As observed in the case of 2,6-dichlorobiphenyl (106, 165) and in the case of DDT (169), Phe336 is too large to enable productive binding with large substrates. In addition, the fact that Gly321 is constrained through a network of hydrogen bonding significantly hinders binding with these substrates (165). In a previous report we showed that replacing Thr335 with Ala335 in BphAE_{LB400} relieved constraints on the Val320-Gly321-Gln322 segment allowing for more movement during substrate binding. This feature enables BphAE_{p4} to accommodate bulkier substrates, such as 2,6-dichlorobiphenyl (165). Similarly to Ala335 of BphAE_{p4}, the corresponding residue Gly333 of BphAE_{B356} is too short to form any contact with this segment (not shown). Therefore, Gly319 of BphAE_{B356} is more relaxed than Gly321 of BphAE_{LB400}, which explains in part why BphAE_{B356} can metabolize substrates such as 2,6-dichlorobiphenyl (106) or flavonoids that BphAE_{LB400} metabolizes poorly. However, other unidentified structural features influence binding to flavonoids. For example, it is noteworthy that BphAE_{LB400} was found to catalyze the oxidation of flavanone more efficiently than flavone. The superior properties of the enzyme toward flavanone were attributed to the fact that the oxo group of the chromane moiety was placed away from Phe336. This indicates that protein structures involved in the binding process interacted differently with the chromene and chromane moiety of the molecule.

This is also supported by the superior catalytic abilities of BphAE_{B356} compared to those of BphAE_{p4} toward flavanone, flavone and isoflavone in spite of the fact that both

BphAE_{B356} and BphAE_{p4} comprise a smaller amino acid than Phe336 of BphAE_{LB400} at position 336 and, in addition, the fact that the correspondence of Gly321 of BphAE_{p4} to Gly319 of BphAE_{B356} is less constrained than that of Gly321 of BphAE_{LB400}. The docking experiments did not allow us to identify precisely the BphAE_{B356} structural features that conferred to the enzyme an ability superior to that of BphAE_{p4} to catalyze the reaction. In a previous report it was shown that the helix between residues 282 and 288 moved considerably more toward the substrate during substrate binding with BphAE_{p4} than with BphAE_{LB400}. This movement was attributed to the Thr335Ala substitution that has altered the intramolecular hydrogen bonding networks involving residues of this helix (165). It was suggested (106) that the mobile character of this helix may influence binding to substrate larger than biphenyl. Furthermore, residue 283 is at the entranceway of the catalytic pocket and both residues Ile283 of BphAE_{B356} and Ser283 of BphAE_{p4} are very close (less than 3 Å) from ring A of flavone (**Figure 4.5**) in the flavone-docked enzyme. In the biphenyl-bound form of BphAE_{LB400}, Ser283 is far from the substrate. Although its precise role in substrate binding is not clear, residue 283 and the helix to which it belongs appear to be likely candidates for engineering enzymes exhibiting altered substrate specificity and regiospecificity toward flavonoids. However, we cannot exclude other residues that are not in contact with the substrate but that may influence substrate binding by other mechanisms. For example, in a recent report, residue 338 and 409 of BphAE_{LB400} were found to act synergistically to influence the catalytic properties of the enzyme by interacting with residues that are involved in subunit assembly and electron transport (206).

In previous reports, *E. coli* cells producing *P. alcaligenes* KF707 BPDO were found to catalyze the hydroxylation of flavone (152) and of flavanone (112). BphA1A2 from strain KF707 is more than 95% homologous to BphAE_{LB400}, except that like BphAE_{B356}, residue 335 (corresponding to Phe336 of BphAE_{LB400}) is an Ile and residue 334 (corresponding to Thr335 of BphAE_{LB400}) is an Ala. Therefore, with respect to the catalytic properties toward flavonoids, the structural features of BphA1A2_{KF707} and BphAE_{p4} are expected to be comparable. However, a BphA1A2_{KF707} variant was obtained which exhibited enhanced activity towards flavonoids (142). This variant was obtained by substitution of His255Gln, Val256Ile, Gly266Ala, and Phe277Tyr. It is not clear whether all these residues together or a combination of some of them were required to enhance the activity toward flavonoids. The likely involvement in substrate specificity and selectivity of the mobile loop between residues

240 and 260 that overhang the entranceway of the catalytic pocket has been discussed previously (165). In addition, the likely involvement of residue 266 and 267 in the catalytic properties of BphAE_{B356} toward DDT has also been discussed (169). Nevertheless, our data with BphAE_{B356} and BphAE_{LB400} and data related to BphA1A2_{KF707} variants show the complexity of the substrate binding process, which involves interaction between the substrate and many protein atoms that either contact the substrate or modulate the conformation of protein structures that are required to enable a productive binding.

Together, our investigation identified residues that are involved in substrate binding with simple flavonoids and provided lines of evidence that BphAE_{B356} has evolved to be better fitted than BphAE_{LB400} to metabolize these PSMs. Moreover, the fact that the biphenyl catabolic pathway of strain B356 was induced by isoflavone provides additional evidence supporting the hypothesis brought forward by Focht (79) and others (285) that the biphenyl catabolic pathways have evolved in bacteria to serve ecological functions, perhaps related to the metabolism of plants secondary metabolites in soil.

In this work, by singling out simple flavonoids and comparing the ability of two well-characterized biphenyl-degrading bacteria to metabolize them, we have shown that both the metabolism of flavonoids and the response to them as signal molecule to trigger the biphenyl catabolic pathway vary considerably among bacteria. This conclusion is significant for the development of more rational approaches for designing efficient rhizoremediation processes. Hence our data imply that the efficiency of the process will depend on the choice of appropriate bacterial strains responding to the specific PSMs produced by the plants with which they are associated.

4.10. Acknowledgements

This work was supported by the Natural Sciences and Engineering Research Council of Canada (NSERC) (Grants #RGPIN/39579-2007 and STPSC 356996-07)

5. Presentation of article 3

5.1. The context of the article

Data obtained presented in Article 1 and 2 and in other reports suggested that the bacterial biphenyl catabolic pathway may have evolved divergently to serve other functions than biphenyl degradation. In article 2 we suggested that they may have evolved to play a role in the metabolism of PSMs. We pursued on this subject, focusing on two other biphenyl analogs: Diphenylmethane and benzophenone, in which the two phenyl rings are bonded to a single carbon. They are both of environmental concern and their structure may serve as carbon skeletons for some plant metabolites. We investigated the abilities of the biphenyl catabolic enzymes of *P. pnomenusa* B356 and *B. xenovorans* LB400 to metabolize these two compounds. Unexpectedly, we found that, unlike strain LB400, strain B356 grew as well on diphenylmethane as on biphenyl and this substrate was also as good an inducer of the biphenyl catabolic pathway of strain B356 as biphenyl. In order to better understand how these two strains differ with regard to their ability to metabolize these substrates, in this work, we have also resolved and compared the profile of metabolites generated during their oxidation by the biphenyl catabolic pathway of the two strains. We also compared the structures of diphenylmethane- and benzophenone-docked forms BphAE_{B356} and BphAE_{LB400} and examined the biochemical properties of these two enzymes toward the two substrates.

The results were presented in Article 3, which was published in **Journal of Bacteriology**.

5.2. Contribution of the student to article 3

All the experiments performed in this work were planned by the student and Michel Sylvestre, and they were performed by the student. The student performed experiments to assess the ability of diphenylmethane and benzophenone to support the growth of strains B356 and LB400 and to induce their biphenyl catabolic pathway. She produced the preparations of purified enzymes that were used to analyze the metabolites and to determine the steady-state kinetic parameters. She also performed the enzymatic assays. The student identified the metabolites on the basis of their GC-MS and/or NMR spectra. She did the GC-MS analyzes and purified the metabolites for NMR analyzes. The NMR spectra were obtained at the QANUC NMR facility, and they were interpreted by the student. The student also performed the docking experiments. The docking structure analysis was done by Michel Sylvestre. The article was written by the student and Michel Sylvestre.

5.3. Article 3

Has the bacterial biphenyl catabolic pathway evolved primarily to degrade biphenyl? The diphenylmethane case

Thi Thanh My Pham and Michel Sylvestre[#]

Institut National de la Recherche Scientifique

INRS-Institut Armand-Frappier, Laval, QC H7V 1B7, Canada

[#]Corresponding author: Michel Sylvestre, Institut National de la Recherche Scientifique (INRS-Institut Armand-Frappier), Laval, Québec, H7V 1B7, Canada.

450-687-5010; FAX: 450-686-5501; E-mail: Michel.Sylvestre@iaf.inrs.ca

Running title: Metabolism of diphenylmethane and benzophenone

Reference: **Pham, T. T., and Sylvestre, M.** 2013. Has the bacterial biphenyl catabolic pathway evolved primarily to degrade biphenyl? The diphenylmethane case. *J Bacteriol* **195**:3563-3574

5.4. Résumé

Dans ce travail, nous avons comparé la capacité de *Pandoraea pnomenusa* B356 et de *Burkholderia xenovorans* LB400 à métaboliser le diphénylméthane et la benzophénone, deux analogues du biphenyle, dont les cycles phényles sont liés à un seul carbone. Ces deux produits chimiques sont des contaminants environnementaux préoccupants. *P. pnomenusa* B356 pouvait croître facilement sur un milieu de culture contenant du diphénylméthane comme unique source de carbone. Une comparaison des cinétiques de croissance de la souche B356 sur le diphénylméthane et le biphenyle a permis de montrer que les deux substrats induisent la même voie catabolique. Le profil des métabolites produits au cours de la croissance de la souche B356 sur un milieu contenant du diphénylméthane était identique à celui produit par les enzymes isolées de la voie catabolique du biphenyle agissant seul ou réaction couplée. La dioxygénase du biphenyle transforme le diphénylméthane efficacement pour générer du 3-benzylcyclohexa-3,5-diène-1,2-diol, qui est ultimement transformé en acide phénylacétique par les autres enzymes de la voie catabolique. Ce dernier est ensuite métabolisé par une voie inférieure. La souche B356 pouvait aussi cométaboliser la benzophénone en utilisant les enzymes de sa voie du biphenyle. Cependant, dans ce cas, la dégradation était incomplète résultant en l'accumulation de 2-hydroxy-6,7-dioxo-7-phénylheptanoïque dans le milieu de culture, et de plus, le substrat était incapable d'induire la voie du biphenyle. Contrairement à la souche B356, la souche *B. xenovorans* LB400 était incapable de croître sur un milieu de culture contenant du diphénylméthane comme seule source de carbone. Ses enzymes de la voie catabolique du biphenyle pouvaient métaboliser le diphénylméthane, mais elles métabolisaient la benzophénone difficilement. Le fait que la voie catabolique de la souche B356 métabolise le diphénylméthane et la benzophénone plus efficacement que celle de la souche LB400, nous permet de postuler que chez la souche B356, cette voie a évolué de façon divergente afin de servir d'autres fonctions non liées à la dégradation du biphenyle.

5.5. Abstract

In this work, we have compared the ability of *Pandoraea pnomenusa* B356 and of *Burkholderia xenovorans* LB400 to metabolize diphenylmethane and benzophenone, two biphenyl analogs in which the phenyl rings are bonded to a single carbon. Both chemicals are of environmental concern. *P. pnomenusa* B356 grew well on diphenylmethane. On the basis of growth kinetics analyses, diphenylmethane and biphenyl were shown to induce the same catabolic pathway. The profile of metabolites produced during growth of strain B356 on diphenylmethane was the same as the one produced by isolated enzymes of the biphenyl catabolic pathway acting individually or in coupled reactions. The BPDO oxidizes diphenylmethane to 3-benzylcyclohexa-3,5-diene-1,2-diol very efficiently, and ultimately this metabolite is transformed to phenylacetic acid, which is further metabolized by a lower pathway. Strain B356 was also able to cometabolize benzophenone through its biphenyl pathway although in this case, this substrate was unable to induce the biphenyl catabolic pathway, and the degradation was incomplete, with accumulation of 2-hydroxy-6,7-dioxo-7-phenylheptanoic acid (7-phenyl DODA). Unlike strain B356, *B. xenovorans* LB400 did not grow on diphenylmethane. Its biphenyl pathway enzymes metabolized diphenylmethane, but they poorly metabolize benzophenone. The fact that the biphenyl catabolic pathway of strain B356 metabolized diphenylmethane and benzophenone more efficiently than that of strain LB400 brings us to postulate that in strain B356, this pathway evolved divergently to serve other functions not related to biphenyl degradation.

5.6. Introduction

Many investigations have shown that the bacterial biphenyl catabolic pathway enzymes, especially the biphenyl dioxygenase (BPDO), which initiates the degradation process, are very versatile (311). The biphenyl pathway, also called the upper pathway, comprises four enzymatic steps that transform biphenyl into benzoic acid, which is further metabolized by a lower pathway (Figure 5.1).

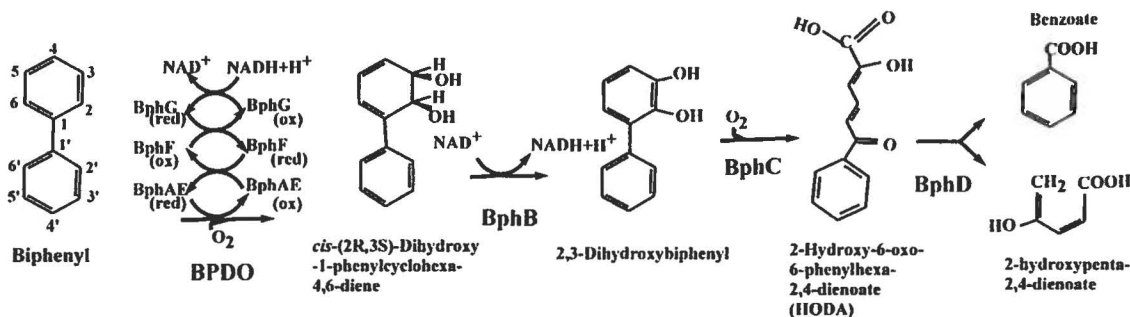


Figure 5.1: Biphenyl catabolic pathway enzymes and metabolites

Aside from its ability to metabolize PCBs (311), BPDO metabolizes many biphenyl analogs (29, 44, 142, 201, 271, 277) to generate hydroxylated aromatics. BPDO is composed of three components (Figure 5.1). The catalytic component, which is a Rieske-type dioxygenase (RO) (BphAE), is a hetero hexamer made up of three α (BphA) and three β (BphE) subunits. The other two components are the ferredoxin (BphF) and the ferredoxin reductase (BphG), both of which are involved in electron transfer from NADH to BphAE. The catalytic center of the enzyme is located on the C-terminal portion of BphAE α subunit, which also carries the major structural determinants for substrate specificity (165). There are three phylogenetically distinct clusters of BphAEs (300, 344, 357), and the structure of a representative BphAE (also called BphA1A2) from each of these three clusters has now been elucidated. Thus, the Protein Data Bank (PDB) coordinate file for *B. xenovorans* LB400 BphAE (BphAE_{LB400}) is available (165), as are those for *P. pnomenusa* B356 BphAE (BphAE_{B356}) (46) and for *R. jostii* RHA1 BphA1A2 (BphA1A2_{RHA1}) (99).

BphAE_{LB400} has been thoroughly investigated, because *B. xenovorans* LB400 is considered one of the best PCB degrader (165). However, recent studies have shown that BphAE_{B356} metabolizes flavone, isoflavone, and flavanone (236), as well as 2,6-

dichlorobiphenyl (106) and DDT (169), significantly more efficiently than BphAE_{LB400}. In this work, we compared the ability of strain LB400 and B356 BPDOs and of further enzymes of their biphenyl catabolic pathway to metabolize two biphenyl analogs (diphenylmethane and benzophenone) in which two phenyl rings are bonded to a single carbon. Both are chemicals of environmental importance. According to U.S. Environmental Protection Agency, in 2003, benzophenone was classified as a high volume chemical, with an annual production exceeding 450,000 kg (<http://toxnet.nlm.nih.gov/>). Benzophenone is widely used as photoinitiator (11). Hydroxybenzophenones are useful building blocks for chemical syntheses and they are also used as photosensitisers (11). Benzophenones and their xanthone analogs are common plant metabolites with medicinal properties (118), but because of their high demand, they are synthesized industrially. A major synthetic process is through atmospheric oxidation of diphenylmethane in the presence of metal catalysts (11). Aside from being a precursor for benzophenones, diphenylmethane and many of its analogs are used in various other industrial applications. The benzhydryl motif is a fundamental component in antiallergenic agents. It is also a component of hexachlorophene and DDT, and diphenylmethane diisocyanate is a major component of polyurethane. However, very few investigations have addressed the bacterial degradation of diphenylmethane (80, 202) or benzophenone (179). Focht and Alexander (82) have described a *Hydrogenomonas* isolate that grew on diphenylmethane and was able to cometabolize benzophenone and several related chlorinated analogs. However, the ability of this isolate to metabolize biphenyl has not been examined. More recently, Misawa et al. (2002) (202) have shown that *P. alcaligenes* KF707 BPDO and variants derived from it were able to metabolize diphenylmethane. However, the metabolites produced have not been identified, and the steady-state kinetics of these BPDOs toward diphenylmethane were not determined. On the other hand, the ability of BPDO to metabolize benzophenone has never been examined.

While examining the ability of the biphenyl catabolic enzymes of *P. pnomenusa* B356 and of *B. xenovorans* LB400 to metabolize these two chemicals, we unexpectedly found that strain B356 grows well on diphenylmethane. In this context, we further investigated diphenylmethane metabolism by strain B356 and we obtained evidence that during growth of the strain on either biphenyl or diphenylmethane, both substrates are metabolized by the same catabolic pathway. This led us to postulate that in strain B356, the biphenyl catabolic pathway evolved to serve other functions not related to biphenyl degradation.

5.7. Materials and methods

5.7.1. Bacterial strains, plasmids, chemicals and general protocols

E. coli DH11S (175) and *E. coli* C41(DE3) (200) were used in this study. Wild-type strains *P. pnomenusa* B356 and *B. xenovorans* LB400 were described previously (19, 70). BphAE_{p4} is a mutant of BphAE_{LB400}, described previously (165), which was obtained by substitution at two residues, Thr335Ala and Phe336Met. This mutant exhibits an expanded substrate range compared to the parent enzyme. Most plasmids used in this study were described previously and are listed in **Table 5.1**. Plasmids pET14b[B356-*bphF*] and pET14b[B356-*bphG*] carry the genes encoding BphF_{B356} and BphG_{B356}, respectively, and they were prepared by sub-cloning the respective genes from pQE31[B356-*bphF*] and pQE31[B356-*bphG*] (128) into pET14b. The culture media used were LB broth (260), basal medium M9 (260), or MM30 (310) amended with various sources of carbon and antibiotics, depending on the experiment. DNA general protocols were done according to Sambrook et al. (1989) (260). Diphenylmethane and benzophenone (99% pure) were from Sigma-Aldrich.

Table 5.1: Plasmids used in the study

Plasmid	Proteins expressed	Reference or source
pET14b[LB400- <i>bphAE</i>]	BphAE _{LB400}	(165)
pET14b[p4- <i>bphAE</i>]	BphAE _{p4}	(165)
pET14b[B356- <i>bphAE</i>]	BphAE _{B356}	(169)
pQE31[B356- <i>bphAE</i>]	BphAE _{B356}	(169)
pDB31[LB400- <i>bphFG</i>]	BphF _{LB400} , BphG _{LB400}	(21)
pYH31[LB400- <i>bphFGBC</i>]	BphF _{LB400} , BphG _{LB400} , BphB _{LB400} , BphC _{LB400}	(20)
pET14b[B356- <i>bphF</i>]	BphF _{B356}	This study
pET14b[B356- <i>bphG</i>]	BphG _{B356}	This study
pET14b[B356- <i>bphB</i>]	BphB _{B356}	(57)
pQE31[B356- <i>bphC</i>]	BphC _{B356}	(117)

5.7.2. Assays to assess ability of diphenylmethane and benzophenone to support growth of strains B356 and LB400 and to induce their biphenyl catabolic pathway

Induction of the biphenyl catabolic pathway of strains B356 and LB400 by diphenylmethane and benzophenone was assessed by monitoring the amount of 4-chlorobenzoate produced from 4-chlorobiphenyl as described previously (236). We have also evaluated the ability of wild-type strains B356 and LB400 to grow on diphenylmethane or benzophenone as the sole growth substrate. Cells grown overnight in LB broth were washed twice in MM30 and suspended in MM30 to an OD_{600nm} of 0.5. This cell suspension was used (100 µl) to inoculate 20 ml of MM30 containing 2 mM of biphenyl or diphenylmethane. The cultures were incubated with shaking at 28 °C. Cell growth was monitored by determining the CFU. We also used the Bioscreen C system (Growth Curves USA, Piscataway, NJ) to compare the growth kinetics of strain B356 according to the substrate diphenylmethane or biphenyl. In order to prepare the inoculums for the Bioscreen C experiments, cells were grown on 1 mM diphenylmethane or biphenyl or on 30 mM sodium acetate for 16 to 18 h, they were washed twice in MM30, and the cells were suspended in the same medium to an OD_{600nm} of 0.08. Each well of the Bioscreen C microplate contained 237.5 µl of MM30 supplemented with 1 mM biphenyl or diphenylmethane added in 30 µl dimethyl sulfoxide (DMSO) or 30 mM sodium acetate added in 30 µl water, and they were inoculated with 12.5 µl of the suspension described above. A series of cultures also contained 3-chlorobenzoic acid (2 mM) or 3-chlorocatechol (0.2 mM), each added in 5 µl DMSO. Control cultures with no substrate and uninoculated cultures were also run in the experiments. The cultures were incubated at 28 °C and set at low revolution. Both biphenyl and diphenylmethane are poorly soluble in water, but when added at a concentration of 1 mM, the nonsoluble portion of the substrate did not interfere with the OD readings during the Bioscreen C experiments. Each sets of cultures were run in triplicate. Growth was also monitored by determining CFU at various intervals of time during the Bioscreen C experiments.

5.7.3. Analysis of the metabolites produced from diphenylmethane and benzophenone by strains B356 and LB400 and by enzymes of their biphenyl catabolic pathway

The metabolites produced during growth of strain B356 on 2 mM diphenylmethane in 20 ml MM30 were extracted with ethyl acetate at neutral pH and at pH 4 from the supernatant of 22-h-old cultures. They were then treated with *n*-Butylboronate (*n*BuB) or *N,O*-bis(trimethylsilyl)trifluoroacetamide (BSTFA) for gas chromatography-mass spectrometry (GC-MS) analyses according to previously described protocols (330). A similar protocol was used to examine the metabolites produced from benzophenone by biphenyl-induced cells of strain B356. However, in this case, the cells were grown on biphenyl to reach log phase, and then they were suspended at an OD_{600nm} of 3.0 in M9 medium and incubated at 28 °C and 100 rpm for 60 min in the presence of 0.2 mM benzophenone.

Metabolites from diphenylmethane and benzophenone also were analyzed from suspensions of isopropyl β -D-1-thiogalactopyranoside (IPTG)-induced whole cells of *E. coli* [pDB31 B356-*bphFG*] or *E. coli* [pYH31 LB400-*bphFGBC*] also harboring pQE31[B356-*bphAE*] or pQE31[LB400-*bphAE*] according to a previously published protocol (330). The induced cells were suspended at an OD_{600nm} of 5.0 in 50 mM sodium phosphate buffer, pH 7.0, and the metabolites generated after 30 min of incubation at 37 °C were extracted and analyzed by GC-MS.

GC-MS analyses were performed using a Hewlett Packard HP6980 series gas chromatograph interfaced with a HP5973 mass selective detector (Agilent Technologies). The mass selective detector was operated in EI ionization mode and used a quadrupole mass analyzer. Under these conditions, the instrument resolution is 0.1 atomic mass units, which is well sufficient to clearly distinguish between two compounds of atomic masses differing by a single atomic mass unit.

5.7.4. Assays to identify diphenylmethane and benzophenone metabolites produced from *BphAE_{B356}*, *BphAE_{LB400}* and *BphAE_{p4}* and to determine their steady-state kinetics

Reconstituted His-tagged BPDO preparations were used in these experiments. His-tagged purified enzyme components were produced and purified by following protocols published previously (206). The enzyme assays were performed in a volume of 200 μ l in 50 mM MES buffer, pH 6.0, at 37 °C as described previously (129). For metabolites analyses, the reaction medium was incubated for 10 min and the metabolites were extracted at pH 6.0 with ethyl acetate, and then they were treated with *n*BuB or BSTFA for GC-MS analyses as described above. The steady-state kinetics were determined by recording the oxygen consumption rates according to a protocol described previously, using a Clarke-type Hansatech model DW1 oxygraph (205). They were determined from three separately prepared purified preparations of the enzymes.

5.7.5. Purification and NMR analysis of 2,2',3,3'-tetrahydroxybenzophenone

2,2',3,3'-Tetrahydroxybenzophenone was prepared using a coupled reaction composed of His-tagged purified preparations of B356 BPDO (*BphAEFG_{B356}*) plus *BphB_{B356}*. Each enzyme reaction contained 50 nmol benzophenone, 0.6 nmol of each B356 BPDO component (*BphAE_{B356}*, *BphF_{B356}* and *BphG_{B356}*), 2 nmol *BphB_{B356}*, 100 nmol of NADH, and 100 nmol NAD in 200 μ l (total volume) of 50 mM MES buffer (pH 6.0). The mixture was incubated for 15 min at 37 °C and then extracted at pH 6.0 with ethyl acetate. The extract was concentrated 20-fold by evaporation under a stream of nitrogen, and this preparation was injected into an XDB-C8 column (4.6 x 150 mm). The column was eluted at 1ml/min with a linear gradient starting from 80%-HPLC grade water with 0.085% *ortho*-phosphoric acid and 20% acetonitrile to 50% acetonitrile at 12 min. The detector was set at a wavelength of 280 nm. The peak of the metabolite was collected, the solution was immediately adjusted to pH 6.0 with 0.1 M NaOH, and the metabolite was extracted with ethyl acetate. Its identity and purity were verified by GC-MS analysis of its TMS derivative before running the nuclear magnetic resonance (NMR) analysis. The NMR spectra were obtained at the Quebec/Eastern Canada High Field NMR Facility at McGill University (Montreal, Quebec, Canada) with a Bruker 500-mHz spectrometer. The analyses were carried out in deuterated acetone at room temperature.

5.7.6. Docking and structure analysis

Dimer AB of BphAE_{LB400} (RCBS Protein Data Bank, PDB entry 2XRX) and of BphAE_{B356} (PDB entry 3GZX) were used as protein targets, and they were prepared as previously described (169). Ligands all were downloaded as sdf files from pubchem (<http://pubchem.ncbi.nlm.nih.gov>) and converted into pdb format in Discover Studio Visualizer 2.5. Both proteins and ligands were processed with AutoDockTools to obtain their proper pdbqt format. The searching space for the ligand was centered on the mononuclear iron and contained 20 Å in each x, y, and z direction. Autodock 4 (209) with default parameters was used to perform the automatic docking.

5.8. Results

5.8.1. Growth of *P. pnomenusa* B356 and *B. xenovorans* LB400 on diphenylmethane and benzophenone

Neither *P. pnomenusa* B356 nor *B. xenovorans* LB400 grew when benzophenone was used as sole growth substrate. Using a previously described 4-chlorobiphenyl conversion assay (236), we showed that benzophenone was unable to induce the biphenyl catabolic pathway of both strains. Similarly, diphenylmethane did not serve as the growth substrate for strain LB400 and did not induce its biphenyl catabolic pathway. However, remarkably, strain B356 grew very well in MM30 containing 2 mM diphenylmethane as the sole growth substrate. Under those conditions, CFUs values of up to 4×10^9 cells/ml were obtained within 36 h at 28 °C. In addition, using the 4-chlorobiphenyl conversion assay (236), we found that a suspension of log-phase cells grown on 2 mM diphenylmethane and adjusted to an OD_{600nm} of 1.0 produced 329 ± 20 μ M 4-chlorobenzoate from 1.25 mM 4-chlorobiphenyl after 2 h incubation. In comparison, a resting suspension of log-phase cells of strain B356 grown on 2 mM biphenyl and tested under the same conditions produced 330 ± 17 μ M of 4-chlorobenzoate. This suggested that the biphenyl catabolic pathway of B356 was induced during growth on diphenylmethane. Using the Bioscreen C system, we have compared the growth kinetics of strain B356 according to the substrate used, biphenyl or diphenylmethane. In addition, we have determined the effect of interchanging the growth substrate on growth kinetics (biphenyl or diphenylmethane) to prepare the inocula. Results shown in **Figure 5.2** clearly demonstrate that strain B356 grows as well on diphenylmethane as on biphenyl, sometimes even better. Furthermore, replacing diphenylmethane with biphenyl to prepare the inoculum for the Bioscreen C experiments did not affect significantly the growth kinetics on diphenylmethane; the lag phases were identical and the growth rates were similar (0.35 ± 0.01 h⁻¹ and 0.34 ± 0.02 h⁻¹ for diphenylmethane- or biphenyl-induced cells, respectively). Likewise, when biphenyl was used as growth substrate, the lag phases were very similar whether the inocula were prepared by growing the cells on biphenyl or diphenylmethane, and the growth rates were identical (0.25 ± 0.02 h⁻¹). Conversely, when cells were grown on sodium acetate to prepare the inoculum, the cells grew very poorly whether the Bioscreen C experiments were run using biphenyl or diphenylmethane as the substrate, (**Figure 5.2**), exhibiting long lag phases and low growth rates (0.14 h⁻¹), and the CFU count did not exceed

5×10^7 cells/ml at the end of the log phase. We have no data explaining why B356 grew better on diphenylmethane than on biphenyl. This result shows that the combined upper and lower pathways metabolized diphenylmethane more efficiently than biphenyl. However, the fact that interchanging the substrates to prepare the inocula for the Bioscreen C experiments did not affect the growth kinetics and did not prolong the lag phase provide strong evidence that the two substrates were degraded by the same pathway, which they both induced.

As further evidence that growth on diphenylmethane proceeded through the biphenyl catabolic pathway, we have examined the effect of adding 3-chlorocatechol and 3-chlorobenzoate to the growth medium. In the Bioscreen C experiments, 0.2 mM 3-chlorocatechol completely inhibited growth of strain B356 on both biphenyl and diphenylmethane (not shown). In a previous work, we showed that B356 BphC is very sensitive to 3-chlorocatechol (117), and its presence in the growth medium strongly inhibits biphenyl metabolism (297).

It is also noteworthy that in the Bioscreen C experiments, when 3-chlorobenzoate (2 mM) was added as a cosubstrate, cell growth was strongly inhibited (**Figure 5.2**). The same inhibition was observed whether the cells were pregrown on diphenylmethane or biphenyl or whether the Bioscreen C experiments were run using biphenyl or diphenylmethane as substrate. This inhibition was not observed when the Bioscreen C experiments were run using sodium acetate as growth substrate (not shown). The significant inhibitory effect of 3-chlorobenzoate on the metabolism of biphenyl by strain B356 has been reported previously (297). It was attributed to the ability of the lower biphenyl catabolic pathway to convert 3-chlorobenzoate into 3-chlorocatechol, which strongly inhibits the upper biphenyl catabolic pathway (297). Therefore, data obtained in the Bioscreen C experiments suggest that a pathway able to metabolize 3-chlorobenzoate into 3-chlorocatechol is induced during growth on diphenylmethane and 3-chlorocatechol strongly impairs the metabolism of the upper pathway. The fact that both the diphenylmethane, and biphenyl degradation pathways responded similarly to the presence of 3-chlorocatechol and 3-chlorobenzoate provides additional evidence that both substrates are metabolized by the same pathway.

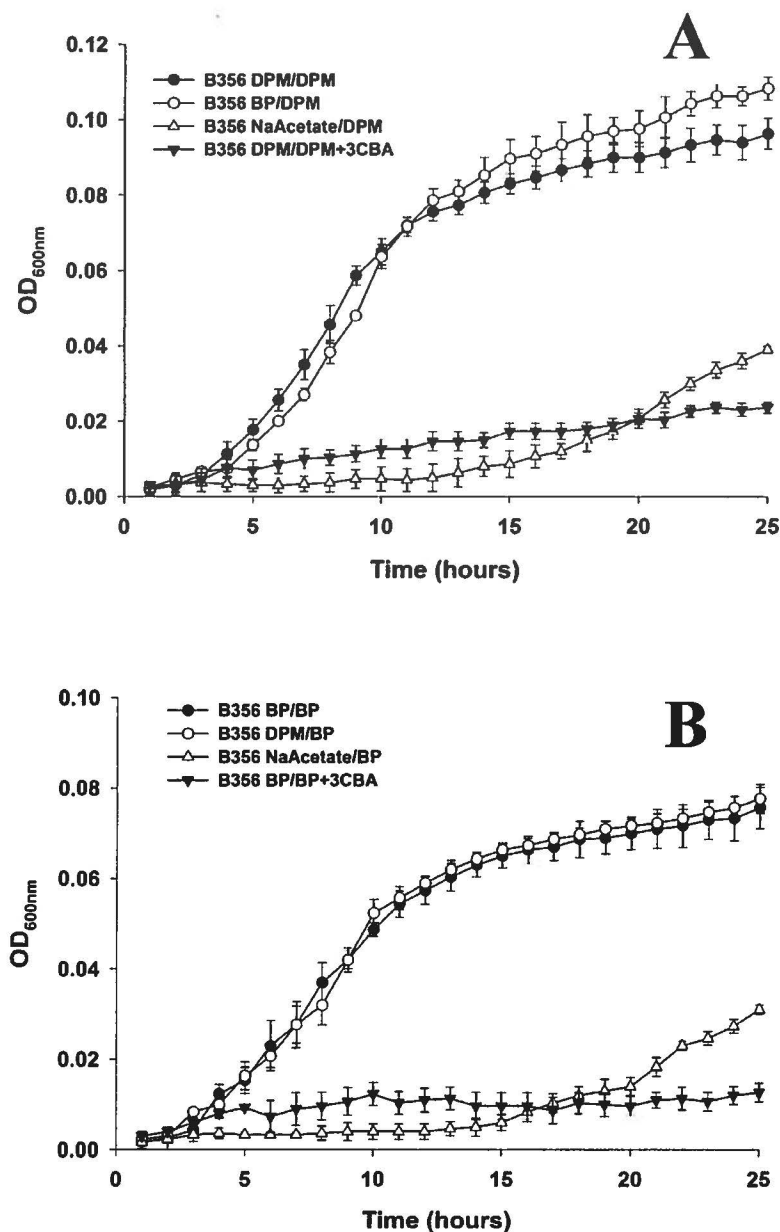


Figure 5.2: Growth curves of strain B356 on diphenylmethane when the inocula were prepared by growing the cells on either diphenylmethane (DPM/DPM), biphenyl (BP/DPM), or sodium acetate (NaAcetate/DPM) (upper) or on biphenyl when the inocula were prepared by growing the cells on either biphenyl (BP/BP), diphenylmethane (DPM/BP), or sodium acetate (NaAcetate/BP) (lower). A growth curve also was obtained for cells pregrown on diphenylmethane and then grown on diphenylmethane plus 3-chlorobenzoate (DPM/DPM + 3CBA) or cells pregrown on biphenyl then then grown on biphenyl plus 3-chlorobenzoate (BP + 3CBA). The growth curves were obtained using a Bioscreen C system as described in the Materials and Methods.

Because phenylacetate would be the expected endproduct if diphenylmethane was metabolized by the enzymes of the upper biphenyl pathway, we have determined whether it could serve as growth substrate for strains B356 and LB400. In both cases, cells grew very well, reaching CFU values exceeding 10^9 cells/ml within 18 h at 28 °C.

5.8.2. Metabolism of diphenylmethane and benzophenone by *P. pnomenusa* B356

When diphenylmethane-grown cells of strain B356 were inoculated in MM30 containing 2 mM diphenylmethane, the substrate (approximately 40 μ mol) was almost completely metabolized after 22 h. The mass spectral features of the major metabolite in the acidic ethyl acetate extract were identical to those of an authentic standard of phenylacetic acid (**Figure 5.3A**, spectra are not shown). Based on the area under the GC-MS peak, approximately 15 nmol was present in the 22-h-old cultures. Among the minor metabolites, one peak eluting at 14.76 min (**Figure 5.3A**) exhibited mass spectral features that correspond to those of a *meta*-fission metabolite resulting from the catalytic cleavage of a catechol derivative of diphenylmethane. This metabolite was tentatively identified as 2-hydroxy-6-oxo-7-phenylhepta-2,4-dienoic acid (7-phenyl HODA) ($m/z = 376$ (M^+), $m/z = 361$ ($M^+ - CH_3$), $m/z = 333$ ($M^+ - CH_3 - CO$), and $m/z = 259$ ($M^+ - COO(CH_3)_3Si$) (see **Figure 5S1** in the supplemental material for the spectrum). This is the metabolite that would be expected if the hydroxylation reaction had occurred on the *ortho-meta* carbons of one benzene ring of diphenylmethane to generate 3-benzylcyclohexa-3,5-diene-1,2-diol. The identity of the acidic metabolite as 7-phenyl HODA is consistent with the fact that a metabolite exhibiting the same mass spectral features was produced from diphenylmethane by resting cells of *E. coli* pQE31[B356-*bphAE*] + pYH31[LB400-*bphFGBC*] (**Figure 5.3A**). The *E. coli* resting cells assay also shows that BphB_{LB400} and BphC_{LB400} can further metabolize 3-benzylcyclohexa-3,5-diene-1,2-diol generated by BphAE_{B356}.

The acidic extracts of cells of strain B356 grown on diphenylmethane also contained a metabolite whose TMS derivative exhibited a molecular mass at m/z 256 corresponding to a mono-hydroxy-diphenylmethane (**Figure 5.3A**, spectrum not shown). This metabolite was presumably generated from the corresponding dihydrodiol metabolite during the extraction procedure at pH 4.

In the culture extracts prepared at neutral pH, 3-benzylcyclohexa-3,5-diene-1,2-diol and 2,3-dihydroxydiphenylmethane were detected only in trace amount (not shown). The fact that only small amounts of acidic and neutral metabolites were detected in the culture medium of 22-h-old cultures shows diphenylmethane metabolism is very efficient, and this is consistent with the rapid growth on this substrate.

Strain B356 was unable to grow on benzophenone. However, biphenyl- or diphenylmethane-grown resting cell suspensions metabolized benzophenone and produced a yellow *meta*-fission metabolite which was detected within minutes after substrate addition. Two metabolites (see **Figure 5.3B**) with similar spectral features were detected by GC-MS analysis of their TMS derivatives ($m/z = 390$ (M^+), $m/z = 375$ ($M^+ - CH_3$), $m/z = 347$ ($M^+ - CH_3 - CO$), $m/z = 273$ ($M^+ - COO(CH_3)_3Si$), $m/z = 258$ ($M^+ - COO(CH_3)_3Si - CH_3$), $m/z = 184$ ($M^+ - COO(CH_3)_3Si - O(CH_3)_3Si$)) (**Figure 5S2** in the supplemental material) and their concentrations increased steadily between 5 min and 30 min of incubation (not shown). These metabolites were tentatively identified as isomers of 2-hydroxy-6,7-dioxo-7-phenylheptanoic acid (7-phenyl DODA) that should be expected from the *meta*-fission of 2,3-dihydroxybenzophenone. Although the formation of isomers of the *meta*-fission products resulting from BphC reaction has been reported in several other investigations (17, 189, 205), their mechanism of formation has not yet been elucidated. However, as proposed previously (189) for the *meta*-fission products of chlorobiphenyls, these isomers may be generated during the oxidative cleavage of catechol where the formation of C-7 keto next to the phenyl ring and C-1 carboxylic functions may promote the isomerization of the double bonds at C-2 and C4.

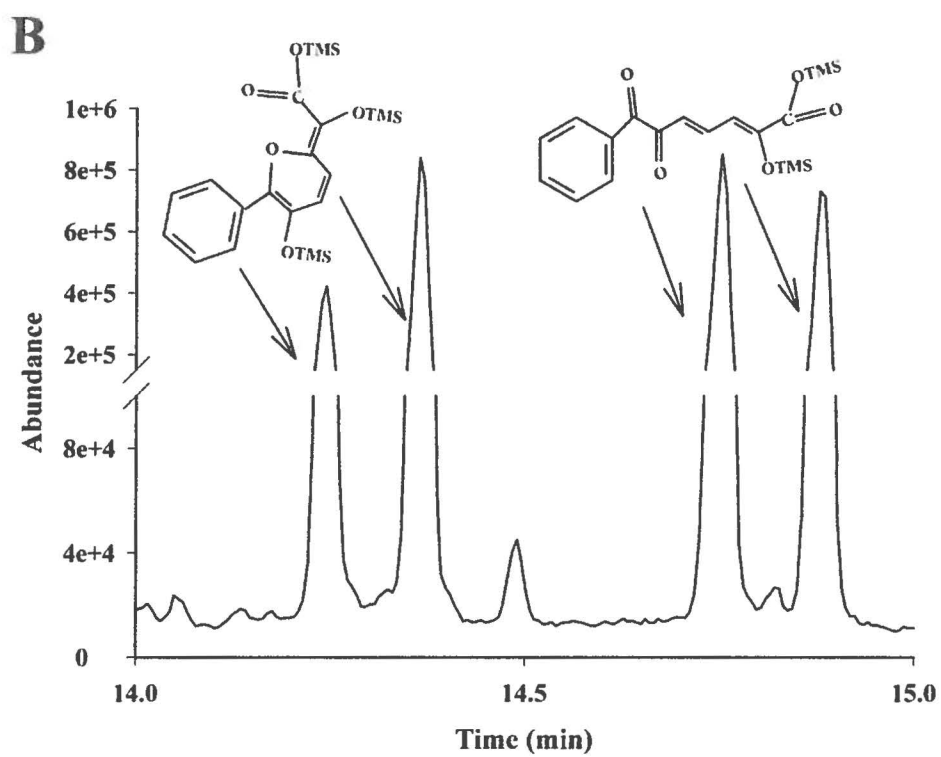
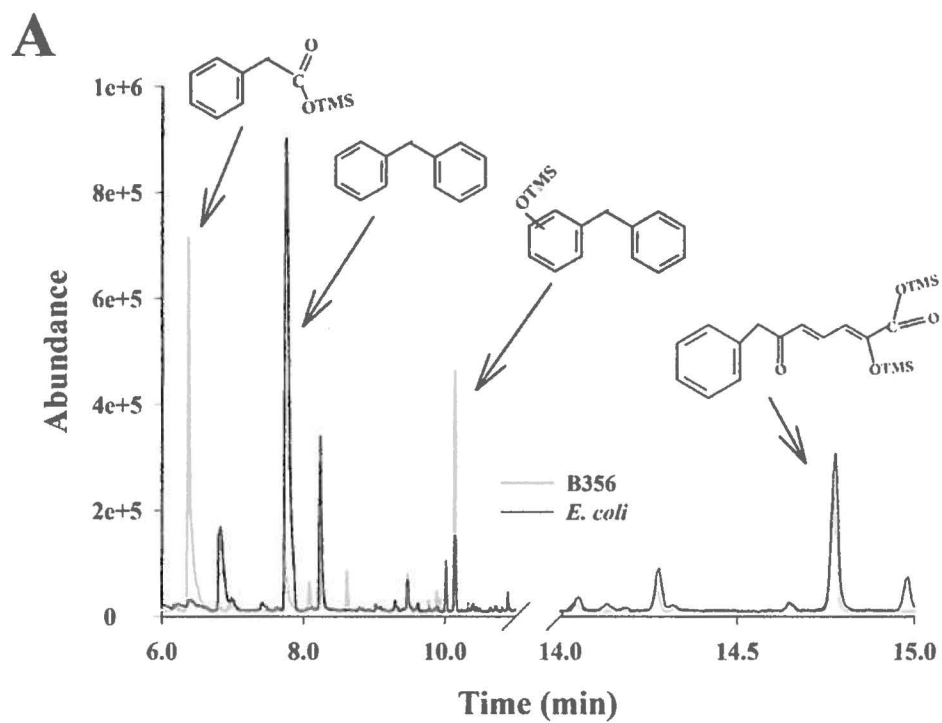


Figure 5.3: Total ion chromatograms of (A) Acidic metabolites detected in 22-h-old cultures of strain B356 grown on diphenylmethane (black line) or in resting cell suspensions of *E. coli* carrying plasmids pQE31[B356-*bphAE*] plus pYH31[LB400-*bphFGBC*] incubated 30 min with diphenylmethane (grey line); (B) Acidic metabolites produced by a suspension of biphenyl-induced cells of strain B356 incubated for 60 min with benzophenone. The protocols are described in the Materials and Methods. Shown are the peak of the TMS-treated metabolites that were identified from their mass spectral features. The unlabelled peaks were also detected in controls unexposed to the substrate. OTMS, trimethylsilyl-oxygen complex.

No 2,3-dioxo-3-phenylpropanoic acid, which presumed is the metabolite produced from 7-phenyl DODA by the phenyl-HODA hydrolase (BphD), was detected, even after 1 h incubation in the presence of the substrate. Therefore, we were unable to obtain evidence that benzophenone metabolism goes beyond the *meta*-fission reaction. On the other hand, two metabolites (**Figure 5.3B**) that exhibited spectral features that could correspond to pyranol isomers ($m/z = 462$ (M^+), $m/z = 447$ ($M^+ - CO$), $m/z = 419$ ($M^+ - CH_3 - CO$), $m/z = 345$ ($M^+ - COO(CH_3)_3Si$)) (**Figure 5.3B**, also see **Figure 5S3** in the supplemental material for the spectrum) were detected. These pyranol isomers may have been generated from a cyclization reaction through intramolecular rearrangements. At this time, there is no documented evidence of spontaneous tautomerization or cyclization of phenyl HODAs. The fact that the same metabolites were produced by an IPTG-induced resting cell suspension of a 1:1 mixture of recombinant *E. coli* pQE31[B356-*bphAE*] + pYH31[LB400-*bphFGB*] plus *E. coli* pQE31[B356-*bphC*] (not shown) suggest they were produced spontaneously from 7-phenyl DODA in the cell suspensions or during the TMS reaction. However, we cannot exclude other mechanisms of formation involving unspecific enzymatic reactions occurring in both strain B356 and *E. coli*. Therefore, their production remains unexplained at this time.

5.8.3. Metabolism of diphenylmethane by purified BphAE_{B356}, BphAE_{LB400}, and BphAE_{p4}

To confirm that the biphenyl catabolic enzymes of strain B356 metabolize diphenylmethane efficiently, we have examined the catalytic properties of BphAE_{B356} toward diphenylmethane, and we have compared them with those of BphAE_{LB400} and BphAE_{p4}. GC-MS analysis of the *n*BuB-treated diphenylmethane metabolites revealed two metabolites

(Figure 5.4A). Since *n*BuB reacts only with vicinal hydroxyl groups, the mass spectral features (see Figure 5S4 in the supplemental material) of the major metabolite (m/z 268 (M^+), and m/z 211 ($M^+ - n\text{Bu}$), 184 ($M^+ - n\text{BuBO}$), 177 ($M^+ - \text{C}_7\text{H}_7$), 168 ($M^+ - n\text{BuBO}_2$) and 156 ($M^+ - n\text{BuBO} - \text{CO}$) must correspond to a dihydrodiol. Docking experiments (see below) suggested the oxygenation occurred on the *ortho-meta* carbons. Therefore, on the basis of its mass spectral features, the major metabolite was tentatively identified as the 3-benzylcyclohexa-3,5-diene-1,2-diol.

The minor metabolite contains two pairs of vicinal hydroxyl groups (Figure 5.4A). This metabolite presumably was generated from the catalytic *ortho-meta* hydroxylation of the non hydroxylated ring of 3-benzylcyclohexa-3,5-diene-1,2-diol. It was tentatively identified as 3-[(5,6-dihydroxycyclohexa-1,3-dien-1-yl)methyl]cyclohexa-3,5-diene-1,2-diol showing ions at m/z 368 (M^+), 284 ($M^+ - n\text{BuBO}$), 200 ($M^+ - n\text{BuBO} - n\text{BuBO}$), 184 ($M^+ - n\text{BuBO} - n\text{BuBO}_2$), 177 ($M^+ - n\text{BuBO}_2 - \text{C}_7\text{H}_7$), 168 ($M^+ - n\text{BuBO}_2 - n\text{BuBO}_2$) and 156 ($M^+ - n\text{BuBO}_2 - n\text{BuBO} - \text{CO}$) (see Figure 5S5 in the supplemental material). The fragmentation ion at m/z 177 provides evidence that both rings were oxidized.

The production of 3-benzylcyclohexa-3,5-diene-1,2-diol and 3-[(5,6-dihydroxycyclohexa-1,3-dien-1-yl)methyl]cyclohexa-3,5-diene-1,2-diol as sole products of the B356 BPDO reaction was confirmed by the fact that a coupled reaction composed of purified preparations of BphAE_{B356} plus BphB_{B356} generated two metabolites. On the basis of the mass spectra of their TMS derivatives, the major one was identified as 2,3-dihydroxydiphenylmethane (3-benzylbenzene-1,2-diol) and the minor one as 2,2',3,3'-tetrahydroxydiphenylmethane (3-[(2,3-dihydroxyphenyl)methyl]benzene-1,2-diol) (Figure 5.4B). The diagnostically important ions for the TMS-derived 2,3-dihydroxydiphenylmethane (see Figure 5S6 in the supplemental material) comprise the molecular ion at m/z 344 and fragmentation ions at m/z 329 ($M^+ - \text{CH}_3$), 271 ($M^+ - (\text{CH}_3)_3\text{Si}$), 255 ($M^+ - \text{O}(\text{CH}_3)_3\text{Si}$), 225 ($M^+ - \text{O}(\text{CH}_3)_3\text{Si} - (\text{CH}_3)_2$). For the TMS-derived 2,2',3,3'-tetrahydroxydiphenylmethane (see Figure 5S7 in the supplemental material), they are m/z 520 (M^+) and 505 ($M^+ - \text{CH}_3$), 447 ($M^+ - (\text{CH}_3)_3\text{Si}$), 431 ($M^+ - \text{O}(\text{CH}_3)_3\text{Si}$), 342 ($M^+ - \text{O}(\text{CH}_3)_3\text{Si} - \text{O}(\text{CH}_3)_3\text{Si}$), 312 ($M^+ - \text{O}(\text{CH}_3)_3\text{Si} - \text{O}(\text{CH}_3)_3\text{Si} - (\text{CH}_3)_2$), 253 ($M^+ - \text{O}(\text{CH}_3)_3\text{Si} - \text{O}(\text{CH}_3)_3\text{Si} - \text{O}(\text{CH}_3)_3\text{Si}$). The vicinity of the two hydroxyl groups in these metabolites was confirmed by the mass spectra of the *n*BuB derivatives (not shown).

When BphAE_{LB400} was incubated for 10 min with the substrate, it produced approximately the same amount of 3-benzylcyclohexa-3,5-diene-1,2-diol from diphenylmethane as BphAE_{B356}, but no 3-[(5,6-dihydroxycyclohexa-1,3-dien-1-yl)methyl]cyclohexa-3,5-diene-1,2-diol was produced (Figure 5.4A). The metabolic pattern of BphAE_{p4} toward diphenylmethane was very similar to that of the parental enzyme BphAE_{LB400} (not shown). Therefore, BphAE_{B356} was the only one of the three enzymes to further oxidizes the dihydroxylated metabolite.

The steady-state kinetic parameters of purified preparations of BphAE_{B356}, BphAE_{p4}, and BphAE_{LB400} toward diphenylmethane were calculated from the initial oxygen consumption, and they were consistent with the GC-MS analysis. Diphenylmethane was as good a substrate as biphenyl for all three enzymes. Thus, the k_{cat} and k_{cat}/K_m values for BphAE_{B356} (Table 5.2) were in the range reported for biphenyl (4.3 s^{-1} and $63 \times 10^3 \text{ M}^{-1} \text{ s}^{-1}$, respectively) (169) when this enzyme was used under the same reaction conditions. Similarly, the k_{cat} and k_{cat}/K_m values for BphAE_{LB400} and for BphAE_{p4} (Table 5.2) were very close to those obtained when biphenyl was the substrate and the reactions run under identical conditions (the reported values were 0.9 s^{-1} and $41 \times 10^3 \text{ M}^{-1} \text{ s}^{-1}$ for BphAE_{LB400}, respectively and 1.0 s^{-1} and $31 \times 10^3 \text{ M}^{-1} \text{ s}^{-1}$ for BphAE_{p4}, respectively) (206).

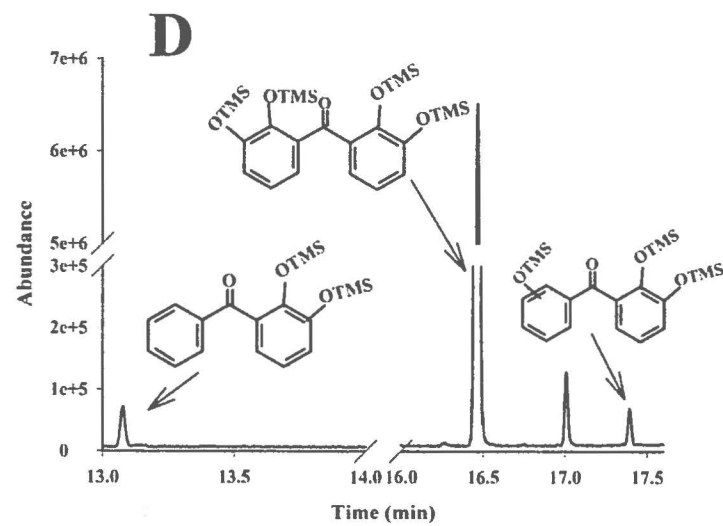
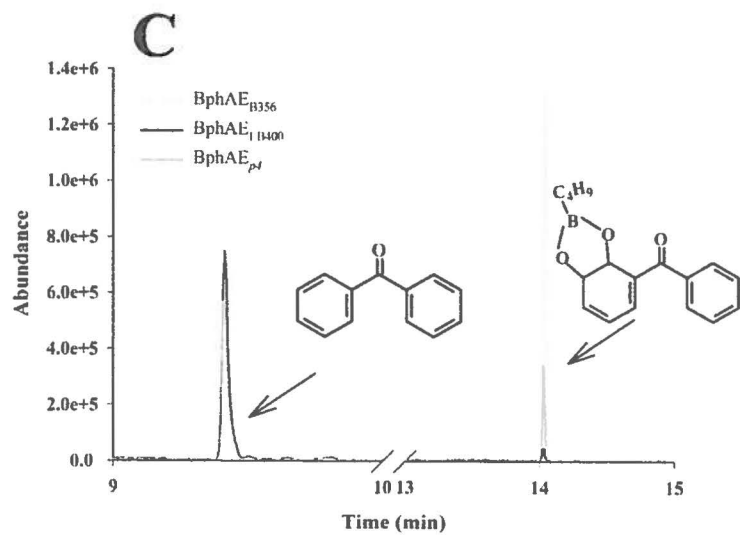
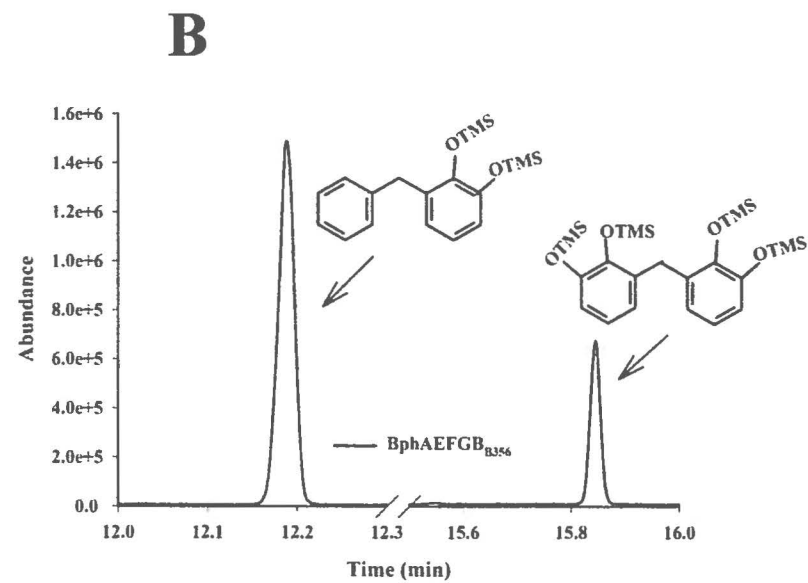
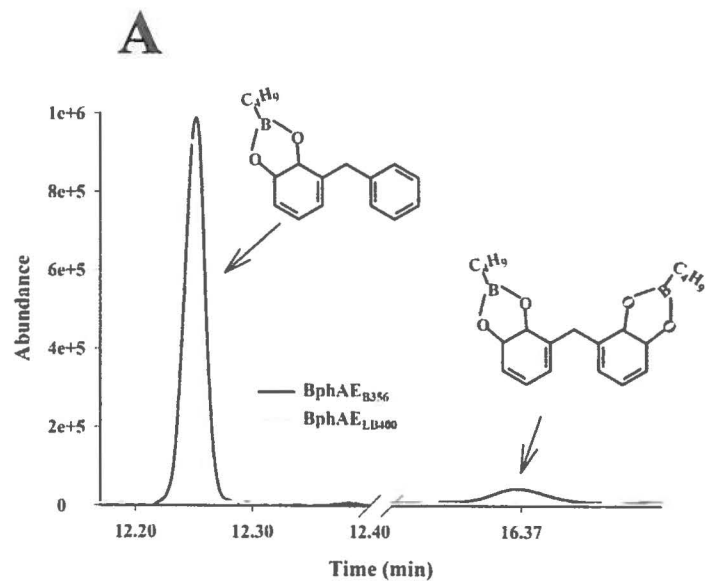


Figure 5.4: Total ion chromatograms of metabolites produced from diphenylmethane (A) By purified preparations of BphAE_{B356} (black line) and BphAE_{LB400} (grey line); (B) By a coupled reaction composed of purified BphAE_{B356} + BphB_{B356}; (C) Total ion chromatograms of metabolites produced from benzophenone by purified preparations of BphAE_{B356} (light grey line), BphAE_{LB400} (black line) and BphAE_{p4} (dark grey line); (D) Total ion chromatograms of metabolites produced from benzophenone by a coupled reaction composed of purified BphAE_{B356} plus BphB_{B356}. The procedures to purify the enzymes, to set up the reactions, and to extract the metabolites for GC-MS analysis are described in the Materials and Methods. Shown are the peaks of *n*BuB- or TMS-treated metabolites that were identified from their mass spectral features. The unlabelled peaks were also present in controls unexposed to the substrate.

Table 5.2: Steady-state kinetic parameters^a of BphAE_{B356}, BphAE_{LB400}, and BphAE_{p4} toward diphenylmethane and benzophenone

Substrate	Enzyme	K_m (μ M)	k_{cat} (s^{-1})	k_{cat}/K_m ($10^3 \cdot M^{-1} \cdot s^{-1}$)
Diphenylmethane	BphAE _{B356}	63.0 (5.6)	8.9 (0.3)	141.3 (7.5)
	BphAE _{LB400}	15.4 (1.1)	1.0 (0.1)	64.9 (2.7)
	BphAE _{p4}	17.9 (2.2)	1.6 (0.1)	89.4 (5.5)
Benzophenone	BphAE _{B356}	65.3 (8.5)	1.2 (0.2)	18.4 (0.6)
	BphAE _{LB400}	ND ^b	ND	ND
	BphAE _{p4}	9.1 (2.1)	0.1 (0.0)	11.0 (1.6)

^a The steady-states kinetics were determined from the oxygen consumption rates as described in the Materials and Methods. The values are results \pm standard deviations from three independently produced enzyme preparations.

^b ND, not determined; the metabolism was too slow to determine values accurately.

5.8.4. Benzophenone metabolism by purified BphAE_{B356}, BphAE_{LB400}, and BphAE_{p4}

Unlike diphenylmethane, benzophenone is metabolized differently by BphAE_{B356} and BphAE_{LB400}. A purified preparation of BphAE_{B356} completely oxidized 50 nmol benzophenone in 10 min to generate a single metabolite (**Figure 5.4C**), tentatively identified as 3-benzoylcyclohexa-3,5-diene-1,2-diol from the GC-MS spectrum of its *n*BuB derivative (see **Figure 5S8** in the supplemental material) (ions at m/z 282 (M^+) and at 225 ($M^+ - nBu$), 198 ($M^+ - nBuBO$), 182 ($M^+ - nBuBO_2$) and 170 ($M^+ - nBuBO - CO$). Under the same conditions, BphAE_{LB400} and BphAE_{p4} oxidized only a fraction of the added 50 nmol benzophenone, but both enzymes produced the same metabolite as BphAE_{B356} (**Figure 5.4C**). This is consistent with the steady-state kinetics shown in **Table 5.2**, where the turnover rate of reaction of BphAE_{B356} toward benzophenone was 12 times higher than that for BphAE_{p4}, and the turnover rate of reaction of BphAE_{LB400} was too low to obtain reliable values.

When BphB_{B356} was used to oxidize 3-benzoylcyclohexa-3,5-diene-1,2-diol, 2,3-dihydroxybenzophenone was produced (not shown) and was identified from the GC-MS spectral features of its TMS derivative (ions at m/z 358 (M^+) and m/z 343 ($M^+ - CH_3$), 270 ($M^+ - (CH_3)_4Si$) and 212 ($M^+ - (CH_3)_4Si - (CH_3)_2Si$) (see **Figure 5S9** in the supplemental material).

Remarkably, when benzophenone at a concentration of 50 nmol was the substrate for the coupled reaction composed of BphAE_{B356} plus BphB_{B356}, it was almost completely metabolized to 2,2',3,3'-tetrahydroxybenzophenone (**Figure 5.4D**), which was identified from its GC-MS and NMR spectra. The other two metabolites, 2,3-dihydroxybenzophenone and 2,2',3- or 2,3,3'-trihydroxybenzophenone, represented less than 1% of total metabolites produced by this reaction. The spectral features of the TMS-treated major metabolite (see **Figure 5S10** in the supplemental material) was comprised of a molecular ion at m/z 534 plus fragmentation ions at m/z 519 ($M^+ - CH_3$), 446 ($M^+ - (CH_3)_4Si$), and 358 ($M^+ - (CH_3)_4Si - (CH_3)_4Si$). The position of the hydroxyl groups was confirmed by NMR analysis. The spectrum showed only three signals for six protons between 6.80 and 7.10 ppm. This indicates that there are two identical aromatic rings, and each one contains 3 protons. The chemical shifts for the protons labeled H₄, H₅ and H₆ in **Figure 5.5** were recorded at 6.824 ppm (triplet) (H₅), at 7.096 (doublet of doublets) and 6.969 (doublet of doublets) (H₄ and H₆). The coupling constant between the three protons (**Figure 5.5**) and the shape of the peaks (1

triplet and 2 doublet of doublets) revealed that the 3 protons of each aromatic ring were vicinal to each other. With this in mind, the only possibility for the structure of the metabolite was 2,2',3,3'-tetrahydroxybenzophenone.

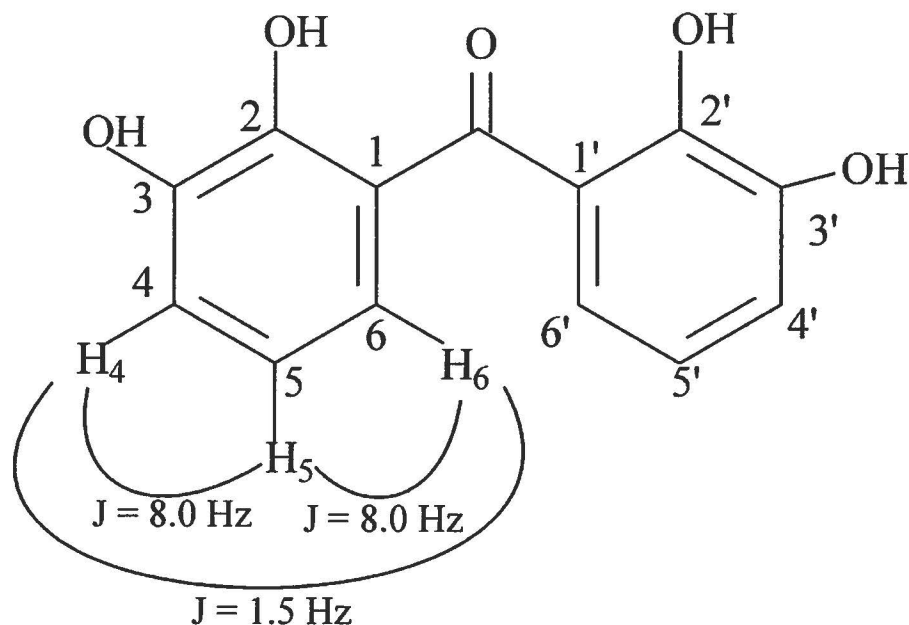


Figure 5.5: Structural features of the hydroxylated metabolites obtained from benzophenone by the coupled reaction of BphAE_{B356} plus BphB_{B356}, which was identified as 2,2',3,3'-tetrahydroxybenzophenone by NMR analysis.

5.8.5. Docking experiments with diphenylmethane and benzophenone

We docked diphenylmethane and benzophenone in the substrate-bound form of BphAE_{B356} and BphAE_{LB400} after removing biphenyl. For both substrates, the conformation of the top-ranked docked molecules in BphAE_{B356} exhibited an orientation that would enable an oxygenation of the *ortho-meta* carbons of the phenyl ring. In both cases, the *ortho-meta* carbons closely aligned with carbons 2 and 3 of the oxidized ring of biphenyl in the complexed form (**Figure 5.6A and B**). This suggests BphAE_{B356} produces 3-benzylcyclohexa-3,5-diene-1,2-diol from diphenylmethane and 3-benzoylcyclohexa-3,5-diene-1,2-diol from benzophenone, and it is consistent with the NMR spectral data that confirm that 2,2',3,3'-tetrahydroxybenzophenone was produced from benzophenone by the combined reaction of BphAE_{B356} plus BphB_{B356}.

As shown in **Figure 5.6A and B**, the conformation of benzophenone inside the catalytic pocket of BphAE_{B356} differs from that of diphenylmethane. Therefore, the carbonyl group strongly influences the interaction between the substrate and the amino acid residues that line the catalytic pocket. However, the *ortho-meta* carbons of the docked benzophenone aligned very well with the reactive carbons of biphenyl in the biphenyl-bound form of BphAE_{B356} (**Figure 5.6A**). In the case of BphAE_{LB400}, the top-ranked conformations for benzophenone were at a distance from the catalytic iron that may have allowed catalytic hydroxylation (**Figure 5.6C**). However, the reactive ring did not align as well as for BphAE_{B356} with the reactive ring of biphenyl, and this may explain why BphAE_{LB400} catalyzed the oxygenation of benzophenone poorly. On the other hand, we cannot exclude the possibility that other types of interactions between protein structures and the substrate, which could not be reproduced in the docking experiments, prevent its productive binding to BphAE_{LB400} catalytic pocket. Since the conformation of benzophenone in the docked BphAE_{B356} structure appears to be more favorable for the catalytic reaction, we have superposed the benzophenone docked structure of BphAE_{B356} on the structure of the biphenyl-bound BphAE_{LB400} after biphenyl removal (**Figure 5.6D**). As shown in the figure, the benzophenone carbonyl oxygen was very close to both Gly321 and Phe336 of BphAE_{LB400}. Therefore, in this conformation of the substrate, the proximity of these two residues relative to the carbonyl oxygen may hinder proper binding. This is consistent with previous observations (165, 169) where Gly321 and Phe336, two residues lining the catalytic pocket, appeared to play a significant role in binding substrate's analogs. It is also consistent with the observation that BphAE_{p4}, the doubly substituted Thr335Ala/Phe336Met mutant of BphAE_{LB400} metabolized benzophenone more efficiently than its parent (**Table 5.2**). In this case, the Thr335Ala mutation releases constraints imposed by Thr335 on Gly321 allowing movement of its carbonyl group during substrate binding to create more space to accommodate larger substrates.

On the other hand, in the case of 2,3-dihydroxybenzophenone, none of the 20 top-ranked conformations of the docked substrate were at a distance from BphAE_{B356} catalytic iron that could have allowed a catalytic reaction. Therefore, perhaps structural features, involving an induced-fit mechanism that the docking experiment could not reproduce are required to allow productive binding of this substrate to the catalytic pocket of BphAE_{B356}.

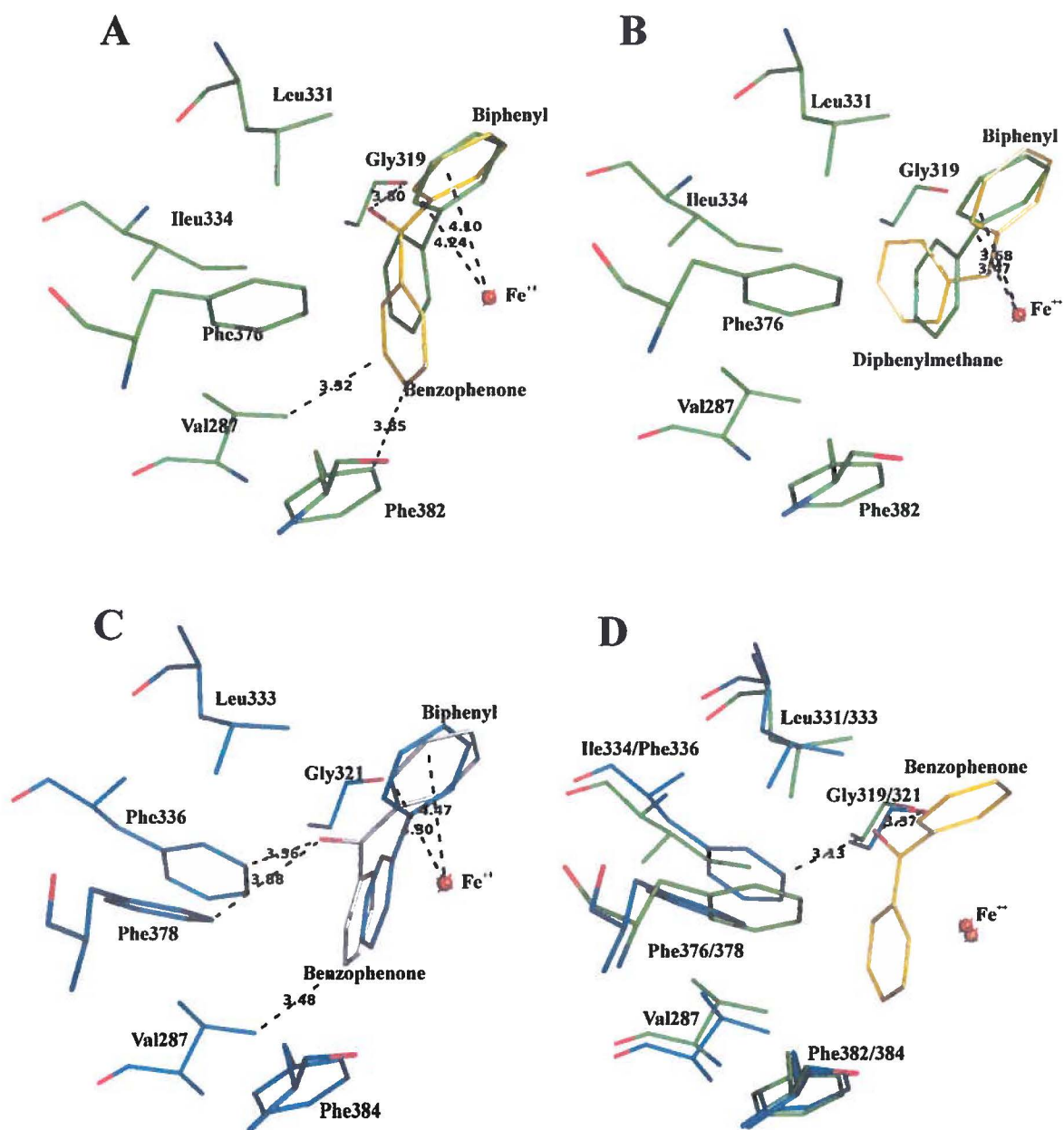


Figure 5.6: (A) Superposition of catalytic center residues of benzophenone-docked (yellow) and biphenyl-bound (green) forms of BphAE_{B356}. (B) Superposition of catalytic center residues of diphenylmethane-docked (yellow) and biphenyl-bound (green) forms of BphAE_{B356}. (C) Superposition of catalytic center residues of benzophenone-docked (white) and biphenyl-bound (blue) forms of BphAE_{LB400}. (D) Superposition of the biphenyl-bound form of BphAE_{LB400} (blue) after removal of biphenyl substrate and the benzophenone-docked (yellow) BphAE_{B356} (green). The oxygen atoms are in red.

5.9. Discussion

Unlike *B. xenovorans* LB400, *P. pnomenusa* B356 grew remarkably well on diphenylmethane, and many observations made in this work are supportive of the idea that it was metabolized by the enzymes of the biphenyl catabolic pathway to produce phenylacetate, which was further metabolized by a lower pathway. Cells of strain B356 produced the same metabolites from diphenylmethane during their growth on this substrate as those isolated from enzymes of the biphenyl catabolic pathway (Figure 5.7). Furthermore, the kinetic parameters of BphAE_{B356} toward diphenylmethane were in same range as those for biphenyl, suggesting this enzyme metabolizes diphenylmethane during growth on this substrate. It is noteworthy that when purified preparations of B356 BPDO or B356 BPDO plus BphB_{B356} were used to metabolize diphenylmethane, significant amount of tetrahydroxylated metabolites were detected in the reaction medium. However, the tetrahydroxylated metabolites were present in very small amount in cultures of B356 growing on diphenylmethane (not shown). This shows that during growth of strain B356 on diphenylmethane, 3-benzylcyclohexa-3,5-diene-1,2-diol and subsequent metabolites were oxidized very efficiently by the downstream enzymes of the catabolic pathway, thus preventing further BPDO oxidation of the dihydrodiol and the catechol metabolites.

Judging by its steady-state kinetics toward diphenylmethane, BphAE_{LB400} metabolized this substrate as well as biphenyl. In addition, we found that BphC_{LB400} catalyzed the ring-cleavage of 2,3-dihydroxydiphenylmethane and the strain grew well on phenylacetate. However, unlike strain B356, cells of strain LB400 grown cometabolically on diphenylmethane plus sodium acetate were unable to metabolize 4-chlorobiphenyl, showing that diphenylmethane did not induce the biphenyl catabolic pathway of strain LB400. Therefore, the inability of diphenylmethane to induce the biphenyl catabolic pathway in strain LB400 most likely is the reason why this strain is unable to grow on this substrate.

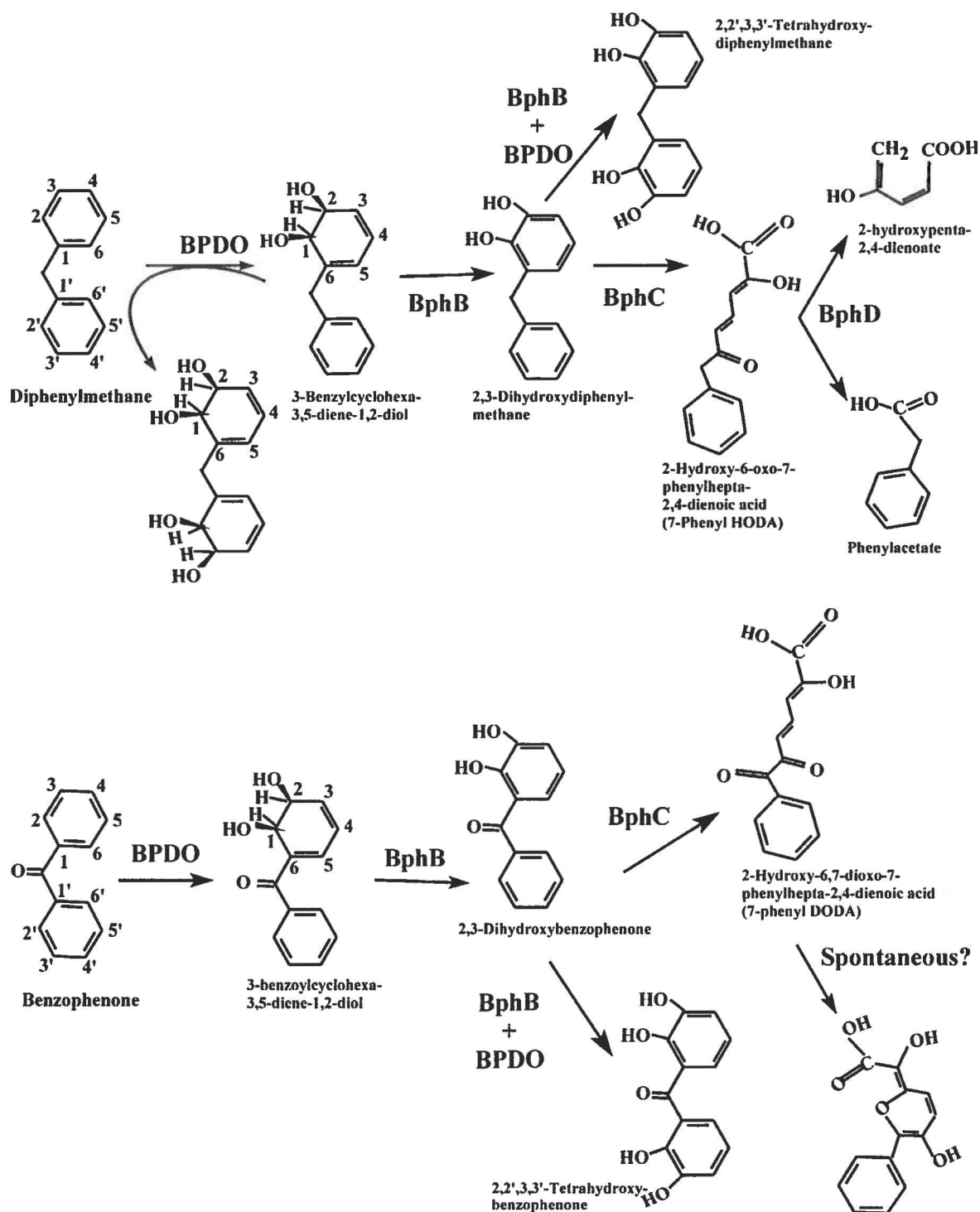


Figure 5.7: Profile of metabolites generated during the oxidation of diphenylmethane (upper) or benzophenone (lower) by diphenylmethane- or biphenyl-induced cells of strain B356 or by isolated enzymes of its biphenyl catabolic pathway.

Growth kinetics data provided strong evidence that both diphenylmethane and biphenyl induced the same catabolic enzymes during growth of strain B356. Uninduced cells grew poorly on diphenylmethane or biphenyl, which was the case when the inocula were prepared by growing the cells on sodium acetate. However, interchanging the growth substrates to prepare the inocula did not affect the growth kinetics on diphenylmethane or on biphenyl, which strongly suggests that both substrates induced the same catabolic pathway.

Remarkably, although further work will be needed to confirm the conclusion, data suggest that a benzoate pathway is induced when cells are grown on diphenylmethane. This was supported by the fact that 3-chlorobenzoate strongly inhibited growth on diphenylmethane. Based on a previous report (297), in order to inhibit growth on biphenyl, 3-chlorobenzoate must be converted to 3-chlorocatechol, which is a very potent inhibitor of BphC. In this study, we have not elucidated the enzymatic steps involved in phenylacetate catabolism during growth of strain B356 on diphenylmethane. However, since phenylacetate is a key metabolite in the metabolism of many aromatic chemicals, including phenylalanine, most bacteria have the ability to metabolize it through a pathway that proceeds via the formation of a Coenzyme A-thioester derivative (328). Strain LB400 can metabolize 3- and 4-hydroxyphenylacetate through the homogentisate pathway (249), but the ability of this strain to metabolize phenylacetate through this pathway has not been demonstrated. Focht and Alexander (81, 82) have described a *Hydrogenomonas* isolate that metabolizes diphenylmethane through a pathway that presumably involves the meta-cleavage of a catechol metabolite, which is further metabolized to generate phenylacetate. Since cells grown on diphenylmethane readily metabolized homogentisate, they postulated that phenylacetate was metabolized via a homogentisic pathway in that *Hydrogenomonas* strain. However, neither the phenylacetyl-coenzyme A, nor the homogentisate pathway involves production of a 2,3-catechol derivative, as is the case for the metabolism of benzoic acid in strain B356. Therefore, the growth inhibition caused by 3-chlorobenzoate suggests that diphenylmethane or one of its metabolites induces a pathway involving a benzoate 2,3-dioxygenase, namely, the biphenyl-associated benzoate pathway. Indeed, strain B356 carries two benzoate pathways, only one of which, the one induced when cells are grown on biphenyl, is able to produce 3-chlorocatechol from 3-chlorobenzoate (297).

Few investigations have assessed the ability of the bacterial biphenyl catabolic enzymes to metabolize diphenylmethane or one of its derivatives, such as DDT or 1,1-

dichloro-2,2-(4-chlorophenyl)ethane (DDD) (114, 115, 169, 202, 213), but no studies have examined the ability of biphenyl-degrading bacteria to grow on diphenylmethane. Therefore, strain B356 might not be the only one with the ability to use the biphenyl catabolic pathway to grow on this substrate.

Neither strain B356 nor LB400 could use benzophenone as growth substrate; however, BphAE_{B356} metabolized this diphenylmethane analog significantly more efficiently than BphAE_{LB400}. Structural analysis of the docked substrate showed that residues Phe336 and Gly321 were partly responsible for preventing productive binding of this substrate with BphAE_{LB400}. Structural analyses of substrate-bound crystals and docking experiments have shown that the combined effect of these two substitutions increases the space required in the catalytic pocket to accommodate bulkier substrates (165, 169). The replacement of Thr335 of BphAE_{LB400} by Gly333 in BphAE_{B356} produces a similar effect (169). However, other structural features that our docking experiments could not identify also may have an influence on the ability of the enzyme to metabolize this substrate, since, on the basis of their steady-state kinetics, BphAE_{B356} metabolized benzophenone more efficiently than BphAE_{p4}, which is a doubly substituted Thr335Ala/Phe336Met mutant of BphAE_{LB400}.

Generally, the investigations related to the biphenyl-degrading bacteria during the last 5 decades were initiated with the objective of designing a biological process to degrade PCBs and other chlorinated aromatics, such as chlorodibenzofurans (164, 238). These bacteria were obtained by enrichments on biphenyl, and traditionally it was believed that the four-enzymatic-step biphenyl pathway evolved in bacteria primarily to transform biphenyl into benzoic acid. However, data presented in the current and previous works (236) bring us to question this belief. Biphenyl is a naturally occurring chemical, but it is not universally distributed in nature. It is noteworthy that bacteria carrying the biphenyl catabolic pathway enzymes were obtained from pristine soils not exposed to biphenyl or chlorobiphenyls (344).

On the basis of their primary amino acid sequence, BphAE_{B356} and BphAE_{LB400} belong to distinct phylogenetic clusters of BphAE (300, 344, 357). Recent data suggested that each has acquired a distinct PCB-degrading pattern (106, 300), as well as distinct abilities to metabolize simple flavonoids (236), DDT (169) or DDD (115). In this work, we found that BphAE_{B356} and BphAE_{LB400} metabolized diphenylmethane similarly but benzophenone and 2,3-dihydroxybenzophenone very differently. Furthermore, the fact that the biphenyl

catabolic pathway of strain B356 is inducible by diphenylmethane allows the strain to use it as growth substrate. As a result, under natural conditions, strain B356 has the potential to metabolize or cometabolize many chemicals that strain LB400 metabolizes poorly.

Although the enzymes of the peripheral pathways, such as those of the biphenyl catabolic pathway, have evolved to metabolize a broad range of substrates, on the basis of the observations made in this work and a previous one (236), we postulate that the biphenyl catabolic pathway enzymes have evolved divergently in bacteria, in such a way that each phylogenetic branch has specialized to play distinct ecophysiological functions with regard to chemicals naturally found in nature.

5.10. Acknowledgements

This work was supported by the Natural Sciences and Engineering Research Council of Canada (NSERC) (Grants #RGPIN/39579-2012). We thank Sameer Al-Abdul-Wahid, QANUC NMR Facility (McGill University, Montreal, Quebec, Canada) for his help in NMR analysis. We also thank Eric Déziel, INRS-Institut Armand-Frappier, for the use of his Bioscreen C system.

5.11. Supplemental materials

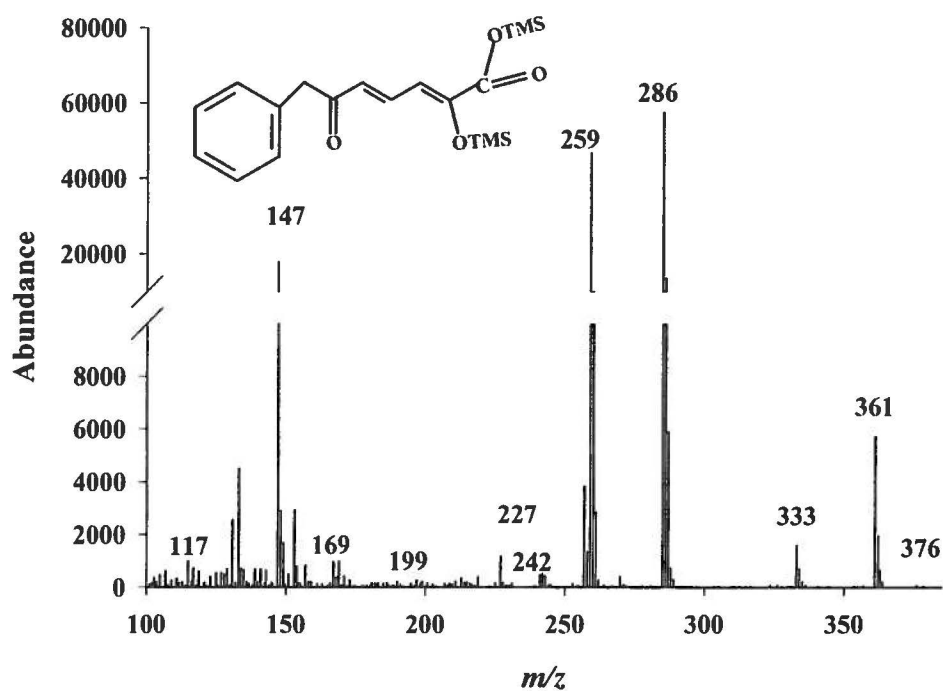


Figure 5S1: Mass spectrum of the TMS-derived acidic metabolite produced from diphenylmethane by cells of strain B356 grown on diphenylmethane. Based on spectral features, the metabolite was identified as 7-phenyl HODA.

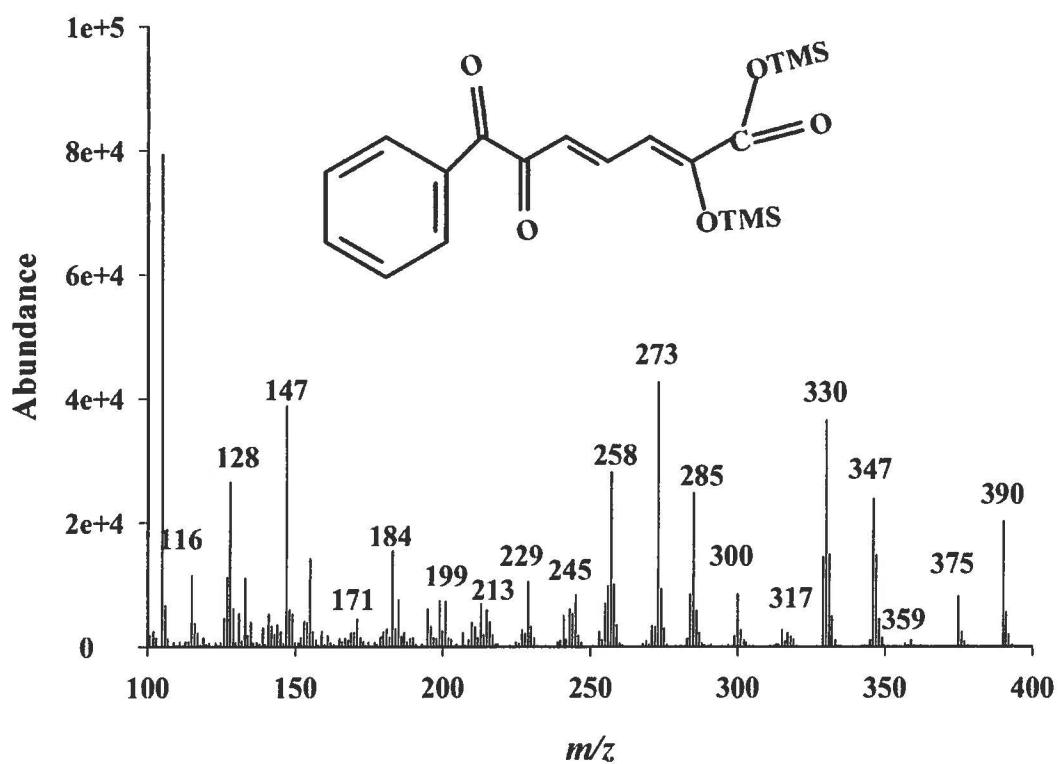


Figure 5S2: Mass spectrum of the TMS-derived acidic metabolite produced from benzophenone by biphenyl-induced cells of strain B356. Based on spectral features, the metabolite was identified as 7-phenyl DODA.

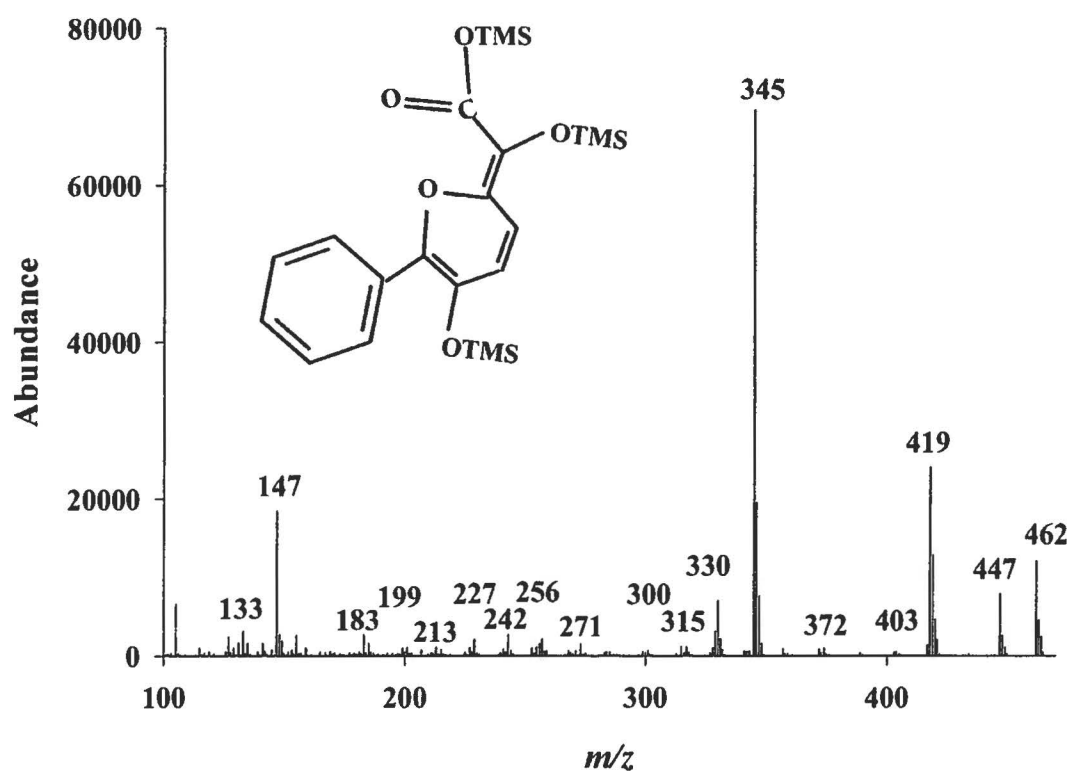


Figure 5S3: Mass spectrum of the TMS-derived acidic metabolite produced from benzophenone by biphenyl-induced cells of strain B356. Based on spectral features, the metabolite was identified as a pyranol presumedly generated from a cyclization reaction of 6,7-dioxo-7-phenylheptanoic acid.

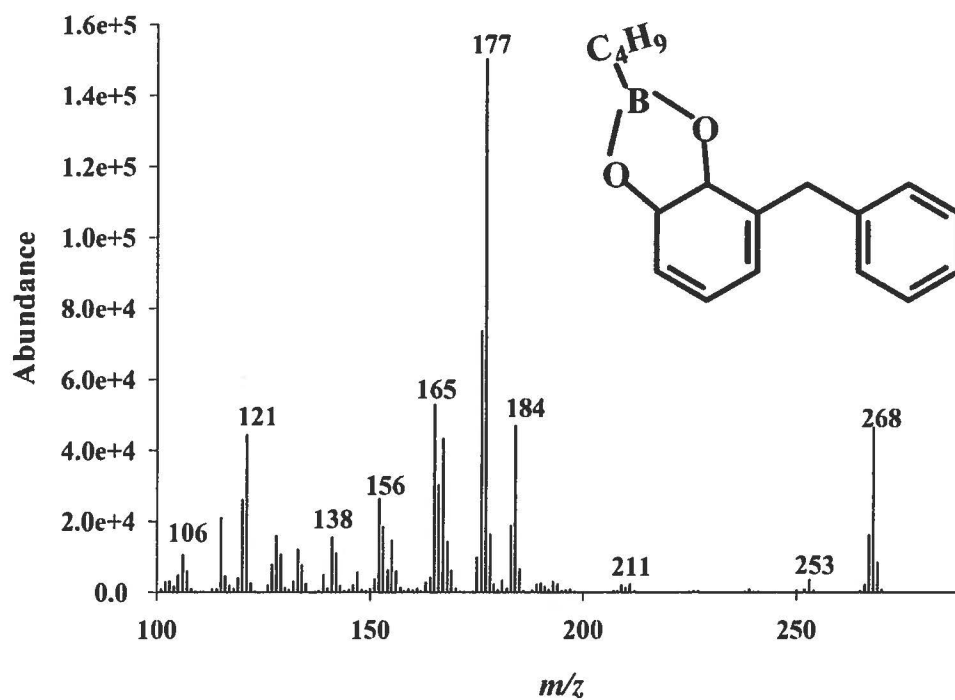


Figure 5S4: Mass spectrum of a *n*BuB-derived metabolite produced from diphenylmethane by BphAE_{B356}. Based on spectral features, the metabolite was identified as 3-benzylcyclohexa-3,5-diene-1,2-diol.

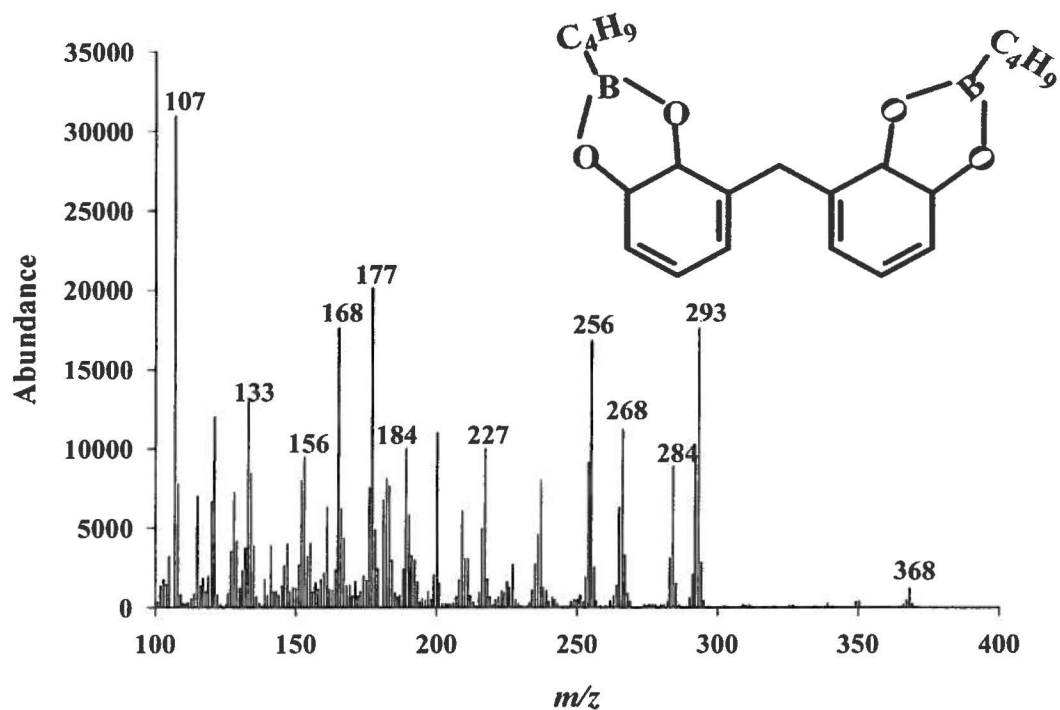


Figure 5S5: Mass spectrum of a *n*BuB-derived metabolite produced from diphenylmethane by BphAE_{B356}. Based on spectral features, the metabolite was identified as 3-[(5,6-dihydroxycyclohexa-1,3-dien-1-yl)methyl]cyclohexa-3,5-diene-1,2-diol.

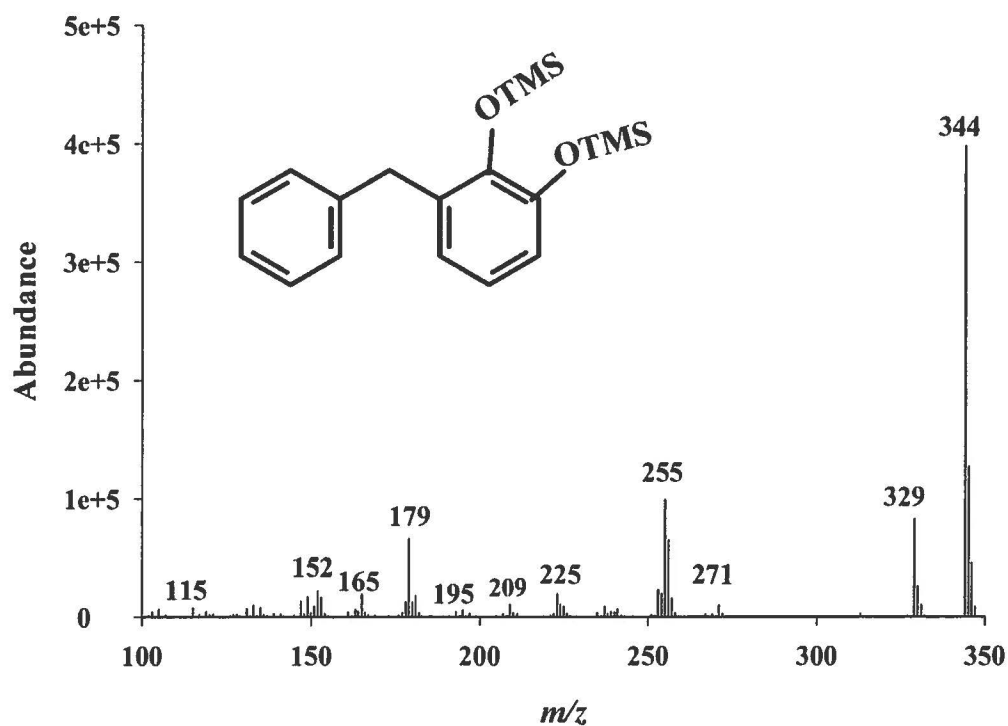


Figure 5S6: Mass spectrum of the TMS-derived major metabolite produced from diphenylmethane by a coupled reaction composed of purified preparations of BphAE_{B356} plus BphB_{B356}. Based on spectral features, the metabolite was identified as 2,3-dihydroxydiphenylmethane.

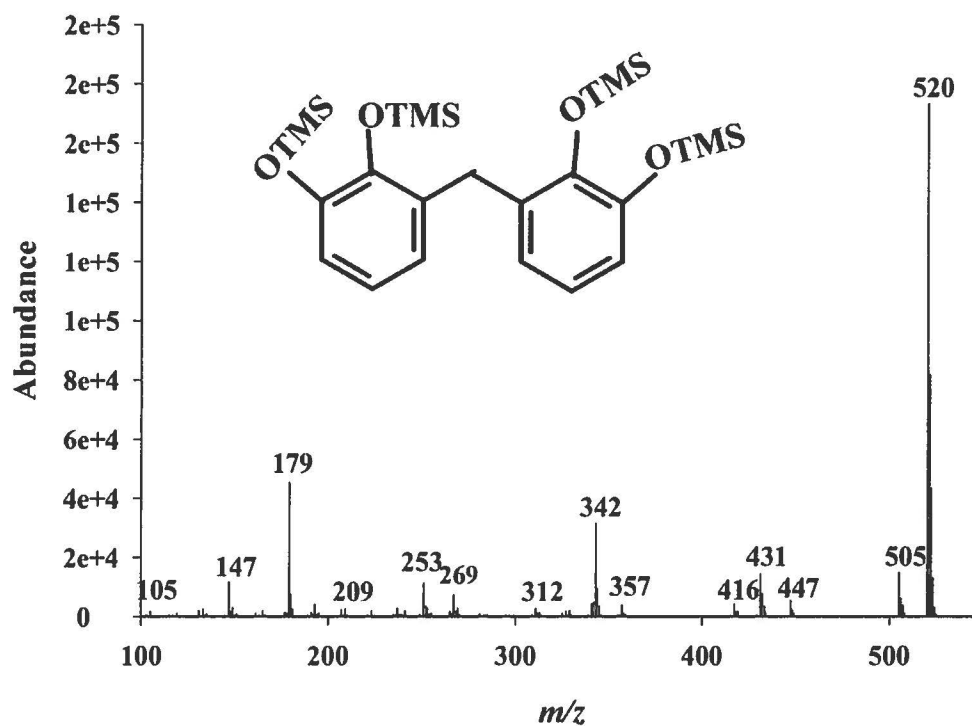


Figure 5S7: Mass spectrum of the TMS-derived minor metabolite produced from diphenylmethane by a coupled reaction composed of purified preparations of BphAE_{B356} plus BphB_{B356}. Based on spectral features, the metabolite was identified as 2,2',3,3'-tetrahydroxydiphenylmethane.

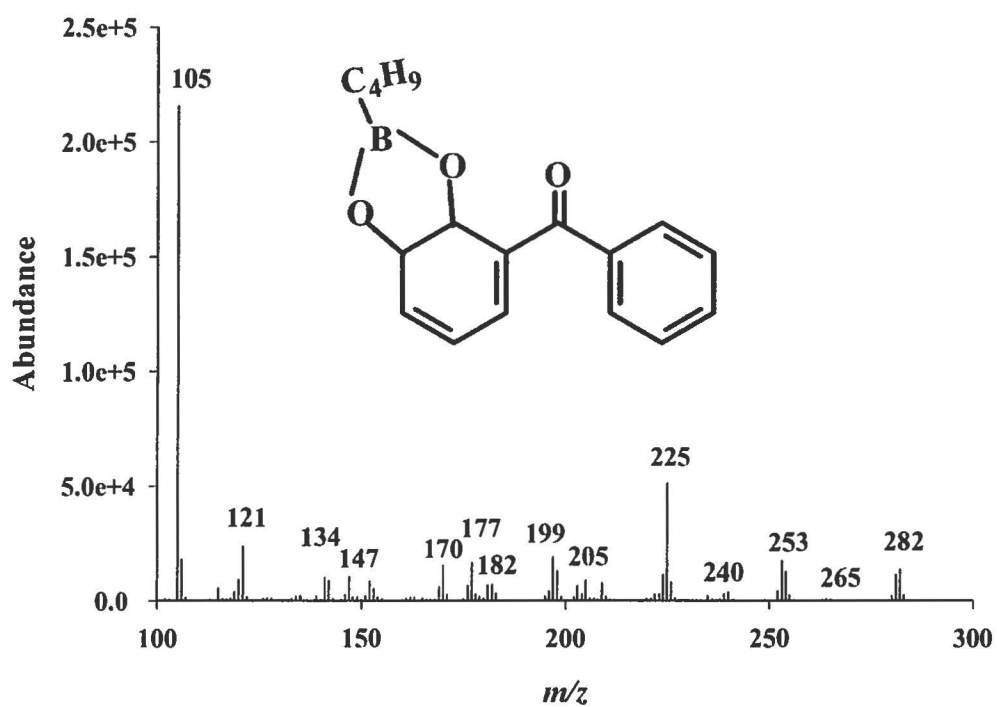


Figure 5S8: Mass spectrum of the *n*BuB-derived metabolite produced from benzophenone by a BphAE_{B356}. Based on spectral features, the metabolite was identified as 3-benzoylcyclohexa-3,5-diene-1,2-diol.

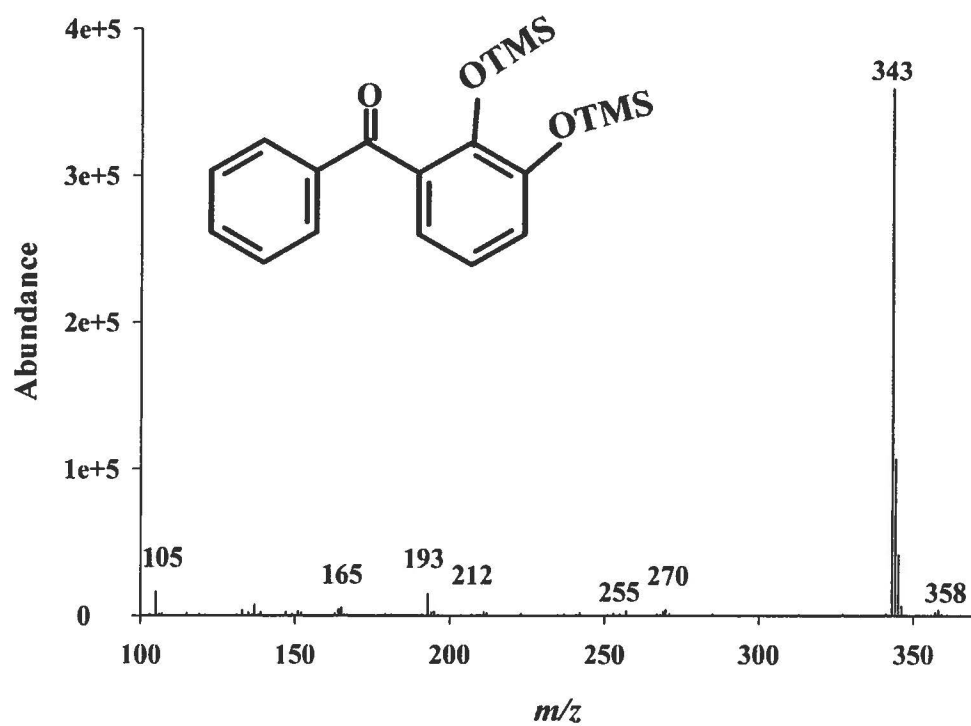


Figure 5S9: Mass spectrum of the TMS-derived metabolite produced from 3-benzoylcyclohexa-3,5-diene-1,2-diol by BphB_{B356}. Based on spectral features, the metabolite was identified as 2,3-dihydroxybenzophenone.

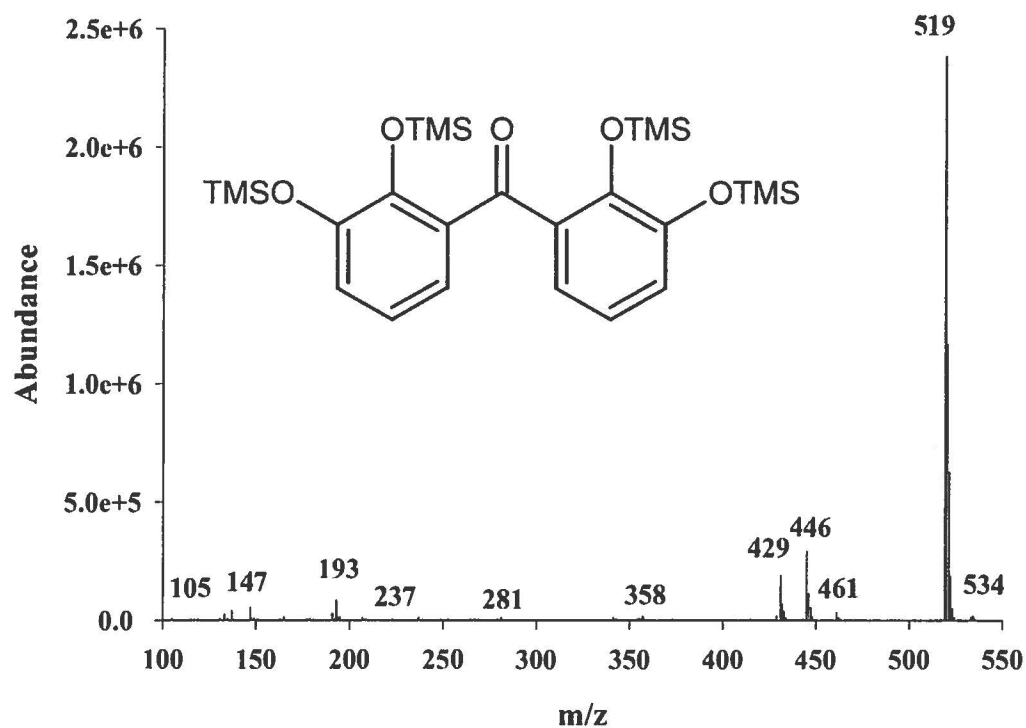


Figure 5S10: Mass spectrum of the TMS-derived major metabolite produced from benzophenone by a coupled reaction composed of purified preparations of BphAE_{B356} plus BphB_{B356}. Based on spectral features, the metabolite was identified as 2,2',3,3'-tetrahydroxybenzophenone.

6. Presentation of article 4

6.1. The context of the article

The ability of biphenyl catabolic pathway to degrade PCBs has been well investigated. However, few studies have paid attention to hydroxylated-PCBs, which may also be toxic and persistent, and therefore, their impacts may be as considerable on the ecosystem as PCBs. Hydroxylated-PCBs are key intermediates produced from PCBs and other xenobiotics such as chlorodibenzofurans, by the bacterial biphenyl catabolic enzymes or by plants enzymatic systems.

In this work, we investigated the ability of the biphenyl catabolic enzymes of *P. pnomenusa* B356 and *B. xenovorans* LB400 to transform hydroxylated-PCBs. We have determined the profile of metabolites generated from selected doubly *para*-substituted hydroxy-chlorobiphenyl by the biphenyl catabolic pathway of strain B356. We found that the dihydro-dihydroxy derivatives of doubly *para*-substituted hydroxy-chlorobiphenyls resulting from the BPDO reaction are prone to rearrangement or they are further transformed inside the catalytic pocket of the BPDO to generate unexpected metabolites. Some of these metabolites are not further degraded by downstream enzymes and they accumulate in the medium.

The results were presented in **Article 4** which was submitted to **Journal of biological chemistry**.

6.2. Contribution of the student to article 4

Results shown in this article were obtained in part by student and in part by Mohammad Sondossi (Prof. Weber State University, Utah). The analysis of the metabolites produced by the wild-type strains B356 and LB400 was made by M. Sondossi. The student planned and performed the experimental part done with the purified enzymes preparations. She purified the enzymes, performed the assays to identify the metabolites. She identified the metabolites by GC-MS analysis. She also purified and identified some of the metabolites by NMR spectroscopy. The NMR spectra were obtained at the QANUC NMR facility and they were interpreted by the student. The student also performed docking experiments with selected hydroxy-chlorobiphenyls. Structural analysis of the docked-enzymes was done by Michel Sylvestre. The article was written by the student and Michel Sylvestre and was verified by Mohammad Sondossi.

6.3. Article 4

The metabolism of doubly *para*-substituted hydroxychlorobiphenyls by bacterial biphenyl dioxygenases generates unexpected metabolites

Thi Thanh My Pham¹, Mohammad Sondossi^{2*} and Michel Sylvestre^{1*}

¹ Institut National de la Recherche Scientifique, INRS-Institut Armand-Frappier, Laval, QC H7V 1B7, Canada, ² Department of Microbiology, Weber State University, Ogden, Utah 84408

Running head: metabolites profile of *para*-hydroxychlorobiphenyls

Address correspondance to: Michel Sylvestre, Institut National de la Recherche Scientifique (INRS-Institut Armand-Frappier), Laval, Québec, H7V 1B7, Canada. 450-687-5010; FAX: 450-686-5501; E-mail: Michel.Sylvestre@iaf.inrs.ca; Mohammad Sondossi, Department of Microbiology, Weber State University, Ogden, Utah 84408, phone: (801) 626-6884; E-mail: msondossi@weber.edu

This article was submitted to Journal of biological chemistry

6.4. Résumé

Dans ce travail, nous avons déterminé le profil des métabolites produits à partir du 4,4'-dihydroxybiphényle, du 4-hydroxy-4'-chlorobiphényle, du 3-hydroxy-4,4'-dichlorobiphényle et du 3,3'-dihydroxy-4,4'-dichlorobiphényle par la souche *Pandoraea pnomenusa* B356 induite au biphényle et par sa biphényle dioxygenase. Lorsque les analogues du biphényle doublement substitués en position *para* servaient de substrats pour la réaction catalysée par la dioxygénase du biphényle de la souche B356, aucun des métabolites dihydrodihydroxy attendus n'a pas été détecté. Dans le cas du 4-hydroxy-4'-chlorobiphényle, les données suggèrent qu'il a été converti principalement en 3,4-dihydroxy-4'-chlorobiphényle qui a été ré-oxydé en 3,4,5-trihydroxy-4'-chlorobiphényle. Dans le cas du 3-hydroxy-4,4'-dichlorobiphényle, le noyau ne contenant pas de groupe hydroxyle a été oxygéné et le produit dihydrotrihydroxy a subi un réarrangement ayant conduit à une réaction de déshalogénéation pour produire le 2,3,3'-trihydroxy-4'-chlorobiphényle. Des métabolites similaires ont été produits lorsque de la dioxygénase du biphényle de *Burkholderia xenovorans* LB400 a été utilisée pour catalyser les réactions, sauf que pour tous les substrats qui ont été testés, l'enzyme de LB400 était moins efficace que celle de la souche B356, et contrairement à la souche B356, la BPDO de la souche LB400 était incapable d'oxyder les produits de la réaction. Les mécanismes impliqués dans la production de ces métabolites et d'autres ayant été identifiés dans ce travail restent inconnus, mais l'ensemble de nos données montre que les dérivés du dihydrodihydroxy de l'hydroxychlorobiphenyl doublement substitué en position *para* sont sujet à un réarrangement après la libération du produit ou à l'intérieur de la poche catalytique de la biphényle dioxygénase pour soit générer des métabolites que les autres enzymes de la voie cataboliques sont incapables de métaboliser et qui s'accumulent dans les milieux de culture, ou pour générer des métabolites déshalogénés qui sont ensuite métabolisés en leur acide benzoïque correspondant.

6.5. Abstract

In this work, we have examined the profile of metabolites produced from 4,4'-dihydroxybiphenyl, 4-hydroxy-4'-chlorobiphenyl, 3-hydroxy-4,4'-dichlorobiphenyl, and 3,3'-dihydroxy-4,4'-chlorobiphenyl by biphenyl-induced *Pandoraea pnomenusa* B356 and by its biphenyl dioxygenase. For all of these doubly *para*-substituted biphenyl analogs, the expected dihydrodihydroxy metabolite was not detected when the biphenyl dioxygenase of strain B356 was used to catalyze the hydroxylation. In the case of 4-hydroxy-4'-chlorobiphenyl, data suggested that it was converted principally to 3,4-dihydroxy-4'-chlorobiphenyl which was re-oxidized to 3,4,5-trihydroxy-4'-chlorobiphenyl. In the case of 3-hydroxy-4,4'-dichlorobiphenyl, the ring containing no hydroxyl group was oxygenated and the dihydrotrihydroxy product was rearranged through a dehalogenation reaction to generate 2,3,3'-trihydroxy-4'-chlorobiphenyl. Similar metabolites were produced when the biphenyl dioxygenase of *Burkholderia xenovorans* LB400 was used to catalyze the reactions, except that for all substrates that were tested, the LB400 enzyme was less efficient than that of strain B356 and unlike B356, LB400 BPDO was unable to further oxidize the reaction products. The mechanism involved in the production of the unexpected metabolites identified in this work has not been clearly demonstrated, but together data show that the dihydrodihydroxy derivatives of doubly *para*-substituted hydroxychlorobiphenyls are prone to rearrangement after product release or inside the catalytic pocket of the biphenyl dioxygenase to generate dehalogenated metabolites which are further metabolized to the corresponding benzoic acid or to dead-end metabolites which accumulate in the culture media.

6.6. Introduction

The toxicity of hydroxybiphenyls has been exploited for many years in antimicrobial preparations used as biocides (240). In addition, hydroxybiphenyls are key intermediates produced from multiple sources. For example, they are produced from microbial metabolism of dibenzofuran, fluorene, and carbazole (205, 223). In polychlorinated biphenyl (PCB)-contaminated sites, hydroxychlorobiphenyls are generated by the bacterial biphenyl catabolic enzymes (311) and by plants enzymatic systems (183, 244). The presence of these hydroxylated metabolites in the environment may have a considerable impact on the ecosystem in which they are generated since they may be toxic for living organisms, including bacteria. Because of the numerous concerns about their environmental impacts, hydroxychlorobiphenyls are increasingly considered as a new class of environmental contaminants (328). However, their fate in the environment has been scarcely investigated. The hydroxybiphenyl-degrading *Pseudomonas sp.* strain HBP1 and its 2-hydroxybiphenyl 3-monooxygenase have been well characterized (308). The pathway used by aerobic bacteria to degrade biphenyl is also able to metabolize or cometabolize several hydroxy- and hydroxychlorobiphenyls (328). However, the profile of metabolites generated by this pathway has been determined for only few of these biphenyl analogs (87, 296, 298).

The biphenyl catabolic pathway is composed of the four enzymatic steps shown in **Figure 6.1**. The three-component biphenyl dioxygenase (BPDO) initiates the metabolism by insertion of molecular oxygen onto vicinal *ortho-meta* carbons to generate the *cis*-2,3-dihydro-2,3-dihydroxybiphenyl which is then oxidized to a catechol. The encoding genes in *Pandoraea pnomenusa* B356 are *bphAEFG* for the biphenyl dioxygenase and *bphBCD* for the 2,3-dihydro-2,3-dihydroxybiphenyl dehydrogenase (BphB), the 2-3-dihydroxybiphenyl 1,2-dioxygenase (BphC) and the 2-hydroxy-6-oxo-6-phenylhexa-2,4-dienoic acid (HODA) hydrolase (BphD) (**Figure 6.1**). The enzymes of the biphenyl catabolic pathway are very versatile. Beside PCBs they may also metabolize diphenylmethane as well as heterocyclic aromatics including dibenzofuran, quinoline and many phenolics such as flavonoids derived from plants (87, 205, 236, 271, 288, 296, 327).

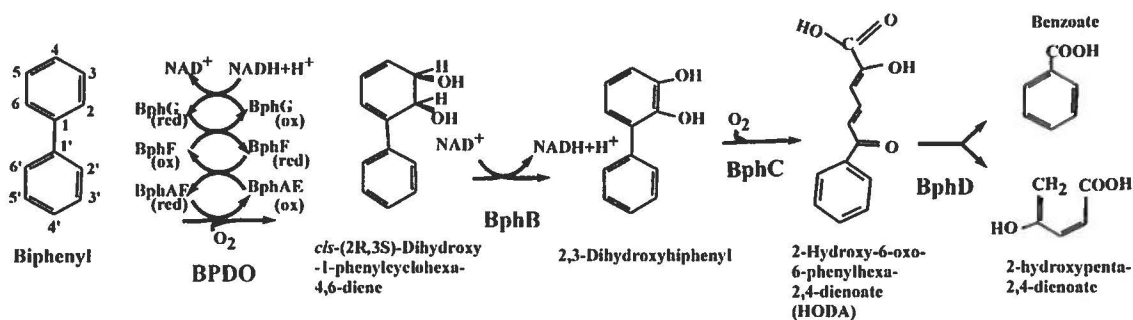


Figure 6.1: The first four enzymatic steps of the bacterial biphenyl catabolic pathway.

The specificity of the BPDO is crucial to determine the range of biphenyl analogs metabolized by the biphenyl catabolic pathway. For this reason, lots of efforts were invested to characterize this enzyme and the three-dimensional structure of the oxygenase component (BphAE) of strain B356 and of *Burkholderia xenovorans* LB400 BPDO have been resolved (46, 165). It is now well established that the range of biphenyl analogs metabolized by B356 and LB400 BPDOs differs considerably. Although *B. xenovorans* LB400 is considered to be the best PCB-degrading bacteria of natural occurrence, recent reports have shown that BphAE_{B356} metabolizes many biphenyl analogs significantly more efficiently than BphAE_{LB400} (106, 235, 236, 300).

It has clearly been established that bacterial BPDOs oxidize chlorinated biphenyls principally on the least substituted or non-substituted ring (311). In the case of plants, the position of hydroxylation has not been clearly established for most PCB congeners. However, using *in vitro* plant cells cultures, Kucerova et al. (2000) (161) have shown that 4-chlorobiphenyl is hydroxylated onto the 4'-carbon and Rezek et al. (2008) (244) have shown that the least substituted ring is the one that is most often hydroxylated. Therefore, it would be important to investigate the ability of the biphenyl catabolic enzymes to metabolize hydroxy- and hydroxychlorobiphenyls carrying a substituent on both rings. The profiles of metabolites generated from 2,2'- and 3,3'-dihydroxybiphenyl by biphenyl-induced cells of strain B356 have been determined in a previous study (296). The ability of the biphenyl catabolic pathway of *B. xenovorans* LB400 to metabolize 4-hydroxy-4'-chlorobiphenyl has recently been demonstrated (327) but the profile of metabolites produced from doubly *para*-substituted hydroxy- or hydroxychlorobiphenyls has never been reported. In this work we

have determined the profile of metabolites produced from selected doubly *para*-substituted hydroxychlorobiphenyls by the biphenyl catabolic pathway enzymes. Since many unexpected metabolites were produced, in order to explain their production, we have examined in more details the catalytic reaction of *P. pnomenusa* B356 and *B. xenovorans* LB400 BPDOs toward these biphenyl analogs. Our data show that frequently, the dihydrodihydroxy metabolites generated during BPDO catalytic oxidation of doubly *para*-substituted biphenyl analogs are prone to rearrangement, leading to the production of unexpected metabolites, some of which may not be metabolized by the downstream enzymes of the pathway and they accumulate in the environment.

6.7. Materials and methods

6.7.1. Bacterial strains, plasmids, chemicals and general protocols

Wild-type strains *P. pnomenusa* B356, *E. coli* DH11S [pDB31 LB400-*bphFG*] + pQE31[B356-*bphAE*] and *E. coli* DH11S [pDB31 LB400-*bphFG*] + pQE31[LB400-*bphAE*] were described previously (20, 235, 344). These *E. coli* strains express an active BPDO exhibiting the biochemical features of B356 and LB400 BPDOs respectively. The culture media used were Luria–Bertani (LB) broth (260), basal medium M9 (260) or minimal mineral medium no. 30 (MM30) (310) amended with various sources of carbon and antibiotics depending on the experiment. 4,4'-Dihydroxybiphenyl, 4-chlorobenzoate, 4-hydroxybenzoate (99% pure) were from Sigma-Aldrich; 4-hydroxy-4'-chlorobiphenyl, 3-hydroxy-4,4'-dichlorobiphenyl and 3,3'-dihydroxy-4,4'-dichlorobiphenyl (99% pure) were from Ultra Scientific.

6.7.2. Whole cell assays to assess the metabolism of the various hydroxychlorobiphenyls by the biphenyl catabolic pathway enzymes

Strain B356 was grown at 28 °C on MM30 plus biphenyl to reach log phase. Cultures were filtered through packed glass wool to remove particulates, cell aggregates, and crystals of growth substrate. Cells were harvested by centrifugation, washed with phosphate buffer (30 mM, pH 7.2) or M9 medium and suspended to an OD_{600nm} of 2.0 in MM30 plus the appropriate substrate (344). *E. coli* DH11S [pDB31 LB400-*bphFG*] + pQE31[B356-*bphAE*] and *E. coli* DH11S [pDB31 LB400-*bphFG*] + pQE31[LB400-*bphAE*] were grown at 37 °C to log phase in LB broth with appropriate antibiotics. The cultures were induced for 4 h with 0.5 mM isopropyl-β-D-thiogalactoside (IPTG) and then washed and suspended to an OD_{600nm} of 2.0 in M9 medium containing 0.5 mM IPTG, 0.1% (wt/vol) sodium acetate and the appropriate hydroxychlorobiphenyls. For short term assays, the induced *E. coli* cells were suspended at an OD_{600nm} of 5.0 in 50 mM sodium phosphate buffer, pH 7.0 containing appropriate hydroxychlorobiphenyls at concentrations between 0.5-2 mM.

After periods varying between 1 to 18 h depending on experiments, the cell suspensions were extracted at neutral and acidic pH with ethyl acetate, and the extracts were treated with butylboronate (*n*BuB) or *N,O*-bis-trimethylsilyl trifluoroacetamide (BSTFA) for

gas chromatography-mass spectrometry (GC-MS) analysis according to previously described protocols (330). GC-MS analyses were performed as described previously (235), using a Hewlett Packard HP6980 series gas chromatograph interfaced with an HP5973 mass selective detector (Agilent Technologies).

We also assessed the ability of reconstituted His-tagged BPDO preparations to metabolize hydroxychlorobiphenyls. His-tagged enzyme components were produced and purified following protocols published previously (206). The enzyme assays containing between 100 to 800 nmol substrate, were performed in a volume of 200 μ l in 50 mM morpholinethanesulfonic (MES) buffer pH 6.0, at 37 °C as described previously (129). For metabolites analyses, the reaction medium was incubated for 5 to 15 min and the metabolites were extracted at pH 6.0 with ethyl acetate, then treated with *n*BuB or BSTFA as described above for GC-MS analysis.

6.7.3. Purification and NMR analysis of 3,4-dihydroxy-4'-chlorobiphenyl, 3,4,5-trihydroxy-4'-chlorobiphenyl, and 4-(4-chlorophenyl)-cis-5,6-dihydroxycyclohex-3-en-1-one

4-Hydroxy-4'-chlorobiphenyl metabolites were produced by a reconstituted His-tagged-purified preparation of B356 BPDO comprised of BphAEFG_{B356}. Each enzyme reaction performed as described above, contained 800 nmol 4-hydroxy-4'-chlorobiphenyl and the mixture was incubated for 15 min at 37 °C. The ethyl acetate extract was concentrated 20 fold by evaporation under a stream of nitrogen, and this preparation was injected into a XDB-C8 column (4.6 x 150 mm). The HPLC conditions were identical to those used in a previous report (235) to purify benzophenone metabolites produced by purified B356 BPDO. The identity and purity of the purified metabolites were confirmed by GC-MS analysis of TMS derivatives before running the NMR analysis. The NMR spectra were obtained at the Quebec/Eastern Canada High Field NMR Facility at McGill University (Montreal, Quebec, Canada) with a Bruker 500-mHz spectrometer. The analyses were carried out in deuterated acetone at room temperature.

6.7.4. Docking and structure analysis

Dimer AB of BphAE_{B356} (RCBS protein databank 3GZX) were used as protein targets and they were prepared as previously described (169). Ligands were all downloaded as sdf files from pubchem (<http://pubchem.ncbi.nlm.nih.gov>) and converted into pdb format in Discover Studio Visualizer 2.5. Both proteins and ligands were processed with AutoDockTools to obtain their proper pdbqt format. The searching space for the ligand was centered on the mononuclear iron and contained 20 Å in each x, y, and z direction. Autodock 4 (209) with the default parameters was used to perform the automatic docking. Structures were analyzed using the PyMOL software (DeLano Scientific LLC).

6.8. Results

6.8.1. Analysis of metabolites produced from 4-hydroxy-4'-chlorobiphenyl by purified B356 BPDO

When a purified preparation of B356 BPDO was used to metabolize 4-hydroxy-4'-chlorobiphenyl, several metabolites were produced, but one of them, metabolite 7 was by far the major one (**Figure 6.2**). On the basis of previous reports (189, 296), the mass spectral features of metabolite 7 (**Table 6.1**) corresponded to a trihydroxychlorobiphenyl [M^+ at m/z 452 and fragmentation ions at m/z 437 ($M^+ - CH_3$), 417 ($M^+ - Cl$), 379 ($M^+ - (CH_3)_3Si$), 364 ($M^+ - (CH_3)_4Si$), 349 ($M^+ - (CH_3)_4Si - CH_3$)]. Among the minor metabolites, metabolite 1 (**Figure 6.2**) exhibited spectral features that were identical to those of authentic 2,3-dihydroxy-4'-chlorobiphenyl which is produced from 4-chlorobiphenyl (189). The mass spectral features of metabolite 2 (**Table 6.1**) were similar to those of metabolite 3 [M^+ at m/z 382 and fragmentation ions at m/z 367 ($M^+ - CH_3$), 340 ($M^+ - CO - CH_2$), 292 ($M^+ - (CH_3)_3SiOH$), 277 ($M^+ - (CH_3)_3SiOH - CH_3$), 264 ($M^+ - (CH_3)_3SiO - CH - O$), 252 ($M^+ - (CH_3)_3SiO - CH - CO$), 217 ($M^+ - (CH_3)_3SiO - CH - CO - Cl$)] which has been identified as 4-(4-chlorophenyl)-*cis*-5,6- dihydroxycyclohex-3-en-1-one by NMR spectrometry (see below). The TMS-treated metabolite 4 exhibited mass spectral features that on the basis of previous reports (189, 296), were characteristic of a dihydroxychlorobiphenyl (**Table 6.1**) and this metabolite was also identified by NMR spectroscopy (see below). Those of metabolite 5 corresponded to a trihydroxychlorobiphenyl (**Table 6.1**) and those of metabolite 6 to a dihydrotrihydroxychlorobiphenyl (**Table 6.1**).

Table 6.1: Metabolites produced from 4-hydroxy-4'-chlorobiphenyl by B356 BPDO

METABOLITE # ^{ab}	Spectral features (TMS derivatives)		
	M ⁺	M-15	Other ions
<u>1</u>	364	349	276, 261, 246, 210, 147, 139
<u>2</u>	382	367	339, 264, 249, 217, 204, 147
<u>3</u>	382	367	340, 264, 252, 217, 204, 147
<u>4</u>	364	349	276, 261, 246, 210, 147, 139
<u>5</u>	452	437	364, 349
<u>6</u>	454	439	364, 341, 279, 264, 147
<u>7</u>	452	437	417, 379, 364, 349, 321, 314

^aMetabolite numbering follows the order of elution on the GC-MS spectrum

^bStructures are shown on **Figure 6.2**

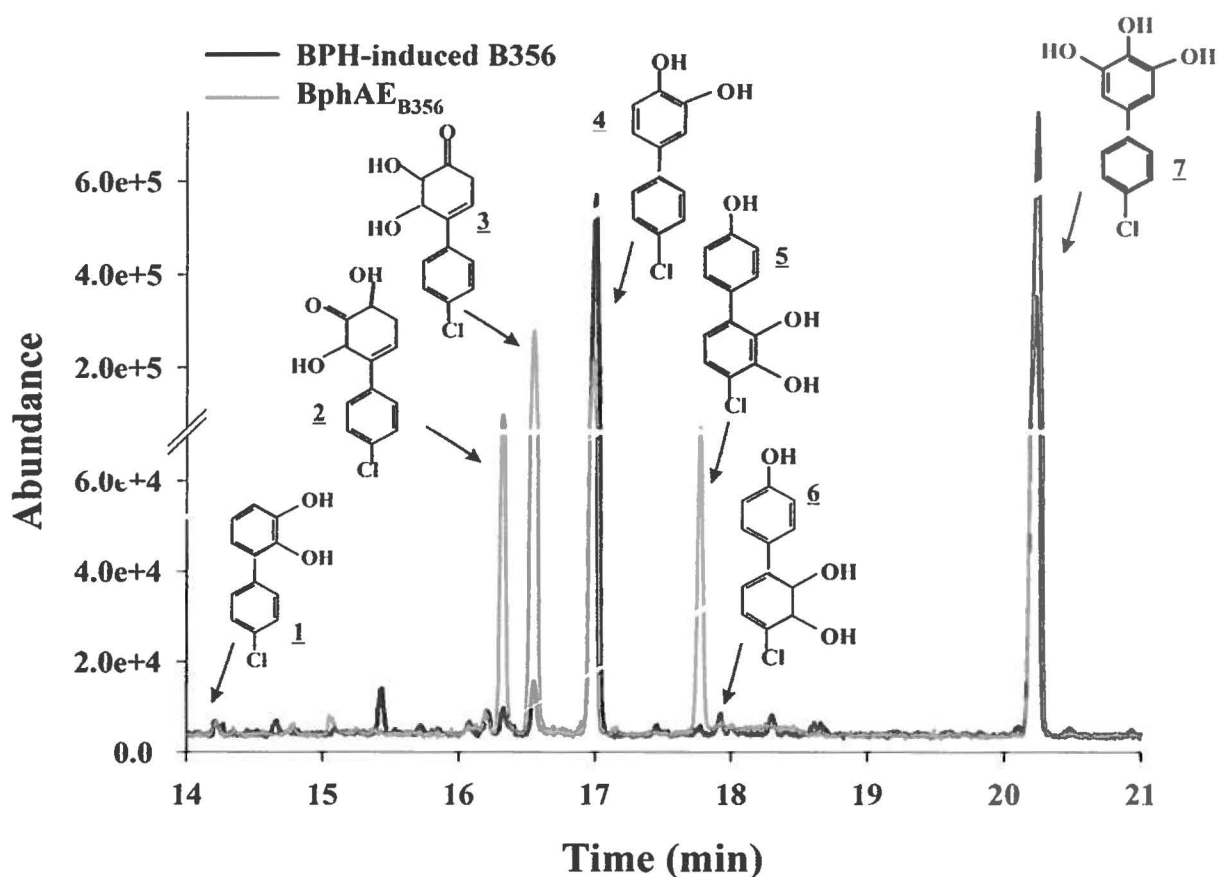


Figure 6.2: Total ion chromatogram of the metabolites produced from 4-hydroxy-4'-chlorobiphenyl by biphenyl-induced cells of strain B356 incubated 90 min with the substrate as indicated in the Materials and Methods section (black line) or by a purified preparation of BphAE_{B356} incubated for 7 min with the substrate (grey line). The metabolite numbering is the same as in the text and in **Table 6.1**

6.8.2. Analysis of the metabolites produced from 4-hydroxy-4'-chlorobiphenyl by biphenyl-induced resting cells of strain B356

When a resting suspension of biphenyl-induced B356 cells was incubated with 1.6 $\mu\text{mol/ml}$ of 4-hydroxy-4'-chlorobiphenyl, about 10% of the added substrate was left after two hours of incubation. In the acidic extract, we detected approximately 10 nmol/ml each of 4-

chlorobenzoic acid and 4-hydroxybenzoic acid, both were identified by comparing their spectral features with those of authentic standards. We also detected traces of a metabolite whose spectral features were identical to those of 2-hydroxy-6-oxo-6-[4'-chlorophenyl]-hexa-2,4-dienoic acid (chlorophenyl-HODA) which is also produced from 2,3-dihydroxy-4'-chlorobiphenyl during the metabolism of 4-chlorobiphenyl (189). The major metabolites were detected in the neutral extract of the 2-h old culture (**Figure 6.2**). Two major peaks were observed, together representing more than 95% of the total neutral plus acidic metabolites, and their GC-MS features were identical to those of metabolites 4 and 7. Since both 4-hydroxybenzoate and 4-chlorobenzoate are poor growth substrates for strain B356 and poorly metabolized by biphenyl-induced cells of strain B356 (not shown), most of the added 1.6 $\mu\text{mol/ml}$ substrate should have been converted to the benzoic acid derivatives by the resting cell suspension, after 2 h of incubation. The fact that only small amounts of acidic metabolites were detected suggested that the major metabolites 4 and 7 were dead-end metabolites that accumulated in the growth medium.

6.8.3. Identity of metabolite 3, 4 and 7

Metabolite 7 was purified as a single peak by HPLC and analyzed by NMR spectrometry. Metabolite 3 was also purified by HPLC but the purified preparation contained small amount of metabolite 4. This mixture was also analyzed by NMR spectrometry.

On the basis of its NMR features reported in **Table 6.2**, compound 7 was identified as 3,4,5-trihydroxy-4'-chlorobiphenyl. The presence of only 3 signals (1 singlet and two doublets) for 6 protons shows the metabolite is perfectly symmetric, thus two hydroxyl groups are located on two symmetrical positions of one of the aromatic rings. A 2D HMBC experiment showed a correlation between the singlet proton at 6.716 ppm and carbon C1' at 141.12 ppm (**Figure 6.3A**) which gives only two possible positions for these hydroxyl groups at either 3,5 or 3',5'. Metabolite 7 was identified as 3,4,5-trihydroxy-4'-chlorobiphenyl on the basis of the experimental chemical shifts values for the ^{13}C -NMR which were very close to the calculated theoretical values for this compound (**Table 6.2**).

Table 6.2: NMR features of metabolite 7

No	Chemical shifts (ppm)			
	¹ H	¹³ C	¹³ C theoretical	¹³ C theoretical
		Experimental	Molecule A ^a	Molecule B ^a
1		133.99	136.5	132.5
2	6.716 (s)	106.88	107.0	129.5
3		147.16	143.5	115.0
4		n/a	126.5	153.5
5		147.16	143.5	115.0
6	6.716 (s)	106.88	107.0	129.5
1'		141.12	139.5	143.5
2'	7.557 (d)	129.50	129.0	106.5
3'	7.428 (d)	128.98	128.5	157.0
4'		132.88	133.0	106.0
5'	7.428 (d)	128.98	128.5	157.0
6'	7.557 (d)	129.50	129.0	106.5

^aMolecule A is 3,4,5-trihydroxy-4'-chlorobiphenyl, Molecule B is 3',4,5'-trihydroxy-4'-chlorobiphenyl

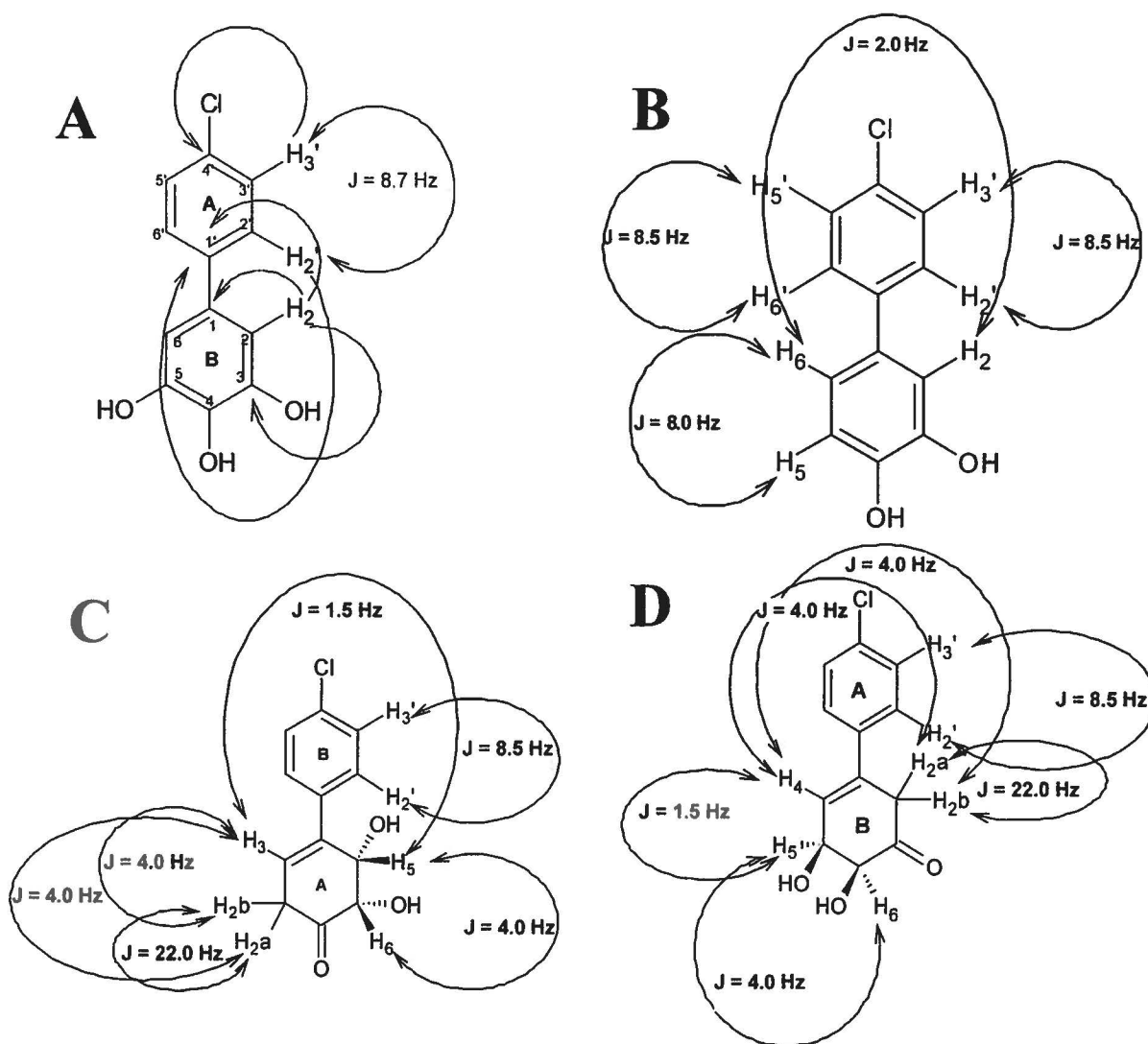


Figure 6.3: NMR coupling constants and HMBC correlations of A) 3,4,5-trihydroxy-4'-chlorobiphenyl (metabolite 7); and NMR coupling constants of B) 3,4-dihydroxy-4'-chlorobiphenyl (metabolite 4); C) 4-(4-chlorophenyl)- *cis*-5,6-dihydroxycyclohex-3-en-1-one] (metabolite 3A); D) 3-(4-chlorophenyl)-*cis*-5,6-dihydroxycyclohex-3-en-1-one (metabolite 3B).

Metabolite 4, was also identified from its NMR spectral features. This metabolite was detected as a minor contaminant of the HPLC peak containing metabolite 3 but the resolution and peak height for the ^1H -NMR and the 2D COSY spectra were good enough to allow its identification. The ^1H -NMR spectrum showed 5 signals representing 7 protons [peaks at 7.60 ppm (d, 2H) ($\text{H2}'$, $\text{H6}'$ or $\text{H3}'$, $\text{H5}'$) and 7.38 ppm (d, 2H) ($\text{H3}'$, $\text{H5}'$ or $\text{H2}'$, $\text{H6}'$), at 7.15 ppm (d, 1H) (H2), 7.03 ppm (dd, 1H) (H6) and at 6.94 ppm (d, 1H) (H5)]. The structure and coupling constants shown in **Figure 6.3B** are identical to those already reported for 3,4-dihydroxy-4'-chlorobiphenyl in the same solvent (197). The identity of metabolites 4 and 7 as 3,4-dihydroxy-4'-chlorobiphenyl and 3,4,5-dihydroxy-4'-chlorobiphenyl is consistent with the observation that they accumulated in the strain B356 cell suspensions since they would not be metabolized by BphC (17).

The ^1H -NMR spectrum of compound 3 showed 9 protons, including two couples of symmetrical vicinal aromatic protons (AA'BB' system) [7.424 ppm (d), 8.5 Hz (2H) and 7.658 ppm (d), 8.5 Hz (2H)]. The correlation between these four protons and the carbon at position 4' observed from a 2D HMBC spectrum, as well as the ^{13}C chemical shifts (**Table 6.3**) confirmed that one of the two phenyl rings was not transformed during the enzymatic reaction.

Signals for the other ring were: one carbonyl ($\text{C}=\text{O}$) (207.813 ppm); one methylene (CH_2) (C: 39.749 ppm; H_a : 3.365 ppm; H_b : 3.123 ppm); two (CH-OH) groups (C: 77.605 ppm and 73.706 ppm; H : 4.892 ppm and 4.649 ppm, respectively); one ($\text{CH}=\text{}$) (C: 125.868 ppm; H : 6.371 ppm). On the basis of HMBC correlations, there were two possible structures, 3A [4-(4-chlorophenyl)-*cis*-5,6-dihydroxycyclohex-3-en-1-one] (**Figure 6.3C**) or 3B [3-(4-chlorophenyl)-*cis*-5,6-dihydroxycyclohex-3-en-1-one] (**Figure 6.3D**). The correlations for compound 3A are listed in **Table 6.3** (data not shown for compound 3B). However, in the case of 3B (**Figure 6.3D**) there are several unjustifiable coupling constants, such as $^3J_{\text{H4-H5}} = 1.5$ Hz; $^4J_{\text{H2a-H4}}$ and $^4J_{\text{H2b-H4}} = 4.0$ Hz. In addition, no four-bond TOCSY correlation was observed between protons H4-H5-H6 of compound 3B.

Table 6.3: ^{13}C and ^1H chemical shifts and HMBC correlations of metabolite 3

No	Chemical shifts (ppm)		HMBC Correlation
	^{13}C	^1H	
1	207.813		
2	39.749	2a: 3.365 (dd); 2b: 3.123 (dd)	H2-C1-C3-C4-C6-C5-C1'-C2'
3	125.868	6.371 (dt)	H3-C4-C1'-C5-C2-C1
4	138.203		
5	77.605	4.892 (d)	H5-C6-C3-C4-C1'-C1
6	73.706	4.649 (d)	H6-C5-C1
1'	139.837		
2'	128.372	7.658 (d)	H2'-C3'-C4'-C1
3'	129.423	7.424 (d)	H3'-C2'-C4'-C1'
4'	133.610		
5'	129.423	7.424 (d)	H5'-C2'-C4'-C1'
6'	128.372	7.658 (d)	H6'-C3'-C4'-C1

On the other hand, all coupling constant values were consistent with the structure of 3A, and also consistent with the TOCSY experiment which did not show any three vicinal protons. The $^3J_{\text{H5-H6}}$ coupling value at 4.0 Hz reveals a 45 degree dihedral angle (calculated by Karplus equations (145) consistent with a *cis*-conformation. With these lines of evidence, 3 was identified as 3A which is 4-(4-chlorophenyl)-*cis*-5,6-dihydroxycyclohex-3-en-1-one. The carbonyl group at the *para* position of the oxidized ring is consistent with a rearrangement of part of the *cis*-2,3-dihydro-2,3,4-trihydroxy-4'-chlorobiphenyl produced from the oxidation of the hydroxylated ring of 4-hydroxy-4'-chlorobiphenyl during or after the catalytic reaction.

6.8.4. Metabolism of 4-hydroxy-4'-chlorobiphenyl by *E. coli* cells expressing B356 BPDO

Additional experimental evidence that metabolite 7 was produced from further oxidation of metabolite 4 was obtained from the analysis of the metabolites produced from 4-hydroxy-4'-chlorobiphenyl by recombinant *E. coli* cells expressing B356 BPDO. An IPTG-induced cell suspension metabolized 0.8 mM 4-hydroxy-4'-chlorobiphenyl completely within two hours and 3,4,5-trihydroxy-4'-chlorobiphenyl was by far the major metabolite detected in the 2 h-old culture (not shown). Consistent with a further oxidation of metabolite 4, this metabolite was detected in significant amounts in younger cultures but only in trace amount in older cultures. The other metabolites 1, 2, 3, 5 and 6 were also detected, but in very small amount, when the cell suspensions were incubated for periods between 1 and 2 h and in older cultures, they completely disappeared most likely due to polymerization through oxidation. Interestingly, under the same conditions, *E. coli* cells producing LB400 BPDO metabolized less than 10% of the added 4-hydroxy-4'-chlorobiphenyl in 18 h and 3,4-dihydroxy-4'-chlorobiphenyl was the sole metabolite detected in those suspensions. Therefore, unlike B356 BPDO, LB400 BPDO metabolized 4-hydroxy-4'-chlorobiphenyl poorly and was unable to further metabolize the reaction product.

6.8.5. Docking experiments and suggested pathway for the metabolism of 4-hydroxy-4'-chlorobiphenyl

We docked 4-hydroxy-4'-chlorobiphenyl in the substrate-bound form of BphAE_{B356} after removal of biphenyl. The conformation of 19 of the 20 top-ranked docked molecules in BphAE_{B356} exhibited an orientation that would enable an oxygenation of the *ortho-meta* carbons of the hydroxylated ring (**Figure 6.4A**) and one docked molecule exhibited conformation that would enable an oxygenation of the *ortho-meta* carbons of the chlorinated ring (**Figure 6.4B**). For both structures, the *ortho-meta* carbons did not closely aligned with carbons 2 and 3 of the oxidized ring of biphenyl in the complexed form (**Figure 6.4A and B**) but their *ortho-meta* carbons were at a distance from the catalytic iron that would allow an oxygenation of the molecule onto those positions. A similar observation was made in a previous work (169) with 1,1,1-trichloro-2,2-bis(4-chlorophenyl)ethane (DDT), a doubly

para-substituted biphenyl analog, where the *ortho-meta* carbons of DDT did not closely aligned those of the oxidized ring of biphenyl in the complexed form. It is likely that without this distortion, the *para*-substituent would be too close to Gln226 and Phe227, two residues that are involved in the catalytic reaction (206). Therefore, these analogs are either placed differently than biphenyl inside the catalytic pocket of the enzyme or they may require induced-fit conformational changes of the protein that our docking experiments could not reproduce. However, although imperfect, none of the docking experiments placed 4-hydroxy-4'-chlorobiphenyl in an orientation that would allow a *meta-para* reaction. Therefore, the docking experiments suggest this substrate would be metabolized principally through an *ortho-meta* oxygenation. The fact that no 2,3-dihydro-2,3,4-trihydroxy-4'-chlorobiphenyl was detected when the reaction was catalyzed by B356 or LB400 BPDO suggests that this metabolite is very susceptible to rearrangement. The fact that many metabolites were produced during the BPDO reaction indicates that 2,3-dihydro-2,3,4-trihydroxy-4'-chlorobiphenyl rearrangement may involve different mechanisms. However, the major route appears to involve a spontaneous water removal at position 2 to generate 3,4-dihydroxy-4'-chlorobiphenyl (metabolite 4). This metabolite is then rapidly further oxidized by B356 BPDO to generate 3,4,5-trihydroxy-4'-chlorobiphenyl (metabolite 7). We have tried to dock 3,4-dihydroxy-4'-chlorobiphenyl into BphAE_{B356} but none of the 20 top-ranked molecules exhibited a productive conformation (not shown). Therefore, other structural features that our docking experiments could not reproduce are required for productive binding of this substrate.

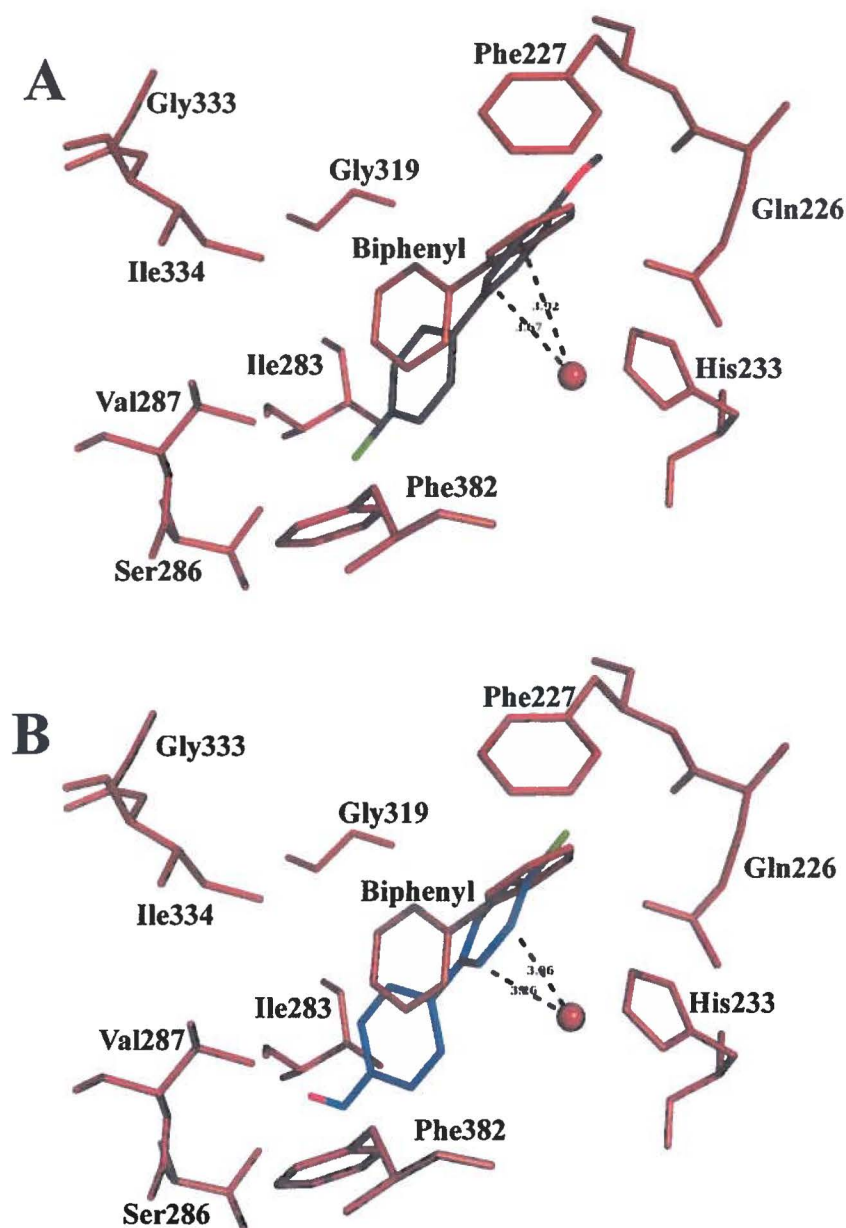


Figure 6.4: A-B) Superposition of catalytic center residues of 4-hydroxy-4'-chlorobiphenyl-docked (black and blue) and biphenyl-bound (red) forms of BphAEB₃₅₆. The hydroxyl groups of 4-hydroxy-4'-chlorobiphenyl are in red and the chlorine atom in green.

A small portion of the 2,3-dihydro-2,3,4-trihydroxy-4'-chlorobiphenyl produced from the BPDO reaction may lose one water molecule at position 4 to generate 2,3-dihydroxy-4'-chlorobiphenyl (metabolite 1), but this pathway is minor. When the reaction was catalyzed by a purified B356 BPDO preparation, a small portion of 2,3-dihydro-2,3,4-trihydroxy-4'-chlorobiphenyl was also found to rearrange into metabolites 2 and 3. However, these two metabolites were produced in much lesser amounts by B356 and recombinant *E. coli* cell suspensions than by purified BPDO preparations. This observation may be explained by the fact that the optimal conditions for the BPDO reaction (pH 6.0, 50 mM MES) which were used in this work, differed from the conditions occurring inside the cells. Therefore, under conditions prevailing inside the cells, the rearrangement of *cis*-2,3-dihydro-2,3,4-trihydroxy-4'-chlorobiphenyl to produce 4-(4-chlorophenyl)-*cis*-5,6-dihydroxycyclohex-3-en-1-one may not be favored.

Finally, because 4-hydroxybenzoate was found among the metabolites in the acid extract of B356 resting cell suspensions, we may presume metabolite 5 was 2',3',4-trihydroxy-4'-chlorobiphenyl and metabolite 6 was 2',3'-dihydro-2',3',4-trihydroxy-4'-chlorobiphenyl. This would be consistent with the docking experiments that showed that one of twenty docked molecules exhibited a conformation allowing an oxygenation of the chlorinated ring.

On the basis of these observations, we may propose the metabolic pathway for 4-hydroxy-4'-chlorobiphenyl shown in **Figure 6.5**.

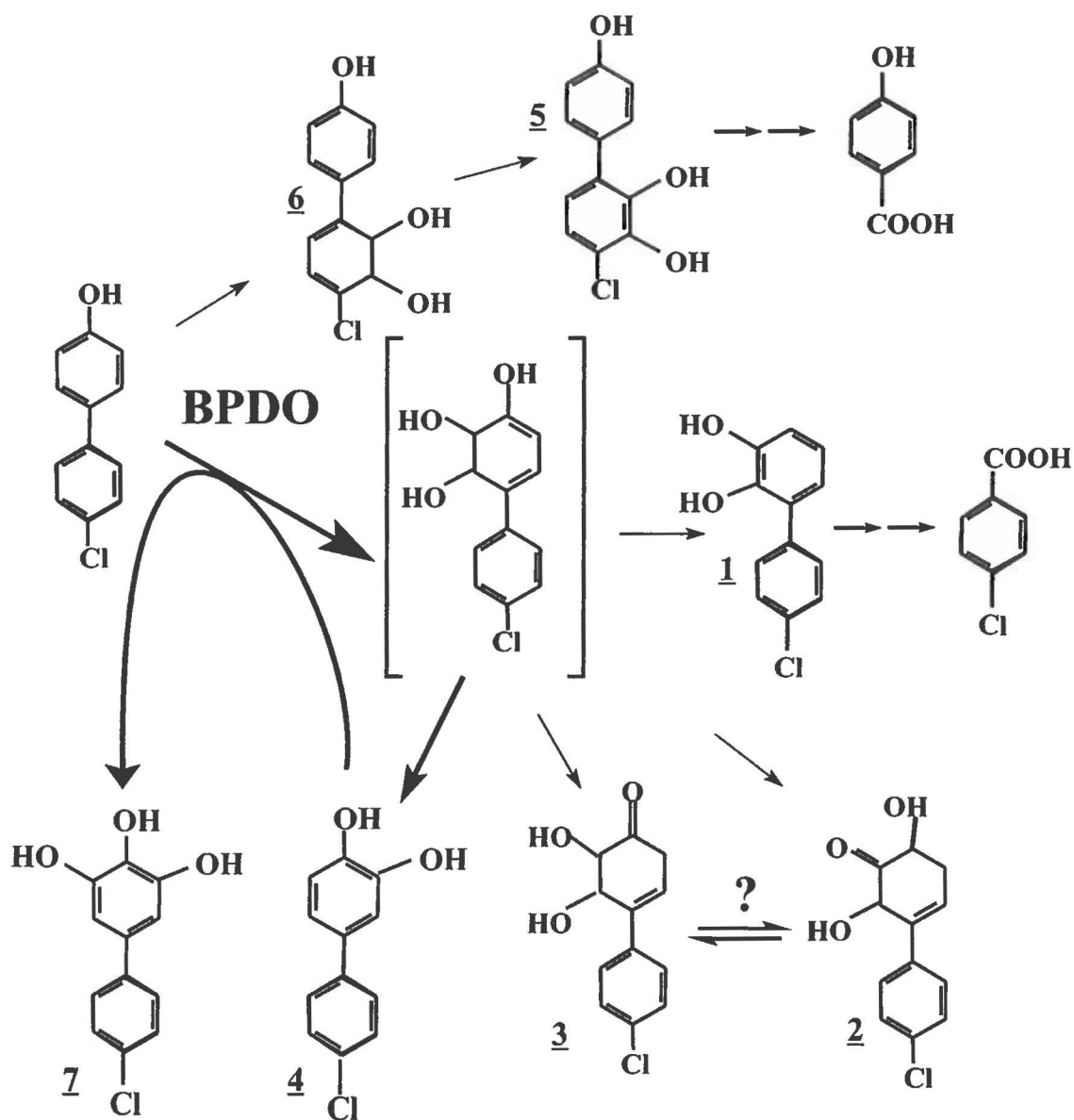


Figure 6.5: Proposed profile of metabolites produced from 4-hydroxy-4'-chlorobiphenyl by B356 BPDO and biphenyl-induced cells of strain B356. The thick arrows indicate the major route of transformation. Brackets indicate the metabolite was not detected. The metabolite numbering is as indicated in Table 6.1.

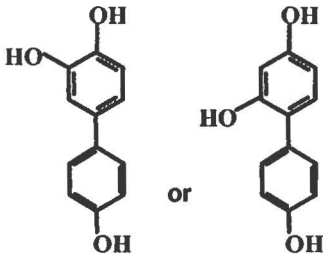
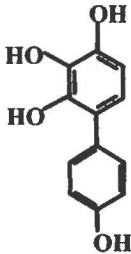
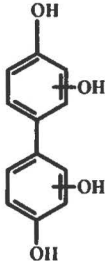
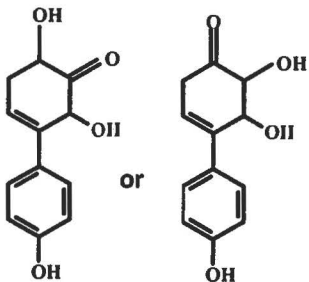
6.8.6. Metabolism of other para-hydroxy- or hydroxychlorobiphenyls

Analysis of the metabolites generated from 4-hydroxy-4'-chlorobiphenyl showed that the dihydrodihydroxy metabolites resulting from the catalytic oxidation of this doubly *para*-substituted biphenyls are unstable and undergo various types of rearrangements. In order to verify that this observation was not a feature unique to this substrate, we have also examined the metabolism of 4,4'-dihydroxybiphenyl, 3-hydroxy-4,4'-dichlorobiphenyl and 3,3'-dihydroxy-4,4'-dichlorobiphenyl.

6.8.6.1. Metabolism of 4,4'-dihydroxybiphenyl by biphenyl-induced cells of strain B356

When a biphenyl-induced resting cell suspension of strain B356 was incubated with 4,4'-dihydroxybiphenyl, several metabolites were detected. We did not investigate in detail the metabolites that were produced, and our data do not allow us to draw a precise profile of metabolites. However, in the acid fraction, we detected small amount of 4-hydroxybenzoic acid (not shown) showing that part of the substrate was metabolized to the end product of the pathway. When the reaction was catalyzed by *E. coli* cells expressing B356 BPDO more than 95% of the substrate was converted to a metabolite exhibiting the spectral features of a trihydroxybiphenyl (metabolite 8, Table 6.4). The fact that this metabolite was not further metabolized by BphC (not shown), allows us to tentatively identify it as 3,4,4'-trihydroxybiphenyl which BphC would be unable to cleave (17) or as 2,4,4'-trihydroxybiphenyl. No dihydrodihydroxy metabolites were detected but two tetrahydroxybiphenyls (metabolites 9, 10, Table 6.4) were produced in small amounts. Together, they represented less than 1% of total metabolites. We also detected trace amounts of a metabolite which, on the basis of its mass spectral features was tentatively identified as 5,6-dihydroxy-4-(4-hydroxyphenyl)-cyclohex-3-en-1-one or 2,6-dihydroxy-4-(4-hydroxyphenyl)-cyclohex-3-en-1-one or any other analogs with other distributions of their hydroxyl and ketone functions (metabolite 11, Table 6.4). Together, these observations plus the absence of 2,3-dihydro-2,3,4,4'-tetrahydroxybiphenyl in recombinant *E. coli* cell evidence that this metabolite is susceptible to rearrangement. When *E. coli* cells expressing LB400 BPDO was used to metabolize 4,4'-dihydroxybiphenyl, the substrate was metabolized poorly compared to those expressing B356 BPDO but metabolite 8 was the only one recovered (in very small amount) in the culture medium. Therefore, LB400 BPDO catalyzed the oxidation of 4,4'-dihydroxybiphenyl less efficiently than B356 BPDO but both of them produced the same major metabolite and they did not produce the expected dihydrodihydroxy metabolites.

Table 6.4: Metabolites produced from 4,4'-dihydroxybiphenyl by strain B356 BPDO

METABOLITE ^a	#	Spectral features (TMS derivatives)		
		M ⁺	M - 15	Other ions
	<u>8</u>	418	403	330, 315, 299, 241, 209, 147, 73,
	<u>9</u>	506	491	418, 403, 300, 253, 207, 147, 73,
	<u>10</u>	506	491	418, 403, 300, 253, 207, 147, 73,
	<u>11</u>	436	421	330, 204

^aMetabolite numbering follows the order of elution on the GC-MS spectrum

6.8.6.2. Metabolism of 3-hydroxy-4,4'-dichlorobiphenyl

When a biphenyl-induced resting cell suspension of strain B356 was used to metabolize 3-hydroxy-4,4'-dichlorobiphenyl, less than 20% of the added substrate was metabolized and the major metabolite, representing approximately 50% of all neutral plus acidic metabolites, was 3-hydroxy-4-chlorobenzoic acid (metabolite 12, **Table 6.5**) which was identified on the basis of its GC-MS spectral features. In the neutral extract several hydroxylated metabolites were detected, only two were produced in significant amount, each of which representing about 25% of the total metabolites. The first one was identified as a dihydroxy-dichlorobiphenyl on the basis of its mass spectral features (metabolite 13, **Table 6.5**). It likely resulted from 2,3-dihydro-2,3,3'-trihydroxy-4,4'-dichlorobiphenyl after elimination of one water molecule. The other one was identified as a monochloro-trihydroxybiphenyl on the basis of its mass spectral features (metabolite 14, **Table 6.5**). When a purified BphAE_{B356} was used to metabolize 3-hydroxy-4,4'-dichlorobiphenyl less than 5% of the substrate was transformed within 10 min and metabolite 13 was a minor one, representing, on the basis of the area under its GC-MS peak, less than 5% of the total metabolites. Two major products were detected at approximately equal amount and together representing about 90% of the total metabolites. The mass spectral features of the first one to elute (spectrum not shown) were identical to those of metabolite 14 produced by biphenyl-induced resting cells of strain B356. We presumed it resulted from the hydroxylation of the non hydroxylated ring and it may be the 2,3,3'-trihydroxy-4'-chlorobiphenyl resulting from the removal of one chlorine atom from 2,3-dihydro-2,3,3'-trihydroxy-4,4'-dichlorobiphenyl. Production of metabolite 14 is consistent with the observation that 3-hydroxy-4-chlorobenzoic acid is a major metabolite of B356 resting cell suspensions. The second major metabolite was also identified on the basis of its mass spectral features to either be 6-chloro-3-(4-chlorophenyl)-4,5-dihydroxycyclohex-2-en-1-one or 6-chloro-3-(4-chlorophenyl)-2,5-dihydroxycyclohex-3-en-1-one (metabolite 15, **Table 6.5**). It exhibited a molecular ion at m/z 416 and fragmentation ions at m/z 401 ($M^+ - CH_3$) and at 381 ($M^+ - Cl$) with a single prominent ion at m/z 266 corresponding to ($M^+ - 150$) which would result from the loss of $[(CH_3)_3SiOH - CH - CH-Cl]$. This is similar to the prominent m/z $M^+ - 116$ ions corresponding to $[(CH_3)_3SiOH - CH - CH_2]$ observed for 3,4- dihydroxy-5-(3-hydroxyphenyl)-5-cyclohexen-1-one (296) which is characterized by the fact that the two *meta* positions of the non-aromatic ring are occupied by respectively a hydroxyl and a carbonyl group and one of the *ortho* positions is occupied by a hydroxyl group. Together data show that both rings of 3-hydroxy-

4,4'-dichlorobiphenyl may be attacked by B356 BPDO and in both cases, the resulting metabolite is very susceptible to rearrangement. When the non-hydroxylated ring is oxidized, the resulting metabolite readily loss the *para* chlorine atom to generate a catechol which is further metabolized by the downstream enzymes whereas, when the hydroxylated ring is metabolized, the resulting metabolite is readily transformed to a dead-end metabolite. A proposed pathway for the metabolism of 4,4'-dichloro-3-hydroxybiphenyl is presented in **Figure 6.6**.

Table 6.5: Metabolites produced from 3-hydroxy-4,4'-dichlorobiphenyl and from 3,3'-dihydroxy-4,4'-dichlorobiphenyl by strain B356 and its BPDO

METABOLITE # ^{ab}	Spectral features (TMS derivatives)		
	M ⁺	M-15	Other ions
<u>12</u>	316,	301	257, 227, 189, 149
<u>13</u>	398	383	363, 348, 333, 275, 239, 181, 152, 131
<u>14</u>	452	437	417, 379, 364, 349, 314, 299, 253, 147
<u>15</u>	416	401	353, 266, 250, 147
<u>16</u>	486	471	398, 383, 348, 219, 147, 131
<u>17</u>	470	455	381, 354, 315, 271, 181, 147, 131

^aMetabolite numbering follows the order of elution on the GC-MS spectrum

^bStructures are shown on **Figure 6.6** and **6.7**

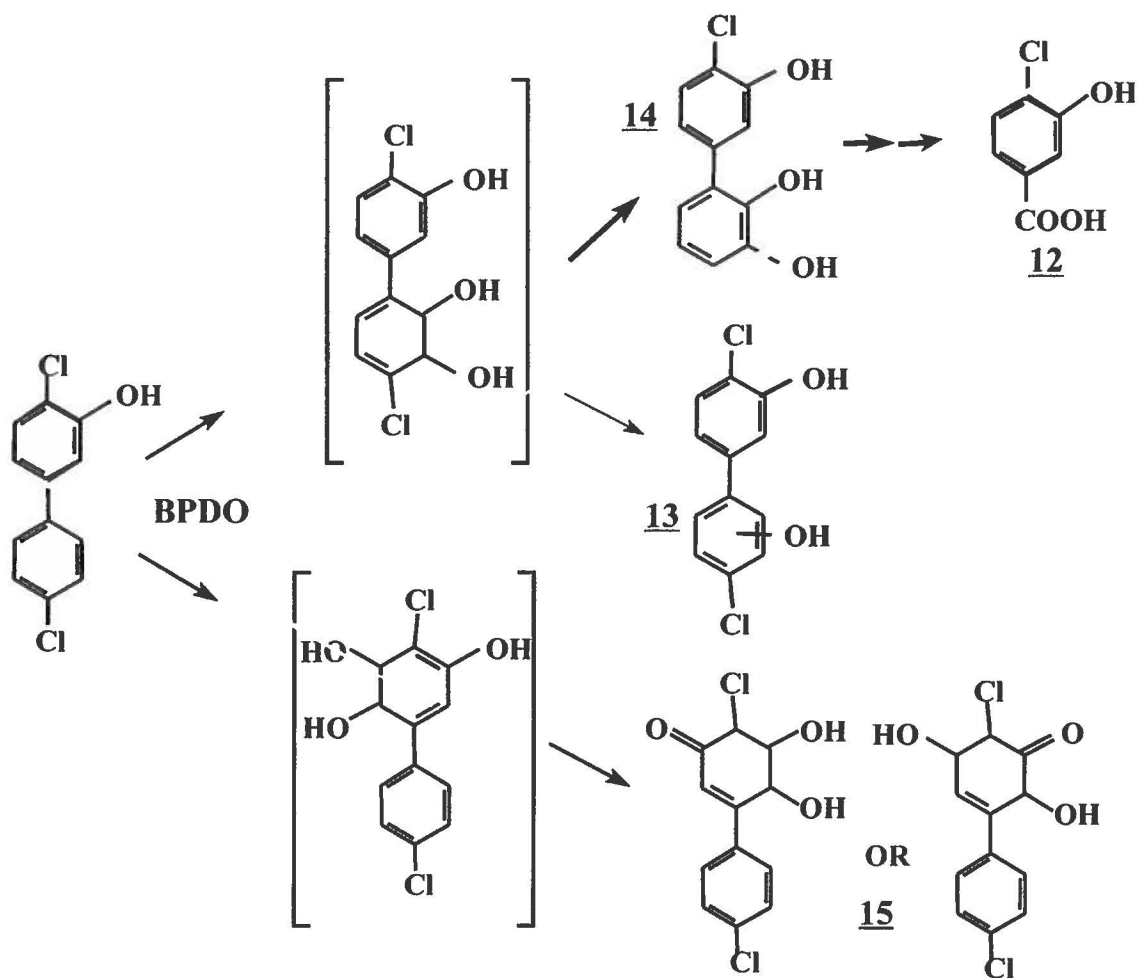


Figure 6.6: Proposed profile of metabolites produced from 3-hydroxy-4,4'-dichlorobiphenyl by B356 BPDO and biphenyl-induced cells of strain B356. The thick arrows indicate the major route of transformation. Brackets indicate the metabolite was not detected. The metabolite numbering is as indicated in Table 6.5.

6.8.6.3. Metabolism of 3,3'-dihydroxy-4,4'-dichlorobiphenyl

3,3'-Dihydroxy-4,4'-dichlorobiphenyl is poorly metabolized by strain B356. About 1% of the substrate added to the biphenyl-induced resting cell suspension was metabolized after 18 h of incubation. The major metabolite, representing about 90% of the total was detected in the acidic extract of the culture and it was identified as 3-hydroxy-4-chlorobenzoic acid on the basis of its GC-MS spectral features which were identical to metabolite 12 (Table 6.5). The other metabolites were hydroxychlorobiphenyls that were found at very low concentrations and were not identified. The observation that the biphenyl catabolic enzymes of strain B356 poorly metabolized 3,3'-dihydroxy-4,4'-dichlorobiphenyl was confirmed by the fact that less than 1% of the added substrate was metabolized after 10 min incubation with a purified preparation of B356 BPDO. Only one major metabolite was detected which exhibited the mass spectral attributes of a trihydroxydichlorobiphenyl (metabolite 16, Table 6.5). Although further work will be required to determine its precise identity, this metabolite may presumably be the 2,3,3'-trihydroxy-4,4'-dichlorobiphenyl that would be further metabolized by the downstream biphenyl catabolic enzymes to generate the 3-hydroxy-4-chlorobenzoic acid found in the resting cell suspensions of strain B356. Metabolite 16 was most likely produced from a 2,3 dioxygenation reaction with concomitant replacement of the *meta* hydroxyl but we cannot exclude its formation from a 5,6 dioxygenation followed by elimination of one water molecule. Another metabolite detected in trace amount in the BPDO reaction medium was identified on the basis of its mass spectral features which was characteristic of a monochlorinated compound, as either 3-(4-chloro-3-hydroxyphenyl)-2,5-dihydroxycyclohex-3-en-1-one or 3-(4-chloro-3-hydroxyphenyl)-4,5-dihydroxycyclohex-2-en-1-one (metabolite 17, Table 6.5). The metabolite exhibited the characteristic single prominent ion at m/z (354, $M^+ - 116$), corresponding to $[(CH_3)_3SiOH - CH - CH_2]$ observed for 3,4-dihydroxy-5-(3-hydroxyphenyl)-5-cyclohexen-1-one (296). This metabolite is not likely to be further metabolized by the biphenyl catabolic pathway and is most likely produced from the concomitant rearrangement and loss of a chlorine atom of 5,6-dihydro-3,3',5,6-tetrahydroxy-4,4'-dichlorobiphenyl that would result from a catalytic oxygenation on carbon 5 and 6. It is noteworthy that in the case of 3-hydroxy-4,4'-dichlorobiphenyl, the attack onto the hydroxylated ring generated a similar metabolite (metabolite 15), but it was not dehalogenated. This suggests that the occurrence of the dehalogenation reaction may depend on the overall electronic distribution of the dihydroxy metabolite. A proposed pathway for the metabolism of 4,4'-dichloro-3,3'-dihydroxybiphenyl is presented in Figure 6.7.

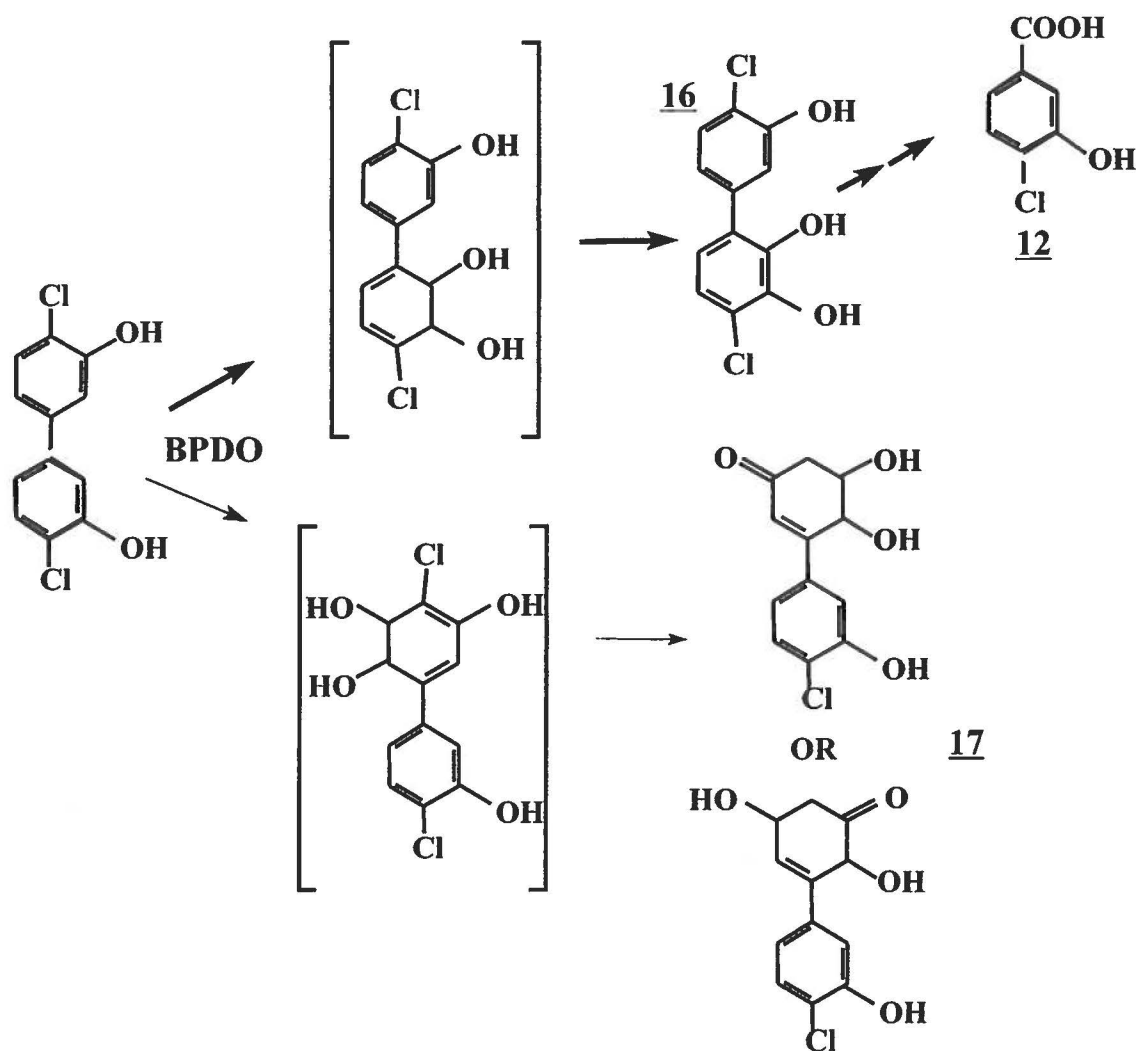


Figure 6.7: Proposed profile of metabolites produced from 3,3'-dihydroxy-4,4'-dichlorobiphenyl by B356 BPDO and biphenyl-induced cells of strain B356. The thick arrows indicate the major route of transformation. Brackets indicate the metabolite was not detected. The metabolite numbering is as indicated in Table 6.5.

6.9. Discussion

According to their primary amino acid sequence, BphAE_{B356} and BphAE_{LB400} belong to distinct phylogenetic clusters of BphAEs. Recent data has suggested that each cluster may have evolved to play distinct ecophysiological roles with respect to the metabolism of aromatic compounds in the environment (235, 236). Although LB400 BPDO was considered as the best PCB metabolizing dioxygenase of natural origin, B356 BPDO was shown to metabolize efficiently, many biphenyl analogs that LB400 BPDO metabolizes poorly (106, 169, 235, 236). Consistent with these findings, in this work we showed that strain B356 BPDO metabolizes several *para*-substituted hydroxy- and hydroxychlorobiphenyl analogs more efficiently than strain LB400 BPDO. Our data also showed that the dihydrodihydroxybiphenyls resulting from catalytic dioxygenation of doubly *para*-substituted hydroxychlorobiphenyls are prone to intramolecular rearrangements which may or may not lead to the loss of water or of a *para*-chlorine atom. Similar instabilities and rearrangements were observed in the case of 5,6-dihydro-3,3',5,6-tetrahydroxybiphenyl which was generated from the catalytic oxygenation of 3,3'-dihydroxybiphenyl by B356 BPDO and which was rapidly converted to (3*S*,4*R*)-3,4-dihydroxy-5-(3-hydroxyphenyl)-5-cyclohexen-1-one, a dead-end metabolite (296).

In a previous work, it was shown that *P. putida* DA261 which expressed B356 BPDO plus BphB produced 2,3-dihydroxy-4'-chlorobiphenyl and 2,3-dihydroxy-2'-chlorobiphenyl from 4,4'-dichlorobiphenyl and 2,4-dichlorobiphenyl respectively. This suggested that a dehalogenation reaction had occurred during catalytic oxygenation of the *para*-chlorinated ring by B356 BPDO (8). During this work we confirmed this observation and found that 2,3-dihydroxy-4'-chlorobiphenyl was a major metabolite produced from 4,4'-dichlorobiphenyl by *E. coli* cells expressing B356 BPDO (not shown). In addition, in this work a similar dehalogenation reaction was observed with other doubly *para*-substituted biphenyls. Thus, we found that 2,3,3'-trihydroxy-4'-chlorobiphenyl (metabolite 14) was a major metabolite produced from 3-hydroxy-4,4'-chlorobiphenyl and small amount of 3-(4-chloro-3-hydroxyphenyl)-2,5-dihydroxycyclohex-3-en-1-one (metabolite 17) was produced from 3,3'-dihydroxy-4,4'-dichlorobiphenyl by a purified preparation of B356 BPDO. These dehalogenation reactions are distinct from the oxygenolytic dehalogenation occurring during the catalytic oxygenation of the *ortho-meta* carbons of 2,2'-dichlorobiphenyl (18) since removal of the *para* chlorine was not replaced by an hydroxyl group.

On the other hand, no dechlorinated metabolite was reported when 4,4'-dichlorobiphenyl and 2,4,4'-trichlorobiphenyl were oxidized by *Pseudomonas pseudoalcaligenes* KF707 BPDO (162, 305). Similarly, the catalytic oxidation of 2,4,4'-trichlorobiphenyl and 2,2',4,4'-tetrachlorobiphenyl by B356 BPDO and by LB400 mutants, generated as major metabolite, for each substrate, the expected, non dechlorinated dihydrodihydroxy metabolite, which was stable (21, 106). It is also noteworthy that in a previous work, *cis*-2,3-dihydro-2,3-dihydroxy-1,1,1-trichloro-2,2-bis(4-chlorophenyl)ethane produced from catalytic oxygenation of DDT was shown to be very stable and no *para*-dehalogenation was observed (169). Furthermore, in the current work no dehalogenated metabolite was detected when 4-hydroxy-4'-chlorobiphenyl was metabolized by B356 BPDO. Therefore, it appears that the dehalogenation reaction occurring during catalytic oxygenation of doubly *para*-substituted chloro- and hydroxychlorobiphenyl analogs may depend on many factors, which may include the number, type and position of the substituents, and perhaps the structural properties of the BPDO used to catalyze the reaction.

Several metabolites detected in this work are most likely generated from a redistribution of the electronic configuration of instable dihydrodihydroxybiphenyls resulting in the loss of a water molecule or chlorine atom. However, many other types of mechanisms may have been involved in the production of some of the unexpected metabolites detected in this work. For example, in the case of the *meta-para* dihydroxylated metabolites 4 and 7 (3,4-dihydroxy-4'-chlorobiphenyl and 3,4,5-trihydroxy-4'-chlorobiphenyl), we cannot exclude the possibility that they were produced inside the catalytic pocket of B356 BPDO during the catalytic reaction.

In a previous report, it was shown that dibenzofuran was displaced from its original binding conformation to another conformation during its catalytic dioxygenation by a mutant of LB400 BPDO (164). This displacement allowed substrate atoms other than the predestined ones to interact with protein atoms involved in the catalytic reaction. As a consequence, although the crystal structure of the substrate-bound form of the enzyme clearly showed the substrate into the conformation that would allow an angular dioxygenation of dibenzofuran, the major metabolites produced from the reaction resulted from a lateral dioxygenation (164). Therefore, in the present study, although the docking experiments were consistent with an *ortho-meta* dioxygenation of 4-hydroxy-4'-chlorobiphenyl, we cannot exclude the possibility that the enzyme regiospecificity toward these substrates may have changed during the

catalytic reaction through a similar mechanism to generate principally *meta-para* hydroxylated metabolites. Likewise, we cannot exclude the possibility that B356 BPDO may have hydroxylated the *meta*-carbon of the *para*-hydroxylated ring through a monooxygenase type reaction similar to the one catalyzed by *P. pseudoalcaligenes* KF707 BPDO on isoflavan-4-ol (278).

One clear observation made in this work is that the dihydrodihydroxybiphenyl metabolites that were expected to be produced from the substrates used in this study were not detected or detected at very low level when B356 and LB400 BPDOs were used to catalyze their oxygenation. A major consequence of this finding is that doubly *para*-substituted hydroxychlorobiphenyls are prone to generate dead-end metabolites when they serve as substrate for the bacterial biphenyl dioxygenase. This was evidenced by the fact that only small amounts of hydroxy- or chlorobenzoic acids were detected in biphenyl-induced cell suspensions of strain B356 incubated with 4,4'-dihydroxy or 4-hydroxy-4'-chlorobiphenyl; most of the metabolites were recovered as hydroxylated derivatives of the tested substrate. The formation of dead-end metabolites may also explain why Tehrani et al. (2012) (327) did not detect any 4-chlorobenzoate in biphenyl-induced cell suspensions of strain LB400 incubated with 4-hydroxy-4'-chlorobiphenyl, though substrate depletion was observed.

Unlike bacteria which metabolize PCBs through the biphenyl dioxygenase to generate a *cis*-dihydrodihydroxybiphenyl derivative, plants and animals produce principally monohydroxylated derivatives from PCBs. In both organisms the hydroxylation may occur on either one of the chlorinated or non chlorinated ring (244, 258). However, in the case of plants several reports indicate that the hydroxylation reaction often occurs onto the *para* carbon of the least chlorinated ring (161, 244). Altogether, our data show that many unexpected hydroxylated metabolites are produced when doubly *para*-substituted hydroxychlorobiphenyls are metabolized by the bacterial BPDOs, some of these metabolites may facilitate further metabolism, such as the one resulting from *para* dehalogenation reactions, but other metabolites may not be further degraded by the biphenyl catabolic enzymes and they may accumulate in the environment. Although further work will be required to clarify precisely the mechanism by which all the metabolites observed in this work were produced, our data show that a clear picture of the fate of PCBs in contaminated sites will require a better understanding of the metabolism of the hydroxychlorobiphenyls

derived from plants and animals and of the chemistry of the dihydrodihydroxylated metabolites produced from them by the bacterial biphenyl dioxygenase.

6.10. Acknowledgements

This work was supported in part by a NSERC grant RGPIN/39579-2012 to MS. We thank Sameer Al-Abdul-Wahid, QANUC NMR Facility (McGill University, Montreal, Quebec, Canada), for his help in NMR analysis.

7. Discussion

7.1. Biphenyl catabolic pathway for the degradation of PCBs

Biphenyl catabolic pathway and PSMs

Plant secondary metabolites, especially flavonoids are known to have a multifunctional role in the rhizospheric plant-microbe direct and indirect interactions. The direct correlations, in which flavonoids act as signal molecules to initiate legume-rhizobia symbioses, or to establish the arbuscular mycorrhizal symbiosis, has been well investigated (23, 33, 121, 332). However, the indirect interactions, in which flavonoids and other PSMs induce plant colonization by plant-growth promoting rhizobacteria or enhance the degradation of soil pollutants in the rhizosphere is largely unknown. A better understanding about these interactions is important in exploitation plants and microbes to rhizoremediate PCBs and other pollutants in soil. In this work, we have examined the ability of certain flavonoids to induce biphenyl catabolic pathway of three strains: *R. erythropolis* U23A (Art.1); *P. pnomenusa* B356 and *B. xenovorans* LB400 (Art.2 and Art.3).

The biphenyl catabolic pathway of strain U23A was shown to be triggered by flavanone at a concentration varying from 0.01 mM to 1.0 mM (Art.1). Under the same conditions, flavanone was found to be as good an inducer, if not even better than biphenyl, the traditional inducer of the pathway. Similarly, isoflavone, at concentrations varying between 0.1 mM and 6 mM, was as efficient as biphenyl to induce the biphenyl catabolic pathway of *P. pnomenusa* B356 (Art.2). Furthermore, the induction was observed at a very low concentrations of flavonoids (0.01mM of flavanone for strain U23A and 0.1mM of isoflavone for strain B356), which were ten times lower than the amount of biphenyl required to induce the pathway under the same conditions (0.1mM and 1mM respectively). However, *B. xenovorans* LB400 reacted differently from the other strains tested (Art.2). None of the three flavonoids tested including flavanone, isoflavone and flavone, could induce its biphenyl catabolic pathway.

The difference in the responses of the three strains toward flavonoids may be explained by the fact that the biphenyl catabolic operons of three strains *R. erythropolis* U23A, *P. pnomenusa* B356 and *B. xenovorans* LB400 are most likely regulated by different mechanisms. The *bph* operon of strain LB400 is controlled by two regulators, Orf0 belonging to the GntR family and BphR2 which is a LysR-type regulator (53). Orf0 is a positive regulator (53). On the other hand, the biphenyl operon of strain U23A is likely to be very similar to those of strains *Rhodococcus sp.* M5 and of *R. jostii* RHA1, which are regulated through a two-component regulatory system (170, 187). The regulation system of strain B356 has not yet been investigated in details. However, a gene (*orf0*B356) encoding a protein exhibiting homology with BphS of *C. oxalaticus* A5 and of *Pseudomonas sp.* KKS102 (211), was found upstream of *bphG* in a previous unpublished work. Unlike Orf0 of strain LB400, BphS was found to be a negative regulator (227). Although little is known about the regulatory mechanisms of *bph* genes of the three strains studied, current knowledge shows the divergence of these mechanisms, which may explain their difference responses to flavonoids.

Besides the capacity of flavonoids to induce the bacterial biphenyl catabolic pathways, we also tested the ability of these natural compounds to support the growth of three biphenyl-degrading strains. Results showed that, none of the simple flavonoids tested could act as carbon source to support the growth of *P. pnomenusa* B356, *B. xenovorans* LB400 or *R. erythropolis* U23A. However, most of the tested flavonoids were metabolized very efficiently by the upper biphenyl pathways of strains U23A and B356. Furthermore, we found that, amazingly, B356 grew on diphenylmethane, another biphenyl analog, as well as on biphenyl and this compound could induce the biphenyl catabolic pathway of strain B356 very efficiently (Art.3). Together these observations are consistent with and extend recent reports suggesting that biphenyl structural analogs may play an important role in the rhizoremediation processes (172, 284, 294).

The ability of a biphenyl analog to support the growth of bacteria depends on its ability to induce the biphenyl catabolic pathways as well as the ability of this pathway to transform this compound into key intermediates that may finally enter into the Krebs cycle. The inability of the simple flavonoids we tested to support the growth of strains U23A, B356 and LB400 may most likely be explained by the fact that no biochemical pathway has evolved in these bacteria to further metabolize the chromene derivatives of the upper

pathway. The accumulation of 4-oxo-3,4-dihydrochromene-2-carboxylic acid (or 4-oxo-2-chromanecarboxylic acid) when flavanone was the substrate for biphenyl-induced cells of strains U23A (Art.1), B356 and LB400 (Art.2) provided evidence of the absence of a lower pathway to metabolize it.

In the case of diphenylmethane (Art.3), results showed that a lower catabolic pathway was induced during the incubation of strain B356 with this substrate. Thus, phenylacetic acid which is the end-product generated from diphenylmethane by the biphenyl upper pathway, was then further metabolized to key intermediates. This conclusion was supported by the observation that strain B356 grew well on phenylacetic acid. On the other hand, the fact that 3-chlorobenzoate inhibited the growth of diphenylmethane-grown cells of strain B356 suggested that one of the diphenylmethane metabolites, presumably phenylacetate may have induced the benzoate degradation pathway of strain B356 (see more detail in Discussion section of Art.3). However, there has been no study investigating the ability of this benzoate pathway to metabolize phenylacetic acid. Therefore, more investigation will be required to confirm this hypothesis.

Most substrates used in our study may be related to PSMs. Flavonoids represent one of the major components of root exudates while benzophenone and diphenylmethane are building blocks for a number of PSMs (156, 176, 291). Therefore, our data support the hypothesis proposed by Fotch (79) and Shaw (285) that the bacterial biphenyl catabolic pathways may have ecological functions, possibly related to PSMs metabolisms in the rhizosphere. Especially, the fact that biphenyl catabolic pathway of strain B356 was inducible by diphenylmethane and was able to use it as growth substrate, brings us to question the current belief whereby the biphenyl catabolic pathway evolved primarily to degrade biphenyl. Furthermore, since our study included one representative strain of each of the three distinct phylogenetic clusters of PCB-degrading bacteria (344), and that each responded differently to PSMs, we may postulate a possibility that in this regard, each phylogenetic branch plays a distinct ecophysiological role. This hypothesis is consistent with the recent results of a PCBs-contaminated soil metagenomic study, (300) suggesting that each biphenyl-degrading lineage has acquired distinct PCB-degrading activities.

Exploiting PSMs to promote PCBs rhizoremediation

Although recently, there has been great progress in the development of bioremediation processes to restore xenobiotic-contaminated soil including PCBs, there are still many bottlenecks remaining to be overcome to improve these processes. Three major bottlenecks were summarized by Sylvestre (311). The first one is the limitation of the biphenyl catabolic pathway enzymes to metabolize PCBs. This limitation may be overcome by engineering enzymes of the pathway to broaden their substrates range. The second bottleneck is the low level of expression of the biphenyl catabolic pathway enzymes in the absence of biphenyl as inducer. Many studies have shown that this limitation may be solved by exploiting a process combining plants and their rhizobacteria (311). The last bottleneck is due to the hydrophobicity of PCBs that lead to the uneven distribution of both pollutants and bacteria in soil and makes them become poorly bioavailable. Sylvestre (311) and other (339) have suggested that some of these bottlenecks may be overcome by using a process based on plants and microbes interactions. In this work, we did not engineer biphenyl catabolic pathway enzymes to broaden their substrates ranges, however our results may suggest practical solutions for the second and the third limitations and therefore help to improve the degradation of PCBs in soil by rhizobacteria.

We showed that several biphenyl analogs, some of which are PSMs, acted as inducers for the biphenyl catabolic pathway (**Art.1**, **Art.2** and **Art.3**). This observation encourages the prospect of using a process exploiting plants and their associated rhizobacteria to clean PCBs decontaminated soil. In such a process, plants would excrete exudates containing flavonoids, sugars, amino acids and other components via their root system into the rhizosphere. While flavonoids from root exudates would serve as inducer of the biphenyl catabolic pathway, sugars and amino acids would serve as growth substrates for the bacteria. However, a number of issues need to be considered in order to achieve successful plants-microbes rhizoremediation process.

The biphenyl catabolic pathways of various bacterial strains react differently toward flavonoids. For example, the biphenyl catabolic pathway of *P. pnomensusa* B356 was induced by isoflavone and diphenylmethane (**Art.2** and **Art.3**) while in the case of strain *R. erythropolis* U23A, this pathway was induced by flavanone (**Art.1**). In addition, each plant will most likely have different impacts on bacterial strains due to difference in their root

exudates composition (105, 167, 173, 194). Therefore, in order to obtain a functional plant-rhizobacteria system, it will be essential to select the most appropriate bacterial strains and plant types. As a first choice we may suggest the use of plant-microbe models that have already been well characterized. For example *M. sativa* or *Beta vulgaris* with *P. fluorescens* (32, 347), *Arabidopsis* with *P. putida* (216) or *R. erythropolis* (Art.1). However, other factors than the plants and microbial species should also be considered when designing a system of plant-rhizobacteria. Those factors will be discussed below.

A concentration of 0.01 mM of flavanone was required to induce the biphenyl catabolic pathway of strain U23A (Art.1) and of 0.1 mM of isoflavone to induce that of strain B356 (Art.2). Although the information regarding the concentrations of individual flavonoids in the rhizosphere is lacking, several flavonoids were estimated to be present in the rhizosphere at concentrations varying from a few to hundreds nmol (285). These concentrations are much lower than the minimum concentration, at which flavonoids were found to induce the biphenyl catabolic pathway in our study. Therefore, transgenic plants that can produce higher concentration of certain flavonoids are necessary. There are several examples of flavonoids-overproducing transgenic plants that may be promising candidates for such a process. Among them, we may cite two variants *tt8* and *ttg* of *A. thaliana* that were studied by Walker et al. (1999) (350) and Nesi et al. (2000) (217) and mutants W92.40 and W92.72 of *Linum usitatissimum* that were able to produce several flavonoids at concentrations twice as high as the wild-type (370). More flavonoids-overproducing transgenic plants candidates are described in section 2.2.3.2. Furthermore, although there has been no study to determine whether various flavonoids may act synergistically to induce the biphenyl catabolic pathway, it is possible that many flavonoids together, even if present at low concentration, may induce this pathway more strongly than a simple one.

Flavonoids overproduction is important to induce the biphenyl catabolic pathway. However, at high concentration, certain flavonoids may inhibit PCBs metabolism or may be toxic for the microorganisms. In this regard, Art.1 shows that strain *R. erythropolis* U23A could not grow on its traditional substrate, biphenyl, in the presence of flavanone. Other data (not yet published) also show that at a concentration higher than 0.1 mM, flavone inhibited the growth of strain U23A in a culture containing sodium acetate as carbon source. Another example is the case of carvone, a terpenoid found in *Mentha spicata*, which enhanced the biphenyl-degrading ability of an *Arthrobacter* strain, but which was toxic to this bacterium

(103). These factors should be considered in the development of the rhizoremediation process.

As presented in the section Literature Review (section 2.3.2), we may also consider the alternative of using transgenic plants containing biphenyl catabolic pathway genes that can metabolize PCBs contaminants. A model of plant-microbe where both components would hold PCBs degradation genes should help not only to strengthen the biphenyl-degrading ability of the system but also to prevent the accumulation of certain toxic metabolites generated by plant enzymes (225, 311, 313).

Together, although many bottlenecks still remain to be overcome, rhizoremediation processes exploiting plant-microbe interactions to decontaminate organic pollutants in soil are very promising.

Degradation of hydroxychlorobiphenyls by the biphenyl catabolic pathway

Bacterial biphenyl catabolic pathway has been shown to be able to degrade PCBs (18, 91, 106, 313, 319, 330, 337, 345) and certain other biphenyl analogs such as dibenzofuran, chlorodibenzofurans (168, 205, 346), dibenzo-*para*-dioxins (168) and dichlorodiphenyltrichloroethane (DDT) (169). In our work, we provided lines of evidence of the ability of the biphenyl catabolic pathway of two bacterial strains *P. pnomenusa* B356 and *B. xenovorans* LB400 to metabolize a broad range of substrates. Aside from the above-cited pollutants, these strains were shown to degrade hydroxychlorobiphenyls (hydroxy-PCBs) and other xenobiotics such as diphenylmethane and benzophenone.

Hydroxy-PCBs are intermediate metabolites produced during the transformation of PCBs and chlorodibenzofuran by the bacterial biphenyl catabolic pathway, or by plant enzymatic systems (87, 149, 185, 244, 311). Although these compounds are toxic, only few studies have examined the ability of biphenyl-degrading bacteria to metabolize hydroxy-PCBs. These studies were discussed in a review of Tehrani et al. (2013) (328). In this work, we have determined the metabolite profiles of four *para*-hydroxy-PCBs including 4-4'-dihydroxybiphenyl, 4-hydroxy-4'-chlorobiphenyl, 3-hydroxy-4,4'-dichlorobiphenyl and 3,3'-

dihydroxy-4,4'-dichlorobiphenyl by the biphenyl catabolic pathway of strains *P. pnomenuma* B356 and *B. xenovorans* LB400 (Art.4).

Biphenyl and simple PCBs are oxidized by BPDOs to produce *cis*-dihydrodihydroxy-metabolites, which are rapidly further metabolized by the downstream enzymes to generate benzoic acid or chlorobenzoic acid. Unlike these compounds, the metabolite profiles of hydroxy-PCBs are more complex, where unexpected metabolites were produced. Although we have not clearly demonstrated the mechanisms by which these metabolites were produced, we may postulate that some of the *cis*-dihydrodihydroxy-metabolites are unstable and they would rearrange through a spontaneous loss of water or chlorine atom. Alternatively, it is possible that, in a way similar to dibenzofurans substrate (164), some of the hydroxy-PCBs may be displaced inside the BPDOs catalytic pocket during the catalytic reaction, leading to the formation of unexpected metabolites. In other cases, BPDOs may have acted as monooxygenase, by catalyzing the addition of a single, instead of two oxygen atoms to the substrate (278). Our data also suggest that BPDOs may also operate a reductive dehalogenation reaction onto the *para*-substituted chlorine, but in this case, the mechanism remains largely unknown and we cannot exclude the possibility that the dehalogenation reaction may have occurred through the redistribution of the electronic configuration of the unstable dihydrodihydroxybiphenyls. It would, therefore, be of interest to further explore this reaction since it may help enhance the degradation of some PCBs and hydroxy-PCBs.

In the case of 4,4'-dihydroxybiphenyl and 4-hydroxy-4'-chlorobiphenyl (Art.4). Aside from a small portion of substrate that was transformed normally by the biphenyl catabolic pathway enzymes to generate the corresponding benzoic acids, the major metabolites generated from these substrates were produced unexpectedly via either one of the mechanisms mentioned above. In the case of 3-hydroxy-4,4'-dichlorobiphenyl and 3,3'-dihydroxy-4,4'-dichlorobiphenyl, the two doubly-*para*-chlorobiphenyl, only BPDO_{B356} was able to metabolize these compounds (Art.4). Besides the dioxygenase reaction that generated a *cis*-dihydrodihydroxy-metabolites, we also observed metabolites that were likely to be produced through a dehalogenation or a monooxygenase reaction.

These unexpected reactions may be interesting to generate novel chemical of interest with regard to the manufacturing of fine chemical. However they represent a disadvantage for the degradation pollutants. Most of these reactions generate dead-end metabolites, as they

cannot be further transformed by the downstream enzymes of the pathway. Therefore, they accumulate, and in the worse case, these metabolites may be more toxic than the parent compounds (35, 244). On the other hand, dehalogenation reactions are helpful in PCBs decontamination, since the most chlorinated congeners are the most persistent to biodegradation (105, 311, 316). Further work should therefore be required to assess the toxicity of the dead-end metabolites generated by the biphenyl catabolic enzymes.

7.2. Biphenyl catabolic pathway for molecular manufacturing

The biphenyl-degrading bacterial strains that we investigated were unable to grow on flavonoids, and most of other chemical tested, however they were able to cometabolize them. Three simple flavonoids including flavone, flavanone, and isoflavone (**Art.1** and **Art.2**) and two other compounds including diphenylmethane and benzophenone (**Art.3**) were used as substrates for the BPDOs. We resolved the metabolite profiles of these compounds by using purified BPDO preparations or used recombinant *E. coli* strains expressing these enzymes. We also used whole cells of *P. pnomenus* B356 and *B. xenovorans* LB400, and *R. erythropolis* U23A.

BPDO_{LB400} has been shown to degrade a wide range of PCB congeners (18, 21, 109, 206, 345), however we have demonstrated that BPDO_{B356} metabolizes PSMs significantly more efficiently than BPDO_{LB400}. Thus BPDO_{B356} oxidized all five substrates investigated (flavone, flavanone, isoflavone, diphenylmethane and benzophenone) with a higher turnover rate (k_{cat}) value than BPDO_{LB400} (**Art.2** and **Art.3**). Especially, we found that BPDO_{B356} k_{cat} values for flavanone (**Art.2**) and diphenylmethane (**Art.3**) were in the same range, or even slightly higher, than for biphenyl. BPDO_{LB400} also transformed all five compounds, however, for many of the tested substrates including isoflavone, flavone (**Art.2**) and benzophenone (**Art.3**), the kinetic parameters were very low. However, it is noteworthy that although strain LB400 did not grow on diphenylmethane, this compound was a substrate as good as biphenyl for BPDO_{LB400} (**Art.3**).

The fact that BPDO may transform several PSMs provides an opportunity to synthesize new compounds through a greener way than by chemical syntheses. We have summarized in a previous section (section 2.3.2) the beneficial effects of flavonoids on

human health. Using a three-dimensional quantitative structure-activity relationship (3D-QSAR) approach, Park et al. (2009) (231) examined the scavenging effect of flavone and of its hydroxy-derivatives. Results showed that, the biological activities of the derivatives containing two or more hydroxy groups were predicted to be higher than flavone, the parent compound. Notably, their results suggested that 2',3'/2',4'/3',4'-dihydroxyflavone would be respectively 88; 40; and 84% more active than flavone. These compounds are difficult to be synthesized by chemical synthesis since the hydroxylation is one of the most challenging reactions in organic synthesis (224). Fortunately, BPDO_{B356} was shown to catalyze the hydroxylation of flavone to generate 2',3'-dihydrodihydroxyflavones and 3',4'-dihydrodihydroxyflavones (Art.2). BphB_{B356}, which can catalyze the dehydrogenation of a wide range of dihydrodihydroxy-metabolites, then can rapidly transform these two dihydrodihydroxyflavones to generate 2',3'- and 3',4'-dihydroxyflavone. Therefore, it would be worth examining a process using BPDO_{B356} plus BphB_{B356} to generate these active compounds.

Besides their interesting pharmacological properties, flavonoids are also important in floral industry since flower colors are mainly controlled by flavonoids (83, 324, 356). These compounds provide a wide range of colors varying from red, blue, pale yellow to deep violet (323, 368, 369). Flowers synthesize a limited range of flavonoids and therefore exhibit a limited range of color. For this reason, genetic engineering has been applied to broaden the color spectrum of flowers (214, 221, 222, 322-324). Some derivatives of anthocyanin (hydroxyflavonoids), especially the one containing hydroxy groups on ring B, are interesting candidates, since these compounds exhibit deep colors such as blue and dark purple that are rarely expressed in certain flowers especially the roses, and therefore have a high value in the flower market (364). Attempts were recently made to generate transgenic carnations and transgenic roses that can use certain enzymes, such as flavonoid 3'-hydroxylase and flavonoid 3',5'-hydroxylase to produce anthocyanin derivatives, especially delphinidin, to have novel blue flowers. However, the success was limited (272, 323). Besides these two enzymes, BPDOs are also worth to be considered, since these enzymes can also catalyze the hydroxylation especially on ring B of flavonoids. However, no study have investigated the ability of BPDOs to transform anthocyanin, thus more study would be needed to engineer BPDOs in order to apply this enzyme in floral genetics.

To summarize, our work revealed that some BPDOs can catalyze the hydroxylation of certain flavonoids as efficiently as biphenyl, their traditional substrate. This observation is useful for green chemistry and for metabolic engineering as well. For green chemistry, it would be interesting to use BPDOs to generate effectively hydroxyflavonoids that have stronger beneficial effect on human health than the parent compounds. For metabolic engineering, it would be worth considering using BPDOs to create hydroxyflavonoids that exhibit deep color flowers that are very rare in nature and therefore have high value in flowers market.

7.3. Mechanistic interactions between BPDOs and substrates

Along with the efforts to investigate metabolic profiles of flavonoids, diphenylmethane and benzophenone by biphenyl catabolic pathway, as well as to determine the kinetic parameters of BPDOs toward these compounds, we studied also the mechanistic interactions between BPDOs and these substrates. In this case, using the Autodock software, we docked the substrate into the enzymes crystal structures from Protein Data Banks. Although the information obtained from this approach is limited, in our case, it was useful to identify some of the protein residues that bind with biphenyl analogs substrates, and some of those that may interact with these substrates in a way that prevents a productive binding.

BPDO_{LB400} metabolized five of the tested substrates less efficiently than its mutant, BPDO_{p4} which was created by changing residue Thr335 by Ala (2 .) (Art.2 and Art.3). These two enzymes differed not only in terms of their reaction rates, but also in terms of their substrate regiospecificity. Thus, BPDO_{p4} oxidized flavonoids at several positions on both rings B and A while the metabolites generated by BPDO_{LB400} were less abundant and they were oxidized on ring B only (Art.2 and Art.3). Our structural and biochemical analyses highlighted the importance of residue Thr335, which hinders the activity of BPDO_{LB400}. The ability of residue Thr335 to hinder the activity of BPDO_{LB400} toward chlorobiphenyls was demonstrated by Kumar et al. (2011) (165). They showed that, hydrogen bonds between residue Thr335 and the Val320-Gln322 segment prevent the productive binding of certain PCB congeners to the enzyme catabolic pocket of BPDO_{LB400}. Changing Thr335 by Ala in BPDO_{p4}, reduces the constraints on the Val320-Gln322 segment, resulting in a more plastic

catalytic pocket that may allow the accommodation of larger PCB congeners. Our modeling study suggested that, a similar mechanism may be responsible for enhancing BPDO_{pt} catalytic properties toward flavonoids (Art.2). However, further structural analyses of substrate-bound crystal forms of the enzyme will be required to confirm this hypothesis.

Our modeling strategy has helped us get more insights about the mechanistic interactions between BPDOs and some of the tested substrates. However, for others, such as hydroxybenzophenone and certain hydroxy-PCBs (Art.3 and Art.4), the Autodock software did not allow us to obtain structural models showing the substrate in a productive orientation inside the catalytic pocket. This limitation showed that, other factors may also affect the enzymatic reaction that our modeling software could not reproduce. Among the likely limitations of our analyses, we may point out that we have run the Autodock software under rigid protein conditions. Under these conditions, the Autodock software was unable to reproduce some of the conformational changes that may occur inside the catalytic pocket during the substrate binding process, to accommodate substrate analogs. The occurrence of such conformational changes has been documented in recent investigations about the binding process of dichlorobiphenyl and dibenzofuran by BPDO_{LB400} and some of its mutants (165, 206). In order to get a more realistic model of the substrate binding process, we may suggest using the Autodock software under flexible protein conditions. This approach may help resolve some of the limitations we have faced during our modeling study.

In addition to the rigid protein conditions mentioned above, there may be an under-utilization of data which is produced by the software. Currently, the application generates various data regarding the enzymatic reaction, of which only one parameter, the total energy, is investigated. Until now, the other parameters, such as electrostatic energy, ligand efficiency, inhibition constant, etc... have not been analyzed in any reports. Further investigation of these parameters may be warranted in order to maximize the exploitation of this approach.

The first of these is the fact that the
majority of the population are
of African descent, and the
majority of the population are
of African descent.

The second of these is the fact that
the majority of the population are
of African descent, and the
majority of the population are
of African descent. The third
of these is the fact that the
majority of the population are
of African descent, and the
majority of the population are
of African descent.

The fourth of these is the fact that
the majority of the population are
of African descent, and the
majority of the population are
of African descent. The fifth
of these is the fact that the
majority of the population are
of African descent, and the
majority of the population are
of African descent.

The sixth of these is the fact that
the majority of the population are
of African descent, and the
majority of the population are
of African descent. The seventh
of these is the fact that the
majority of the population are
of African descent, and the
majority of the population are
of African descent.

8. Conclusion

This work broadens our knowledge about the bacterial biphenyl catabolic pathway. Although our data did not provide enough evidences to firmly confirm it, our results were consistent with the hypothesis whereby the various phylogenetic clusters of the bacterial biphenyl catabolic pathway would each have evolved to play distinct ecophysiological roles not essentially related to the degradation of biphenyl. Our work, therefore, opens the prospect for exploring further studies addressing the role of this pathway in natural ecosystems.

In this work, considerable achievements have been attained with respect to PCB rhizoremediation. As a first achievement, we have identified some of the PSMs that may trigger the bacterial PCB-degrading abilities. When used as co-substrate with another compound that can support bacterial growth, these PSMs were found to act as well as biphenyl to induce the biphenyl catabolic pathway. This finding may help to solve one of the major limitations of exploiting the bacterial biphenyl catabolic pathway to remediate PCBs which is the biphenyl requirement to trigger PCB degradation. Our study allowed us to propose a model for explaining how plants promote PCB degradation in soil. In the rhizosphere, labile chemicals such as the sugar moiety of the conjugated PSMs might provide a substrate on which to grow, whereas the flavonoids or other phenylpropanoids would then induce the biphenyl pathway of PCB-degrading rhizobacteria. This opens the opportunity of expanding the effectiveness of soil decontamination by using combined plant-bacteria systems.

However, our work also highlights that the metabolism of biphenyl analogs as well as the ability of these compounds to trigger the biphenyl catabolic pathway vary considerably among bacteria. Furthermore, we found the amount of PSMs present in plant exudates is significantly lower than what would be required to fully induce the pathway. These observations emphasize the importance of a rational choice of plants and bacteria for an effective rhizoremediation treatment. A further research using quantitative PCR to measure level of gene expression can help to compare the biphenyl catabolic pathway-inducing ability of the different inducers found in this work. This information should be helpful to facilitate the choice of the most appropriate plants and bacteria for the remediation process. In this regard, we may also propose to engineer plants in order to increase the amount of PSMs that are most appropriate to trigger PCB degradation or we may propose to examine the plant physiological factors that may influence the amount of PSMs they release in soil.

In order to apply these achievements in the *in-situ* PCBs rhizoremediation, besides the interaction between PSMs and biphenyl-degrading bacteria that was studied in this work, other factors such as the effect of weather condition, soil characteristics, the presence of other pollutants and microorganisms should also be studied. Especially, since 80% of vascular plants are believed to form symbiosis with mycorrhizal fungi in one hand, and on the other hand this class of fungi has been shown to degrade a wide range of persistent organic pollutants, the interaction between PSMs, mycorrhizal fungi and biphenyl-degrading bacteria is interesting and should be further investigated.

In the context of molecular manufacturing, our work showed a perspective of using biphenyl catabolic pathway enzymes, especially BPDO plus BphB to produce hydroxy-flavonoids, which have many beneficial effects on human health. The fact that both strains *R. erythropolis* U23A and *P. pnomenusa* B356 were able to effectively generate dihydroxy-flavanone from flavanone raised a green way to synthesize these compounds. A promising future of flavonoids manufacturing by using enzymes of this pathway is, therefore, opened, although more studies will be required to fully discover other efficient substrate-enzyme pairs.

This work points out the prospect of using bacterial biphenyl catabolic pathway in PCBs decontamination processes and in manufacturing fine chemicals, especially flavonoids. However, to maximize the application of this pathway, expanding its substrate range is essential. Thus, a better knowledge about the interactions between the enzyme catalytic pocket and the substrates is important. With the help of modeling strategy, we identified protein residues that are likely to prevent or facilitate the catalytic reaction, however, the success was limited. The limitation of modeling method makes crystallization process essential in this case. Information obtained from enzyme crystallization will help to design more efficient enzymes exhibiting more specific chemo-, regio-, and enantio selection toward biphenyl analogs which will promote their application for the synthesis of chemical production, or for the degradation of highly chlorinated PCBs.

Finally, as a second objective, we found that several hydroxy-PCBs were metabolized by enzymes of the biphenyl catabolic pathway, generating unexpected dead-end metabolites that may accumulate in the environment and cause concern. The mechanisms involve in the production of these metabolites were not clearly demonstrated, therefore, further studies are required to elucidate the mechanism by which these problematic compounds are produced. These studies will help to establish a clear picture of the fate of PCBs in environment as well.

9. List of references

1. 2002. Destruction and decontamination technologies for PCBs and other POPs wastes. United Nations Environment Programme.
2. 2013. Health Effects of PCBs. U.S. Environmental Protection Agency.
3. 2004. Polychlorinated Biphenyl Inspection Manual. U.S. Environmental Protection Agency.
4. **Abraham, W. R., Nogales, B., Golyshin, P. N., Pieper, D. H., and Timmis, K. N.** 2002. Polychlorinated biphenyl-degrading microbial communities in soils and sediments. *Curr Opin Microbiol* **5**:246-253.
5. **Abramowicz, D. A.** 1990. Aerobic and anaerobic biodegradation of PCBs - a review. *Crit Rev Biotechnol* **10**:241-249.
6. **Abramowicz, D. A.** 1995. Aerobic and anaerobic PCB biodegradation in the environment. *Environ Health Persp* **103**:97-99.
7. **Ahmad, D., Masse, R., and Sylvestre, M.** 1990. Cloning and expression of genes involved in 4-chlorobiphenyl transformation by *Pseudomonas testosteroni*: homology to polychlorobiphenyl-degrading genes in other bacteria. *Gene* **86**:53-61.
8. **Ahmad, D., Sylvestre, M., and Sondossi, M.** 1991. Subcloning of *bph* genes from *Pseudomonas testosteroni* B-356 in *Pseudomonas putida* and *Escherichia coli* - Evidence for dehalogenation during initial attack on chlorobiphenyls. *Appl Environ Microb* **57**:2880-2887.
9. **Alcalde, M., Ferrer, M., Plou, F. J., and Ballesteros, A.** 2006. Environmental biocatalysis: from remediation with enzymes to novel green processes. *Trends Biotechnol* **24**:281-287.
10. **Allouche, N., Damak, M., Ellouz, R., and Sayadi, S.** 2004. Use of whole cells of *Pseudomonas aeruginosa* for synthesis of the antioxidant hydroxytyrosol via conversion of tyrosol. *Appl Environ Microbiol* **70**:2105-2109.
11. **Anonymous.** 2012. Some chemicals present in industrial and consumer products, food and drinking-water p. 285-305, IARC Monographs on the evaluation of carcinogenic risks to humans, vol. 101. World Health Organization Press.
12. **Arai, H., Kosono, S., Taguchi, K., Maeda, M., Song, E., Fuji, F., Chung, S. Y., and Kudo, T.** 1998. Two sets of biphenyl and PCB degradation genes on a linear plasmid in *Rhodococcus erythropolis* TA421. *J Ferment Bioeng* **86**:595-599.
13. **Asturias, J. A., Moore, E., Yakimov, M. M., Klatte, S., and Timmis, K. N.** 1994. Reclassification of the polychlorinated biphenyl-degraders *Acinetobacter* sp. strain P6 and *Corynebacterium* sp. strain MB1 as *Rhodococcus globerulus*. *Syst Appl Microbiol* **17**:226-231.
14. **Asturias, J. A., and Timmis, K. N.** 1993. Three different 2,3-dihydroxybiphenyl-1,2-dioxygenase genes in the gram-positive polychlorobiphenyl-degrading bacterium *Rhodococcus globerulus* P6. *J Bacteriol* **175**:4631-4640.
15. **Azerad, R.** 2001. Chemical biotechnology - Better enzymes for green chemistry - Editorial overview. *Curr Opin Biotech* **12**:533-534.
16. **Bais, H. P., Park, S. W., Weir, T. L., Callaway, R. M., and Vivanco, J. M.** 2004. How plants communicate using the underground information superhighway. *Trends Plant Sci* **9**:26-32.

17. Barriault, D., Durand, J., Maaroufi, H., Eltis, L. D., and Sylvestre, M. 1998. Degradation of polychlorinated biphenyl metabolites by naphthalene-catabolizing enzymes. *Appl Environ Microbiol* **64**:4637-4642.
18. Barriault, D., Lépine, F., Mohammadi, M., Milot, S., Leberre, N., and Sylvestre, M. 2004. Revisiting the regiospecificity of *Burkholderia xenovorans* LB400 biphenyl dioxygenase toward 2,2'-dichlorobiphenyl and 2,3,2',3'-tetrachlorobiphenyl. *J Biol Chem* **279**:47489-47496.
19. Barriault, D., Pelletier, C., Hurtubise, Y., and Sylvestre, M. 1997. Substrate selectivity pattern of *Comamonas testosteroni* strain B-356 towards dichlorobiphenyls. *Int Biodeter Biodegr* **39**:311-316.
20. Barriault, D., Plante, M. M., and Sylvestre, M. 2002. Family shuffling of a targeted *bphA* region to engineer biphenyl dioxygenase. *J Bacteriol* **184**:3794-3800.
21. Barriault, D., and Sylvestre, M. 2004. Evolution of the biphenyl dioxygenase BphA from *Burkholderia xenovorans* LB400 by random mutagenesis of multiple sites in region III. *J Biol Chem* **279**:47480-47488.
22. Barriault, D., Vedadi, M., Powlowski, J., and Sylvestre, M. 1999. *cis*-2,3-dihydro-2,3-dihydroxybiphenyl dehydrogenase and *cis*-1,2-dihydro-1,2-dihydroxynaphthalene dehydrogenase catalyze dehydrogenation of the same range of substrates. *Biochem Biophys Res Commun* **260**:181-187.
23. Becard, G., Douds, D. D., and Pfeffer, P. E. 1992. Extensive in vitro hyphal growth of vesicular-arbuscular mycorrhizal fungi in the presence of CO₂ and flavonols. *Appl Environ Microbiol* **58**:821-825.
24. Bedard, D. L., Unterman, R., Bopp, L. H., Brennan, M. J., Haberl, M. L., and Johnson, C. 1986. Rapid assay for screening and characterizing microorganisms for the ability to degrade polychlorinated biphenyls. *Appl Environ Microbiol* **51**:761-768.
25. Bedard, D. L., Unterman, R., Bopp, L. H., Brennan, M. J., Haberl, M. L., and Johnson, C. 1986. Rapid assay for screening and characterizing microorganisms for the ability to degrade polychlorinated biphenyls. *Appl Environ Microbiol* **51**:761-768.
26. Bedard, D. L., Wagner, R. E., Brennan, M. J., Haberl, M. L., and Brown, J. F., Jr. 1987. Extensive degradation of Aroclors and environmentally transformed polychlorinated biphenyls by *Alcaligenes eutrophus* H850. *Appl Environ Microbiol* **53**:1094-1102.
27. Beltrametti, F., Reniero, D., Backhaus, S., and Hofer, B. 2001. Analysis of transcription of the *bph* locus of *Burkholderia* sp. strain LB400 and evidence that the *orf0* gene product acts as a regulator of the *bphA1* promoter. *Microbiology* **147**:2169-2182.
28. Borja, J., Taleon, D. M., Auresenia, J., and Gallardo, S. 2005. Polychlorinated biphenyls and their biodegradation. *Process Biochem* **40**:1999-2013.
29. Boyd, D. R., and Bugg, T. D. 2006. Arene *cis*-dihydrodiol formation: from biology to application. *Org Biomol Chem* **4**:181-192.
30. Boyd, D. R., Sharma, N. D., Belhocine, T., Malone, J. F., McGregor, S., and Allen, C. C. 2006. Dioxygenase-catalysed dihydroxylation of arene *cis*-dihydrodiols and acetone derivatives: a new approach to the synthesis of enantiopure tetraoxygenated bioproducts from arenes. *Chem Commun (Camb)*:4934-4936.
31. Boyd, D. R., Sharma, N. D., Bowers, N. I., Dalton, H., Garrett, M. D., Harrison, J. S., and Sheldrake, G. N. 2006. Dioxygenase-catalysed oxidation of disubstituted benzene substrates:

- benzylic monohydroxylation versus aryl *cis*-dihydroxylation and the *meta* effect. *Org Biomol Chem* **4**:3343-3349.
32. **Brazil, G. M., Kenefick, L., Callanan, M., Haro, A., Delorenzo, V., Dowling, D. N., and Ogara, F.** 1995. Construction of a rhizosphere pseudomonad with potential to degrade polychlorinated-biphenyls and detection of *bph* gene-expression in the rhizosphere. *Appl Environ Microb* **61**:1946-1952.
 33. **Broughton, W. J., Jabbouri, S., and Perret, X.** 2000. Keys to symbiotic harmony. *J Bacteriol* **182**:5641-5652.
 34. **Burton, S. G.** 2003. Oxidizing enzymes as biocatalysts. *Trends Biotechnol* **21**:543-549.
 35. **Camara, B., Herrera, C., Gonzalez, M., Couve, E., Hofer, B., and Seeger, M.** 2004. From PCBs to highly toxic metabolites by the biphenyl pathway. *Environ Microbiol* **6**:842-850.
 36. **Campanella, B. F., Bock, C., and Schroder, P.** 2002. Phytoremediation to increase the degradation of PCBs and PCDD/Fs. Potential and limitations. *Environ Sci Pollut Res Int* **9**:73-85.
 37. **Carredano, E., Karlsson, A., Kauppi, B., Choudhury, D., Parales, R. E., Parales, J. V., Lee, K., Gibson, D. T., Eklund, H., and Ramaswamy, S.** 2000. Substrate binding site of naphthalene 1,2-dioxygenase: functional implications of indole binding. *J Mol Biol* **296**:701-712.
 38. **Chang, M. C., Eachus, R. A., Trieu, W., Ro, D. K., and Keasling, J. D.** 2007. Engineering *Escherichia coli* for production of functionalized terpenoids using plant P450s. *Nat Chem Biol* **3**:274-277.
 39. **Chaudhry, Q., Blom-Zandstra, M., Gupta, S., and Joner, E. J.** 2005. Utilising the synergy between plants and rhizosphere microorganisms to enhance breakdown of organic pollutants in the environment. *Environ Sci Pollut Res Int* **12**:34-48.
 40. **Chebrou, H., Hurtubise, Y., Barriault, D., and Sylvestre, M.** 1999. Heterologous expression and characterization of the purified oxygenase component of *Rhodococcus globerulus* P6 biphenyl dioxygenase and of chimeras derived from it. *J Bacteriol* **181**:4805-4811.
 41. **Chekol, T., Vough, L. R., and Chaney, R. L.** 2004. Phytoremediation of polychlorinated biphenyl-contaminated soils: the rhizosphere effect. *Environ Int* **30**:799-804.
 42. **Chong, M. N., Jin, B., Chow, C. W., and Saint, C.** 2010. Recent developments in photocatalytic water treatment technology: a review. *Water Res* **44**:2997-3027.
 43. **Christensen, A., Gurol, M. D., and Garoma, T.** 2009. Treatment of persistent organic compounds by integrated advanced oxidation processes and sequential batch reactor. *Water Res* **43**:3910-3921.
 44. **Chun, H. K., Ohnishi, Y., Shindo, K., Misawa, N., Furukawa, K., and Horinouchi, S.** 2003. Biotransformation of flavone and flavanone by *Streptomyces lividans* cells carrying shuffled biphenyl dioxygenase genes. *J Mol Catal B-Enzym* **21**:113-121.
 45. **Chung, S. Y., Maeda, M., Song, E., Horikoshi, K., and Kudo, T.** 1994. A gram-positive polychlorinated biphenyl-degrading bacterium, *Rhodococcus erythropolis* strain TA421, isolated from a termite ecosystem. *Biosci Biotechnol Biochem* **58**:2111-2113.
 46. **Colbert, C. L., Agar, N. Y., Kumar, P., Chakko, M. N., Sinha, S. C., Powlowski, J. B., Eltis, L. D., and Bolin, J. T.** 2013. Structural characterization of *Pandoraea pnomenusa* B-356 biphenyl dioxygenase reveals features of potent polychlorinated biphenyl-degrading enzymes. *PloS one* **8**:e52550.

47. **Compant, S., Duffy, B., Nowak, J., Clement, C., and Barka, E. A.** 2005. Use of plant growth-promoting bacteria for biocontrol of plant diseases: principles, mechanisms of action, and future prospects. *Appl Environ Microbiol* **71**:4951-4959.
48. **Cundy, A. B., Hopkinson, L., and Whitby, R. L.** 2008. Use of iron-based technologies in contaminated land and groundwater remediation: a review. *Sci Total Environ* **400**:42-51.
49. **Daar, A. S., Thorsteinsdottir, H., Martin, D. K., Smith, A. C., Nast, S., and Singer, P. A.** 2002. Top ten biotechnologies for improving health in developing countries. *Nat Genet* **32**:229-232.
50. **De Lorenzo, V., and Pérez-Martin, J.** 1996. Regulatory noise in prokaryotic promoters: How bacteria learn to respond to novel environmental signals. *Mol Microbiol* **19**:1177-1184.
51. **De, S., Perkins, M., and Dutta, S. K.** 2006. Nitrate reductase gene involvement in hexachlorobiphenyl dechlorination by *Phanerochaete chrysosporium*. *J Hazard Mater* **135**:350-354.
52. **De Voogt, B.** 1989. Production, properties and usage of polychlorinated biphenyls, p. 3-45. *In* Kimbrough, R.D. and Jensen, A.A. (ed.), *Halogenated biphenyls, terphenyls, naphthalenes, dibenzodioxins and related products. Topics in environmental health.* Elsevier.
53. **Denef, V. J., Park, J., Tsoi, T. V., Rouillard, J. M., Zhang, H., Wibbenmeyer, J. A., Verstraete, W., Gulari, E., Hashsham, S. A., and Tiedje, J. M.** 2004. Biphenyl and benzoate metabolism in a genomic context: outlining genome-wide metabolic networks in *Burkholderia xenovorans* LB400. *Appl Environ Microbiol* **70**:4961-4970.
54. **Dercova, K., Tandlich, R., and Brezna, B.** 2003. Application of terpenes as possible inducers of biodegradation of PCBs. *Fresen Environ Bull* **12**:286-290.
55. **Deweerd, K. A., and Suflita, J. M.** 1990. Anaerobic aryl reductive dehalogenation of halobenzoates by cell extracts of "*Desulfomonile tiedjei*". *Appl Environ Microbiol* **56**:2999-3005.
56. **Déziel, E., Comeau, Y., and Villemur, R.** 2001. Initiation of biofilm formation by *Pseudomonas aeruginosa* 57RP correlates with emergence of hyperpilated and highly adherent phenotypic variants deficient in swimming, swarming, and twitching motilities. *J Bacteriol* **183**:1195-1204.
57. **Dhindwal, S., Patil, D. N., Mohammadi, M., Sylvestre, M., Tomar, S., and Kumar, P.** 2011. Biochemical studies and ligand-bound structures of biphenyl dehydrogenase from *Pandoraea pnomenusa* strain B-356 reveal a basis for broad specificity of the enzyme. *J Biol Chem* **286**:37011-37022.
58. **Dietrich, D., Hickey, W. J., and Lamar, R.** 1995. Degradation of 4,4'-dichlorobiphenyl, 3,3',4,4'-tetrachlorobiphenyl, and 2,2',4,4',5,5'-hexachlorobiphenyl by the white rot fungus *Phanerochaete chrysosporium*. *Appl Environ Microbiol* **61**:3904-3909.
59. **Dixon, R. A.** 2001. Natural products and plant disease resistance. *Nature* **411**:843-847.
60. **Dmochewitz, S., and Ballschmiter, K.** 1988. Microbial transformation of technical mixtures of polychlorinated biphenyls (PCB) by the fungus *Aspergillus niger*. *Chemosphere* **17**:111-121.
61. **Dong, X. S., Fushinobu, S., Fukuda, E., Terada, T., Nakamura, S., Shimizu, K., Nojiri, H., Omori, T., Shoun, H., and Wakagi, T.** 2005. Crystal structure of the terminal oxygenase component of cumene dioxygenase from *Pseudomonas fluorescens* IP01. *J Bacteriol* **187**:2483-2490.

62. **Donnelly, P. K., Hegde, R. S., and Fletcher, J. S.** 1994. Growth of PCB-degrading bacteria on compounds from photosynthetic plants. *Chemosphere* **28**:981-988.
63. **Doty, S. L.** 2008. Enhancing phytoremediation through the use of transgenics and endophytes. *New Phytol* **179**:318-333.
64. **Ducrocq, V., Pandardb, P., Hallier-Souliera, S., Thybaudb, E., and Truffaut, N.** 1999. The use of quantitative PCR, plant and earthworm bioassays, plating and chemical analysis to monitor 4-chlorobiphenyl biodegradation in soil microcosms. *Appl Soil Ecol* **12**:15-27.
65. **Duetz, W. A., Van Beilen, J. B., and Witholt, B.** 2001. Using proteins in their natural environment: potential and limitations of microbial whole-cell hydroxylations in applied biocatalysis. *Curr Opin Biotechnol* **12**:419-425.
66. **Ecobichon, D. J., and Comeau, A. M.** 1974. Comparative effects of commercial Aroclors on rat liver enzyme activities. *Chem Biol Interact* **9**:341-350.
67. **Edwards, U., Rogall, T., Blocker, H., Emde, M., and Bottger, E. C.** 1989. Isolation and direct complete nucleotide determination of entire genes. Characterization of a gene coding for 16S ribosomal RNA. *Nucleic Acids Res* **17**:7843-7853.
68. **Eltis, L. D., Hofmann, B., Hecht, H. J., Lunsdorf, H., and Timmis, K. N.** 1993. Purification and crystallization of 2,3-dihydroxybiphenyl 1,2-dioxygenase. *J Biol Chem* **268**:2727-2732.
69. **Erickson, B. D., and Mondello, F. J.** 1993. Enhanced biodegradation of polychlorinated biphenyls after site-directed mutagenesis of a biphenyl dioxygenase gene. *Appl Environ Microbiol* **59**:3858-3862.
70. **Erickson, B. D., and Mondello, F. J.** 1992. Nucleotide sequencing and transcriptional mapping of the genes encoding biphenyl dioxygenase, a multicomponent polychlorinated-biphenyl-degrading enzyme in *Pseudomonas* strain LB400. *J Bacteriol* **174**:2903-2912.
71. **Faber, K.** 2004. Biotransformations in organic chemistry. Springer, Berlin.
72. **Farre, M. J., Maldonado, M. I., Gernjak, W., Oller, I., Malato, S., Domenech, X., and Peral, J.** 2008. Coupled solar photo-Fenton and biological treatment for the degradation of diuron and linuron herbicides at pilot scale. *Chemosphere* **72**:622-629.
73. **Fava, F., and Bertin, L.** 1999. Use of exogenous specialised bacteria in the biological detoxification of a dump site-polychlorobiphenyl-contaminated soil in slurry phase conditions. *Biotechnol Bioeng* **64**:240-249.
74. **Ferraro, D. J., Brown, E. N., Yu, C. L., Parales, R. E., Gibson, D. T., and Ramaswamy, S.** 2007. Structural investigations of the ferredoxin and terminal oxygenase components of the biphenyl 2,3-dioxygenase from *Sphingobium yanoikuyae* B1. *Bmc Struct Biol* **7**:10.
75. **Ferraro, D. J., Gakhar, L., and Ramaswamy, S.** 2005. Rieske business: structure-function of Rieske non-heme oxygenases. *Biochem Biophys Res Commun* **338**:175-190.
76. **Field, J. A., and Sierra-Alvarez, R.** 2008. Microbial degradation of chlorinated dioxins. *Chemosphere* **71**:1005-1018.
77. **Fish, K. M., and Principe, J. M.** 1994. Biotransformations of Aroclor 1242 in Hudson river test tube microcosms. *Appl Environ Microbiol* **60**:4289-4296.
78. **Fletcher, J. S., and Hegde, R. S.** 1995. Release of phenols by perennial plant-roots and their potential importance in bioremediation. *Chemosphere* **31**:3009-3016.
79. **Focht, D. D.** 1995. Strategies for the improvement of aerobic metabolism of polychlorinated biphenyls. *Curr Opin Biotech* **6**:341-346.

80. Focht, D. D., and Alexander, M. 1971. Aerobic cometabolism of DDT analogues by *Hydrogenomonas* sp. *J Agric Food Chem* **19**:20-22.
81. Focht, D. D., and Alexander, M. 1970. Bacterial degradation of diphenylmethane, a DDT model substrate. *Appl Microbiol* **20**:608-611.
82. Focht, D. D., and Alexander, M. 1970. DDT metabolites and analogs: ring fission by *Hydrogenomonas*. *Science* **170**:91-92.
83. Forkmann, G., and Martens, S. 2001. Metabolic engineering and applications of flavonoids. *Curr Opin Biotechnol* **12**:155-160.
84. Formica, J. V., and Regelson, W. 1995. Review of the biology of Quercetin and related bioflavonoids. *Food Chem Toxicol* **33**:1061-1080.
85. Fortin, P. D., Macpherson, I., Neau, D. B., Bolin, J. T., and Eltis, L. D. 2005. Directed evolution of a ring-cleaving dioxygenase for polychlorinated biphenyl degradation. *J Biol Chem* **280**:42307-42314.
86. Francis, I., Holsters, M., and Vereecke, D. 2010. The Gram-positive side of plant-microbe interactions. *Environ Microbiol* **12**:1-12.
87. Francova, K., Mackova, M., Macek, T., and Sylvestre, M. 2004. Ability of bacterial biphenyl dioxygenases from *Burkholderia* sp. LB400 and *Comamonas testosteroni* B-356 to catalyze oxygenation of *ortho*-hydroxychlorobiphenyls formed from PCBs by plants. *Environ Pollut* **127**:41-48.
88. Friemann, R., Lee, K., Brown, E. N., Gibson, D. T., Eklund, H., and Ramaswamy, S. 2009. Structures of the multicomponent Rieske non-heme iron toluene 2,3-dioxygenase enzyme system. *Acta Crystallogr D* **65**:24-33.
89. Frydman, A., Weissshaus, O., Huhman, D. V., Sumner, L. W., Bar-Peled, M., Lewinsohn, E., Fluhr, R., Gressel, J., and Eyal, Y. 2005. Metabolic engineering of plant cells for biotransformation of hesperedin into neohesperidin, a substrate for production of the low-calorie sweetener and flavor enhancer NHDC. *J Agric Food Chem* **53**:9708-9712.
90. Fujihara, H., Yoshida, H., Matsunaga, T., Goto, M., and Furukawa, K. 2006. Cross-regulation of biphenyl- and salicylate-catabolic genes by two regulatory systems in *Pseudomonas pseudoalcaligenes* KF707. *J Bacteriol* **188**:4690-4697.
91. Fukuda, M., Shimizu, S., Okita, N., Seto, M., and Masai, E. 1998. Structural alteration of linear plasmids encoding the genes for polychlorinated biphenyl degradation in *Rhodococcus* strain RHA1. *Antonie Van Leeuwenhoek* **74**:169-173.
92. Fukuda, M., Yasukochi, Y., Kikuchi, Y., Nagata, Y., Kimbara, K., Horiuchi, H., Takagi, M., and Yano, K. 1994. Identification of the *bphA* and *bphB* genes of *Pseudomonas* sp. strains KKS102 involved in degradation of biphenyl and polychlorinated biphenyls. *Biochem Biophys Res Commun* **202**:850-856.
93. Furukawa, K. 1986. Modification of PCBs by bacteria and other microorganisms, p. 89-100. *In* John, S.W. (ed.), *PCBs and the environment*. CRC Press, Florida.
94. Furukawa, K., and Fujihara, H. 2008. Microbial degradation of polychlorinated biphenyls: Biochemical and molecular features. *J Biosci Bioeng* **105**:433-449.
95. Furukawa, K., Hirose, J., Suyama, A., Zaiki, T., and Hayashida, S. 1993. Gene components responsible for discrete substrate specificity in the metabolism of biphenyl (*bph* operon) and toluene (*tod* operon). *J Bacteriol* **175**:5224-5232.

96. Furukawa, K., Matsumura, F., and Tonomura, K. 1978. *Alcaligenes* and *Acinetobacter* strains capable of degrading polychlorinated biphenyls. *Agric Biol Chem* **42** (3):543-548.
97. Furukawa, K., and Miyazaki, T. 1986. Cloning of a gene cluster encoding biphenyl and chlorobiphenyl degradation in *Pseudomonas pseudoalcaligenes*. *J Bacteriol* **166**:392-398.
98. Furukawa, K., Suenaga, H., and Goto, M. 2004. Biphenyl dioxygenases: functional versatilities and directed evolution. *J Bacteriol* **186**:5189-5196.
99. Furusawa, Y., Nagarajan, V., Tanokura, M., Masai, E., Fukuda, M., and Senda, T. 2004. Crystal structure of the terminal oxygenase component of biphenyl dioxygenase derived from *Rhodococcus* sp. strain RHA1. *J Mol Biol* **342**:1041-1052.
100. Gescher, J., Zaar, A., Mohamed, M., Schagger, H., and Fuchs, G. 2002. Genes coding for a new pathway of aerobic benzoate metabolism in *Azoarcus evansii*. *J Bacteriol* **184**:6301-6315.
101. Gibson, D. T., Cruden, D. L., Haddock, J. D., Zylstra, G. J., and Brand, J. M. 1993. Oxidation of polychlorinated biphenyls by *Pseudomonas* sp. strain LB400 and *Pseudomonas pseudoalcaligenes* KF707. *J Bacteriol* **175**:6735-6735.
102. Gibson, D. T., and Parales, R. E. 2000. Aromatic hydrocarbon dioxygenases in environmental biotechnology. *Curr Opin Biotech* **11**:236-243.
103. Gilbert, E. S., and Crowley, D. E. 1997. Plant compounds that induce polychlorinated biphenyl biodegradation by *Arthrobacter* sp. strain B1B. *Appl Environ Microb* **63**:1933-1938.
104. Glass, D. J. 1999. U.S. and international markets for phytoremediation, 1999-2000. D. Glass Associates, MA, USA.
105. Glick, B. R. 2010. Using soil bacteria to facilitate phytoremediation. *Biotechnol Adv* **28**:367-374.
106. Gomez-Gil, L., Kumar, P., Barriault, D., Bolin, J. T., Sylvestre, M., and Eltis, L. D. 2007. Characterization of biphenyl dioxygenase of *Pandoraea pnomenusa* B-356 as a potent polychlorinated biphenyl-degrading enzyme. *J Bacteriol* **189**:5705-5715.
107. Gonzalez, L. F., Sarria, V., and Sanchez, O. F. 2010. Degradation of chlorophenols by sequential biological-advanced oxidative process using *Trametes pubescens* and TiO₂/UV. *Bioresour Technol* **101**:3493-3499.
108. Gordillo, F., Chavez, F. P., and Jerez, C. A. 2007. Motility and chemotaxis of *Pseudomonas* sp. B4 towards polychlorobiphenyls and chlorobenzoates. *FEMS Microbiol Ecol* **60**:322-328.
109. Goris, J., De Vos, P., Caballero-Mellado, J., Park, J., Falsen, E., Quensen, J. F., 3rd, Tiedje, J. M., and Vandamme, P. 2004. Classification of the biphenyl- and polychlorinated biphenyl-degrading strain LB400^T and relatives as *Burkholderia xenovorans* sp. nov. *Int J Syst Evol Microbiol* **54**:1677-1681.
110. Guieysse, B., Viklund, G., Toes, A. C., and Mattiasson, B. 2004. Combined UV-biological degradation of PAHs. *Chemosphere* **55**:1493-1499.
111. Haddock, J. D., and Gibson, D. T. 1995. Purification and characterization of the oxygenase component of biphenyl 2,3-dioxygenase from *Pseudomonas* sp. strain LB400. *J Bacteriol* **177**:5834-5839.
112. Han, J., Kim, S. Y., Jung, J., Lim, Y., Ahn, J. H., Kim, S. I., and Hur, H. G. 2005. Epoxide formation on the aromatic B ring of flavanone by biphenyl dioxygenase of *Pseudomonas pseudoalcaligenes* KF707. *Appl Environ Microb* **71**:5354-5361.

113. Harwood, C. S., and Parales, R. E. 1996. The *beta*-ketoadipate pathway and the biology of self-identity. *Annu Rev Microbiol* **50**:553-590.
114. Hay, A. G., and Focht, D. D. 1998. Cometabolism of 1,1-dichloro-2,2-bis(4-chlorophenyl)ethane by *Pseudomonas acidovorans* M3GY grown on biphenyl. *Appl Environ Microbiol* **64**:2141-2146.
115. Hay, A. G., and Focht, D. D. 2000. Transformation of 1,1-dichloro-2,2-(4-chlorophenyl)ethane (DDD) by *Ralstonia eutropha* strain A5. *FEMS Microbiol Ecol* **31**:249-253.
116. He, N., Li, P., Zhou, Y., Fan, S., and Ren, W. 2009. Degradation of pentachlorobiphenyl by a sequential treatment using Pd coated iron and an aerobic bacterium (H1). *Chemosphere* **76**:1491-1497.
117. Hein, P., Powlowski, J., Barriault, D., Hurtubise, Y., Ahmad, D., and Sylvestre, M. 1998. Biphenyl-associated *meta*-cleavage dioxygenases from *Comamonas testosteroni* B-356. *Can. J. Microbiol.* **44**:42-49.
118. Hemshekhar, M., Sunitha, K., Santhosh, M. S., Devaraja, S., Kemparaju, K., Vishwanath, B. S., Niranjana, S. R., and Girish, K. S. 2011. An overview on genus *Garcinia*: phytochemical and therapeutical aspects. *Phytochem Rev* **10**:325-351.
119. Hernandez, B. S., Koh, S. C., Chial, M., and Focht, D. D. 1997. Terpene-utilizing isolates and their relevance to enhanced biotransformation of polychlorinated biphenyls in soil. *Biodegradation* **8**:153-158.
120. Hirose, J., Suyama, A., Hayashida, S., and Furukawa, K. 1994. Construction of hybrid biphenyl (*bph*) and toluene (*tod*) genes for functional analysis of aromatic ring dioxygenases. *Gene* **138**:27-33.
121. Hocher, V., Auguy, F., Argout, X., Laplace, L., Franche, C., and Bogusz, D. 2006. Expressed sequence-tag analysis in *Casuarina glauca* actinorhizal nodule and root. *New Phytol* **169**:681-688.
122. Hofer, B., Backhaus, S., and Timmis, K. N. 1994. The biphenyl/polychlorinated biphenyl-degradation locus (*bph*) of *Pseudomonas* sp. LB400 encodes four additional metabolic enzymes. *Gene* **144**:9-16.
123. Holliger C, W. G., Diekert G. . 1998. Reductive dechlorination in the energy metabolism of anaerobic bacteria. *FEMS Microbiol Rev* **22**:383-398.
124. Hollmann, F., Arends, I. W. C. E., Buehler, K., Schallmeyer, A., and B"Uhler, B. 2011. Enzyme-mediated oxidations for the chemist. *Green chem* **13**:226-265.
125. Horsman, G. P., Bhowmik, S., Seah, S. Y., Kumar, P., Bolin, J. T., and Eltis, L. D. 2007. The tautomeric half-reaction of BphD, a C-C bond hydrolase. Kinetic and structural evidence supporting a key role for histidine 265 of the catalytic triad. *J Biol Chem* **282**:19894-19904.
126. Horsman, G. P., Ke, J., Dai, S., Seah, S. Y., Bolin, J. T., and Eltis, L. D. 2006. Kinetic and structural insight into the mechanism of BphD, a C-C bond hydrolase from the biphenyl degradation pathway. *Biochemistry* **45**:11071-11086.
127. Hsu, S., Wu, S., Yeh, C., and Wu, S. 1985. Discovery and epidemiology of PCB poisoning in Taiwan. *Enviro Health Perspect* **59**:5-10.
128. Hurtubise, Y., Barriault, D., Powlowski, J., and Sylvestre, M. 1995. Purification and characterization of the *Comamonas testosteroni* B356 biphenyl dioxygenase components. *J Bacteriol* **177**:6610-6618.

129. Hurtubise, Y., Barriault, D., and Sylvestre, M. 1996. Characterization of active recombinant His-tagged oxygenase component of *Comamonas testosteroni* B-356 biphenyl dioxygenase. *J Biol Chem* **271**:8152-8156.
130. Hurtubise, Y., Barriault, D., and Sylvestre, M. 1998. Involvement of the terminal oxygenase *beta* subunit in the biphenyl dioxygenase reactivity pattern toward chlorobiphenyls. *J Bacteriol* **180**:5828-5835.
131. Hutzinger, O., Jamieson, W. D., Safe, S., Paulmann, L., and Ammon, R. 1974. Identification of metabolic dechlorination of highly chlorinated biphenyl in rabbit. *Nature* **252**:698-699.
132. Ibrahim, A. R., and Abul-Hajj, Y. J. 1990. Microbiological transformation of (+/-)-flavanone and (+/-)-isoflavanone. *J Nat Prod* **53**:644-656.
133. Ibrahim, A. R., and Abul-Hajj, Y. J. 1990. Microbiological transformation of flavone and isoflavone. *Xenobiotica* **20**:363-373.
134. Imbeault, N. Y., Powlowski, J. B., Colbert, C. L., Bolin, J. T., and Eltis, L. D. 2000. Steady-state kinetic characterization and crystallization of a polychlorinated biphenyl-transforming dioxygenase. *J Biol Chem* **275**:12430-12437.
135. Iniguez, A. L., Dong, Y., and Triplett, E. W. 2004. Nitrogen fixation in wheat provided by *Klebsiella pneumoniae* 342. *Mol Plant Microbe Interact* **17**:1078-1085.
136. Iwasaki, T., Miyauchi, K., Masai, E., and Fukuda, M. 2006. Multiple-subunit genes of the aromatic-ring-hydroxylating dioxygenase play an active role in biphenyl and polychlorinated biphenyl degradation in *Rhodococcus* sp. strain RHA1. *Appl Environ Microbiol* **72**:5396-5402.
137. Iwasaki, T., Takeda, H., Miyauchi, K., Yamada, T., Masai, E., and Fukuda, M. 2007. Characterization of two biphenyl dioxygenases for biphenyl/PCB degradation in A PCB degrader, *Rhodococcus* sp. strain RHA1. *Biosci Biotechnol Biochem* **71**:993-1002.
138. Jakoncic, J., Jouanneau, Y., Meyer, C., and Stojanoff, V. 2007. The crystal structure of the ring-hydroxylating dioxygenase from *Sphingomonas* CHY-1. *Febs J* **274**:2470-2481.
139. Jarrell, K. F., and McBride, M. J. 2008. The surprisingly diverse ways that prokaryotes move. *Nature Rev Microbiol* **6**:466-476.
140. Jeon, J. R., Murugesan, K., Nam, I. H., and Chang, Y. S. 2013. Coupling microbial catabolic actions with abiotic redox processes: a new recipe for persistent organic pollutant (POP) removal. *Biotechnol Adv* **31**:246-256.
141. Jung, W., Yu, O., Lau, S. M., O'Keefe, D. P., Odell, J., Fader, G., and McGonigle, B. 2000. Identification and expression of isoflavone synthase, the key enzyme for biosynthesis of isoflavones in legumes. *Nat Biotechnol* **18**:208-212.
142. Kagami, O., Shindo, K., Kyojima, A., Takeda, K., Ikenaga, H., Furukawa, K., and Misawa, N. 2008. Protein engineering on biphenyl dioxygenase for conferring activity to convert 7-hydroxyflavone and 5,7-dihydroxyflavone (chrysin). *J Biosci Bioeng* **106**:121-127.
143. Kamei, I., Kogura, R., and Kondo, R. 2006. Metabolism of 4,4'-dichlorobiphenyl by white-rot fungi *Phanerochaete chrysosporium* and *Phanerochaete* sp. MZ142. *Appl Microbiol Biotechnol* **72**:566-575.
144. Karlsson, A., Parales, J. V., Parales, R. E., Gibson, D. T., Eklund, H., and Ramaswamy, S. 2003. Crystal structure of naphthalene dioxygenase: side-on binding of dioxygen to iron. *Science* **299**:1039-1042.

145. **Karplus, M.** 1963. Vicinal proton coupling in nuclear magnetic resonance. *J Am Chem Soc* **85**:2870-2871.
146. **Kauppi, B., Lee, K., Carredano, E., Parales, R. E., Gibson, D. T., Eklund, H., and Ramaswamy, S.** 1998. Structure of an aromatic-ring-hydroxylating dioxygenase-naphthalene 1,2-dioxygenase. *Structure* **6**:571-586.
147. **Kearns, D. B.** 2010. A field guide to bacterial swarming motility. *Nature Rev Microbiol* **8**:634-644.
148. **Keasling, J. D.** 2010. Manufacturing molecules through metabolic engineering. *Science* **330**:1355-1358.
149. **Keum, Y. S., and Li, Q. X.** 2004. Fungal laccase-catalyzed degradation of hydroxy polychlorinated biphenyls. *Chemosphere* **56**:23-30.
150. **Kim, B. H., Oh, E. T., So, J. S., Ahn, Y., and Koh, S. C.** 2003. Plant terpene-induced expression of multiple aromatic ring hydroxylation oxygenase genes in *Rhodococcus* sp. strain T104. *J Microbiol* **41**:349-352.
151. **Kim, J. H., Tratnyek, P. G., and Chang, Y. S.** 2008. Rapid dechlorination of polychlorinated dibenzo-*p*-dioxins by bimetallic and nanosized zerovalent iron. *Environ Sci Technol* **42**:4106-4112.
152. **Kim, S.-Y., Jung, J., Lim, Y., Ahn, J.-H., Kim, S.-Y., and Hur, H.-G.** 2003. *Cis*-2', 3'-dihydrodiol production on flavone B-ring by biphenyl dioxygenase from *Pseudomonas pseudoalcaligenes* KF707 expressed in *Escherichia coli*. *Antonie van Leeuwenhoek* **84**:261-268.
153. **Kimbara, K., Hashimoto, T., Fukuda, M., Koana, T., Takagi, M., Oishi, M., and Yano, K.** 1989. Cloning and sequencing of two tandem genes involved in degradation of 2,3-dihydroxybiphenyl to benzoic acid in the polychlorinated biphenyl-degrading soil bacterium *Pseudomonas* sp. strain KKS102. *J Bacteriol* **171**:2740-2747.
154. **Kimbrough, R. D., Squire, R. A., Linder, R. E., Strandberg, J. D., Montalli, R. J., and Burse, V. W.** 1975. Induction of liver tumor in Sherman strain female rats by polychlorinated biphenyl aroclor 1260. *J Natl Cancer Inst* **55**:1453-1459.
155. **Kimura, N., Nishi, A., Goto, M., and Furukawa, K.** 1997. Functional analyses of a variety of chimeric dioxygenases constructed from two biphenyl dioxygenases that are similar structurally but different functionally. *J Bacteriol* **179**:3936-3943.
156. **Klundt, T., Bocola, M., Lutge, M., Beuerle, T., Liu, B., and Beerhues, L.** 2009. A single amino acid substitution converts benzophenone synthase into phenylpyrone synthase. *J Biol Chem* **284**:30957-30964.
157. **Kosono, S., Maeda, M., Fujii, F., Arai, H., and Kudo, T.** 1997. Three of the seven *bphC* genes of *Rhodococcus erythropolis* TA421, isolated from a termite ecosystem, are located on an indigenous plasmid associated with biphenyl degradation. *Appl Environ Microbiol* **63**:3282-3285.
158. **Krechel, A., Faupel, A., Hallmann, J., Ulrich, A., and Berg, G.** 2002. Potato-associated bacteria and their antagonistic potential towards plant-pathogenic fungi and the plant-parasitic nematode *Meloidogyne incognita* (Kofoid & White) Chitwood. *Can J Microbiol* **48**:772-786.
159. **Krumholz, L. R.** 1997. *Desulfuromonas chloroethenica* sp. nov. Uses tetrachloroethylene and trichloroethylene as electron acceptors. *Int J Syst Evol Microbiol* **47**:1262-1263.

160. Kubatova, A., Erbanova, P., Eichlerova, I., Homolka, L., Nerud, F., and Sasek, V. 2001. PCB congener selective biodegradation by the white rot fungus *Pleurotus ostreatus* in contaminated soil. *Chemosphere* **43**:207-215.
161. Kucerovala, P., Mackova, M., Chroma, L., Burkhard, J., Triska, J., Demnerova, K., and Macek, T. 2000. Metabolism of polychlorinated biphenyls by *Solanum nigrum* hairy root clone SNC-90 and analysis of transformation products. *Plant Soil* **225**:109-115.
162. Kumamaru, T., Suenaga, H., Mitsuoka, M., Watanabe, T., and Furukawa, K. 1998. Enhanced degradation of polychlorinated biphenyls by directed evolution of biphenyl dioxygenase. *Nat Biotechnol* **16**:663-666.
163. Kumar, P., Gomez-Gil, L., Mohammadi, M., Sylvestre, M., Eltis, L. D., and Bolin, J. T. 2011. Anaerobic crystallization and initial X-ray diffraction data of biphenyl 2,3-dioxygenase from *Burkholderia xenovorans* LB400: addition of agarose improved the quality of the crystals. *Acta Crystallogr Sect F Struct Biol Cryst Commun* **67**:59-63.
164. Kumar, P., Mohammadi, M., Dhindwal, S., Pham, T. T., Bolin, J. T., and Sylvestre, M. 2012. Structural insights into the metabolism of 2-chlorodibenzofuran by an evolved biphenyl dioxygenase. *Biochem Biophys Res Commun* **421**:757-762.
165. Kumar, P., Mohammadi, M., Viger, J. F., Barriault, D., Gomez-Gil, L., Eltis, L. D., Bolin, J. T., and Sylvestre, M. 2011. Structural insight into the expanded PCB-degrading abilities of a biphenyl dioxygenase obtained by directed evolution. *J Mol Biol* **405**:531-547.
166. Kuratsune, M., Yoshimura, T., Matsuzaka, J., and Yamaguchi, A. 1972. Epidemiologic study on Yusho, a poisoning caused by ingestion of rice oil contaminated with a commercial brand of polychlorinated biphenyls. *Environ Health Perspect* **1**:119-128.
167. Kurzawova, V., Stursa, P., Uhlik, O., Norkova, K., Strohalm, M., Lipov, J., Kochankova, L., and Mackova, M. 2012. Plant-microorganism interactions in bioremediation of polychlorinated biphenyl-contaminated soil. *Nat Biotechnol* **30**:15-22.
168. L'abbée, J. B., Barriault, D., and Sylvestre, M. 2005. Metabolism of dibenzofuran and dibenzo-*p*-dioxin by the biphenyl dioxygenase of *Burkholderia xenovorans* LB400 and *Comamonas testosteroni* B-356. *Appl Microbiol Biotechnol* **67**:506-514.
169. L'abbée, J. B., Tu, Y., Barriault, D., and Sylvestre, M. 2011. Insight into the metabolism of 1,1,1-trichloro-2,2-bis(4-chlorophenyl)ethane (DDT) by biphenyl dioxygenases. *Arch Biochem Biophys* **516**:35-44.
170. Labbé, D., Garnon, J., and Lau, P. C. 1997. Characterization of the genes encoding a receptor-like histidine kinase and a cognate response regulator from a biphenyl/polychlorobiphenyl-degrading bacterium, *Rhodococcus* sp. strain M5. *J Bacteriol* **179**:2772-2776.
171. Lau, P. C., Garnon, J., Labbé, D., and Wang, Y. 1996. Location and sequence analysis of a 2-hydroxy-6-oxo-6-phenylhexa-2,4-dienoate hydrolase-encoding gene (*bpdF*) of the biphenyl/polychlorinated biphenyl degradation pathway in *Rhodococcus* sp. M5. *Gene* **171**:53-57.
172. Leigh, M. B., Fletcher, J. S., Fu, X., and Schmitz, F. J. 2002. Root turnover: an important source of microbial substrates in rhizosphere remediation of recalcitrant contaminants. *Environ Sci Technol* **36**:1579-1583.
173. Leigh, M. B., Prouzova, P., Mackova, M., Macek, T., Nagle, D. P., and Fletcher, J. S. 2006. Polychlorinated biphenyl (PCB)-degrading bacteria associated with trees in a PCB-contaminated site. *Appl Environ Microb* **72**:2331-2342.

174. Li, F. X., Jin, Z. P., Zhao, D. X., Cheng, L. Q., Fu, C. X., and Ma, F. 2006. Overexpression of the *Saussurea medusa* chalcone isomerase gene in *S. involucrata* hairy root cultures enhances their biosynthesis of apigenin. *Phytochemistry* **67**:553-560.
175. Lin, J. J., Smith, M., Jessee, J., and Bloom, F. 1992. DH11s: an *E. coli* strain for preparation of single-standed DNA from phagemid vectors. *BioTechniques* **12**:718-721.
176. Liu, B., Falkenstein-Paul, H., Schmidt, W., and Beerhues, L. 2003. Benzophenone synthase and chalcone synthase from *Hypericum androsaemum* cell cultures: cDNA cloning, functional expression, and site-directed mutagenesis of two polyketide synthases. *Plant J* **34**:847-855.
177. Liu, C. J., Blount, J. W., Steele, C. L., and Dixon, R. A. 2002. Bottlenecks for metabolic engineering of isoflavone glycoconjugates in *Arabidopsis*. *Proc Natl Acad Sci U S A* **99**:14578-14583.
178. Liu, R., Hu, Y., Li, J., and Lin, Z. 2007. Production of soybean isoflavone genistein in non-legume plants via genetically modified secondary metabolism pathway. *Metab Eng* **9**:1-7.
179. Liu, Y. S., Ying, G. G., Shareef, A., and Kookana, R. S. 2012. Biodegradation of the ultraviolet filter benzophenone-3 under different redox conditions. *Environ Toxicol Chem* **31**:289-295.
180. Lucas Garcia, J. A., Barbas, C., Probanza, A., Barrientos, M. L., and Gutierrez Manero, F. J. 2001. Low molecular weight organic acids and fatty acids in root exudates of two *Lupinus cultivars* at flowering and fruiting stages. *Phytochem Anal* **12**:305-311.
181. Lugtenberg, B., and Kamilova, F. 2009. Plant-growth-promoting rhizobacteria. *Annu Rev Microbiol* **63**:541-556.
182. Luo, W. S., D'Angelo, E. M., and Coyne, M. S. 2007. Plant secondary metabolites, biphenyl, and hydroxypropyl- β -cyclodextrin effects on aerobic polychlorinated biphenyl removal and microbial community structure in soils. *Soil Biol Biochem* **39**:735-743.
183. Mackova, M., Vrchotova, B., Francova, K., Sylvestre, M., Tomaniova, M., Lovecka, P., Demnerova, K., and Macek, T. 2007. Biotransformation of PCBs by plants and bacteria-consequences of plant-microbe interactions. *Eur J Soil Biol* **43**:233-241.
184. Mano, H., and Morisaki, H. 2008. Endophytic bacteria in the rice plant. *Microbes Environ* **23**:109-117.
185. Marek, R. F., Martinez, A., and Hornbuckle, K. C. 2013. Discovery of hydroxylated polychlorinated biphenyls (OH-PCBs) in sediment from a lake Michigan waterway and original commercial aroclors. *Environ Sci Technol* **47**:8204-8210.
186. Martin, V. J., Pitera, D. J., Withers, S. T., Newman, J. D., and Keasling, J. D. 2003. Engineering a mevalonate pathway in *Escherichia coli* for production of terpenoids. *Nat Biotechnol* **21**:796-802.
187. Masai, E., Yamada, A., Healy, J. M., Hatta, T., Kimbara, K., Fukuda, M., and Yano, K. 1995. Characterization of biphenyl catabolic genes of Gram-positive polychlorinated biphenyl degrader *Rhodococcus* sp. strain RHA1. *Appl Environ Microbiol* **61**:2079-2085.
188. Masak, J., Cejkova, A., Jirku, V., Kotrba, D., Hron, P., and Siglova, M. 2005. Colonization of surfaces by phenolic compounds utilizing microorganisms. *Environ Int* **31**:197-200.
189. Massé, R., Messier, F., Ayotte, C., Lévesque, M.-F., and Sylvestre, M. 1989. A comprehensive gas chromatographic/mass spectrometric analysis of 4-chlorobiphenyl bacterial degradation products. *Biomed Environ Mass Spectrom* **18**:24-47.

190. **Master, E. R., and Mohn, W. W.** 1998. Psychrotolerant bacteria isolated from arctic soil that degrade polychlorinated biphenyls at low temperatures. *Appl Environ Microbiol* **64**:4823-4829.
191. **Mastretta, C., Barac, T., Vangronsvelde, J., Newman, L., Taghavi, S., and Van Der Lelie, D.** 2006. Endophytic bacteria and their potential application to improve the phytoremediation of contaminated environments. *Biotechnol Genet Eng Rev* **23**:175-207.
192. **Mayak, S., Tirosh, T., and Glick, B. R.** 2004. Plant growth-promoting bacteria confer resistance in tomato plants to salt stress. *Plant Physiol Biochem* **42**:565-572.
193. **Maymo-Gatell, X., Anguish, T., and Zinder, S. H.** 1999. Reductive dechlorination of chlorinated ethenes and 1, 2-dichloroethane by "*Dehalococcoides ethenogenes*" 195. *Appl Environ Microbiol* **65**:3108-3113.
194. **McGuinness, M., and Dowling, D.** 2009. Plant-associated bacterial degradation of toxic organic compounds in soil. *Int J Environ Res Public Health* **6**:2226-2247.
195. **McKay, D. B., Prucha, M., Reineke, W., Timmis, K. N., and Pieper, D. H.** 2003. Substrate specificity and expression of three 2,3-dihydroxybiphenyl 1,2-dioxygenases from *Rhodococcus globulus* strain P6. *J Bacteriol* **185**:2944-2951.
196. **McKay, D. B., Seeger, M., Zielinski, M., Hofer, B., and Timmis, K. N.** 1997. Heterologous expression of biphenyl dioxygenase-encoding genes from a Gram-positive broad-spectrum polychlorinated biphenyl degrader and characterization of chlorobiphenyl oxidation by the gene products. *J Bacteriol* **179**:1924-1930.
197. **McLean, M. R., Bauer, U., Amaro, A. R., and Robertson, L. W.** 1996. Identification of catechol and hydroquinone metabolites of 4-monochlorobiphenyl. *Chem Res Toxicol* **9**:158-164.
198. **McNaught, A. D., and Wilkinson, A.** 1997. Flavonoids (isoflavonoids and neoflavonoids), IUPAC compendium of chemical terminology (2 ed.). Oxford: Blackwell Scientific.
199. **McNear, D. H. J.** 2013. The rhizosphere-roots, soil and everything in between. *Nature Education Knowledge* **4**(3):1.
200. **Miroux, B., and Walker, J. E.** 1996. Over-production of proteins in *Escherichia coli*: mutant hosts that allow synthesis of some membrane proteins and globular proteins at high levels. *J Mol Biol* **260**:289-298.
201. **Misawa, N., Nakamura, R., Kagiya, Y., Ikenaga, H., Furukawa, K., and Shindo, K.** 2005. Synthesis of vicinal diols from various arenes with a heterocyclic, amino or carboxyl group by using recombinant *Escherichia coli* cells expressing evolved biphenyl dioxygenase and dihydrodiol dehydrogenase genes. *Tetrahedron* **61**:195-204.
202. **Misawa, N., Shindo, K., Takahashi, H., Suenaga, H., Iguchi, K., Okazaki, H., Harayama, S., and Furukawae, K.** 2002. Hydroxylation of various molecules including heterocyclic aromatics using recombinant *Escherichia coli* cells expressing modified biphenyl dioxygenase genes. *Tetrahedron* **58**:9605-9612.
203. **Miya, R. K., and Firestone, M. K.** 2001. Enhanced phenanthrene biodegradation in soil by slender oat root exudates and root debris. *J Environ Qual* **30**:1911-1918.
204. **Mohammadi, M., Chalavi, V., Novakova-Sura, M., Laliberte, J. F., and Sylvestre, M.** 2007. Expression of bacterial biphenyl-chlorobiphenyl dioxygenase genes in tobacco plants. *Biotechnol Bioeng* **97**:496-505.

205. **Mohammadi, M., and Sylvestre, M.** 2005. Resolving the profile of metabolites generated during oxidation of dibenzofuran and chlorodibenzofurans by the biphenyl catabolic pathway enzymes. *Chem Biol* **12**:835-846.
206. **Mohammadi, M., Viger, J. F., Kumar, P., Barriault, D., Bolin, J. T., and Sylvestre, M.** 2011. Retuning Rieske-type oxygenases to expand substrate range. *J Biol Chem* **286**:27612-27621.
207. **Mondello, F. J.** 1989. Cloning and expression in *Escherichia coli* of *Pseudomonas* strain LB400 genes encoding polychlorinated biphenyl degradation. *J Bacteriol* **171**:1725-1732.
208. **Mondello, F. J., Turcich, M. P., Lobos, J. H., and Erickson, B. D.** 1997. Identification and modification of biphenyl dioxygenase sequences that determine the specificity of polychlorinated biphenyl degradation. *Appl Environ Microbiol* **63**:3096-3103.
209. **Morris, G. M., Huey, R., Lindstrom, W., Sanner, M. F., Belew, R. K., Goodsell, D. S., and Olson, A. J.** 2009. AutoDock4 and AutoDockTools4: Automated docking with selective receptor flexibility. *J Comput Chem* **30**:2785-2791.
210. **Morris, P. J., Mohn, W. W., Quensen, J. F., Tiedje, J. M., and Boyd, S. A.** 1992. Establishment of polychlorinated biphenyl-degrading enrichment culture with predominantly *meta* dechlorination. *Appl Environ Microbiol* **58**:3088-3094.
211. **Mouz, S., Merlin, C., Springael, D., and Toussaint, A.** 1999. A GntR-like negative regulator of the biphenyl degradation genes of the transposon Tn4371. *Mol Gen Genet* **262**:790-799.
212. **Murray, T. S., and Kazmierczak, B. I.** 2008. *Pseudomonas aeruginosa* exhibits sliding motility in the absence of type IV pili and flagella. *J Bacteriol* **190**:2700-2708.
213. **Nadeau, L. J., Menn, F. M., Breen, A., and Sayler, G. S.** 1994. Aerobic degradation of 1,1,1-trichloro-2,2-bis(4-chlorophenyl)ethane (DDT) by *Alcaligenes eutrophus* A5. *Appl Environ Microbiol* **60**:51-55.
214. **Nakatsuka, T., Mishiba, K., Kubota, A., Abe, Y., Yamamura, S., Nakamura, N., Tanaka, Y., and Nishihara, M.** 2010. Genetic engineering of novel flower colour by suppression of anthocyanin modification genes in gentian. *J Plant Physiol* **167**:231-237.
215. **Nandhagopal, N., Yamada, A., Hatta, T., Masai, E., Fukuda, M., Mitsui, Y., and Senda, T.** 2001. Crystal structure of 2-hydroxyl-6-oxo-6-phenylhexa-2,4-dienoic acid (HPDA) hydrolase (BphD enzyme) from the *Rhodococcus* sp. strain RHA1 of the PCB degradation pathway. *J Mol Biol* **309**:1139-1151.
216. **Narasimhan, K., Basheer, C., Bajic, V. B., and Swarup, S.** 2003. Enhancement of plant-microbe interactions using a rhizosphere metabolomics-driven approach and its application in the removal of polychlorinated biphenyls. *Plant Physiology* **132**:146-153.
217. **Nesi, N., Debeaujon, I., Jond, C., Pelletier, G., Caboche, M., and Lepiniec, L.** 2000. The *TT8* gene encodes a basic helix-loop-helix domain protein required for expression of *DFR* and *BAN* genes in *Arabidopsis siliques*. *Plant Cell* **12**:1863-1878.
218. **Nichenametla, S. N., Taruscio, T. G., Barney, D. L., and Exon, J. H.** 2006. A review of the effects and mechanisms of polyphenolics in cancer. *Crit Rev Food Sci Nutr* **46**:161-183.
219. **Nijveldt, R. J., Van Nood, E., Van Hoorn, D. E., Boelens, P. G., Van Norren, K., and Van Leeuwen, P. A.** 2001. Flavonoids: a review of probable mechanisms of action and potential applications. *Am J Clin Nutr* **74**:418-425.
220. **Niraula, N. P., Bhattarai, S., Lee, N. R., Sohng, J. K., and Oh, T. J.** 2012. Biotransformation of flavone by CYP105P2 from *Streptomyces peucetius*. *J Microbiol Biotechnol* **22**:1059-1065.

221. Nishihara, M., and Nakatsuka, T. 2011. Genetic engineering of flavonoid pigments to modify flower color in floricultural plants. *Biotechnol Lett* **33**:433-441.
222. Nishihara, M., and Nakatsuka, T. 2010. Genetic engineering of novel flower colors in floricultural plants: recent advances via transgenic approaches. *Methods Mol Biol* **589**:325-347.
223. Nojiri, H., and Omori, T. 2002. Molecular bases of aerobic bacterial degradation of dioxins: Involvement of angular dioxygenation. *Biosci Biotechnol Biochem* **66**:2001-2016.
224. Nolan, L. C., and O'Connor, K. E. 2008. Dioxygenase- and monooxygenase-catalysed synthesis of *cis*-dihydrodiols, catechols, epoxides and other oxygenated products. *Biotechnol Lett* **30**:1879-1891.
225. Novakova, M., Mackova, M., Chrastilova, Z., Viktorova, J., Szekeres, M., Demnerova, K., and Macek, T. 2009. Cloning the bacterial *bphC* gene into *Nicotiana tabacum* to improve the efficiency of PCB phytoremediation. *Biotechnol Bioeng* **102**:29-37.
226. O'Toole, G., Kaplan, H. B., and Kolter, R. 2000. Biofilm formation as microbial development. *Ann Rev Microbiol* **54**:49-79.
227. Ohtsubo, Y., Delawary, M., Kimbara, K., Takagi, M., Ohta, A., and Nagata, Y. 2001. BphS, a key transcriptional regulator of *bph* genes involved in polychlorinated biphenyl/biphenyl degradation in *Pseudomonas* sp. KKS102. *J Biol Chem* **276**:36146-36154.
228. Ohtsubo, Y., Nagata, Y., Kimbara, K., Takagi, M., and Ohta, A. 2000. Expression of the *bph* genes involved in biphenyl/PCB degradation in *Pseudomonas* sp. KKS102 induced by the biphenyl degradation intermediate, 2-hydroxy-6-oxo-6-phenylhexa-2,4-dienoic acid. *Gene* **256**:223-228.
229. Oller, I., Malato, S., and Sanchez-Perez, J. A. 2011. Combination of advanced oxidation processes and biological treatments for wastewater decontamination-a review. *Sci Total Environ* **409**:4141-4166.
230. Parales, R. E., Lee, K., Resnick, S. M., Jiang, H., Lessner, D. J., and Gibson, D. T. 2000. Substrate specificity of naphthalene dioxygenase: effect of specific amino acids at the active site of the enzyme. *J Bacteriol* **182**:1641-1649.
231. Park, Y. B., Lee, S., Woo, Y., and Lim, Y. 2009. Relationships between structure and anti-oxidative effects of hydroxyflavones. *Bull Korean Chem Soc* **30**:43-47.
232. Parnell, J. J., Denef, V. J., Park, J., Tsoi, T., and Tiedje, J. M. 2010. Environmentally relevant parameters affecting PCB degradation: carbon source- and growth phase-mitigated effects of the expression of the biphenyl pathway and associated genes in *Burkholderia xenovorans* LB400. *Biodegradation* **21**:147-156.
233. Parsons, J. R., Sijm, D. T. H. M., Van Laar, A., and Hutzinger, O. 1988. Biodegradation of chlorinated biphenyls and benzoic acids by a *Pseudomonas* strain. *Appl Microbiol Biotechnol* **29**:81-84.
234. Paul, N. D., Hatcher, P. E., and Taylor, J. E. 2000. Coping with multiple enemies: an integration of molecular and ecological perspectives. *Trends Plant Sci* **5**:220-225.
235. Pham, T. T., and Sylvestre, M. 2013. Has the bacterial biphenyl catabolic pathway evolved primarily to degrade biphenyl? The diphenylmethane case. *J Bacteriol* **195**:3563-3574.
236. Pham, T. T. M., Tu, Y. B., and Sylvestre, M. 2012. Remarkable ability of *Pandoraea pnomenusa* B356 biphenyl dioxygenase to metabolize simple flavonoids. *Appl Environ Microbiol* **78**:3560-3570.

237. **Pieper, D. H.** 2005. Aerobic degradation of polychlorinated biphenyls. *Appl Environ Microbiol* **67**:170-191.
238. **Pieper, D. H., and Seeger, M.** 2008. Bacterial metabolism of polychlorinated biphenyls. *J Mol Microb Biotech* **15**:121-138.
239. **Pilon-Smits, E.** 2005. Phytoremediation. *Annu Rev Plant Biol* **56**:15-39.
240. **Prindle, R. F.** 1983. Phenolic compounds, p. 197-224. *In* Block, S.S. (ed.), *Disinfection, sterilization, and preservation*. Lea and Fegiger, Philadelphia.
241. **Quensen, J. F., Boyd, S. A., and Tiedje, J. M.** 1990. Dechlorination of four commercial polychlorinated biphenyl mixtures (Aroclors) by anaerobic microorganisms from sediments. *Appl Environ Microbiol* **56**:2360-2369.
242. **Quensen, J. F., Tiedje, J. M., and Boyd, S. A.** 1988. Reductive dechlorination of polychlorinated biphenyls by anaerobic microorganisms from sediments. *Science* **242**:752-754.
243. **Reetz, M. T., and Jaeger, K. E.** 2000. Enantioselective enzymes for organic synthesis created by directed evolution. *Chemistry* **6**:407-412.
244. **Rezek, J., Macek, T., Mackova, M., Triska, J., and Ruzickova, K.** 2008. Hydroxy-PCBs, methoxy-PCBs and hydroxy-methoxy-PCBs: metabolites of polychlorinated biphenyls formed in vitro by tobacco cells. *Environ Sci Technol* **42**:5746-5751.
245. **Ro, D. K., Paradise, E. M., Ouellet, M., Fisher, K. J., Newman, K. L., Ndungu, J. M., Ho, K. A., Eachus, R. A., Ham, T. S., Kirby, J., Chang, M. C., Withers, S. T., Shiba, Y., Sarpong, R., and Keasling, J. D.** 2006. Production of the antimalarial drug precursor artemisinic acid in engineered yeast. *Nature* **440**:940-943.
246. **Roberts, S. M., Teaf, M. C., and Bean, A. J.** 1999. Hazardous waste incineration: Evaluating the human health and environmental risks. CRC Press.
247. **Rodriguez, H., and Fraga, R.** 1999. Phosphate solubilizing bacteria and their role in plant growth promotion. *Biotechnol Adv* **17**:319-339.
248. **Roelfes, G., Vraijmasu, V., Chen, K., Ho, R. Y., Rohde, J. U., Zondervan, C., La Crois, R. M., Schudde, E. P., Lutz, M., Spek, A. L., Hage, R., Feringa, B. L., Munck, E., and Que, L., Jr.** 2003. End-on and side-on peroxo derivatives of non-heme iron complexes with pentadentate ligands: models for putative intermediates in biological iron/dioxygen chemistry. *Inorg Chem* **42**:2639-2653.
249. **Romero-Silva, M. J., Mendez, V., Agullo, L., and Seeger, M.** 2013. Genomic and functional analyses of the gentisate and protocatechuate ring-cleavage pathways and related 3-hydroxybenzoate and 4-hydroxybenzoate peripheral pathways in *Burkholderia xenovorans* LB400. *Plos One* **8**:e56038.
250. **Rosenberg, M.** 2006. Microbial adhesion to hydrocarbons: twenty-five years of doing MATH. *FEMS Microbiol Lett* **262**:129-134.
251. **Rosenberg, M., Gutnick, D., and Rosenberg, E.** 1980. Adherence of bacteria to hydrocarbons: a simple method for measuring cell-surface hydrophobicity. *FEMS Microbiol Lett* **9**:29-33.
252. **Rudel, R. A., Seryak, L. M., and Brody, J. G.** 2008. PCB-containing wood floor finish is a likely source of elevated PCBs in residents' blood, household air and dust: a case study of exposure. *Environ Health* **7**:2.

253. Rump, A. F., Schussler, M., Acar, D., Cordes, A., Ratke, R., Theisohn, M., Rosen, R., Klaus, W., and Fricke, U. 1995. Effects of different inotropes with antioxidant properties on acute regional myocardial ischemia in isolated rabbit hearts. *Gen Pharmacol* **26**:603-611.
254. Russo, L., Rizzo, L., and Belgiorno, V. 2012. Ozone oxidation and aerobic biodegradation with spent mushroom compost for detoxification and benzo(a)pyrene removal from contaminated soil. *Chemosphere* **87**:595-601.
255. Ruzzini, A. C., Ghosh, S., Horsman, G. P., Foster, L. J., Bolin, J. T., and Eltis, L. D. 2012. Identification of an acyl-enzyme intermediate in a *meta*-cleavage product hydrolase reveals the versatility of the catalytic triad. *J Am Chem Soc* **134**:4615-4624.
256. Ryan, P., Delhaize, E., and Jones, D. 2001. Function and mechanism of organic anion exudation from plant roots. *Annu Rev Plant Physiol Plant Mol Biol* **52**:527-560.
257. Saavedra, J. M., Acevedo, F., Gonzalez, M., and Seeger, M. 2010. Mineralization of PCBs by the genetically modified strain *Cupriavidus necator* JMS34 and its application for bioremediation of PCBs in soil. *Appl Microbiol Biotechnol* **87**:1543-1554.
258. Safe, S. H. 1994. Polychlorinated biphenyls (PCBs): environmental impact, biochemical and toxic responses, and implications for risk assessment. *Crit Rev Toxicol* **24**:87-149.
259. Salt, D. E., Smith, R. D., and Raskin, I. 1998. Phytoremediation. *Annu Rev Plant Physiol Plant Mol Biol* **49**:643-668.
260. Sambrook, J., Fritsch, E. F., and Maniatis, T. 1989. Molecular cloning: a laboratory manual. Cold Spring Harbor Laboratory Press, Cold Spring Harbor, NY.
261. Sanchez-Contreras, M., Martin, M., Villaceros, M., O'gara, F., Bonilla, I., and Rivilla, R. 2002. Phenotypic selection and phase variation occur during alfalfa root colonization by *Pseudomonas fluorescens* F113. *J Bacteriol* **184**:1587-1596.
262. Sanford, R. A., Cole, J. R., Löffler, F. E., and Tiedje, J. M. 1996. Characterization of *Desulfitobacterium chlororespirans* sp. nov., which grows by coupling the oxidation of lactate to the reductive dechlorination of 3-chloro-4-hydroxybenzoate. *Appl Environ Microbiol* **62**:3800-3808.
263. Sayler, G. S., Shon, M., and Colwell, R. R. 1977. Growth of an estuarine *Pseudomonas* sp. on polychlorinated biphenyl. *Microb Ecol* **3**:241-255.
264. Scher, F. M., Ziegler, J. S., and Kloepper, J. W. 1984. A method for assessing the root-colonizing capacity of bacteria on maize. *Can J Microbiol* **30**:151-157.
265. Schijlen, E., Ric De Vos, C. H., Jonker, H., Van Den Broeck, H., Molthoff, J., Van Tunen, A., Martens, S., and Bovy, A. 2006. Pathway engineering for healthy phytochemicals leading to the production of novel flavonoids in tomato fruit. *Plant Biotechnol J* **4**:433-444.
266. Schirmer, A., Rude, M. A., Li, X., Popova, E., and Del Cardayre, S. B. 2010. Microbial biosynthesis of alkanes. *Science* **329**:559-562.
267. Schmid, A., Dordick, J. S., Hauer, B., Kiener, A., Wubbolts, M., and Witholt, B. 2001. Industrial biocatalysis today and tomorrow. *Nature* **409**:258-268.
268. Seah, S. Y., Ke, J., Denis, G., Horsman, G. P., Fortin, P. D., Whiting, C. J., and Eltis, L. D. 2007. Characterization of a C-C bond hydrolase from *Sphingomonas wittichii* RW1 with novel specificities towards polychlorinated biphenyl metabolites. *J Bacteriol* **189**:4038-4045.

269. Seah, S. Y., Labbé, G., Kaschabek, S. R., Reifenrath, F., Reineke, W., and Eltis, L. D. 2001. Comparative specificities of two evolutionarily divergent hydrolases involved in microbial degradation of polychlorinated biphenyls. *J Bacteriol* **183**:1511-1516.
270. Seeger, M., Camara, B., and Hofer, B. 2001. Dehalogenation, denitration, dehydroxylation, and angular attack on substituted biphenyls and related compounds by a biphenyl dioxygenase. *J Bacteriol* **183**:3548-3555.
271. Seeger, M., Gonzalez, M., Camara, B., Munoz, L., Ponce, E., Mejias, L., Mascayano, C., Vasquez, Y., and Sepulveda-Boza, S. 2003. Biotransformation of natural and synthetic isoflavonoids by two recombinant microbial enzymes. *Appl Environ Microbiol* **69**:5045-5050.
272. Seitz, C., Eder, C., Deiml, B., Kellner, S., Martens, S., and Forkmann, G. 2006. Cloning, functional identification and sequence analysis of flavonoid 3'-hydroxylase and flavonoid 3',5'-hydroxylase cDNAs reveals independent evolution of flavonoid 3',5'-hydroxylase in the *Asteraceae* family. *Plant Mol Biol* **61**:365-381.
273. Senda, M., Kimura, S., Kishigami, S., and Senda, T. 2006. Crystallization and preliminary X-ray analysis of the Rieske-type [2Fe-2S] ferredoxin component of biphenyl dioxygenase from *Pseudomonas* sp. strain KKS102. *Acta Crystallogr Sect F Struct Biol Cryst Commun* **62**:590-592.
274. Senda, M., Kishigami, S., Kimura, S., Fukuda, M., Ishida, T., and Senda, T. 2007. Molecular mechanism of the redox-dependent interaction between NADH-dependent ferredoxin reductase and Rieske-type [2Fe-2S] ferredoxin. *J Mol Biol* **373**:382-400.
275. Senda, T., Yamada, T., Sakurai, N., Kubota, M., Nishizaki, T., Masai, E., Fukuda, M., and Mitsuidagger, Y. 2000. Crystal structure of NADH-dependent ferredoxin reductase component in biphenyl dioxygenase. *J Mol Biol* **304**:397-410.
276. Seo, J., Kang, S. I., Kim, M., Han, J., and Hur, H. G. 2011. Flavonoids biotransformation by bacterial non-heme dioxygenases, biphenyl and naphthalene dioxygenase. *Appl Microbiol Biot* **91**:219-228.
277. Seo, J., Kang, S. I., Ryu, J. Y., Lee, Y. J., Park, K. D., Kim, M., Won, D., Park, H. Y., Ahn, J. H., Chong, Y., Kanaly, R. A., Han, J., and Hur, H. G. 2010. Location of flavone B-ring controls regioselectivity and stereoselectivity of naphthalene dioxygenase from *Pseudomonas* sp. strain NCIB 9816-4. *Appl Microbiol Biotechnol* **86**:1451-1462.
278. Seo, J., Kang, S. I., Won, D., Kim, M., Ryu, J. Y., Kang, S. W., Um, B. H., Pan, C. H., Ahn, J. H., Chong, Y., Kanaly, R. A., Han, J., and Hur, H. G. 2011. Absolute configuration-dependent epoxide formation from isoflavan-4-ol stereoisomers by biphenyl dioxygenase of *Pseudomonas pseudoalcaligenes* strain KF707. *Appl Microbiol Biotechnol* **89**:1773-1782.
279. Seto, M., Ida, M., Okita, N., Hatta, T., Masai, E., and Fukuda, M. 1996. Catabolic potential of multiple PCB transformation systems in *Rhodococcus* sp. strain RHA1. *Biotechnol Lett* **18**:1305-1308.
280. Seto, M., Kimbara, K., Shimura, M., Hatta, T., Fukuda, M., and Yano, K. 1995. A novel transformation of polychlorinated biphenyls by *Rhodococcus* sp. strain RHA1. *Appl Environ Microbiol* **61**:3353-3358.
281. Seto, M., Masai, E., Ida, M., Hatta, T., Kimbara, K., Fukuda, M., and Yano, K. 1995. Multiple polychlorinated biphenyl transformation systems in the Gram-positive bacterium *Rhodococcus* sp. strain RHA1. *Appl Environ Microbiol* **61**:4510-4513.

282. **Sharma, A., and Johri, B. N.** 2003. Combat of iron-deprivation through a plant growth promoting fluorescent *Pseudomonas* strain GRP3A in mung bean (*Vigna radiata* L. Wilzeck). *Microbiol Res* **158**:77-81.
283. **Sharma, A., and Johri, B. N.** 2003. Growth promoting influence of siderophore-producing *Pseudomonas* strains GRP3A and PRS9 in maize (*Zea mays* L.) under iron limiting conditions. *Microbiol Res* **158**:243-248.
284. **Shaw, L. J., and Burns, R. G.** 2003. Biodegradation of organic pollutants in the rhizosphere. *Adv Appl Microbiol* **53**:1-60.
285. **Shaw, L. J., Morris, P., and Hooker, J. E.** 2006. Perception and modification of plant flavonoid signals by rhizosphere microorganisms. *Environ Microbiol* **8**:1867-1880.
286. **Shimizu, S., Kobayashi, H., Masai, E., and Fukuda, M.** 2001. Characterization of the 450-kb linear plasmid in a polychlorinated biphenyl degrader, *Rhodococcus* sp. strain RHA1. *Appl Environ Microbiol* **67**:2021-2028.
287. **Shindo, K., Kagiya, Y., Nakamura, R., Hara, A., Ikenaga, H., Furukawa, K., and Misawa, N.** 2003. Enzymatic synthesis of novel antioxidant flavonoids by *Escherichia coli* cells expressing modified metabolic genes involved in biphenyl catabolism. *J Mol Catal B Enzym* **23**:9-16.
288. **Shindo, K., Nakamura, R., Osawa, A., Kagami, O., Kanoh, K., Furukawa, K., and Misawa, N.** 2005. Biocatalytic synthesis of monocyclic arene-dihydrodiols and -diols by *Escherichia coli* cells expressing hybrid toluene/biphenyl dioxygenase and dihydrodiol dehydrogenase genes. *J Mol Catal B Enzym* **35**:134-141.
289. **Shindo, K., Osawa, A., Nakamura, R., Kagiya, Y., Sakuda, S., Shizuri, Y., Furukawa, K., and Misawa, N.** 2004. Conversion from arenes having a benzene ring to those having a picolinic acid by simple growing cell reactions using *Escherichia coli* that expressed the six bacterial genes involved in biphenyl catabolism. *J Am Chem Soc* **126**:15042-15043.
290. **Shindo, K., Shindo, Y., Hasegawa, T., Osawa, A., Kagami, O., Furukawa, K., and Misawa, N.** 2007. Synthesis of highly hydroxylated aromatics by evolved biphenyl dioxygenase and subsequent dihydrodiol dehydrogenase. *Appl Microbiol Biotechnol* **75**:1063-1069.
291. **Shu, J. C., Chou, G. X., and Wang, Z. T.** 2012. One new diphenylmethane glycoside from the leaves of *Psidium guajava* L. *Nat Prod Res* **26**:1971-1975.
292. **Sietmann, R., Gesell, M., Hammer, E., and Schauer, F.** 2006. Oxidative ring cleavage of low chlorinated biphenyl derivatives by fungi leads to the formation of chlorinated lactone derivatives. *Chemosphere* **64**:672-685.
293. **Singer, A.** 2006. The chemical ecology of pollutant biodegradation. Bioremediation and phytoremediation from mechanistic and ecological perspectives, p. 5-19. *In* Mackova, M., Dowling, D.N., Macek, T (ed.), *Phytoremediation and rhizoremediation. Theoretical background*. Springer, Dordrecht
294. **Singer, A. C., Crowley, D. E., and Thompson, I. P.** 2003. Secondary plant metabolites in phytoremediation and biotransformation. *Trends Biotechnol* **21**:123-130.
295. **Slater, H., Gouin, T., and Leigh, M. B.** 2011. Assessing the potential for rhizoremediation of PCB contaminated soils in northern regions using native tree species. *Chemosphere* **84**:199-206.

296. **Sondossi, M., Barriault, D., and Sylvestre, M.** 2004. Metabolism of 2,2'- and 3,3'-dihydroxybiphenyl by the biphenyl catabolic pathway of *Comamonas testosteroni* B-356. *Appl Environ Microbiol* **70**:174-181.
297. **Sondossi, M., Sylvestre, M., and Ahmad, D.** 1992. Effects of chlorobenzoate transformation on the *Pseudomonas testosteroni* biphenyl and chlorobiphenyl degradation pathway. *Appl Environ Microbiol* **58**:485-495.
298. **Sondossi, M., Sylvestre, M., Ahmad, D., and Massé, R.** 1991. Metabolism of hydroxybiphenyl and chloro-hydroxybiphenyl by biphenyl/chlorobiphenyl degrading *Pseudomonas testosteroni* strain B-356. *J Ind Microbiol Biot* **7**:77-88.
299. **Spencer, J. P.** 2008. Flavonoids: modulators of brain function? *Brit J Nutr* **99 E Suppl 1**:ES60-77.
300. **Standfuss-Gabisch, C., Al-Halbouni, D., and Hofer, B.** 2012. Characterization of biphenyl dioxygenase sequences and activities encoded by the metagenomes of highly polychlorobiphenyl-contaminated soils. *Appl Environ Microbiol* **78**:2706-2715.
301. **Stangl, V., Lorenz, M., and Stangl, K.** 2006. The role of tea and tea flavonoids in cardiovascular health. *Mol Nutr Food Res* **50**:218-228.
302. **Steen, E. J., Kang, Y., Bokinsky, G., Hu, Z., Schirmer, A., McClure, A., Del Cardayre, S. B., and Keasling, J. D.** 2010. Microbial production of fatty-acid-derived fuels and chemicals from plant biomass. *Nature* **463**:559-562.
303. **Suenaga, H., Goto, M., and Furukawa, K.** 2006. Active-site engineering of biphenyl dioxygenase: effect of substituted amino acids on substrate specificity and regiospecificity. *Appl Microbiol Biotechnol* **71**:168-176.
304. **Suenaga, H., Mitsuoka, M., Ura, Y., Watanabe, T., and Furukawa, K.** 2001. Directed evolution of biphenyl dioxygenase: emergence of enhanced degradation capacity for benzene, toluene, and alkylbenzenes. *J Bacteriol* **183**:5441-5444.
305. **Suenaga, H., Nishi, A., Watanabe, T., Sakai, M., and Furukawa, K.** 1999. Engineering a hybrid pseudomonad to acquire 3,4-dioxygenase activity for polychlorinated biphenyls. *J Biosci Bioeng* **87**:430-435.
306. **Suenaga, H., Nonaka, K., Fujihara, H., Goto, M., and Furukawa, K.** 2010. Hybrid pseudomonads engineered by two-step homologous recombination acquire novel degradation abilities toward aromatics and polychlorinated biphenyls. *Appl Microbiol Biotechnol* **88**:915-923.
307. **Suenaga, H., Watanabe, T., Sato, M., Ngadiman, and Furukawa, K.** 2002. Alteration of regiospecificity in biphenyl dioxygenase by active-site engineering. *J Bacteriol* **184**:3682-3688.
308. **Suske, W. A., Van Berkel, W. J., and Kohler, H. P.** 1999. Catalytic mechanism of 2-hydroxybiphenyl 3-monooxygenase, a flavoprotein from *Pseudomonas azelaica* HBP1. *J Biol Chem* **274**:33355-33365.
309. **Sylvestre, M.** 2004. Genetically modified organisms to remediate polychlorinated biphenyls. Where do we stand? *Int Biodeter Biodegr* **54**:153-162.
310. **Sylvestre, M.** 1980. Isolation method for bacterial isolates capable of growth on *p*-chlorobiphenyl. *Appl Environ Microbiol* **39**:1223-1224.
311. **Sylvestre, M.** 2012. Prospects for using combined engineered bacterial enzymes and plant systems to rhizoremediate polychlorinated biphenyls. *Environ Microbiol* **15**:907-915.

312. Sylvestre, M., Hurtubise, Y., Barriault, D., Bergeron, J., and Ahmad, D. 1996. Characterization of active recombinant 2,3-dihydro-2,3-dihydroxybiphenyl dehydrogenase from *Comamonas testosteroni* B-356 and sequence of the encoding gene (*bphB*). *Appl Environ Microbiol* **62**:2710-2715.
313. Sylvestre, M., Macek, T., and Mackova, M. 2009. Transgenic plants to improve rhizoremediation of polychlorinated biphenyls (PCBs). *Curr Opin Biotechnol* **20**:242-247.
314. Sylvestre, M., Sirois, M., Hurtubise, Y., Bergeron, J., Ahmad, D., Shareck, F., Barriault, D., Guillemette, I., and Juteau, J. M. 1996. Sequencing of *Comamonas testosteroni* strain B-356-biphenyl/chlorobiphenyl dioxygenase genes: evolutionary relationships among Gram-negative bacterial biphenyl dioxygenases. *Gene* **174**:195-202.
315. Sylvestre, M., and Sondossi, M. 1994. Selection of enhanced PCB-degrading bacterial strains for bioremediation: consideration of branching pathways, p. 47-73. *In* Chaudhry, G.R. (ed.), *Biological degradation and remediation of toxic chemicals*. Chapman and Hall, New York.
316. Sylvestre, M., and Toussaint, J.-P. 2011. Engineering microbial enzymes and plants to promote PCB degradation in soil: current state of knowledge, p. 177-196. *In* Koukkou, A.I. (ed.), *Microbial bioremediation of non-metals current research*. Caister Academic Press, Norfolk, UK.
317. Taghavi, S., Garafola, C., Monchy, S., Newman, L., Hoffman, A., Weyens, N., Barac, T., Vangronsveld, J., and Van Der Lelie, D. 2009. Genome survey and characterization of endophytic bacteria exhibiting a beneficial effect on growth and development of poplar trees. *Appl Environ Microbiol* **75**:748-757.
318. Tahara, S. 2007. A journey of twenty-five years through the ecological biochemistry of flavonoids. *Biosci Biotechnol Biochem* **71**:1387-1404.
319. Taira, K., Hirose, J., Hayashida, S., and Furukawa, K. 1992. Analysis of *bph* operon from the polychlorinated biphenyl-degrading strain of *Pseudomonas pseudoalcaligenes* KF707. *J Biol Chem* **267**:4844-4853.
320. Takeda, H., Shimodaira, J., Yukawa, K., Hara, N., Kasai, D., Miyauchi, K., Masai, E., and Fukuda, M. 2010. Dual two-component regulatory systems are involved in aromatic compound degradation in a polychlorinated-biphenyl degrader, *Rhodococcus jostii* RHA1. *J Bacteriol* **192**:4741-4751.
321. Takeda, H., Yamada, A., Miyauchi, K., Masai, E., and Fukuda, M. 2004. Characterization of transcriptional regulatory genes for biphenyl degradation in *Rhodococcus* sp. strain RHA1. *J Bacteriol* **186**:2134-2146.
322. Tanaka, Y., Brugliera, F., and Chandler, S. 2009. Recent progress of flower colour modification by biotechnology. *Int J Mol Sci* **10**:5350-5369.
323. Tanaka, Y., Brugliera, F., Kalc, G., Senior, M., Dyson, B., Nakamura, N., Katsumoto, Y., and Chandler, S. 2010. Flower color modification by engineering of the flavonoid biosynthetic pathway: practical perspectives. *Biosci Biotechnol Biochem* **74**:1760-1769.
324. Tanaka, Y., Tsuda, S., and Kusumi, T. 1998. Metabolic Engineering to Modify Flower Color. *Plant Cell Physiol.* **39**:1119-1126.
325. Tandlich, R., Brezna, B., and Dercova, K. 2001. The effect of terpenes on the biodegradation of polychlorinated biphenyls by *Pseudomonas stutzeri*. *Chemosphere* **44**:1547-1555.

326. **Tao, Y., Fishman, A., Bentley, W. E., and Wood, T. K. 2004.** Altering toluene 4-monooxygenase by active-site engineering for the synthesis of 3-methoxycatechol, methoxyhydroquinone, and methylhydroquinone. *J Bacteriol* **186**:4705-4713.
327. **Tehrani, R., Lyv, M. M., Kaveh, R., Schnoor, J. L., and Van Aken, B. 2012.** Biodegradation of mono-hydroxylated PCBs by *Burkholderia xenovorans*. *Biotechnol Lett* **34**:2247-2252.
328. **Tehrani, R., and Van Aken, B. 2013.** Hydroxylated polychlorinated biphenyls in the environment: sources, fate, and toxicities. *Environ Sci Pollut Res Int* **10.1007/s11356-013-1742-6**.
329. **Thrane, C., Harder Nielsen, T., Neiendam Nielsen, M., Sorensen, J., and Olsson, S. 2000.** Viscosinamide-producing *Pseudomonas fluorescens* DR54 exerts a biocontrol effect on *Pythium ultimum* in sugar beet rhizosphere. *FEMS Microbiol Ecol* **33**:139-146.
330. **Toussaint, J. P., Pham, T. T., Barriault, D., and Sylvestre, M. 2012.** Plant exudates promote PCB degradation by a rhodococcal rhizobacteria. *Appl Microbiol Biotechnol* **95**:1589-1603.
331. **Trivedi, P., Pandey, A., and Sa, T. M. 2007.** Chromate reducing and plant growth promoting activities of psychrotrophic *Rhodococcus erythropolis* MtCC 7905. *J Basic Microb* **47**:513-517.
332. **Tsai, S. M., and Phillips, D. A. 1991.** Flavonoids released naturally from alfalfa promote development of symbiotic *glomus* spores in vitro. *Appl Environ Microbiol* **57**:1485-1488.
333. **Tsao, D. T. 2003.** Overview of phytotechnologies. *Adv Biochem Eng Biotechnol* **78**:1-50.
334. **Uhlik, O., Musilova, L., Ridl, J., Hroudova, M., Vlcek, C., Koubek, J., Holecova, M., Mackova, M., and Macek, T. 2013.** Plant secondary metabolite-induced shifts in bacterial community structure and degradative ability in contaminated soil. *Appl Microbiol Biotechnol* **20**:9245-9256.
335. **Ullrich, R., and Hofrichter, M. 2007.** Enzymatic hydroxylation of aromatic compounds. *Cell Mol Life Sci* **64**:271-293.
336. **Unterman, R. 1996.** A history of PCB biodegradation. In Crawford, R.L. and Crawford, D.L. (ed.), *Bioremediation: Principles and Applications*. Cambridge University Press.
337. **Vaillancourt, F. H., Haro, M. A., Drouin, N. M., Karim, Z., Maaroufi, H., and Eltis, L. D. 2003.** Characterization of extradiol dioxygenases from a polychlorinated biphenyl-degrading strain that possess higher specificities for chlorinated metabolites. *J Bacteriol* **185**:1253-1260.
338. **Vaillancourt, F. H., Labbé, G., Drouin, N. M., Fortin, P. D., and Eltis, L. D. 2002.** The mechanism-based inactivation of 2,3-dihydroxybiphenyl 1,2-dioxygenase by catecholic substrates. *J Biol Chem* **277**:2019-2027.
339. **Van Aken, B., Correa, P. A., and Schnoor, J. L. 2010.** Phytoremediation of polychlorinated biphenyls: New trends and promises. *Environ Sci Technol* **44**:2767-2776.
340. **Van Beilen, J. B., Duetz, W. A., Schmid, A., and Witholt, B. 2003.** Practical issues in the application of oxygenases. *Trends Biotechnol* **21**:170-177.
341. **Vasilyeva, G. K., and Strijakova, E. R. 2007.** Bioremediation of soils and sediments contaminated by polychlorinated biphenyls. *Microbiology* **76**:639-653.
342. **Verhoeven, M. E., Bovy, A., Collins, G., Muir, S., Robinson, S., De Vos, C. H., and Colliver, S. 2002.** Increasing antioxidant levels in tomatoes through modification of the flavonoid biosynthetic pathway. *J Exp Bot* **53**:2099-2106.

343. Ververidis, F., Trantas, E., Douglas, C., Vollmer, G., Kretzschmar, G., and Panopoulos, N. 2007. Biotechnology of flavonoids and other phenylpropanoid-derived natural products. Part I: Chemical diversity, impacts on plant biology and human health. *Biotechnol J* 2:1214-1234.
344. Vezina, J., Barriault, D., and Sylvestre, M. 2008. Diversity of the C-terminal portion of the biphenyl dioxygenase large subunit. *J Mol Microbiol Biotechnol* 15:139-151.
345. Vezina, J., Barriault, D., and Sylvestre, M. 2007. Family shuffling of soil DNA to change the regiospecificity of *Burkholderia xenovorans* LB400 biphenyl dioxygenase. *J Bacteriol* 189:779-788.
346. Viger, J. F., Mohammadi, M., Barriault, D., and Sylvestre, M. 2012. Metabolism of chlorobiphenyls by a variant biphenyl dioxygenase exhibiting enhanced activity toward dibenzofuran. *Biochem Biophys Res Commun* 419:362-367.
347. Villaceros, M., Whelan, C., Mackova, M., Molgaard, J., Sanchez-Contreras, M., Lloret, J., Aguirre De Carcer, D., Oruezabal, R. I., Bolanos, L., Macek, T., Karlson, U., Dowling, D. N., Martin, M., and Rivilla, R. 2005. Polychlorinated biphenyl rhizoremediation by *Pseudomonas fluorescens* F113 derivatives, using a *Sinorhizobium meliloti* nod system to drive *bph* gene expression. *Appl Environ Microbiol* 71:2687-2694.
348. Wackett, L. P. 2002. Mechanism and applications of Rieske non-heme iron dioxygenases. *Enzyme Microb Tech* 31:577-587.
349. Wackett, L. P., and Hershberger, C. D. 2001. Biocatalysis and biodegradation: Microbial transformation of organic compounds. ASM Press, Washington D.C.
350. Walker, A. R., Davison, P. A., Bolognesi-Winfield, A. C., James, C. M., Srinivasan, N., Blundell, T. L., Esch, J. J., Marks, M. D., and Gray, J. C. 1999. The *TRANSPARENT TESTA GLABRA1* locus, which regulates trichome differentiation and anthocyanin biosynthesis in *Arabidopsis*, encodes a WD40 repeat protein. *Plant Cell* 11:1337-1350.
351. Warren, R., Hsiao, W. W., Kudo, H., Myhre, M., Dosanjh, M., Petrescu, A., Kobayashi, H., Shimizu, S., Miyauchi, K., Masai, E., Yang, G., Stott, J. M., Schein, J. E., Shin, H., Khattra, J., Smailus, D., Butterfield, Y. S., Siddiqui, A., Holt, R., Marra, M. A., Jones, S. J., Mohn, W. W., Brinkman, F. S., Fukuda, M., Davies, J., and Eltis, L. D. 2004. Functional characterization of a catabolic plasmid from polychlorinated-biphenyl-degrading *Rhodococcus* sp. strain RHA1. *J Bacteriol* 186:7783-7795.
352. Watanabe, T., Fujihara, H., and Furukawa, K. 2003. Characterization of the second LysR-type regulator in the biphenyl-catabolic gene cluster of *Pseudomonas pseudoalcaligenes* KF707. *J Bacteriol* 185:3575-3582.
353. Watanabe, T., Inoue, R., Kimura, N., and Furukawa, K. 2000. Versatile transcription of biphenyl catabolic *bph* operon in *Pseudomonas pseudoalcaligenes* KF707. *J Biol Chem* 275:31016-31023.
354. Weyens, N., Van Der Lelie, D., Taghavi, S., Newman, L., and Vangronsveld, J. 2009. Exploiting plant-microbe partnerships to improve biomass production and remediation. *Trends Biotechnol* 27:591-598.
355. Wiegel, J., and Wu, Q. 2000. Microbial reductive dehalogenation of polychlorinated biphenyls. *FEMS Microbiol Ecol* 32:1-15.
356. Winkel-Shirley, B. 2001. Flavonoid biosynthesis. A colorful model for genetics, biochemistry, cell biology, and biotechnology. *Plant Physiol* 126:485-493.


357. **Witzig, R., Junca, H., Hecht, H. J., and Pieper, D. H.** 2006. Assessment of toluene/biphenyl dioxygenase gene diversity in benzene-polluted soils: links between benzene biodegradation and genes similar to those encoding isopropylbenzene dioxygenases. *Appl Environ Microbiol* **72**:3504-3514.
358. **Xu, L., Teng, Y., Li, Z. G., Norton, J. M., and Luo, Y. M.** 2010. Enhanced removal of polychlorinated biphenyls from alfalfa rhizosphere soil in a field study: The impact of a rhizobial inoculum. *Sci Total Environ* **408**:1007-1013.
359. **Yagi, O., and Sudo, R.** 1980. Degradation of polychlorinated biphenyls by microorganisms. *Journal (Water Pollution Control Federation)* **52**:1035-1043.
360. **Yamada, A., Kishi, H., Sugiyama, K., Hatta, T., Nakamura, K., Masai, E., and Fukuda, M.** 1998. Two nearly identical aromatic compound hydrolase genes in a strong polychlorinated biphenyl degrader, *Rhodococcus* sp. strain RHA1. *Appl Environ Microbiol* **64**:2006-2012.
361. **Yang, X., Liu, X., Song, L., Xie, F., Zhang, G., and Qian, S.** 2007. Characterization and functional analysis of a novel gene cluster involved in biphenyl degradation in *Rhodococcus* sp. strain R04. *J Appl Microbiol* **103**:2214-2224.
362. **Yang, X. Q., Sun, Y., and Qian, S. J.** 2004. Biodegradation of seven polychlorinated biphenyls by a newly isolated aerobic bacterium (*Rhodococcus* sp. R04). *J Ind Microbiol Biot* **31**:415-420.
363. **Yin, L., Shen, Z., Niu, J., Chen, J., and Duan, Y.** 2010. Degradation of pentachlorophenol and 2,4-dichlorophenol by sequential visible-light driven photocatalysis and laccase catalysis. *Environ Sci Technol* **44**:9117-9122.
364. **Yoshida, K., Mori, M., and Kondo, T.** 2009. Blue flower color development by anthocyanins: from chemical structure to cell physiology. *Nat Prod Rep* **26**:884-915.
365. **Yu, C. L., Liu, W., Ferraro, D. J., Brown, E. N., Parales, J. V., Ramaswamy, S., Zylstra, G. J., Gibson, D. T., and Parales, R. E.** 2007. Purification, characterization, and crystallization of the components of a biphenyl dioxygenase system from *Sphingobium yanoikuyae* B1. *J Ind Microbiol Biot* **34**:311-324.
366. **Yun, Q., Lin, Z., and Xin, T.** 2009. Cometabolism and immobilized degradation of monochlorobenzoate by *Rhodococcus erythropolis*. *Afr J Microbiol Res* **3**:482-486.
367. **Zhang, G. Q., Yang, X. Q., Xie, F. H., Chao, Y. P., and Qian, S. J.** 2009. Cometabolic degradation of mono-chloro benzoic acids by *Rhodococcus* sp. R04 grown on organic carbon sources. *World J Microb Biot* **25**:1169-1174.
368. **Zhao, D., Tao, J., Han, C., and Ge, J.** 2012. Flower color diversity revealed by differential expression of flavonoid biosynthetic genes and flavonoid accumulation in herbaceous peony (*Paeonia lactiflora* Pall.). *Mol Biol Rep* **39**:11263-11275.
369. **Zhu, M., Zheng, X., Shu, Q., Li, H., Zhong, P., Zhang, H., Xu, Y., and Wang, L.** 2012. Relationship between the composition of flavonoids and flower colors variation in tropical water lily (*Nymphaea*) cultivars. *Plos One* **7**:e34335.
370. **Zuk, M., Kulma, A., Dyminska, L., Szoltysek, K., Prescha, A., Hanuza, J., and Szopa, J.** 2011. Flavonoid engineering of flax potentiate its biotechnological application. *BMC Biotechnol* **11**:10.

Annex

Article 1

Plant exudates promote PCB degradation by a rhodococcal rhizobacteria

(published in Applied Microbiology and Biotechnology)

Plant secondary metabolites in *Arabidopsis thaliana* root exudates detected by HPLC 

Article 2

Remarkable ability of *Pandoraea pnomenusa* B356 biphenyl dioxygenase to metabolize simple flavonoids

(published in Applied and Environmental Microbiology)

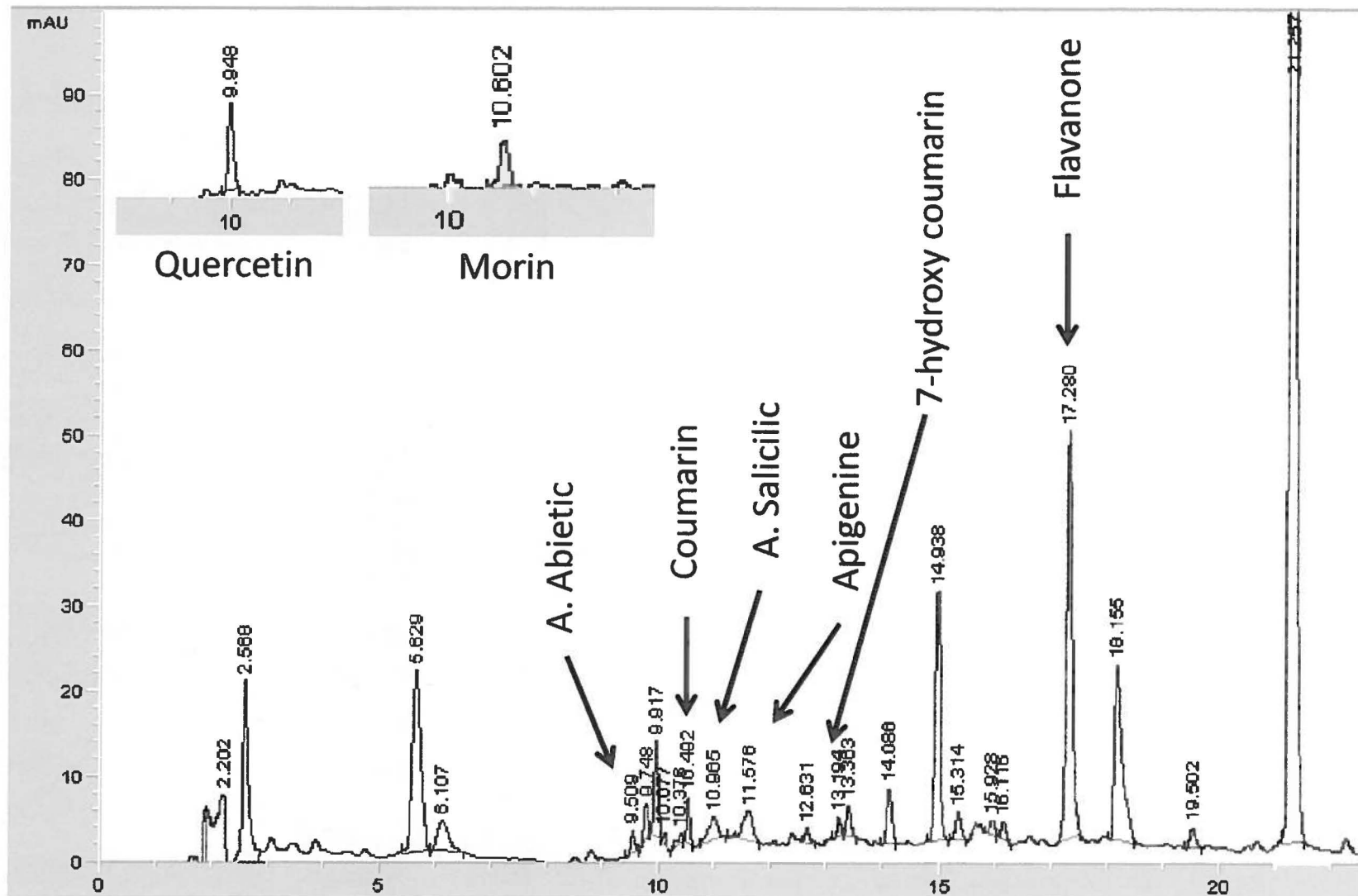
Article 3

Has the bacterial biphenyl catabolic pathway evolved primarily to degrade biphenyl ? The diphenylmethane case

(published in Journal of Bacteriology)

Bioscreen C system

Plant secondary metabolites in *A.thaliana* root exudates detected by HPLC



Method is described in section 3.7.4

Remarkable Ability of *Pandoraea pnomenusa* B356 Biphenyl Dioxygenase To Metabolize Simple Flavonoids

Thi Thanh My Pham, Youbin Tu and Michel Sylvestre
Appl. Environ. Microbiol. 2012, 78(10):3560. DOI:
10.1128/AEM.00225-12.
Published Ahead of Print 16 March 2012.

Updated information and services can be found at:
<http://aem.asm.org/content/78/10/3560>

REFERENCES

These include:

This article cites 36 articles, 14 of which can be accessed free
at: <http://aem.asm.org/content/78/10/3560#ref-list-1>

CONTENT ALERTS

Receive: RSS Feeds, eTOCs, free email alerts (when new
articles cite this article), [more»](#)

Information about commercial reprint orders: <http://aem.asm.org/site/misc/reprints.xhtml>
To subscribe to to another ASM Journal go to: <http://journals.asm.org/site/subscriptions/>

Remarkable Ability of *Pandoraea pnomenusa* B356 Biphenyl Dioxygenase To Metabolize Simple Flavonoids

Thi Thanh My Pham, Youbin Tu, and Michel Sylvestre

Institut National de la Recherche Scientifique, INRS-Institut Armand-Frappier, Laval, Quebec, Canada

Many investigations have provided evidence that plant secondary metabolites, especially flavonoids, may serve as signal molecules to trigger the abilities of bacteria to degrade chlorobiphenyls in soil. However, the bases for this interaction are largely unknown. In this work, we found that BphAE_{B356}, the biphenyl/chlorobiphenyl dioxygenase from *Pandoraea pnomenusa* B356, is significantly better fitted to metabolize flavone, isoflavone, and flavanone than BphAE_{LB400} from *Burkholderia xenovorans* LB400. Unlike those of BphAE_{LB400}, the kinetic parameters of BphAE_{B356} toward these flavonoids were in the same range as for biphenyl. In addition, remarkably, the biphenyl catabolic pathway of strain B356 was strongly induced by isoflavone, whereas none of the three flavonoids induced the catabolic pathway of strain LB400. Docking experiments that replaced biphenyl in the biphenyl-bound form of the enzymes with flavone, isoflavone, or flavanone showed that the superior ability of BphAE_{B356} over BphAE_{LB400} is principally attributable to the replacement of Phe336 of BphAE_{LB400} by Ile334 and of Thr335 of BphAE_{LB400} by Gly333 of BphAE_{B356}. However, biochemical and structural comparison of BphAE_{B356} with BphAE_{p4}, a mutant of BphAE_{LB400} which was obtained in a previous work by the double substitution Phe336Met Thr335Ala of BphAE_{LB400}, provided evidence that other residues or structural features of BphAE_{B356} whose precise identification the docking experiment did not allow are also responsible for the superior catalytic abilities of BphAE_{B356}. Together, these data provide supporting evidence that the biphenyl catabolic pathways have evolved divergently among proteobacteria, where some of them may serve ecological functions related to the metabolism of plant secondary metabolites in soil.

Aryl hydroxylating Rieske-type dioxygenases (ROs) catalyze a *cis*-dioxygenation of aryl compounds to generate a *cis*-dihydrodiol metabolite. ROs are promising biocatalysts that metabolize many substituted benzene or diphenyl rings, as well as bicyclic- or tricyclic-fused heterocyclic aromatics, such as quinoline, dibenzofuran, phenanthridine, and flavonoids (3, 4, 15, 22, 29, 30, 33). The biphenyl dioxygenase (BPDO) which catalyzes the first reaction of the bacterial biphenyl catabolic pathway is an RO that has been extensively studied because of its ability to metabolize several polychlorinated biphenyl (PCB) congeners. The BPDO reaction (Fig. 1) requires three components (10, 12, 13). The catalytic component (BphAE) is an RO protein which is a heterohexamer made up of three α (BphA) and three β subunits (BphE). The ferredoxin (BphF) and the ferredoxin reductase (BphG) are involved in electron transfer from NADH to BphAE. The encoding genes for both *Burkholderia xenovorans* LB400 and *Pandoraea pnomenusa* B356 are *bphA* (BphAE α subunit), *bphE* (BphAE β subunit), *bphF* (BphF), and *bphG* (BphG) (6, 36). The α subunit is the one involved in the catalytic activity. It comprises two domains; the Rieske domain containing a 2Fe-2S Rieske cluster receives the electrons from BphF and transfers them to the catalytic mononuclear iron center of the catalytic domain (7).

Several investigations have shown that BPDO can metabolize flavonoids (4, 15, 29, 30). These plant secondary metabolites (PSMs) are regarded as very promising for the prevention and treatment of cancers (26) and cardiovascular diseases (35). Plants are currently the major source for these chemicals, but the synthesis of novel derivatives exhibiting improved biological properties is often difficult or impractical (22). Furthermore, in the context of the green chemistry concept, new, more selective and more environmentally friendly approaches to manufacture these biologically specific fine chemicals will be required.

Seeger et al. have shown that *B. xenovorans* LB400 BPDO

(BphAE_{LB400}) is able to dihydroxylate several isoflavonoids on ring B (29). BphAE_{LB400} has been extensively investigated because it is regarded as one of the most efficient dioxygenases of natural origin for the degradation of a wide range of chlorobiphenyls. However, in recent years, *P. pnomenusa* B356 BPDO (BphAE_{B356}) was shown to exhibit superior abilities to degrade several biphenyl analogs, including 2,6-dichlorobiphenyl, 2,4,4'-trichlorobiphenyl, and dichlorodiphenyltrichloroethane (DDT), that BphAE_{LB400} metabolizes poorly (9, 20). Furthermore, preliminary unpublished experiments have suggested that BphAE_{B356} metabolizes flavonoids more efficiently than BphAE_{LB400}. On the other hand, a mutant of BphAE_{LB400}, BphAE_{p4}, an evolved BPDO derived from BphAE_{LB400} by the substitutions Thr335Ala Phe336Met, was shown to metabolize a broader range of chlorobiphenyls and dibenzofurans than the parent BphAE_{LB400} (2). The new catalytic properties of this mutant were attributed to the single Thr335Ala substitution. Thr335 exerts constraints on a segment comprised of Val320-Gln322 that lines the catalytic pocket. Replacing Thr335 with Ala releases the constraints on this segment, allowing for more movement during substrate binding (18, 23).

The bacterial metabolism of flavonoids may also have an impact on soil microbiology and on plant-microbe interactions. Many investigations have provided evidence that PSMs may act as signal molecules to trigger the PCB-degrading abilities of soil bacteria (for a review, see reference 34). These signal molecules may have a major impact on the success of rhizoremediation processes

Received 24 January 2012 Accepted 6 March 2012

Published ahead of print 16 March 2012

Address correspondence to Michel Sylvestre, Michel.Sylvestre@iaf.inrs.ca.

Copyright © 2012, American Society for Microbiology. All Rights Reserved.

doi:10.1128/AEM.00225-12

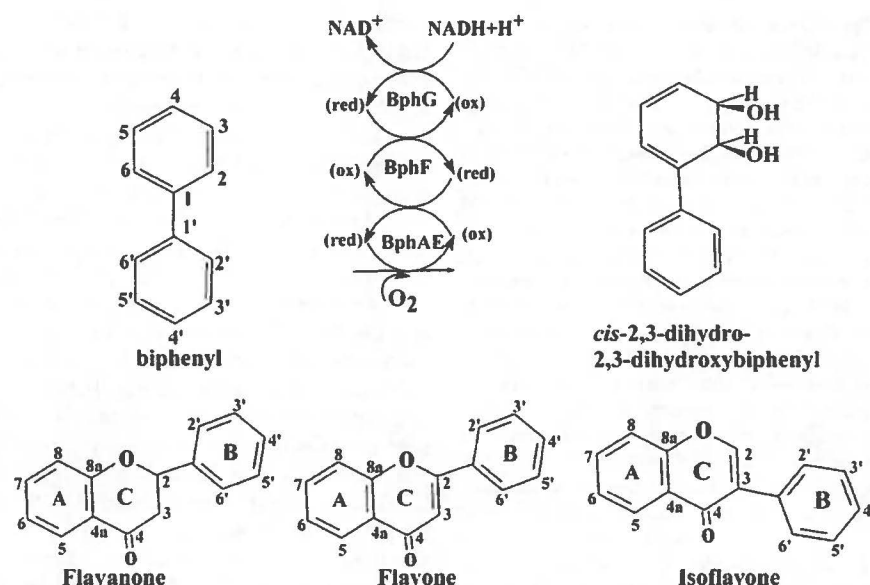


FIG 1 Biphenyl dioxygenase reaction (top) and structures of flavone, flavanone, and isoflavone (bottom).

aiming at the destruction of PCBs in soil. However, the bases for the PCB-degrading bacterium-plant secondary metabolite interactions are largely unknown. In a recent work (37), we showed that *Arabidopsis thaliana* root exudates trigger the PCB catabolic abilities of *Rhodococcus erythropolis* U23A, a rhodococcal rhizobacterium isolated from the rhizosphere of PCB-contaminated-plant roots. Flavanone, one of the major component of these root exudates, was unable to support the growth of strain U23A, but it was metabolized by this strain through its biphenyl catabolic pathway (37). In addition, when used as a cosubstrate with sodium acetate, flavanone was as efficient as biphenyl at inducing the biphenyl catabolic pathway of strain U23A (37). These observations are consistent with the proposed hypothesis whereby flavonoids would act as a signal molecule in soil to modulate the quantity and quality of phenylpropanoids in the rhizosphere (31).

Given the significant impacts the bacterial metabolism of flavonoids may have on green chemistry and on PCB remediation processes and given the preliminary data showing that the two well-characterized *P. pnomenusa* B356 and *B. xenovorans* LB400 BPDOs metabolized flavonoids differently, we compared the catalytic properties of BphAE_{LB400} and BphAE_{B356} toward the simple flavonoids flavone, isoflavone, and flavanone and we assessed the ability of these flavonoids to induce the biphenyl catabolic pathway of these two organisms. In order to get more insights about structural features of BphAE conferring the ability to metabolize these flavonoids, we also docked these chemicals in these protein structures and compared the structure of the docked enzymes with that of BphAE_{p4}.

MATERIALS AND METHODS

Bacterial strains, plasmids, and chemicals. Wild-type strains *P. pnomenusa* B356 and *B. xenovorans* LB400 were described previously (1, 6). All plasmids used in this study were described previously. pET14b[LB400-*bphAE*] and pET14b[*p4-bphAE*] carry the genes encoding the wild-type BphAE_{LB400} and its mutant BphAE_{p4} (Thr335Ala Phe336Met) (2, 17), plasmid pET14b[B356-*bphAE*] carries the genes encoding BphAE_{B356} (20), and plasmids pET14b[LB400-*bphF*] and

pET14b[LB400-*bphG*] carry the genes encoding strain LB400 BphF and BphG (23). Flavone and flavanone were from Sigma-Aldrich, and isoflavone from Indofine Chemical Company, Inc. They were all 99% pure.

Whole-cell assays to determine the ability of *P. pnomenusa* B356 and *B. xenovorans* LB400 to metabolize flavanone. The metabolism of flavanone by resting-cell suspensions of biphenyl-induced cells of *P. pnomenusa* B356 and *B. xenovorans* LB400 was examined according to a protocol described previously to investigate the metabolism of flavanone by *R. erythropolis* U23A (37). Briefly, each strain was grown overnight on medium MM30 (37) containing 3.4 mM biphenyl, and the cells were harvested, washed, and suspended in M9 medium (37) with no carbon source to an optical density at 600 nm (OD₆₀₀) of 5. This cell suspension was distributed (5-ml amounts) among 50-ml glass tubes, and flavanone was added to a final concentration of 200 μM. The resting-cell suspensions were incubated at either 28°C or 15°C for various periods of between 5 min and 18 h. They were then extracted with ethyl acetate, the organic phase was evaporated, and the residues were treated with *n*-butylboronate (*n*BuB) or *N,O*-bis(trimethylsilyl)trifluoroacetamide (BSTFA) (Supelco, Sigma-Aldrich) as described previously for gas chromatography-mass spectrometry (GC-MS) analyses (37).

Assays to identify the metabolites produced from flavone, flavanone, and isoflavone by BphAE_{B356}, BphAE_{LB400}, and BphAE_{p4} and to determine their kinetic parameters. Reconstituted His-tagged BPDO preparations were used in the experiments to identify the metabolites and kinetics of the enzymes and substrates. His-tagged purified enzyme components were produced in recombinant *Escherichia coli* strains and purified according to published protocols (23). The enzyme assays were performed at 37°C as described previously in a volume of 200 μl in 50 mM morpholinethanesulfonic acid (MES) buffer, pH 6.0, containing 100 nmol substrate (13). The metabolites were extracted at pH 6.0 with ethyl acetate and treated with *n*BuB or BSTFA for GC-MS analyses.

Catalytic activities were determined by monitoring substrate depletion and metabolite production after 10 min of incubation under the conditions described above. GC-MS peak areas were used to quantify substrate depletion and metabolite production. GC-MS analyses were performed using a Hewlett Packard HP6980 series gas chromatograph interfaced with an HP5973 mass selective detector (Agilent Technologies). The mass selective detector was operated in electron impact ionization (EI) mode and used a quadrupole mass analyzer. The steady-state

kinetic parameters of all BphAEs were determined by recording oxygen consumption rates using a Clarke-type Hansatech model DW1 oxygraph (14) for various concentrations of flavonoids between 5 and 150 μ M. The kinetic parameters reported in this work were obtained from the analysis of at least two independently produced preparations tested in triplicate.

Assays to assess the ability of flavone, flavanone, and isoflavone to induce the biphenyl catabolic pathway of strains B356 and LB400. The induction of the biphenyl catabolic pathway of strains B356 and LB400 was assessed on the basis of the amount of 4-chlorobenzoate produced from 4-chlorobiphenyl by resting-cell suspensions previously grown on sodium acetate plus variable concentrations of flavonoids or biphenyl. This assay was performed according to the same method as the previously described assay to assess the ability of flavanone to induce the biphenyl catabolic pathway of *R. erythropolis* U23A (37). Briefly, cells were grown overnight in medium MM30 amended with 30 mM sodium acetate or with 30 mM sodium acetate plus variable amounts (6 mM, 1 mM, 0.01 mM, or 0.001 mM) of flavone, isoflavone, flavanone, or biphenyl. Cells were harvested and washed in M9 medium without carbon source. The suspensions were adjusted to an OD₆₀₀ of 1 with M9 medium and distributed in portions of 200 μ l into 1.5-ml Eppendorf tubes. 4-Chlorobiphenyl was added to a final concentration of 1.25 mM, and the reaction vials were incubated for 120 min at 28°C in an Eppendorf Thermomixer 5436. The suspensions were then acidified with HCl before the metabolites were extracted with ethyl acetate. The extracts were evaporated, and the residues were derivatized with BSFTA for GC-MS analysis (37).

Docking and structure analysis. BphAE_{LB400} (RCSB Protein Databank PDB ID 2XRX), BphAE_{B356} (RCSB Protein Databank PDB ID 3GZX), and BphAE_{U23A} (RCSB Protein Databank PDB ID 2XSH) were used as protein targets, and they were prepared as previously described (20). In the case of BphAE_{LB400} and BphAE_{U23A}, we used the structural coordinates of dimer AB for the docking. Ligands were all downloaded as sdf files from PubChem (<http://pubchem.ncbi.nlm.nih.gov>) and converted into pdb format in Discover Studio Visualizer 2.5. Both proteins and ligands were processed with AutoDockTools to obtain their proper pdbqt format. The searching space for the ligand was centered on the mononuclear iron and contained 20 Å in each x, y, and z direction. Autodock Vina 1.1.2 (24) with the default parameters was used to perform the automatic docking.

RESULTS

Metabolism of flavanone by biphenyl-induced resting cells of strains B356 and LB400. In a previous report, we showed that although flavanone could not support the growth of *R. erythropolis* U23A, biphenyl-induced cells of strain U23A metabolized this plant metabolite (37). The induced cells of strain U23A produced small amounts of 2-(2,3-dihydro-2,3-dihydroxyphenyl)chromane-4-one and 2-(3,4-dihydro-3,4-dihydroxyphenyl)chromane-4-one when they were incubated in the presence of flavanone, but the major and ultimate metabolite exhibited mass spectral features corresponding to those of 4-oxo-2-chromanecarboxylic acid (37). Neither strain B356 nor strain LB400 could grow on flavone, isoflavone, or flavanone, but biphenyl-induced cells of both converted flavanone to 4-oxo-2-chromanecarboxylic acid as a dead-end metabolite. 4-Oxo-2-chromanecarboxylic acid was identified from the mass spectral features of its trimethylsilyl (TMS) derivative, which exhibited diagnostically important ions at m/z 264 (M^+), 249 ($M^+ - CH_3$), 219 ($M^+ - 3CH_3$), 205 ($M^+ - CH_3 - O - CO$), 174 ($M^+ - COOTMS$), and 131 ($M^+ - COOTMS - O$).

When the resting cell suspensions of strain B356 were incubated at 15°C and for less than 5 min, in addition to 4-oxo-2-chromanecarboxylic acid, small amounts of 2-(2,3-dihydro-2,3-dihydroxyphenyl)chromane-4-one and 2-(3,4-dihydro-3,4-dihydroxyphenyl)chromane-4-one were detected. These two metabolites were identified on the basis of their GC-MS spectral features as described below for the

purified enzyme preparation. When the resting cells were incubated at a higher temperature and for longer incubation periods, 4-oxo-2-chromanecarboxylic acid was the only metabolite detected in the culture. This shows that the biphenyl catabolic enzymes of this organism were very efficient in transforming flavanone to 4-oxo-2-chromanecarboxylic acid. In addition, while cells of strain B356 metabolized more than 80% of the added substrate within 5 min at 15°C, cells of strain LB400 metabolized less than 20% of the substrate when they were incubated for 1 h at 28°C. This shows the superiority of strain B356 over strain LB400 in metabolizing flavanone.

Induction of the biphenyl catabolic pathway of strains B356 and LB400 by flavonoids. Flavanone induction was assessed by monitoring the 4-chlorobenzoate produced from 4-chlorobiphenyl which, in both strains B356 and LB400, accumulates as a dead-end metabolite of the biphenyl catabolic pathway. In a recent report, it was shown that the biphenyl catabolic genes are expressed constitutively at low levels during the growth of *B. xenovorans* LB400 on succinate (28). Furthermore, the level of expression of the pathway enzymes appeared to be influenced by posttranscriptional regulation factors and by the physiological state of the cells, which may significantly influence the chlorobiphenyl degradation abilities of cells (28). In spite of these difficulties, we reasoned that the assay monitoring 4-chlorobenzoate should allow us to determine if strains B356 and LB400 respond similarly to the presence of simple flavonoids during growth on sodium acetate and if the enzymes of the upper biphenyl catabolic pathway are induced by flavonoids.

When cells of strain B356 were grown on sodium acetate alone, small amounts of chlorobenzoate were produced in the growth medium (Fig. 2A). However, when cells were grown in the presence of sodium acetate plus variable amounts of biphenyl, the amount of 4-chlorobenzoate varied depending on the amount of biphenyl added to the culture medium (Fig. 2A). This response was similar to that observed for strain U23A grown in the presence of sodium acetate plus biphenyl (37). Cells of strain LB400 grown on sodium acetate alone produced slightly larger amounts of 4-chlorobenzoate than cells of strain B356, and the addition of biphenyl to the growth medium did not induce the biphenyl catabolic enzymes as strongly as for strain B356 (Fig. 2B).

When strain B356 was grown on sodium acetate plus flavanone, for concentrations ranging between 1 mM and 0.01 mM, the amount of 4-chlorobenzoate produced during the assay was not significantly higher than for cells grown on sodium acetate alone (Fig. 2A). Similar results were obtained when cells were grown on sodium acetate plus flavone. However, remarkably, the amounts of 4-chlorobenzoate produced from 4-chlorobiphenyl by resting cells grown on sodium acetate plus isoflavone were significantly higher than those produced for cells grown on sodium acetate plus biphenyl (Fig. 2A). We cannot exclude the possibility that posttranscriptional regulation mechanisms exerted by biphenyl metabolites are responsible for the lower enzyme activity found in cells grown on sodium acetate plus biphenyl. Furthermore, since all three flavonoids are metabolized by whole cells of strain B356, we must exclude the possibility that permeation of flavonoids across the cell membrane/wall had affected the cells' activity for substrate. Therefore, the data show that isoflavone is a good inducer of the biphenyl catabolic enzymes of strain B356. In the case of strain LB400, there was no clear-cut effect for any of the three tested flavonoids that would demonstrate

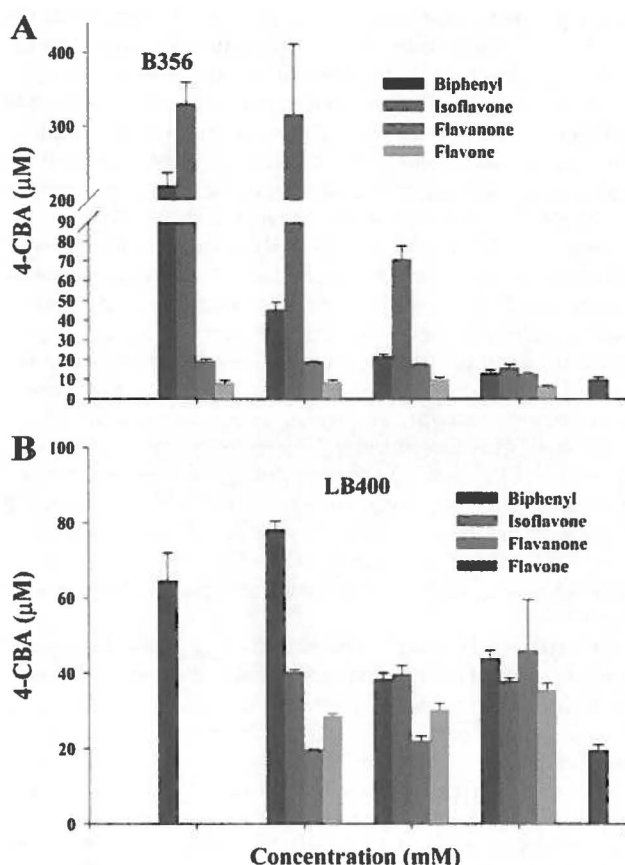


FIG 2 (A) Amounts (μM) of 4-chlorobenzoic acid (4-CBA) produced when standardized resting cell suspensions of strain B356 were incubated with 1,250 μM 4-chlorobiphenyl for 2 h. (B) Amounts (μM) of 4-chlorobenzoic acid produced when standardized resting cell suspensions of strain LB400 were incubated with 1,250 μM 4-chlorobiphenyl for 2 h. Each strain was previously grown overnight at 28°C in MM30 medium amended with 30 mM sodium acetate or with 30 mM sodium acetate plus the indicated concentration of the indicated flavonoid or of biphenyl. Bars represent means ($n = 2$) and standard deviations. The protocol for the standardized 4-chlorobiphenyl assay is described in Materials and Methods. Concentrations of 0.0005 and 0.0001 mM were only used for flavanone.

the ability of these flavonoids to induce the biphenyl catabolic pathway. The amounts of 4-chlorobenzoate produced varied slightly in the presence of flavonoids (Fig. 2B), but the amounts produced were not statistically significantly different from those observed in the absence of flavonoids. Therefore, none of the three flavonoids tested significantly influenced the activity of the biphenyl catabolic enzymes of strain LB400, whereas isoflavone was found to act as an inducer of the biphenyl catabolic pathway of strain B356 when it was added as a cosubstrate with sodium acetate.

Metabolites produced from flavonoids by purified BphAE_{B356}, BphAE_{LB400}, and BphAE_{p4}. Since whole cells of strains B356 and LB400 metabolized flavanone differently and since they responded differently to the presence of flavone, flavanone, and isoflavone in the growth medium, we have compared the ability of purified preparations of their biphenyl dioxygenases to metabolize these three plant metabolites. The purified enzymes were prepared from recombinant *E. coli* cells as described in Ma-

terials and Methods. We have also included BphAE_{p4}, a Thr335Ala Phe336Met mutant of BphAE_{LB400} exhibiting an expanded substrate range compared to that of its parent enzyme (2, 18). In a previous report, we showed that replacing Phe336 of BphAE_{LB400}, which lines the catalytic pocket, with a residue with a smaller side chain (Met336) increases the space inside the catalytic pocket. In a similar manner, the corresponding Ile334 of BphAE_{B356} that lines the catalytic pocket is smaller than Phe336 of BphAE_{LB400} and, thus, allows the enzyme to metabolize bulkier substrates, such as DDT (20). Thr335 is at a remove from the substrate; however, changing this residue to the smaller Ala335 relieves intramolecular constraints on Gly321, allowing for significant movement of this residue during substrate binding and thereby increasing the space available to accommodate bulkier substrates (20). In a manner similar to Ala335 of BphAE_{p4}, Gly333 (corresponding to Thr335 of BphAE_{LB400}) does not interact with Gly319 (corresponding to Gly321 of BphAE_{LB400}). Therefore, although the side chains of Ala335 and Gly333 differ, their effects on the enzyme's structure are likely to be comparable (18).

Based on the GC-MS peak area of the remaining substrate, purified preparations of BphAE_{B356} incubated with 100 nmol flavanone oxidized more than 90 nmol this substrate within 10 min. Under identical conditions, BphAE_{p4} metabolized approximately 20 nmol flavanone and BphAE_{LB400} metabolized less than 10 nmol of this substrate (Fig. 3A). Consistent with these results, the amount of metabolites generated by BphAE_{B356} after 10 min of incubation was significantly higher than for the two other enzymes (Fig. 3A). In addition, the pattern of metabolites generated by the three enzymes differed significantly. BphAE_{B356} produced two metabolites in approximately equal amounts. They both exhibited a very similar mass spectral fragmentation pattern (Table 1). The presence of ions at m/z 147 ($\text{M}^+ - n\text{-BuBO}_2 - \text{C}_6\text{H}_5$) and 120 ($\text{M}^+ - n\text{-BuBO}_2 - \text{C}_6\text{H}_5 - \text{CH} - \text{CH}_2$) was consistent with a dihydroxylation occurring on ring B. BphAE_{LB400} generated only one of the two dihydrodiol metabolites, whereas BphAE_{p4} produced four dihydrodiol metabolites from flavanone. It produced the two metabolites resulting from the oxidation of ring B, but in addition, it produced two other dihydrodiols that could only result from a hydroxylation of ring A. The mass spectral fragmentation patterns of their butylboronate derivatives are shown in Table 1. The ions at m/z 192 ($\text{M}^+ - \text{C}_6\text{H}_5 - \text{C}_3\text{H}_3 - \text{O}$) and 176 ($\text{M}^+ - \text{C}_6\text{H}_5 - \text{C}_3\text{H}_3 - \text{O}_2$) resulting from the loss of the non-hydroxylated ring B (C_6H_5) provide evidence that the hydroxylation occurred on ring A. These data were confirmed by the GC-MS analysis of the trimethylsilyl derivatives of the metabolites, which evidenced the formation of two dihydrodiol metabolites from BphAE_{B356}, a single one from BphAE_{LB400}, and four dihydrodiol metabolites from BphAE_{p4} (not shown).

BphAE_{B356} and BphAE_{p4} metabolized, respectively, 70 nmol and 50 nmol of flavone when they were incubated with 100 nmol of this substrate for 10 min. However, BphAE_{LB400} performed very poorly on flavone, where less than 5% of the added substrate was degraded. As with flavanone, the pattern of metabolites produced from flavone differed significantly among the enzymes (Fig. 3B). Two metabolites were produced when the reaction was catalyzed by BphAE_{B356}, but their proportion differed considerably. Based on the mass spectral fragmentation features of their butylboronate derivatives shown in Table 1, they were identified as 2-(2,3-dihydro-2,3-dihydroxyphenyl)chromene-4-one and 2-(3,4-dihydro-3,4-dihydroxyphenyl)chromene-4-one. On the basis of the

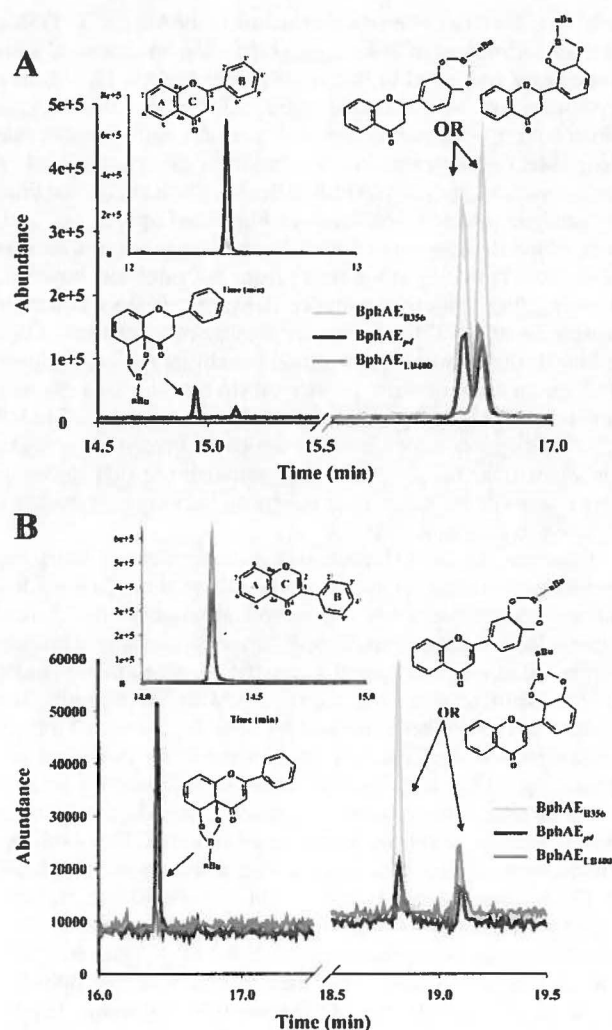


FIG 3 (A) Total ion chromatogram showing the peaks of metabolites produced from flavanone after 10 min by reconstituted His-tagged BphAE_{B356} (gray curve), BphAE_{LB400} (dark gray curve), and BphAE_{p4} (black curve). The inset shows the peak of the substrate remaining in the reaction vial. (B) Total ion chromatogram showing the peaks of metabolites produced from flavone after 10 min by reconstituted His-tagged BphAE_{B356} (gray curve), BphAE_{LB400} (dark gray curve), and BphAE_{p4} (black curve). The inset shows the peak of the substrate remaining in the reaction vial.

TABLE 1 Mass spectral features of the butylboronate-derived metabolites produced from flavanone and flavone by BphAE_{B356}, BphAE_{LB400}, and BphAE_{p4}

Substrate	No. of metabolites produced by:			Metabolite structure ^a	Oxidized ring	M ⁺	Other ions
	BphAE _{B356}	BphAE _{LB400}	BphAE _{p4}				
Flavanone	2	1	2	2-(2,3-Dihydro-2,3-dihydroxyphenyl)chromane-4-one or 2-(3,4-dihydro-3,4-dihydroxyphenyl)chromane-4-one	B	324	308, 267, 240, 224, 147, 120
			2	4a,5-Dihydro-4a,5-dihydroxy-2-phenylchromane-4-one	C	324	308, 267, 240, 224, 192, 176, 131
Flavone	2	1	2	2-(2,3-Dihydro-2,3-dihydroxyphenyl)chromene-4-one or 2-(3,4-dihydro-3,4-dihydroxyphenyl)chromene-4-one	B	322	306, 265, 238, 222, 210, 181, 120
			1	4a,5-Dihydro-4a,5-dihydroxy-2-phenylchromene-4-one	C	322	306, 265, 238, 222, 192, 163, 129

^a Structures were tentatively identified on the basis of their mass spectral fragmentation features and on the orientation of the docked substrates in the enzyme catalytic pocket.

docking experiments described below, the major metabolite would result from a hydroxylation of carbons 2'-3' to generate the 2-(2,3-dihydro-2,3-dihydroxyphenyl)chromene-4-one. BphAE_{p4} produced three metabolites from flavone (Fig. 3B). The GC-MS features of their butylboronate derivatives are shown in Table 1. Two of the metabolites are identical to those produced by BphAE_{B356}. The mass spectral features of the third one, which is a major metabolite, comprise ions at m/z 192 ($M^+ - C_6H_5 - C_3H - O$) and 163 ($M^+ - n\text{-BuB} - C_6H_5 - C_2H$) which are consistent with a hydroxylation on ring A. On the basis of the docking experiments described below, this metabolite would be 4a,5-dihydro-4a,5-dihydroxy-2-phenylchromene-4-one. BphAE_{LB400} produced trace amounts only of the metabolite corresponding to the peak of 2-(3,4-dihydro-3,4-dihydroxyphenyl)chromene-4-one.

As was the case for the previous two substrates, BphAE_{B356} performed better than the other two enzymes toward isoflavone. However, in this case, all three enzymes produced the same two metabolites from this flavonoid (Fig. 4). Both of them exhibited a fragmentation pattern comprising ions at m/z 181 ($M^+ - n\text{-BuBO}_2 - CO - CH$), 165 ($M^+ - n\text{-BuBO}_2 - CO - CH - O$), and 120 ($M^+ - n\text{-BuBO}_2 - C_6H_5 - C_2H$) that was consistent with a dihydroxylation of ring B.

Kinetic parameters of purified BphAE_{B356}, BphAE_{LB400}, and BphAE_{p4} toward flavone, flavanone, and isoflavone. The steady-state kinetic parameters of purified preparations of BphAE_{B356}, BphAE_{p4}, and BphAE_{LB400} toward each of the three flavonoids were calculated from the initial oxygen consumption using a Clark-type oxygraph. Notably, for the three substrates, the k_{cat} and k_{cat}/K_m values for BphAE_{B356} were in the range reported (20) for biphenyl (respectively, 4.3 s^{-1} and $63 \times 10^3 \text{ M}^{-1} \text{ s}^{-1}$) when this enzyme was used under the same reaction conditions (Table 2). Consistent with the whole-cell assays described above, flavanone was the best substrate, exhibiting k_{cat} and k_{cat}/K_m values that were significantly higher than those previously reported for biphenyl (Table 2). However, flavone and isoflavone were also good substrates for the enzyme since their kinetic parameters were in same range as those reported for biphenyl. Furthermore, for all substrates, the steady-state kinetic parameters of BphAE_{B356} were significantly higher than those for BphAE_{p4}. The reported k_{cat} and k_{cat}/K_m values of BphAE_{p4} toward biphenyl (1.0 s^{-1} and $31 \times 10^3 \text{ M}^{-1} \text{ s}^{-1}$) (23) were higher than for all three flavonoids. Therefore, although BphAE_{p4} performed well on these substrates, unlike

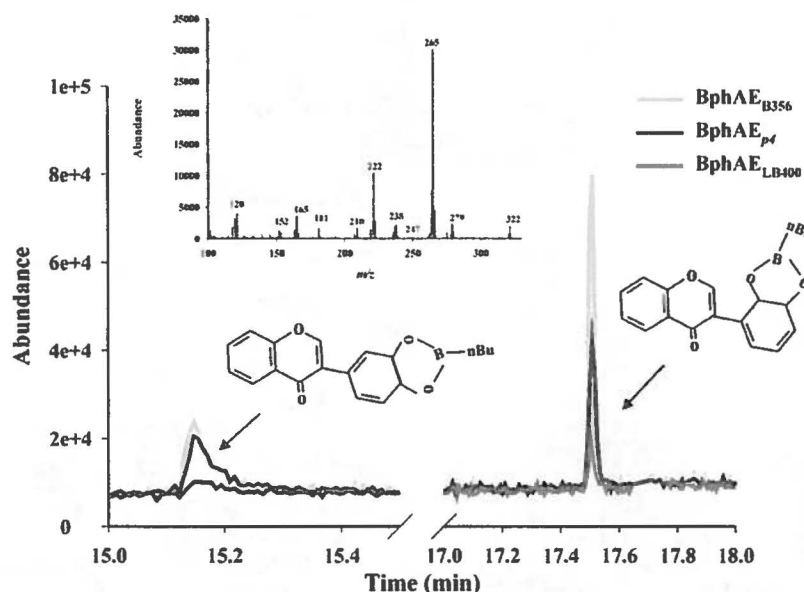


FIG 4 Total ion chromatogram showing the peaks of metabolites produced from isoflavone after 10 min by reconstituted His-tagged BphAE_{B356} (gray curve), BphAE_{LB400} (dark gray curve), and BphAE_{P4} (black curve). The inset shows the mass spectrum of the metabolite exhibiting a retention time of 17.5 min. The mass spectrum for the second metabolite is almost identical (not shown).

BphAE_{B356}, biphenyl remains a better substrate than the flavonoids. Consistent with the time point measurement experiments, BphAE_{LB400} was poorly active toward the three flavonoids. The steady-state kinetic parameters obtained with flavone and isoflavone were too low to be determined accurately and therefore are not reported here. Flavanone was the best substrate; the k_{cat} and k_{cat}/K_m values obtained with this substrate were significantly lower than the values reported when BphAE_{LB400} was used to metabolize biphenyl under identical conditions (respectively, 0.9 s^{-1} and $41 \times 10^3 \text{ M}^{-1} \text{ s}^{-1}$) (23). Together, these data show that in comparison to the activity of BphAE_{LB400}, the double Thr335Ala Phe336Met substitution in BphAE_{P4} contributed to enhancement of the catalytic activity toward the simple flavonoids. However, these mutations did not allow the enzyme to reach the level of activity of the naturally occurring BphAE_{B356}.

TABLE 2 Steady-state kinetic parameters of BphAE_{B356}, BphAE_{LB400}, and BphAE_{P4} toward flavanone, flavone, and isoflavone^a

Substrate, enzyme	K_m (μM)	k_{cat} (s^{-1})	k_{cat}/K_m ($10^3 \text{ M}^{-1} \text{ s}^{-1}$)
Flavanone			
BphAE _{B356}	77.5 ± 4.8	9.0 ± 0.4	116.1 ± 8.9
BphAE _{P4}	27.5 ± 5.7	0.60 ± 0.1	21.8 ± 4.0
BphAE _{LB400}	32.1 ± 3.9	0.36 ± 0.0	11.1 ± 1.3
Flavone			
BphAE _{B356}	121.4 ± 7.2	4.0 ± 1.3	32.9 ± 11.2
BphAE _{P4}	21.4 ± 1.4	0.08 ± 0.0	3.8 ± 0.1
Isoflavone			
BphAE _{B356}	15.8 ± 1.0	1.2 ± 0.0	75.9 ± 4.7
BphAE _{P4}	27.6 ± 0.3	0.59 ± 0.0	21.3 ± 0.0

^a The \pm standard deviations of the results for two independently produced enzyme preparations are shown.

Structural analysis of docked flavonoids at active sites of BphAE_{B356}, BphAE_{LB400}, and BphAE_{P4}. In order to identify the structural features of BphAE_{B356} and BphAE_{LB400} that explain why the two enzymes catalyze flavone, isoflavone, and flavanone oxidation differently, we docked these flavonoids at their active sites. Since previous reports showed that an induced-fit mechanism was required to bind the substrate productively inside the BPDO catalytic pocket (23), we docked the flavonoids in the substrate-bound form of the enzymes after removing biphenyl (or 2,6-dichlorobiphenyl in the case of BphAE_{P4}). When flavone was docked into BphAE_{B356}, consistent with the biochemical data, the conformation of the top-ranked docked molecule exhibited an orientation that would enable an oxygenation of ring B. Carbons 2' and 3' of ring B closely aligned with carbons 2 and 3 of the oxidized ring of biphenyl in the complexed form (Fig. 5A). This suggested that the major metabolite produced from flavone when BphAE_{B356} catalyzed the reaction would be 2-(2,3-dihydro-2,3-dihydroxyphenyl)chromene-4-one. Therefore, the regiospecificity of BphAE_{B356} toward flavone would be similar to that of the previously reported BphA1A2(2072) which was obtained by shuffling *bphA1* from *Pseudomonas alcaligenes* with *bphA* from *B. xenovorans* LB400 (32). In the case of BphAE_{LB400}, none of the docked substrate conformations exhibited a productive orientation toward the catalytic iron. This is consistent with the fact that the catalytic activity of BphAE_{LB400} toward this flavonoid was very low. When BphAE_{B356} docked with flavone was superposed to the biphenyl-bound form of BphAE_{LB400} (without biphenyl), the chromene oxo group of the docked molecule was at less than 3 Å from both Phe336 and Gly321 of BphAE_{LB400} (not shown). Therefore, the proximity of the chromene oxo group to these two residues probably prevents productive binding to BphAE_{LB400}.

Unlike the result for BphAE_{B356}, the conformation of the top-ranked docked flavone molecule in BphAE_{P4} was consistent with the observation that its major metabolite resulted from a dihy-

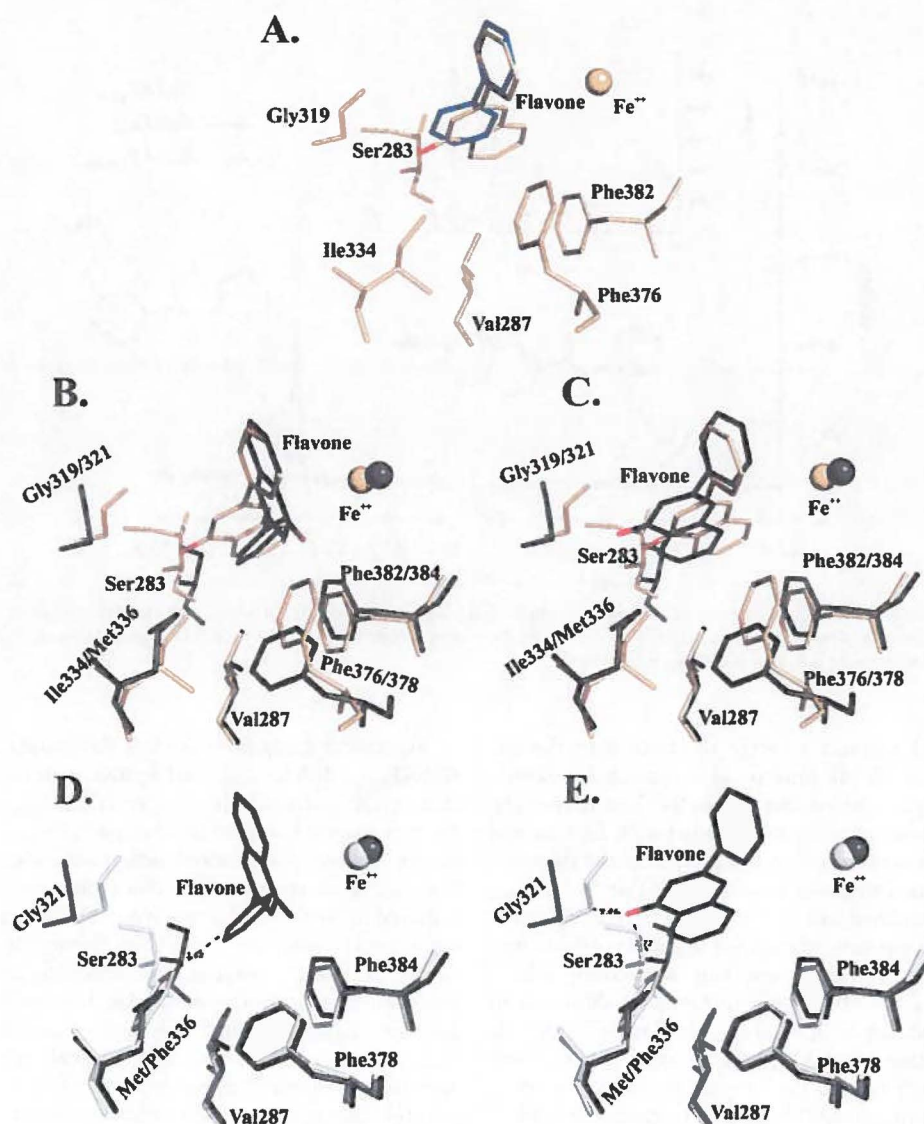


FIG 5 (A) Superposition of catalytic center residues of the flavone-docked (wheat) and biphenyl-bound (blue) forms of BphAE_{B356}. (B and C) Superposition of catalytic center residues of two flavone-docked forms of BphAE_{p4} (black) and the top-ranked flavone-docked form of BphAE_{B356} (wheat). (D and E) Superposition of catalytic center residues of two flavone-docked forms of BphAE_{p4} (black) and the biphenyl-bound form of BphAE_{L400} (white) after removal of biphenyl. The oxygen of the flavone oxo group is in red.

droxylation on ring A. On the basis of the orientation of ring A toward the catalytic Fe^{2+} in the docked form of BphAE_{p4}, the hydroxylation should occur onto carbons 4a and 5 to produce 4a,5-dihydro-4a,5-dihydroxy-2-phenyl chromene-4-one (Fig. 5B). Another of the 10 top-ranked conformations of flavone in BphAE_{p4}'s catalytic pocket was similar to but did not superpose exactly with the molecule docked in BphAE_{B356} (Fig. 5C). In a previous report, the ability of BphAE_{p4} to oxidize 2,6-dichlorobiphenyl on the *meta-para* and *ortho-meta* carbons of biphenyl was attributed to the fact that none of the C-2'-C-3' or C-3'-C-4' pairs of carbons were equidistant from the catalytic Fe^{2+} and they all were within 4.5 Å from it (18). A similar situation was obtained when flavone was docked in BphAE_{p4}. Carbons C-2' and C-3' of ring B were not equidistant from the catalytic Fe^{2+} , and they were

more distant from it than the corresponding atoms of flavone docked in BphAE_{B356} (Fig. 5C). This may explain why both 2-(2,3-dihydro-2,3-dihydroxyphenyl)chromene-4-one and 2-(3,4-dihydro-3,4-dihydroxyphenyl)chromene-4-one were produced and why these metabolites were produced in lesser amounts than when BphAE_{B356} catalyzed the reaction.

As shown in Fig. 5B, when flavone takes an orientation enabling an oxidation of ring A (in black), Phe376 of BphAE_{B356} is too close (1.5 Å) to the chromene oxo group to allow productive binding of this substrate. Therefore, this residue or others that modulate its conformation exert a strong influence on the regio-specificity of the enzyme toward flavone. In order to confirm that Phe336 and Gly321 prevent the binding of flavone to BphAE_{L400}, we superposed both docked conformations of flavone in BphAE_{p4}

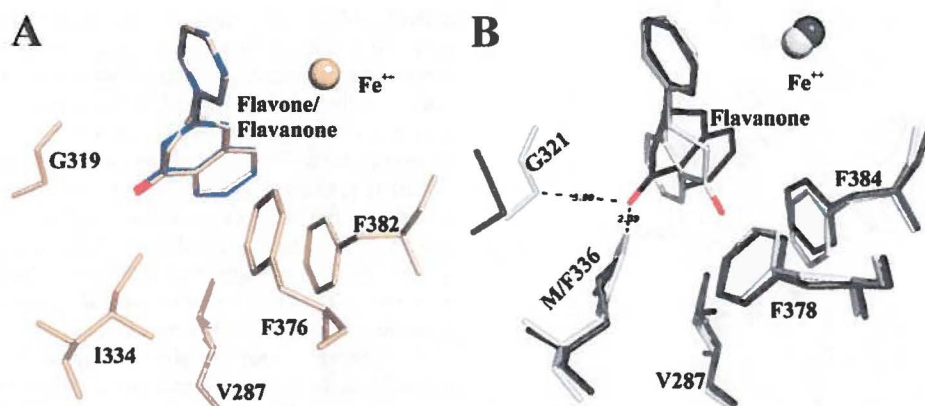


FIG 6 (A) Superposition of catalytic center residues of the flavanone-docked (wheat) and flavone-docked (blue) forms of BphAE_{B356}. (B) Superposition of catalytic center residues of the top-ranked flavanone-docked form of BphAE_{p4} (black) enabling the oxidation of ring B and the top-ranked flavanone-docked form of BphAE_{LB400} (white). The oxygen of the flavanone oxo group is in red.

with the biphenyl-bound form of BphAE_{LB400} after biphenyl removal. This is shown in Fig. 5D and E, where it is clear that for both conformations of the docked substrate in BphAE_{p4}, residues Gly321 and Phe336 of BphAE_{LB400} are both too close to the substrate to allow productive binding. Therefore, the Phe336Met and the Thr335Ala substitution are both required to facilitate flavone binding to BphAE_{p4}. However, as shown from the steady-state kinetic parameters of the enzymes, although BphAE_{p4} can metabolize flavone, its turnover rate of reaction is significantly lower than that of BphAE_{B356}. Therefore, although the two mutations that occurred in BphAE_{p4} enhanced its catalytic activity toward flavone, other structural features of BphAE_{B356} that are not present in BphAE_{p4} are required to facilitate the chemical steps in the catalytic oxygenation reaction. A structural comparison of the catalytic pockets of BphAE_{B356} and BphAE_{p4} identified Phe376/Phe378 and Ser283/Ile283 as likely candidates to explain the different catalytic properties of the two enzymes (Fig. 5).

In the flavanone docking experiment, both flavanone and flavone are placed at the same position in BphAE_{B356} where carbon 2' and 3' of ring B superposed almost perfectly with the reactive carbons of biphenyl (Fig. 6A). Biochemical analysis showed that BphAE_{B356} oxidized both the 2', 3' and 3', 4' carbons of ring B (Fig. 3A). Therefore, the binding of BphAE_{B356} to flavanone can induce other conformations of the substrate that the docking experiment could not reproduce. The docking experiment with BphAE_{p4} showed that flavanone can take an orientation where ring B superposes exactly with ring B of the docked molecule in BphAE_{B356} (not shown). However, similar to flavone docking and consistent with the biochemical data, flavanone can also be docked in BphAE_{p4} in an orientation that would enable a hydroxylation of ring A (not shown). As seen by the observations described above, although BphAE_{LB400} is not as efficient as BphAE_{p4} in oxidizing flavanone, its activity toward this substrate is more efficient than that toward flavone. Consistent with the biochemical data, automatic docking placed flavanone in an orientation that would allow an oxygenation of ring B by BphAE_{LB400}. Structural analysis shows that, unlike the results of the docking experiment done with BphAE_{p4}, in the case of BphAE_{LB400}, the chromane moiety of flavanone is oriented such that the oxo group of ring C is distanced from Phe336 and pulled toward Phe378 and Phe384 (Fig. 6B).

This shows that the chromane moiety of the molecule reacts differently than the chromene moiety of flavone with the surrounding atoms of the catalytic pocket of BphAE_{LB400}. However, the docking experiment has limitations, since it did not allow identification of the protein atoms of BphAE_{LB400} that interact with the chromane moiety of flavanone.

The isoflavone docking experiments are also in agreement with the biochemical data. Ring B of isoflavone superposes well with ring B of flavone in the top-ranked isoflavone-docked form of BphAE_{B356}. The docking experiment suggests that the major metabolite generated by the oxygenation of isoflavone would be 3-(2,3-dihydro-2,3-dihydroxyphenyl)chromene-4-one (Fig. 7A). In the case of BphAE_{p4}, it is not clear why the oxo group is flipped in the opposite orientation for the top-ranked form of isoflavone-docked BphAE_{p4} (Fig. 7B). There are no apparent constraints that would prevent isoflavone from taking the same conformation as in BphAE_{B356}. This shows that as for flavanone, other structural features that the docking experiment could not identify are likely to be involved in the binding process for this flavonoid. It is also interesting that automatic docking places isoflavone in a productive orientation for BphAE_{LB400} (Fig. 7C). However, in this case, unlike the case for BphAE_{p4}, the oxo group is in an orientation similar to that found in the isoflavone-docked BphAE_{B356}. Since isoflavone was a poor substrate for BphAE_{LB400}, it is likely that unidentified structural features that place isoflavone in the opposite orientation in BphAE_{p4} are required to enable the chemical reactions to proceed. Since in the docked form of BphAE_{B356}, the oxo group is at a distance of approximately 4 Å from Fe²⁺ and from the two His that coordinate it, the proximity of the oxo group to the iron may hinder the catalytic activity in BphAE_{LB400}. The iron is at the interface between two α subunits, and it was shown in a previous work that protein structures surrounding the catalytic iron move during binding and that these structures appeared to be involved in maintaining the integrity of the $\alpha_3\beta_3$ conformation of the enzyme (23). However, more structural analyses of the substrate-bound enzymes will be required to determine more precisely why BphAE_{LB400} has poor activity on isoflavone.

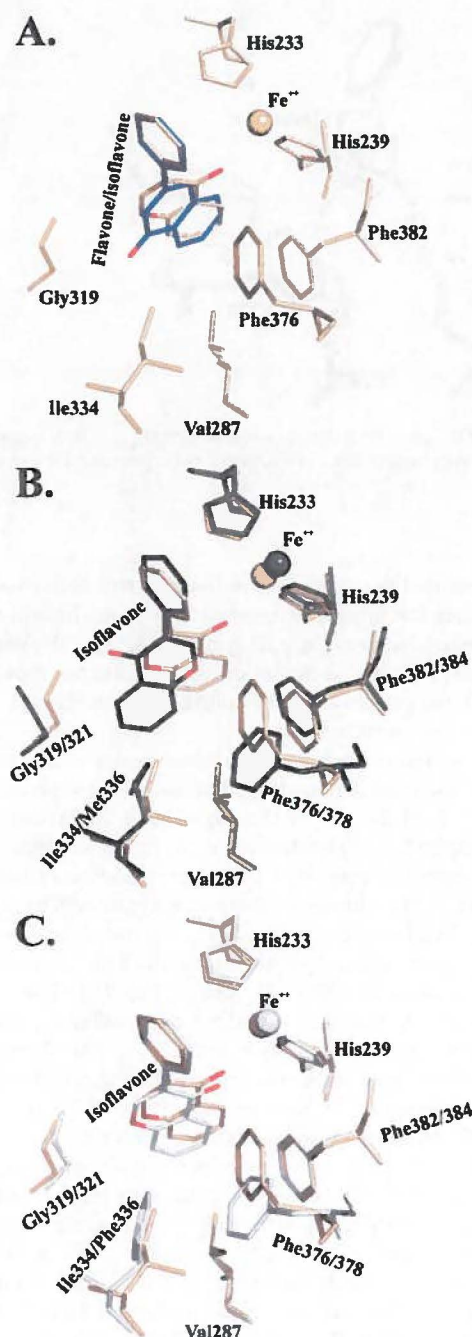


FIG 7 (A) Superposition of catalytic center residues of the top-ranked isoflavone-docked (wheat) and flavone-docked (blue) forms of BphAE_{B356}. (B) Superposition of catalytic center residues of the top-ranked isoflavone-docked forms of BphAE_{B400} (black) and of BphAE_{B356} (wheat). (C) Superposition of catalytic center residues of the top-ranked isoflavone-docked forms of BphAE_{LB400} (white) and of BphAE_{B356} (wheat). The oxygen of the flavanone oxo group is in red.

DISCUSSION

The perception of flavonoids by plant pathogens and their function as signals in the initiation of legume-rhizobium symbiosis have been well characterized (31). However, the potential impacts

of flavonoids on soil and rhizosphere bacteria that do not interact with plants directly in a host-pathogen or symbiotic interaction remain largely unknown. Better insight into this mechanism will help in understanding how plants promote PCB degradation in soil. Many investigations have identified plant secondary metabolites (flavonoids or terpenes) as likely candidates to trigger microbial degradation of PCBs in soil (34). Shaw et al. (31) have hypothesized that PSMs act to shape rhizosphere microbial community structure and, thus, they may have an impact on the rhizosphere function by triggering microbial pathways that can influence the quality and quantity of PSMs in soil. However, this hypothesis remains to be demonstrated.

In a previous report, we showed that the *R. erythropolis* U23A biphenyl catabolic pathway was induced by flavanone (37). In this work, we showed that isoflavone instead of flavanone was an inducer for the biphenyl catabolic pathway of *P. pinoenusa* strain B356, whereas none of the three flavonoids induced the biphenyl catabolic pathway of strain LB400. The observation that strains U23A, B356, and LB400 responded differently to simple flavonoids is consistent with divergent regulation mechanisms for their respective biphenyl catabolic operons. Strain LB400's *bph* operon is controlled by *orf0*, producing a positive regulator belonging to the GntR family, and by *bphR2*, producing a LysR-type regulator (5), whereas the biphenyl operons of *Rhodococcus globululus* P6 and *Rhodococcus jostii* RHA1 are regulated through a two-component regulatory system (19, 21). The regulation of strain U23A's *bph* operon is likely to be very similar to that of other rhodococci. The regulatory system of strain B356's *bph* operon has not yet been elucidated. However, a gene (*orf0B356*, GenBank accession number [JQ322530](https://www.ncbi.nlm.nih.gov/nuclot/JQ322530)) coding for a protein exhibiting 48% homology with BphS of *Cupriavidus oxalaticus* A5 (previously called *Cupriavidus necator* A5, *Alcaligenes eutrophus*, or *Ralstonia eutropha* A5) (25) and exhibiting homology with other members of the GntR family was found in the genome of strain B356 just upstream of *bphG*. Sequence alignment of this protein with other members of GntR family proteins showed it clustering with BphS of strain A5 and of *Pseudomonas* sp. strain KKS102 (not shown) which, unlike Orf0 of strain LB400, were found to be negative regulators (5, 27). The phylogenetic tree obtained when sequences of known BphAs from cultured and uncultured bacteria are aligned (38) shows three branches: two comprise principally Gram-negative proteobacteria, and one comprises exclusively high-GC-content Gram-positive bacteria of the rhodococcal group. It is noteworthy that BphAE_{B356} clusters with BphA1A2 of strain A5 and of strain KKS102, whereas BphAE_{LB400} belongs to a separate branch. The fact that a similar clustering of the phylogenetic tree is obtained for the deduced amino acid sequences of the regulatory protein and of the first enzyme of the biphenyl catabolic pathway of these strains highlights the possibility that the three biphenyl catabolic pathway clusters may have evolved to serve distinct functions in the environment.

In this work, in order to get more insight about how these pathways interact with simple flavonoids, we compared the metabolism of flavanone, flavone, and isoflavone by BphAE_{B356} and BphAE_{LB400}. Biochemical data showed that, unlike BphAE_{LB400}, BphAE_{B356} is well fitted to metabolize these PSMs. Structural analysis identified two features of BphAE_{LB400} that are responsible for the poor ability of the enzyme to metabolize these flavonoids. As observed in the case of 2,6-dichlorobiphenyl (9, 18) and in the case of DDT (20), Phe336 is too large to enable productive binding

with large substrates. In addition, the fact that Gly321 is constrained through a network of hydrogen bonding significantly hinders binding with these substrates (18). In a previous report, we showed that replacing Thr335 with Ala335 in BphAE_{LB400} relieved constraints on the Val320-Gly321-Gln322 segment, allowing for more movement during substrate binding. This feature enables BphAE_{p4} to accommodate bulkier substrates, such as 2,6-dichlorobiphenyl (18). Similar to Ala335 of BphAE_{p4}, the corresponding residue Gly333 of BphAE_{B356} is too short to form any contact with this segment (not shown). Therefore, Gly319 of BphAE_{B356} is more relaxed than Gly321 of BphAE_{LB400}, which explains in part why BphAE_{B356} can metabolize substrates such as 2,6-dichlorobiphenyl (9) or flavonoids that BphAE_{LB400} metabolizes poorly. However, other unidentified structural features influence binding to flavonoids. For example, it is noteworthy that BphAE_{LB400} was found to catalyze the oxidation of flavanone more efficiently than flavone. The superior properties of the enzyme toward flavanone were attributed to the fact that the oxo group of the chromane moiety was placed away from Phe336. This indicates that protein structures involved in the binding process interacted differently with the chromene and chromane moieties of the molecule.

This is also supported by the superior catalytic abilities of BphAE_{B356} compared to those of BphAE_{p4} toward flavanone, flavone, and isoflavone in spite of the fact that both BphAE_{B356} and BphAE_{p4} contain a smaller amino acid than Phe336 of BphAE_{LB400} at position 336 and, in addition, the fact that the correspondence of Gly321 of BphAE_{p4} to Gly319 of BphAE_{B356} is less constrained than that of Gly321 of BphAE_{LB400}. The docking experiments did not allow us to identify precisely the BphAE_{B356} structural features that conferred to the enzyme an ability superior to that of BphAE_{p4} to catalyze the reaction. In a previous report, it was shown that the helix between residues 282 and 288 moved considerably more toward the substrate during substrate binding with BphAE_{p4} than with BphAE_{LB400}. This movement was attributed to the Thr335Ala substitution that altered the intramolecular hydrogen bonding networks involving residues of this helix (18). It was suggested (9) that the mobile character of this helix may influence binding to substrates larger than biphenyls. Furthermore, residue 283 is at the entranceway of the catalytic pocket and both residue Ile283 of BphAE_{B356} and residue Ser283 of BphAE_{p4} are very close (less than 3 Å) to ring A of flavone (Fig. 5) in the flavone-docked enzyme. In the biphenyl-bound form of BphAE_{LB400}, Ser283 is far from the substrate. Although its precise role in substrate binding is not clear, residue 283 and the helix to which it belongs appear to be likely candidates for engineering enzymes exhibiting altered substrate specificity and regiospecificity toward flavonoids. However, we cannot exclude other residues that are not in contact with the substrate but that may influence substrate binding by other mechanisms. For example, in a recent report, residues 338 and 409 of BphAE_{LB400} were found to act synergistically to influence the catalytic properties of the enzyme by interacting with residues that are involved in subunit assembly and electron transport (23).

In previous reports, *E. coli* cells producing *P. alcaligenes* KF707 BPDO were found to catalyze the hydroxylation of flavone (16) and of flavanone (11). BphA1A2 from strain KF707 is more than 95% homologous to BphAE_{LB400}, except that like BphAE_{B356}, residue 335 (corresponding to Phe336 of BphAE_{LB400}) is an Ile and residue 334 (corresponding to Thr335 of BphAE_{LB400}) is an Ala. Therefore, with respect to their catalytic properties toward fla-

vonoids, the structural features of BphA1A2_{KF707} and BphAE_{p4} are expected to be comparable. However, a BphA1A2_{KF707} variant was obtained which exhibited enhanced activity toward flavonoids (15). This variant was obtained by the substitutions His255Gln, Val256Ile, Gly266Ala, and Phe277Tyr. It is not clear whether all these residues together or a combination of some of them were required to enhance the activity toward flavonoids. The likely involvement in substrate specificity and selectivity of the mobile loop between residues 240 and 260 that overhang the entranceway of the catalytic pocket has been discussed previously (18). In addition, the likely involvement of residues 266 and 267 in the catalytic properties of BphAE_{B356} toward DDT has also been discussed (20). Nevertheless, our data with BphAE_{B356} and BphAE_{LB400} and the data related to BphA1A2_{KF707} variants show the complexity of the substrate binding process, which involves interaction between the substrate and many protein atoms that either contact the substrate or modulate the conformation of protein structures that are required to enable a productive binding.

Altogether, our investigation identified residues that are involved in substrate binding with simple flavonoids and provided evidence that BphAE_{B356} has evolved to be better fitted than BphAE_{LB400} to metabolize these PSMs. Moreover, the fact that the biphenyl catabolic pathway of strain B356 was induced by isoflavone provides additional evidence supporting the hypothesis brought forward by Focht (8) and others (31) that the biphenyl catabolic pathways have evolved in bacteria to serve ecological functions, perhaps related to the metabolism of plant secondary metabolites in soil.

In this work, by singling out simple flavonoids and comparing the ability of two well-characterized biphenyl-degrading bacteria to metabolize them, we have shown that both the metabolism of flavonoids and the response to them as signal molecules to trigger the biphenyl catabolic pathway vary considerably among bacteria. This conclusion is significant for the development of more rational approaches for designing efficient rhizoremediation processes. Hence, our data imply that the efficiency of the process will depend on the choice of appropriate bacterial strains responding to the specific PSMs produced by the plants with which they are associated.

ACKNOWLEDGMENTS

This work was supported by the Natural Sciences and Engineering Research Council of Canada (NSERC) (grants RGPIN/39579-2007 and STPSC 356996-07)

REFERENCES

- Barriault D, Pelletier C, Hurtubise Y, Sylvestre M. 1997. Substrate selectivity pattern of *Comminomonas testosteroni* strain B-356 towards dichlorobiphenyls. *Int. Biodeterior. Biodegradation* 39:311-316.
- Barriault D, Sylvestre M. 2004. Evolution of the biphenyl dioxygenase BphA from *Burkholderia xenovorans* LB400 by random mutagenesis of multiple sites in region III. *J. Biol. Chem.* 279:47480-47488.
- Boyd DR, Bugg TDH. 2006. Arene *cis*-dihydrodiol formation: from biology to application. *Org. Biomol. Chem.* 4:181-192.
- Chun HK, et al. 2003. Biotransformation of flavone and flavanone by *Streptomyces lividans* cells carrying shuffled biphenyl dioxygenase genes. *J. Mol. Catal. B Enzym.* 21:113-121.
- Denef VJ, et al. 2004. Biphenyl and benzoate metabolism in a genomic context: outlining genome-wide metabolic networks in *Burkholderia xenovorans* LB400. *Appl. Environ. Microbiol.* 70:4961-4970.
- Erickson BD, Mondello FJ. 1992. Nucleotide sequencing and transcriptional mapping of the genes encoding biphenyl dioxygenase, a multicomponent polychlorinated-biphenyl-degrading enzyme in *Pseudomonas* strain LB400. *J. Bacteriol.* 174:2903-2912.

7. Ferraro DJ, Gakhar L, Ramaswamy S. 2005. Rieske business: structure-function of Rieske non-heme oxygenases. *Biochem. Biophys. Res. Commun.* 338:175–190.
8. Focht DD. 1995. Strategies for the improvement of aerobic metabolism of polychlorinated-biphenyls. *Curr. Opin. Biotechnol.* 6:341–346.
9. Gomez-Gil L, et al. 2007. Characterization of biphenyl dioxygenase of *Pandora phenomena* B-356 as a potent polychlorinated biphenyl-degrading enzyme. *J. Bacteriol.* 189:5705–5715.
10. Haddock JD, Gibson DT. 1995. Purification and characterization of the oxygenase component of biphenyl 2,3-dioxygenase from *Pseudomonas* sp. strain LB400. *J. Bacteriol.* 177:5834–5839.
11. Han J, et al. 2005. Epoxide formation on the aromatic B ring of flavanone by biphenyl dioxygenase of *Pseudomonas pseudoalcaligenes* KF707. *Appl. Environ. Microbiol.* 71:5354–5361.
12. Hurtubise Y, Barriault D, Sylvestre M. 1995. Purification and characterization of the *Comamonas testosteroni* B-356 biphenyl dioxygenase components. *J. Bacteriol.* 177:6610–6618.
13. Hurtubise Y, Barriault D, Sylvestre M. 1996. Characterization of active recombinant his-tagged oxygenase component of *Comamonas testosteroni* B-356 biphenyl dioxygenase. *J. Biol. Chem.* 271:8152–8156.
14. Imbeault NY, Powlowski JB, Colbert CL, Bolin JT, Eltis LD. 2000. Steady-state kinetic characterization and crystallization of a polychlorinated biphenyl-transforming dioxygenase. *J. Biol. Chem.* 275:12430–12437.
15. Kagami O, et al. 2008. Protein engineering on biphenyl dioxygenase for conferring activity to convert 7-hydroxyflavone and 5,7-dihydroxyflavone (chrysin). *J. Biosci. Bioeng.* 106:121–127.
16. Kim SY, et al. 2003. *cis*-2',3'-Dihydrodiol production on flavone B-ring by biphenyl dioxygenase from *Pseudomonas pseudoalcaligenes* KF707 expressed in *Escherichia coli*. *Antonie Van Leeuwenhoek* 84:261–268.
17. Kumar P, et al. 2011. Anaerobic crystallization and initial X-ray diffraction data of biphenyl 2,3-dioxygenase from *Burkholderia xenovorans* LB400: addition of agarose improved the quality of the crystals. *Acta Crystallogr. Sect. F Struct. Biol. Cryst. Commun.* 67:59–62.
18. Kumar P, et al. 2011. Structural insight into the expanded PCB-degrading abilities of a biphenyl dioxygenase obtained by directed evolution. *J. Mol. Biol.* 405:531–547.
19. Labbe D, Garnon J, Lau PCK. 1997. Characterization of the genes encoding a receptor-like histidine kinase and a cognate response regulator from a biphenyl/polychlorobiphenyl-degrading bacterium, *Rhodococcus* sp. strain M5. *J. Bacteriol.* 179:2772–2776.
20. L'Abbée JB, Tu YB, Barriault D, Sylvestre M. 2011. Insight into the metabolism of 1,1,1-trichloro-2,2-bis(4-chlorophenyl)ethane (DDT) by biphenyl dioxygenases. *Arch. Biochem. Biophys.* 516:35–44.
21. Masai E, et al. 1995. Characterization of biphenyl catabolic genes of gram-positive polychlorinated biphenyl degrader *Rhodococcus* sp. strain RHA1. *Appl. Environ. Microbiol.* 61:2079–2085.
22. Misawa N, et al. 2005. Synthesis of vicinal diols from various arenes with a heterocyclic, amino or carboxyl group by using recombinant *Escherichia coli* cells expressing evolved biphenyl dioxygenase and dihydrodiol dehydrogenase genes. *Tetrahedron* 61:195–204.
23. Mohammadi M, et al. 2011. Retuning Rieske-type oxygenases to expand substrate range. *J. Biol. Chem.* 286:27612–27621.
24. Morris GM, et al. 2009. AutoDock4 and AutoDockTools4: automated docking with selective receptor flexibility. *J. Comput. Chem.* 30:2785–2791.
25. Mouz S, Merlin C, Springael D, Toussaint A. 1999. A GntR-like negative regulator of the biphenyl degradation genes of the transposon Tn4371. *Mol. Gen. Genet.* 262:790–797.
26. Nichenametla SN, Taruscio TG, Barney DL, Exon JH. 2006. A review of the effects and mechanisms of polyphenolics in cancer. *Crit. Rev. Food Sci. Nutr.* 46:161–183.
27. Ohtsubo Y, et al. 2001. BphS, a key transcriptional regulator of bph genes involved in polychlorinated biphenyl/biphenyl degradation in *Pseudomonas* sp. KKS102. *J. Biol. Chem.* 276:36146–36154.
28. Parnell JJ, Deneff VJ, Park J, Tsoi T, Tiedje JM. 2010. Environmentally relevant parameters affecting PCB degradation: carbon source- and growth phase-mitigated effects of the expression of the biphenyl pathway and associated genes in *Burkholderia xenovorans* LB400. *Biodegradation* 21:147–156.
29. Seeger M, et al. 2003. Biotransformation of natural and synthetic isoflavonoids by two recombinant microbial enzymes. *Appl. Environ. Microbiol.* 69:5045–5050.
30. Seo J, et al. 2010. Location of flavone B-ring controls regioselectivity and stereoselectivity of naphthalene dioxygenase from *Pseudomonas* sp. strain NCIB 9816-4. *Appl. Microbiol. Biotechnol.* 86:1451–1462.
31. Shaw LJ, Morris P, Hooker JE. 2006. Perception and modification of plant flavonoid signals by rhizosphere microorganisms. *Environ. Microbiol.* 8:1867–1880.
32. Shindo K, et al. 2003. Enzymatic synthesis of novel antioxidant flavonoids by *Escherichia coli* cells expressing modified metabolic genes involved in biphenyl catabolism. *J. Mol. Catal. B Enzym.* 23:9–16.
33. Shindo K, et al. 2005. Biocatalytic synthesis of monocyclic arene-dihydrodiols and -diols by *Escherichia coli* cells expressing hybrid toluene/biphenyl dioxygenase and dihydrodiol dehydrogenase genes. *J. Mol. Catal. B Enzym.* 35:134–141.
34. Singer A. 2006. The chemical ecology of pollutant biodegradation. Bioremediation and phytoremediation from mechanistic and ecological perspectives, p 5–19. In Mackova M, Dowling DN, Macek T (ed), *Phytoremediation and rhizoremediation. Theoretical background*. Springer, Dordrecht, Netherlands.
35. Stangl V, Lorenz M, Stangl K. 2006. The role of tea and tea flavonoids in cardiovascular health. *Mol. Nutr. Food Res.* 50:218–228.
36. Sylvestre M, et al. 1996. Sequencing of *Comamonas testosteroni* strain B-356-biphenyl/chlorobiphenyl dioxygenase genes: evolutionary relationships among Gram-negative bacterial biphenyl dioxygenases. *Gene* 174:195–202.
37. Toussaint JP, Pham TTM, Barriault D, Sylvestre M. 28 December 2011. Plant exudates promote PCB degradation by a rhodococcal rhizobacteria. *Appl. Microbiol. Biotechnol.*
38. Vézina J, Barriault D, Sylvestre M. 2008. Diversity of the C-terminal portion of the biphenyl dioxygenase large subunit. *J. Mol. Microbiol. Biotechnol.* 15:139–151.

Has the Bacterial Biphenyl Catabolic Pathway Evolved Primarily To Degrade Biphenyl? The Diphenylmethane Case

Thi Thanh My Pham, Michel Sylvestre

Institut National de la Recherche Scientifique, INRS-Institut Armand-Frappier, Laval, Quebec, Canada

In this work, we have compared the ability of *Pandoraea pnomenusa* B356 and of *Burkholderia xenovorans* LB400 to metabolize diphenylmethane and benzophenone, two biphenyl analogs in which the phenyl rings are bonded to a single carbon. Both chemicals are of environmental concern. *P. pnomenusa* B356 grew well on diphenylmethane. On the basis of growth kinetics analyses, diphenylmethane and biphenyl were shown to induce the same catabolic pathway. The profile of metabolites produced during growth of strain B356 on diphenylmethane was the same as the one produced by isolated enzymes of the biphenyl catabolic pathway acting individually or in coupled reactions. The biphenyl dioxygenase oxidizes diphenylmethane to 3-benzylcyclohexa-3,5-diene-1,2-diol very efficiently, and ultimately this metabolite is transformed to phenylacetic acid, which is further metabolized by a lower pathway. Strain B356 was also able to cometabolize benzophenone through its biphenyl pathway, although in this case, this substrate was unable to induce the biphenyl catabolic pathway and the degradation was incomplete, with accumulation of 2-hydroxy-6,7-dioxo-7-phenylheptanoic acid. Unlike strain B356, *B. xenovorans* LB400 did not grow on diphenylmethane. Its biphenyl pathway enzymes metabolized diphenylmethane, but they poorly metabolize benzophenone. The fact that the biphenyl catabolic pathway of strain B356 metabolized diphenylmethane and benzophenone more efficiently than that of strain LB400 brings us to postulate that in strain B356, this pathway evolved divergently to serve other functions not related to biphenyl degradation.

Many investigations have shown that the bacterial biphenyl catabolic pathway enzymes, especially biphenyl dioxygenase (BPDO), which initiates the degradation process, are very versatile (1). The biphenyl pathway, also called the upper pathway, comprises four enzymatic steps that transform biphenyl into benzoic acid, which is further metabolized by a lower pathway (Fig. 1).

Aside from its ability to metabolize polychlorinated biphenyls (PCBs) (1), BPDO metabolizes many biphenyl analogs (2–7) to generate hydroxylated aromatics. BPDO is composed of three components (Fig. 1). The catalytic component, which is a Rieske-type dioxygenase (RO) (BphAE), is a heterohexamer made up of three α (BphA) and three β (BphE) subunits. The other two components are ferredoxin (BphF) and ferredoxin reductase (BphG), both of which are involved in electron transfer from NADH to BphAE. The catalytic center of the enzyme is located on the C-terminal portion of the BphAE α subunit, which also carries the major structural determinants for substrate specificity (8). There are three phylogenetically distinct clusters of BphAEs (9–11), and the structure of a representative BphAE (also called BphA1A2) from each of these three clusters has now been elucidated. Thus, the Protein Data Bank (PDB) coordinate file for *Burkholderia xenovorans* LB400 BphAE (BphAE_{LB400}) is available (8), as are those for *Pandoraea pnomenusa* B356 BphAE (BphAE_{B356}) (12) and *Rhodococcus jostii* RHA1 BphA1A2 (BphA1A2_{RHA1}) (13).

BphAE_{LB400} has been thoroughly investigated, because *B. xenovorans* LB400 is considered one of the best PCB degraders (8). However, recent studies have shown that BphAE_{B356} metabolizes flavone, isoflavone, and flavanone (14), as well as 2,6-dichlorobiphenyl (15) and 1,1,1-trichloro-2,2-bis(4-chlorophenyl)ethane (DDT) (16), significantly more efficiently than BphAE_{LB400}. In this work, we compared the abilities of strain LB400 and B356 BPDOs and of further enzymes of their biphenyl catabolic pathway to metabolize two biphenyl analogs (diphenylmethane and benzophenone) in which two phenyl rings are bonded to a single

carbon. Both are chemicals of environmental importance. According to the U.S. Environmental Protection Agency, in 2003, benzophenone was classified as a high-volume chemical, with an annual production exceeding 450,000 kg (<http://toxnet.nlm.nih.gov/>). Benzophenone is widely used as a photoinitiator (17). Hydroxybenzophenones are useful building blocks for chemical syntheses, and they are also used as photosensitizers (17). Benzophenones and their xanthone analogs are common plant metabolites with medicinal properties (18), but because of their high demand, they are synthesized industrially. A major synthetic process is through atmospheric oxidation of diphenylmethane in the presence of metal catalysts (17). Aside from being a precursor for benzophenones, diphenylmethane and many of its analogs are used in various other industrial applications. The benzhydryl motif is a fundamental component in antiallergenic agents. It is also a component of hexachlorophene and DDT, and diphenylmethane diisocyanate is a major component of polyurethane. However, very few investigations have addressed the bacterial degradation of diphenylmethane (19, 20) or benzophenone (21). Focht and Alexander (22) have described a *Hydrogenomonas* isolate that grew on diphenylmethane and was able to cometabolize benzophenone and several related chlorinated analogs. However, the ability of this isolate to metabolize biphenyl has not been examined. More recently, Misawa et al. (19) have shown that *Pseudomonas alcali-*

Received 7 February 2013 Accepted 30 May 2013

Published ahead of print 7 June 2013

Address correspondence to Michel Sylvestre, Michel.Sylvestre@iaf.inrs.ca.

Supplemental material for this article may be found at <http://dx.doi.org/10.1128/JB.00161-13>.

Copyright © 2013, American Society for Microbiology. All Rights Reserved.

doi:10.1128/JB.00161-13

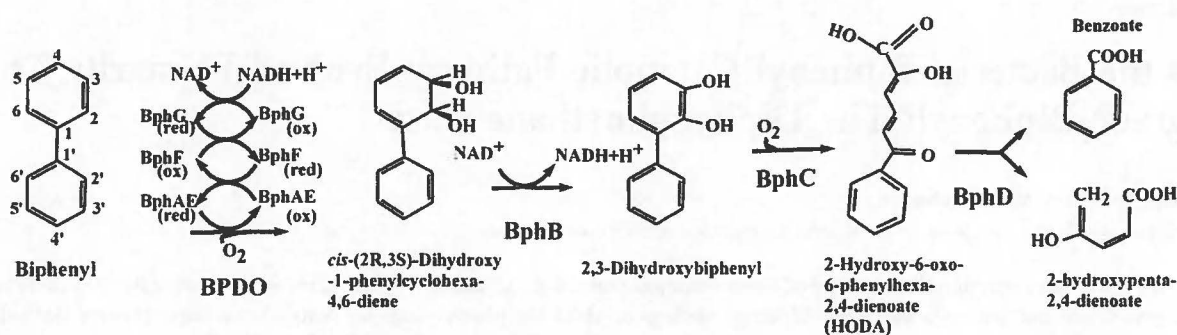


FIG 1 Biphenyl catabolic pathway enzymes and metabolites.

genes KF707 BPDO and variants derived from it were able to metabolize diphenylmethane. However, the metabolites produced have not been identified, and the steady-state kinetics of these BPDOs toward diphenylmethane were not determined. On the other hand, the ability of BPDO to metabolize benzophenone has never been examined.

While examining the ability of the biphenyl catabolic enzymes of *P. pnomenusa* B356 and of *B. xenovorans* LB400 to metabolize these two chemicals, we unexpectedly found that strain B356 grows well on diphenylmethane. In this context, we further investigated diphenylmethane metabolism by strain B356, and we obtained evidence that during growth of the strain on either biphenyl or diphenylmethane, both substrates are metabolized by the same catabolic pathway. This led us to postulate that in strain B356, the biphenyl catabolic pathway evolved to serve other functions not related to biphenyl degradation.

MATERIALS AND METHODS

Bacterial strains, plasmids, chemicals, and general protocols. *Escherichia coli* DH11S (23) and *E. coli* C41(DE3) (24) were used in this study. Wild-type strains *P. pnomenusa* B356 and *B. xenovorans* LB400 were described previously (25, 26). BphAE_{p4} is a mutant of BphAE_{LB400}, described previously (8), which was obtained by substitution at two residues, Thr335Ala and Phe336Met. This mutant exhibits an expanded substrate range compared to that of the parent enzyme. Most plasmids used in this study were described previously and are listed in Table 1. Plasmids pET14b[B356-bphF] and pET14b[B356-bphG] carry the genes encoding BphF_{B356} and BphG_{B356}, respectively, and they were prepared by subcloning the respective genes from pQE31[B356-bphF] and pQE31[B356-bphG] (27) into pET14b. The culture media used were Luria-Bertani (LB)

broth (28), basal medium M9 (28), or minimal mineral medium 30 (MM30) (29) amended with various sources of carbon and antibiotics, depending on the experiment. DNA general protocols were done according to Sambrook et al. (28). Diphenylmethane and benzophenone (99% pure) were from Sigma-Aldrich.

Assays to assess ability of diphenylmethane and benzophenone to support growth of strains B356 and LB400 and to induce their biphenyl catabolic pathway. Induction of the biphenyl catabolic pathway of strains B356 and LB400 by diphenylmethane and benzophenone was assessed by monitoring the amount of 4-chlorobenzoate produced from 4-chlorobiphenyl as described previously (14). We also evaluated the ability of wild-type strains B356 and LB400 to grow on diphenylmethane or benzophenone as the sole growth substrate. Cells grown overnight in LB broth were washed twice in MM30 and suspended in MM30 basal medium to an optical density at 600 nm (OD₆₀₀) of 0.5. This cell suspension was used (100 μl) to inoculate 20 ml of MM30 containing 2 mM biphenyl or diphenylmethane. The cultures were incubated with shaking at 28°C. Cell growth was monitored by determining the CFU. We also used the Bioscreen C system (Growth Curves USA, Piscataway, NJ) to compare the growth kinetics of strain B356 according to the substrate diphenylmethane or biphenyl. In order to prepare the inocula for the Bioscreen C experiments, cells were grown on 1 mM diphenylmethane or biphenyl or on 30 mM sodium acetate for 16 to 18 h, they were washed twice in MM30, and the cells were suspended in the same medium to an OD₆₀₀ of 0.08. Each well of the Bioscreen C microplate contained 237.5 μl of MM30 supplemented with 1 mM biphenyl or diphenylmethane added in 30 μl dimethyl sulfoxide (DMSO) or 30 mM sodium acetate added in 30 μl water, and they were inoculated with 12.5 μl of the suspension described above. A series of cultures also contained 3-chlorobenzoic acid (2 mM) or 3-chlorocatechol (0.2 mM), each added in 5 μl DMSO. Control cultures with no substrate and uninoculated cultures were also run in the experiments. The cultures were incubated at 28°C and set at low revolution. Both biphenyl and diphenylmethane are poorly soluble in water, but when added at a concentration of 1 mM, the nonsoluble portion of the substrate did not interfere with the OD readings during the Bioscreen C experiments. Each set of cultures was run in triplicate. Growth was also monitored by determining the CFU at various intervals of time during the Bioscreen C experiments.

Analysis of the metabolites produced from diphenylmethane and benzophenone by strains B356 and LB400 and by enzymes of their biphenyl catabolic pathway. The metabolites produced during growth of strain B356 on 2 mM diphenylmethane in 20 ml MM30 were extracted with ethyl acetate at neutral pH and at pH 4 from the supernatant of 22-h-old cultures. They were then treated with butylboronate (nBuB) or *N,O*-bis-trimethylsilyl trifluoroacetamide (TMS) for gas chromatography-mass spectrometry (GC-MS) analyses according to previously described protocols (30). A similar protocol was used to examine the metabolites produced from benzophenone by biphenyl-induced cells of strain B356. However, in this case, the cells were grown on biphenyl to

TABLE 1 Plasmids used in the study

Plasmid	Protein(s) expressed	Reference or source
pET14b[LB400-bphAE]	BphAE _{LB400}	8
pET14b[p4-bphAE]	BphAE _{p4}	8
pET14b[B356-bphAE]	BphAE _{B356}	16
pQE31[B356-bphAE]	BphAE _{B356}	16
pDB31[LB400-bphFG]	BphF _{LB400} , BphG _{LB400}	47
pYH31[LB400-bphFGBC]	BphF _{LB400} , BphG _{LB400} , BphB _{LB400}	48
pET14b[B356-bphF]	BphF _{B356}	This study
pET14b[B356-bphG]	BphG _{B356}	This study
pET14b[B356-bphB]	BphB _{B356}	49
pQE31[B356-bphC]	BphC _{B356}	35

reach log phase, and then they were suspended at an OD₆₀₀ of 3.0 in M9 medium and incubated at 28°C and 100 rpm for 60 min in the presence of 0.2 mM benzophenone.

Metabolites from diphenylmethane and benzophenone also were analyzed from suspensions of isopropyl β-D-1-thiogalactopyranoside (IPTG)-induced whole cells of *E. coli*[pDB31 B356-*bphFG*] or *E. coli*[pYH31 LB400-*bphFGBC*] also harboring pQE31[B356-*bphAE*] or pQE31[LB400-*bphAE*] according to a previously published protocol (30). The induced cells were suspended at an OD₆₀₀ of 5.0 in 50 mM sodium phosphate buffer, pH 7.0, and the metabolites generated after 30 min of incubation at 37°C were extracted and analyzed by GC-MS.

GC-MS analyses were performed using a Hewlett Packard HP6980 series gas chromatograph interfaced with an HP5973 mass selective detector (Agilent Technologies). The mass selective detector was operated in electron impact (EI) mode and used a quadrupole mass analyzer. Under these conditions, the instrument resolution is 0.1 atomic mass units, which is sufficient to clearly distinguish between two compounds of atomic masses differing by a single atomic mass unit.

Assays to identify diphenylmethane and benzophenone metabolites produced from BphAE_{B356}, BphAE_{LB400}, and BphAE_{pd} and to determine their steady-state kinetics. Reconstituted His-tagged BPDO preparations were used in these experiments. His-tagged purified enzyme components were produced and purified by following protocols published previously (31). The enzyme assays were performed in a volume of 200 μl in 50 mM morpholineethanesulfonic (MES) buffer, pH 6.0, at 37°C as described previously (32). For metabolite analyses, the reaction medium was incubated for 10 min and the metabolites were extracted at pH 6.0 with ethyl acetate, and then they were treated with nBuB or TMS for GC-MS analyses as described above. The steady-state kinetics were determined by recording the oxygen consumption rates according to a protocol described previously, using a Clarke-type Hansatech model DW1 oxygraph (33). They were determined from three separately prepared purified preparations of the enzymes.

Purification and NMR analysis of 2,2',3,3'-tetrahydroxybenzophenone. 2,2',3,3'-Tetrahydroxybenzophenone was prepared using a coupled reaction composed of His-tagged purified preparations of B356 BPDO (BphAEFG_{B356}) plus BphB_{B356}. Each enzyme reaction mixture contained 50 nmol benzophenone, 0.6 nmol of each B356 BPDO component (BphAE_{B356}, BphF_{B356}, and BphG_{B356}), 2 nmol BphB_{B356}, 100 nmol NADH, and 100 nmol NAD in 200 μl (total volume) of 50 mM MES buffer (pH 6.0). The mixture was incubated for 15 min at 37°C and then extracted at pH 6.0 with ethyl acetate. The extract was concentrated 20-fold by evaporation under a stream of nitrogen, and this preparation was injected into an XDB-C8 column (4.6 by 150 mm). The column was eluted at 1 ml/min with a linear gradient starting from 80% high-performance liquid chromatography (HPLC)-grade water with 0.085% orthophosphoric acid and 20 to 50% acetonitrile at 12 min. The detector was set at a wavelength of 280 nm. The peak of the metabolite was collected, the solution was immediately adjusted to pH 6.0 with 0.1 M NaOH, and the metabolite was extracted with ethyl acetate. Its identity and purity were verified by GC-MS analysis of its TMS derivative before running the nuclear magnetic resonance (NMR) analysis. The NMR spectra were obtained at the Quebec/Eastern Canada High Field NMR Facility at McGill University (Montreal, Quebec, Canada) with a Bruker 500-MHz spectrometer. The analyses were carried out in deuterated acetone at room temperature.

Docking and structure analysis. Dimer AB of BphAE_{LB400} (RCBS Protein Data Bank [PDB] entry 2XRX) and of BphAE_{B356} (PDB entry 3GZX) were used as protein targets, and they were prepared as previously described (16). Ligands all were downloaded as sdf files from PubChem (<http://pubchem.ncbi.nlm.nih.gov>) and converted into pdb format in Discover Studio Visualizer 2.5. Both proteins and ligands were processed with AutoDockTools to obtain their proper pdbqt format. The searching space for the ligand was centered on mononuclear iron and contained 20

Å in each x, y, and z direction. Autodock 4 (34) with default parameters was used to perform the automatic docking.

RESULTS

Growth of *P. pnomenusa* B356 and *B. xenovorans* LB400 on diphenylmethane and benzophenone. Neither *P. pnomenusa* B356 nor *B. xenovorans* LB400 grew when benzophenone was used as the sole growth substrate. Using a previously described 4-chlorobiphenyl conversion assay (14), we showed that benzophenone was unable to induce the biphenyl catabolic pathway of both strains. Similarly, diphenylmethane did not serve as the growth substrate for strain LB400 and did not induce its biphenyl catabolic pathway. However, remarkably, strain B356 grew very well in MM30 containing 2 mM diphenylmethane as the sole growth substrate. Under those conditions, CFU values of up to 4×10^9 cells/ml were obtained within 36 h at 28°C. In addition, using the 4-chlorobiphenyl conversion assay (14), we found that a suspension of log-phase cells grown on 2 mM diphenylmethane and adjusted to an OD₆₀₀ of 1.0 produced 329 ± 20 μM 4-chlorobenzoate from 1.25 mM 4-chlorobiphenyl after 2 h of incubation. In comparison, a resting suspension of log-phase cells of strain B356 grown on 2 mM biphenyl and tested under the same conditions produced 330 ± 17 μM 4-chlorobenzoate. This suggested that the biphenyl catabolic pathway of B356 was induced during growth on diphenylmethane. Using the Bioscreen C system, we have compared the growth kinetics of strain B356 according to the substrate used, biphenyl or diphenylmethane. In addition, we have determined the effect of interchanging the growth substrate on growth kinetics (biphenyl or diphenylmethane) to prepare the inocula. Results shown in Fig. 2 clearly demonstrate that strain B356 grows as well on diphenylmethane as on biphenyl, sometimes even better. Furthermore, replacing diphenylmethane with biphenyl to prepare the inoculum for the Bioscreen C experiments did not affect significantly the growth kinetics on diphenylmethane; the lag phases were identical and the growth rates were similar (0.35 ± 0.01 h⁻¹ and 0.34 ± 0.02 h⁻¹ for diphenylmethane- or biphenyl-induced cells, respectively). Likewise, when biphenyl was used as the growth substrate, the lag phases were very similar whether the inocula were prepared by growing the cells on biphenyl or diphenylmethane, and the growth rates were identical (0.25 ± 0.02 h⁻¹). Conversely, when cells were grown on sodium acetate to prepare the inoculum, the cells grew very poorly whether the Bioscreen C experiments were run using biphenyl or diphenylmethane as the substrate (Fig. 2), exhibiting long lag phases and low growth rates (0.14 h⁻¹), and the CFU count did not exceed 5×10^7 cells/ml at the end of the log phase. We have no data explaining why B356 grew better on diphenylmethane than on biphenyl. This result shows that the combined upper and lower pathways metabolized diphenylmethane more efficiently than biphenyl. However, the facts that interchanging the substrates to prepare the inocula for the Bioscreen C experiments did not affect the growth kinetics and did not prolong the lag phase provide strong evidence that the two substrates were degraded by the same pathway, which they both induced.

As further evidence that growth on diphenylmethane proceeded through the biphenyl catabolic pathway, we examined the effect of adding 3-chlorocatechol and 3-chlorobenzoate to the growth medium. In the Bioscreen C experiments, 0.2 mM 3-chlorocatechol completely inhibited growth of strain B356 on both biphenyl and diphenylmethane (data not shown). In a previous

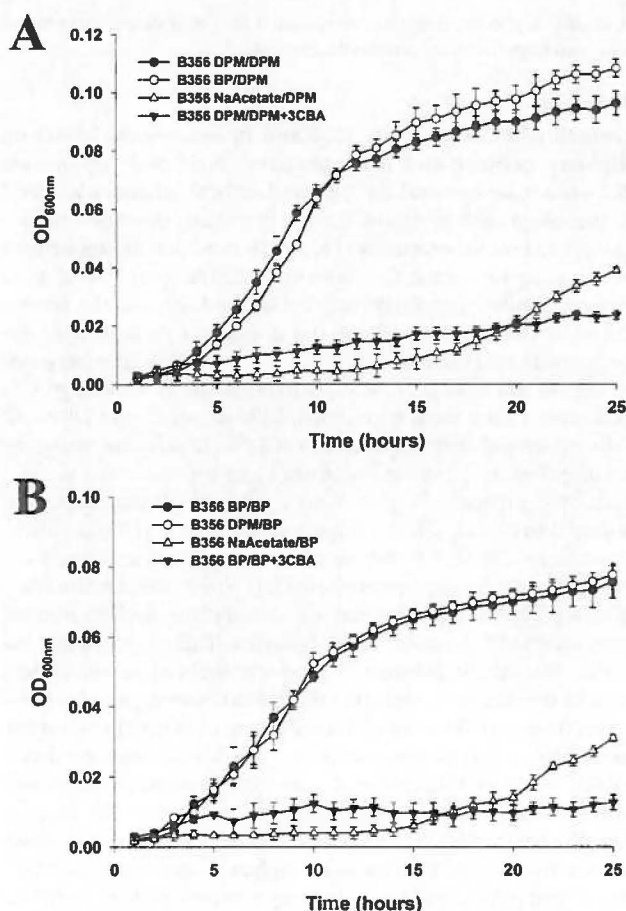


FIG 2 Growth curves of strain B356 on diphenylmethane when the inocula were prepared by growing the cells on either diphenylmethane (DPM/DPM), biphenyl (BP/DPM), or sodium acetate (NaAcetate/DPM) (A) or on biphenyl when the inocula were prepared by growing the cells on either biphenyl (BP/BP), diphenylmethane (DPM/BP), or sodium acetate (NaAcetate/BP) (B). A growth curve also was obtained for cells pregrown on diphenylmethane and then grown on diphenylmethane plus 3-chlorobenzoate (DPM/DPM + 3CBA) or cells pregrown on biphenyl and then grown on biphenyl plus 3-chlorobenzoate (BP + 3CBA). The growth curves were obtained using a Bioscreen C system as described in Materials and Methods.

work, we showed that B356 BphC is very sensitive to 3-chlorocatechol (35), and its presence in the growth medium strongly inhibits biphenyl metabolism (36).

It is also noteworthy that in the Bioscreen C experiments, when 3-chlorobenzoate (2 mM) was added as a cosubstrate, cell growth was strongly inhibited (Fig. 2). The same inhibition was observed whether the cells were pregrown on diphenylmethane or biphenyl or whether the Bioscreen C experiments were run using biphenyl or diphenylmethane as the substrate. This inhibition was not observed when the Bioscreen C experiments were run using sodium acetate as the growth substrate (not shown). The significant inhibitory effect of 3-chlorobenzoate on the metabolism of biphenyl by strain B356 has been reported previously (36). It was attributed to the ability of the lower biphenyl catabolic pathway to convert 3-chlorobenzoate into 3-chlorocatechol, which strongly inhibits the upper biphenyl catabolic pathway (36). Therefore, data obtained in the Bioscreen C experiments suggest that a pathway able

to metabolize 3-chlorobenzoate into 3-chlorocatechol is induced during growth on diphenylmethane, and 3-chlorocatechol strongly impairs the metabolism of the upper pathway. The fact that both the diphenylmethane and biphenyl degradation pathways responded similarly to the presence of 3-chlorocatechol and 3-chlorobenzoate provides additional evidence that both substrates are metabolized by the same pathway.

Because phenylacetate would be the expected end product if diphenylmethane was metabolized by the enzymes of the upper biphenyl pathway, we have determined whether it could serve as the growth substrate for strains B356 and LB400. In both cases, cells grew very well, reaching CFU values exceeding 10^9 cells/ml within 18 h at 28°C.

Metabolism of diphenylmethane and benzophenone by *P. promoenusa* B356. When diphenylmethane-grown cells of strain B356 were inoculated in MM30 containing 2 mM diphenylmethane, the substrate (approximately 40 μ mol) was almost completely metabolized after 22 h. The mass spectral features of the major metabolite in the acidic ethyl acetate extract were identical to those of an authentic standard of phenylacetic acid (Fig. 3A; spectra are not shown). Based on the area under the GC-MS peak, approximately 15 nmol was present in the 22-h-old cultures. Among the minor metabolites, one peak eluting at 14.76 min (Fig. 3A) exhibited mass spectral features that correspond to those of a *meta*-fission metabolite resulting from the catalytic cleavage of a catechol derivative of diphenylmethane. This metabolite was tentatively identified as 2-hydroxy-6-oxo-7-phenylhepta-2,4-dienoic acid (7-phenyl HODA) [m/z 376 (M^+), m/z 361 ($M^+ - CH_3$), m/z 333 ($M^+ - CH_3 - CO$), and m/z 259 [$M^+ - COO(CH_3)_2Si$]] (see Fig. S1 in the supplemental material for the spectrum). This is the metabolite that would be expected if the hydroxylation reaction had occurred on the *ortho*-*meta* carbons of one benzene ring of diphenylmethane to generate 3-benzylcyclohexa-3,5-diene-1,2-diol. The identity of the acidic metabolite as 7-phenyl HODA is consistent with the fact that a metabolite exhibiting the same mass spectral features was produced from diphenylmethane by resting cells of *E. coli* pQE31[B356-*bphAE*] + pYH31[LB400-*bphFGBC*] (Fig. 3A). The *E. coli* resting cell assay also shows that BphB_{LB400} and BphC_{LB400} can further metabolize 3-benzylcyclohexa-3,5-diene-1,2-diol generated by BphAE_{B356}.

The acidic extracts of cells of strain B356 grown on diphenylmethane also contained a metabolite whose TMS derivative exhibited a molecular mass at m/z 256 corresponding to a monohydroxy-diphenylmethane (Fig. 3A; spectrum not shown). This metabolite was presumably generated from the corresponding dihydrodiol metabolite during the extraction procedure at pH 4.

In the culture extracts prepared at neutral pH, 3-benzylcyclohexa-3,5-diene-1,2-diol and 2,3-dihydroxydiphenylmethane were detected only in trace amounts (not shown). The fact that only small amounts of acidic and neutral metabolites were detected in the culture medium of 22-h-old cultures shows diphenylmethane metabolism is very efficient, and this is consistent with the rapid growth on this substrate.

Strain B356 was unable to grow on benzophenone. However, biphenyl- or diphenylmethane-grown resting cell suspensions metabolized benzophenone and produced a yellow *meta*-fission metabolite which was detected within minutes after substrate addition. Two metabolites (Fig. 3B) with similar spectral features were detected by GC-MS analysis of their TMS derivatives [m/z 390 (M^+), m/z 375 ($M^+ - CH_3$), m/z 347 ($M^+ - CH_3 - CO$), m/z

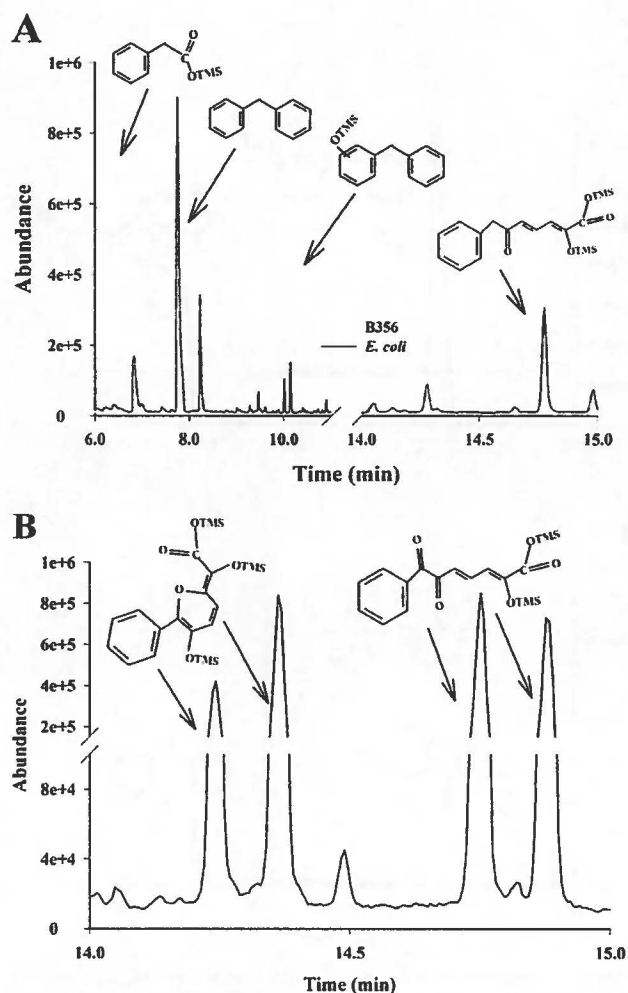


FIG 3 Total ion chromatograms of acidic metabolites detected in 22-h-old cultures of strain B356 grown on diphenylmethane (black line) or in resting cell suspensions of *E. coli* carrying plasmids pQE31[B356-*bphAE*] and pYH31[LB400-*bphFGBC*] incubated for 30 min with diphenylmethane (gray line) (A) or acidic metabolites produced by a suspension of biphenyl-induced cells of strain B356 incubated for 60 min with benzophenone (B). The protocols are described in Materials and Methods. Shown are the peaks of the TMS-treated metabolites that were identified from their mass spectral features. The unlabeled peaks were also detected in controls unexposed to the substrate. OTMS, trimethylsilyl-oxygen complex.

273 [$M^+ - \text{COO}(\text{CH}_3)_3\text{Si}$], m/z 258 [$M^+ - \text{COO}(\text{CH}_3)_3\text{Si} - \text{CH}_3$], m/z 184 [$M^+ - \text{COO}(\text{CH}_3)_3\text{Si} - \text{O}(\text{CH}_3)_3\text{Si}$] (see Fig. S2 in the supplemental material), and their concentrations increased steadily between 5 and 30 min of incubation (not shown). These metabolites were tentatively identified as isomers of 2-hydroxy-6,7-dioxo-7-phenylheptanoic acid (7-phenyl DODA) that should be expected from the *meta*-fission of 2,3-dihydroxybenzophenone. Although the formation of isomers of the *meta*-fission products resulting from the BphC reaction has been reported in several other investigations (33, 37, 38), their mechanism of formation has not yet been elucidated. However, as proposed previously (38) for the *meta*-fission products of chlorobiphenyls, these isomers may be generated during the oxidative cleavage of catechol, where the formation of C-7 keto next to the phenyl ring and

C-1 carboxylic functions may promote the isomerization of the double bonds at C-2 and C-4.

No 2,3-dioxo-3-phenylpropanoic acid, which presumably is the metabolite produced from 7-phenyl DODA by the phenyl HODA hydrolase (BphD), was detected, even after 1 h of incubation in the presence of the substrate. Therefore, we were unable to obtain evidence that benzophenone metabolism goes beyond the *meta*-fission reaction. On the other hand, two metabolites (Fig. 3B) that exhibited spectral features that could correspond to pyranol isomers [m/z 462 (M^+), m/z 447 ($M^+ - \text{CO}$), m/z 419 ($M^+ - \text{CH}_3 - \text{CO}$), m/z 345 [$M^+ - \text{COO}(\text{CH}_3)_3\text{Si}$]] (Fig. 3B; also see Fig. S3 in the supplemental material for the spectrum) were detected. These pyranol isomers may have been generated from a cyclization reaction through intramolecular rearrangements. At this time, there is no documented evidence of spontaneous tautomerization or cyclization of phenyl HODAs. The fact that the same metabolites were produced by an IPTG-induced resting cell suspension of a 1:1 mixture of recombinant *E. coli* pQE31[B356-*bphAE*] + pYH31[LB400-*bphFGBC*] plus *E. coli* pQE31[B356-*bphC*] (not shown) suggests they were produced spontaneously from 7-phenyl DODA in the cell suspensions or during the TMS reaction. However, we cannot exclude other mechanisms of formation involving unspecific enzymatic reactions occurring in both strain B356 and *E. coli*. Therefore, their production remains unexplained at this time.

Metabolism of diphenylmethane by purified BphAE_{B356}, BphAE_{LB400}, and BphAE_{p4}. To confirm that the biphenyl catabolic enzymes of strain B356 metabolize diphenylmethane efficiently, we have examined the catalytic properties of BphAE_{B356} toward diphenylmethane, and we have compared them to those of BphAE_{LB400} and BphAE_{p4}. GC-MS analysis of the nBuB-treated diphenylmethane metabolites revealed two metabolites (Fig. 4A). Since nBuB reacts only with vicinal hydroxyl groups, the mass spectral features (see Fig. S4 in the supplemental material) of the major metabolite (m/z 268 [M^+], m/z 211 [$M^+ - \text{nBu}$], m/z 184 [$M^+ - \text{nBuBO}$], m/z 177 [$M^+ - \text{C}_7\text{H}_7$], m/z 168 [$M^+ - \text{nBuBO}_2$], m/z 156 [$M^+ - \text{nBuBO} - \text{CO}$]) must correspond to a dihydrodiol. Docking experiments (see below) suggested the oxygenation occurred on the *ortho*-*meta* carbons. Therefore, on the basis of its mass spectral features, the major metabolite was tentatively identified as 3-benzylcyclohexa-3,5-diene-1,2-diol.

The minor metabolite contains two pairs of vicinal hydroxyl groups (Fig. 4A). This metabolite presumably was generated from the catalytic *ortho*-*meta* hydroxylation of the nonhydroxylated ring of 3-benzylcyclohexa-3,5-diene-1,2-diol. It was tentatively identified as 3-[(5,6-dihydroxycyclohexa-1,3-dien-1-yl)methyl]cyclohexa-3,5-diene-1,2-diol, showing ions at m/z 368 (M^+), 284 ($M^+ - \text{nBuBO}$), 200 ($M^+ - \text{nBuBO} - \text{nBuBO}$), 184 ($M^+ - \text{nBuBO} - \text{nBuBO}_2$), 177 ($M^+ - \text{nBuBO}_2 - \text{C}_7\text{H}_7$), 168 ($M^+ - \text{nBuBO}_2 - \text{nBuBO}_2$), and 156 ($M^+ - \text{nBuBO}_2 - \text{nBuBO} - \text{CO}$) (see Fig. S5 in the supplemental material). The fragmentation ion at m/z 177 provides evidence that both rings were oxidized.

The production of 3-benzylcyclohexa-3,5-diene-1,2-diol and 3-[(5,6-dihydroxycyclohexa-1,3-dien-1-yl)methyl]cyclohexa-3,5-diene-1,2-diol as sole products of the B356-BPDO reaction was confirmed by the fact that a coupled reaction composed of purified preparations of BphAE_{B356} plus BphB_{B356} generated two metabolites. On the basis of the mass spectra of their TMS derivatives, the major one was identified as 2,3-dihydroxydiphenylmethane (3-benzylbenzene-1,2-diol) and the minor one as 2,2',3,3'-tetra-

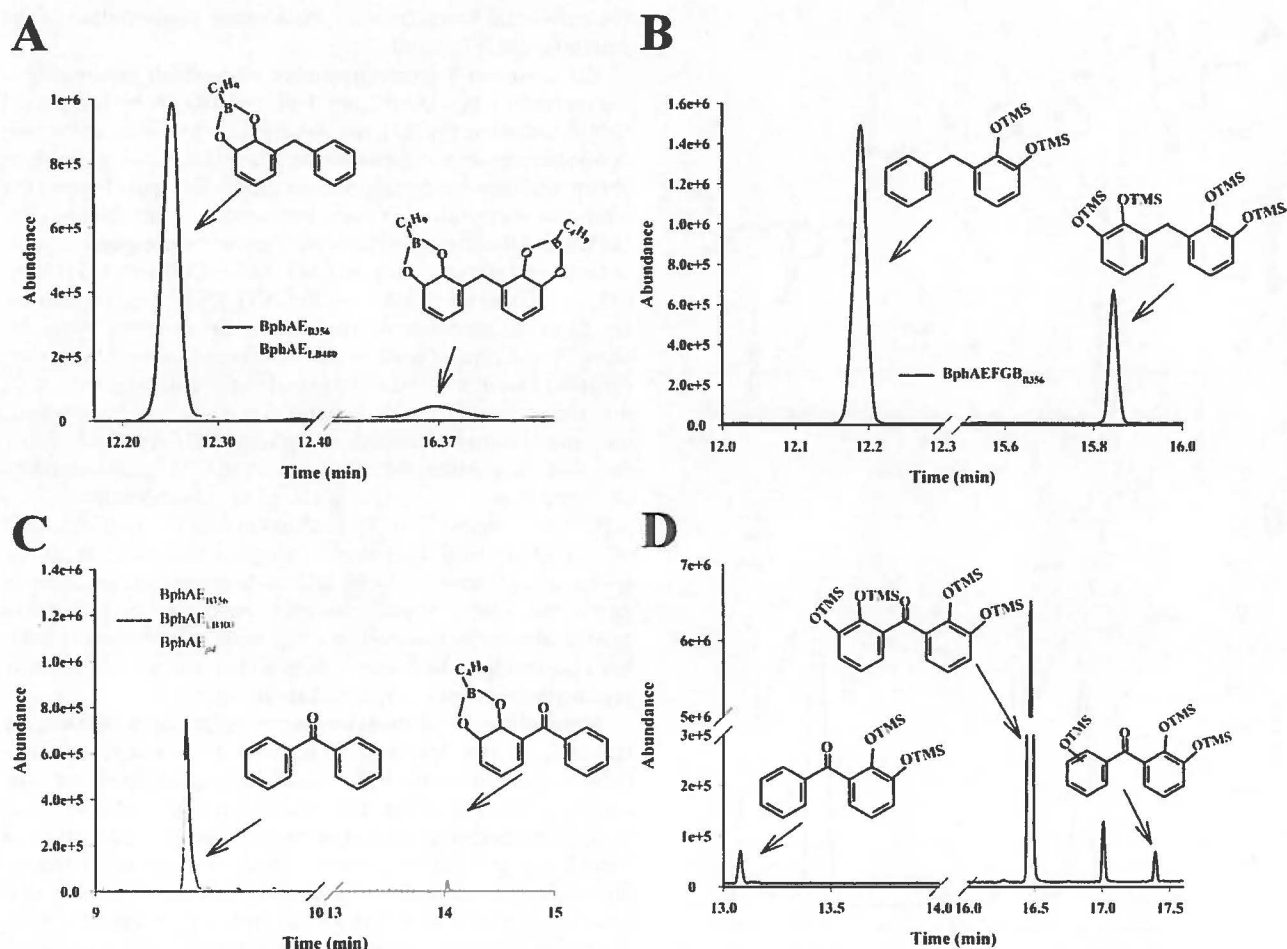


FIG 4 Total ion chromatograms of metabolites produced from diphenylmethane by purified preparations of BphAE_{B356} (black line) and BphAE_{LB400} (gray line) (A) or by a coupled reaction composed of purified BphAE_{B356} plus BphB_{B356} (B). (C) Total ion chromatograms of metabolites produced from benzophenone by purified preparations of BphAE_{B356} (light gray line), BphAE_{LB400} (black line), and BphAE_{p4} (dark gray line). (D) Total ion chromatograms of metabolites produced from benzophenone by a coupled reaction composed of purified BphAE_{B356} plus BphB_{B356}. The procedures to purify the enzymes, to set up the reactions, and to extract the metabolites for GC-MS analysis are described in Materials and Methods. Shown are the peaks of nBuB- or TMS-treated metabolites that were identified from their mass spectral features. The unlabeled peaks were also present in controls unexposed to the substrate.

hydroxydiphenylmethane {3-[(2,3-dihydroxyphenyl)methyl]benzene-1,2-diol} (Fig. 4B). The diagnostically important ions for the TMS-derived 2,3-dihydroxydiphenylmethane (see Fig. S6 in the supplemental material) comprise the molecular ion at m/z 344 and fragmentation ions at m/z 329 ($M^+ - CH_3$), 271 [$M^+ - (CH_3)_3Si$], 255 [$M^+ - O(CH_3)_3Si$], 225 [$M^+ - O(CH_3)_3Si - (CH_3)_2$]. For the TMS-derived 2,2',3,3'-tetrahydroxydiphenylmethane (see Fig. S7), they are m/z 520 (M^+), 505 ($M^+ - CH_3$), 447 [$M^+ - (CH_3)_3Si$], 431 [$M^+ - O(CH_3)_3Si$], 342 [$M^+ - O(CH_3)_3Si - O(CH_3)_3Si$], 312 [$M^+ - O(CH_3)_3Si - O(CH_3)_3Si - (CH_3)_2$], 253 [$M^+ - O(CH_3)_3Si - O(CH_3)_3Si - O(CH_3)_3Si$]. The vicinity of the two hydroxyl groups in these metabolites was confirmed by the mass spectra of the nBuB derivatives (not shown).

When BphAE_{LB400} was incubated for 10 min with the substrate, it produced approximately the same amount of 3-benzylcyclohexa-3,5-diene-1,2-diol from diphenylmethane as BphAE_{B356}, but no 3-[(5,6-dihydroxycyclohexa-1,3-dien-1-yl)methyl]cyclohexa-3,5-diene-1,2-diol was produced (Fig. 4A). The metabolic pattern of BphAE_{p4} toward diphenylmethane was very similar to that of the

parental enzyme BphAE_{LB400} (not shown). Therefore, BphAE_{B356} was the only one of the three enzymes to further oxidize the dihydroxylated metabolite.

The steady-state kinetic parameters of purified preparations of BphAE_{B356}, BphAE_{p4}, and BphAE_{LB400} toward diphenylmethane were calculated from the initial oxygen consumption, and they were consistent with the GC-MS analysis. Diphenylmethane was as good a substrate as biphenyl for all three enzymes. Thus, the k_{cat} and k_{cat}/K_m values for BphAE_{B356} (Table 2) were in the range reported for biphenyl ($4.3 s^{-1}$ and $63 \times 10^3 M^{-1} s^{-1}$, respectively) (16) when this enzyme was used under the same reaction conditions. Similarly, the k_{cat} and k_{cat}/K_m values for BphAE_{LB400} and for BphAE_{p4} (Table 2) were very close to those obtained when biphenyl was the substrate and the reactions were run under identical conditions (the reported values were $0.9 s^{-1}$ and $41 \times 10^3 M^{-1} s^{-1}$ for BphAE_{LB400}, respectively, and $1.0 s^{-1}$ and $31 \times 10^3 M^{-1} s^{-1}$ for BphAE_{p4}, respectively) (31).

Benzophenone metabolism by purified BphAE_{B356}, BphAE_{LB400}, and BphAE_{p4}. Unlike diphenylmethane, benzophe-

TABLE 2 Steady-state kinetic parameters^a of BphAE_{B356}, BphAE_{LB400}, and BphAE_{p4} toward diphenylmethane and benzophenone

Substrate and enzyme	K_m (mM)	k_{cat} (s ⁻¹)	k_{cat}/K_m (10 ³ · M ⁻¹ · s ⁻¹)
Diphenylmethane			
BphAE _{B356}	63.0 (5.6)	8.9 (0.3)	141.3 (7.5)
BphAE _{LB400}	15.4 (1.1)	1.0 (0.1)	64.9 (2.7)
BphAE _{p4}	17.9 (2.2)	1.6 (0.1)	89.4 (5.5)
Benzophenone			
BphAE _{B356}	65.3 (8.5)	1.2 (0.2)	18.4 (0.6)
BphAE _{LB400}	ND ^b	ND	ND
BphAE _{p4}	9.1 (2.1)	0.1 (0.0)	11.0 (1.6)

^a The steady-state kinetics were determined from the oxygen consumption rates as described in Materials and Methods. The values are results ± standard deviations from three independently produced enzyme preparations.

^b ND, not determined; metabolism was too slow to determine values accurately.

none is metabolized differently by BphAE_{B356} and BphAE_{LB400}. A purified preparation of BphAE_{B356} completely oxidized 50 nmol benzophenone in 10 min to generate a single metabolite (Fig. 4C), tentatively identified as 3-benzoylcyclohexa-3,5-diene-1,2-diol from the GC-MS spectrum of its nBuB derivative (see Fig. S8 in the supplemental material) (ions at m/z 282 [M^+] and at 225 [$M^+ - nBu$], 198 [$M^+ - nBuBO$], 182 [$M^+ - nBuBO_2$], and 170 [$M^+ - nBuBO - CO$]). Under the same conditions, BphAE_{LB400} and BphAE_{p4} oxidized only a fraction of the added 50 nmol benzophenone, but both enzymes produced the same metabolite as BphAE_{B356} (Fig. 4C). This is consistent with the steady-state kinetics shown in Table 2, where the turnover rate of the reaction of BphAE_{B356} toward benzophenone was 12 times higher than that for BphAE_{p4}, and the turnover rate of the reaction of BphAE_{LB400} was too low to obtain reliable values.

When BphB_{B356} was used to oxidize 3-benzoylcyclohexa-3,5-diene-1,2-diol, 2,3-dihydroxybenzophenone was produced (not shown) and was identified from the GC-MS spectral features of its TMS derivative (ions at m/z 358 (M^+) and m/z 343 ($M^+ - CH_3$), 270 [$M^+ - (CH_3)_4Si$], and 212 [$M^+ - (CH_3)_4Si - (CH_3)_2Si$]) (see Fig. S9 in the supplemental material).

Remarkably, when benzophenone at a concentration of 50 nmol was the substrate for the coupled reaction composed of BphAE_{B356} plus BphB_{B356}, it was almost completely metabolized to 2,2',3,3'-tetrahydroxybenzophenone (Fig. 4D), which was identified from its GC-MS and NMR spectra. The other two metabolites, 2,3-dihydroxybenzophenone and 2,2',3- or 2,3,3'-trihydroxybenzophenone, represented less than 1% of total metabolites produced by this reaction. The spectral features of the TMS-treated major metabolite (see Fig. S10 in the supplemental material) was comprised of a molecular ion at m/z 534 plus fragmentation ions at m/z 519 ($M^+ - CH_3$), 446 [$M^+ - (CH_3)_4Si$], and 358 [$M^+ - (CH_3)_4Si - (CH_3)_2Si$]. The position of the hydroxyl groups was confirmed by NMR analysis. The spectrum showed only three signals for six protons between 6.80 and 7.10 ppm. This indicates that there are two identical aromatic rings, and each one contains 3 protons. The chemical shifts for the protons labeled H₄, H₅, and H₆ in Fig. 5 were recorded at 6.824 ppm (triplet) (H₅), at 7.096 (doublet of doublets), and 6.969 (doublet of doublets) (H₄ and H₆). The coupling constant between the three protons (Fig. 5) and the shape of the peaks (1 triplet and 2 doublet of doublets) revealed that the 3 protons of each aromatic

ring were vicinal to each other. With this in mind, the only possibility for the structure of the metabolite was 2,2',3,3'-tetrahydroxybenzophenone.

Docking experiments with diphenylmethane and benzophenone. We docked diphenylmethane and benzophenone in the substrate-bound form of BphAE_{B356} and BphAE_{LB400} after removing biphenyl. For both substrates, the conformation of the top-ranked docked molecules in BphAE_{B356} exhibited an orientation that would enable oxygenation of the *ortho-meta* carbons of the phenyl ring. In both cases, the *ortho-meta* carbons closely aligned with carbons 2 and 3 of the oxidized ring of biphenyl in the complexed form (Fig. 6A and B). This suggests BphAE_{B356} produces 3-benzoylcyclohexa-3,5-diene-1,2-diol from diphenylmethane and 3-benzoylcyclohexa-3,5-diene-1,2-diol from benzophenone, and it is consistent with the NMR spectral data that confirm that 2,2',3,3'-tetrahydroxybenzophenone was produced from benzophenone by the combined reaction of BphAE_{B356} plus BphB_{B356}.

As shown in Fig. 6A and B, the conformation of benzophenone inside the catalytic pocket of BphAE_{B356} differs from that of diphenylmethane. Therefore, the carbonyl group strongly influences the interaction between the substrate and the amino acid residues that line the catalytic pocket. However, the *ortho-meta* carbons of the docked benzophenone aligned very well with the reactive carbons of biphenyl in the biphenyl-bound form of BphAE_{B356} (Fig. 6A). In the case of BphAE_{LB400}, the top-ranked conformations for benzophenone were at a distance from the catalytic iron that may have allowed catalytic hydroxylation (Fig. 6C). However, the reactive ring did not align as well as for BphAE_{B356} with the reactive ring of biphenyl, and this may explain why BphAE_{LB400} catalyzed the oxygenation of benzophenone poorly. On the other hand, we cannot exclude the possibility that other types of interactions between protein structures and the substrate, which could not be reproduced in the docking experiments, prevent its productive binding to the BphAE_{LB400} catalytic pocket. Since the conformation of benzophenone in the docked BphAE_{B356} structure appears to be more favorable for the catalytic reaction, we have superposed the benzophenone docked structure of BphAE_{B356} on the structure of the biphenyl-bound BphAE_{LB400} after biphenyl removal (Fig. 6D). As shown in the figure, the benzophenone carbonyl oxygen was very close to both Gly321 and Phe336 of BphAE_{LB400}. Therefore, in this conformation of the substrate, the proximity of these two residues relative to the carbonyl oxygen may hinder proper binding. This is consistent with previous observations (8, 16) where Gly321 and Phe336, two res-

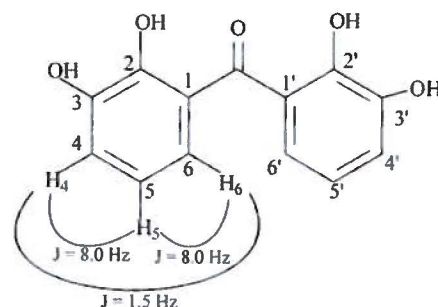


FIG 5 Structural features of the hydroxylated metabolite obtained from benzophenone by the coupled reaction of BphAE_{B356} plus BphB_{B356}, which was identified as 2,2',3,3'-tetrahydroxybenzophenone by NMR analysis.

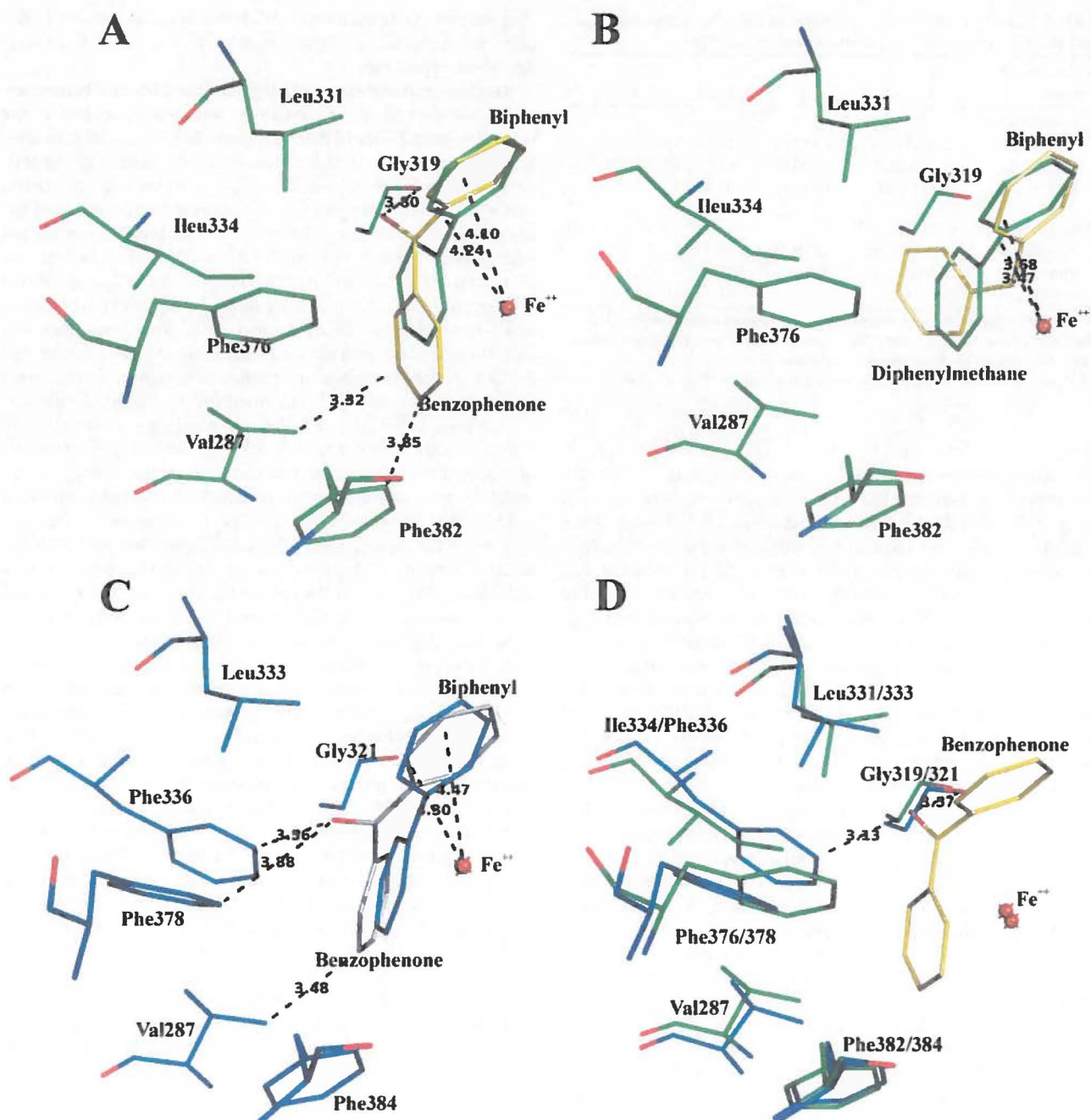


FIG 6 (A) Superposition of catalytic center residues of benzophenone-docked (yellow) and biphenyl-bound (green) forms of BphAE_{B356}. (B) Superposition of catalytic center residues of diphenylmethane-docked (yellow) and biphenyl-bound (green) forms of BphAE_{B356}. (C) Superposition of catalytic center residues of benzophenone-docked (white) and biphenyl-bound (blue) forms of BphAE_{LB400}. (D) Superposition of the biphenyl-bound form of BphAE_{LB400} (blue) after removal of biphenyl substrate and the benzophenone-docked (yellow) BphAE_{B356} (green). The oxygen atoms are in red.

idues lining the catalytic pocket, appeared to play a significant role in binding the substrate's analogs. It is also consistent with the observation that BphAE_{P4}, the doubly substituted Thr335Ala/Phe336Met mutant of BphAE_{LB400}, metabolized benzophenone more efficiently than its parent (Table 2). In this case, the Thr335Ala mutation releases constraints imposed by Thr335 on Gly321, allowing movement of its carbonyl group during substrate binding to create more space to accommodate larger substrates.

On the other hand, in the case of 2,3-dihydroxybenzophenone, none of the 20 top-ranked conformations of the docked substrate were at a distance from BphAE_{B356} catalytic iron that could have allowed a catalytic reaction. Therefore, perhaps structural features involving an induced-fit mechanism that the docking experiment could not reproduce are required to allow productive binding of this substrate to the catalytic pocket of BphAE_{B356}.

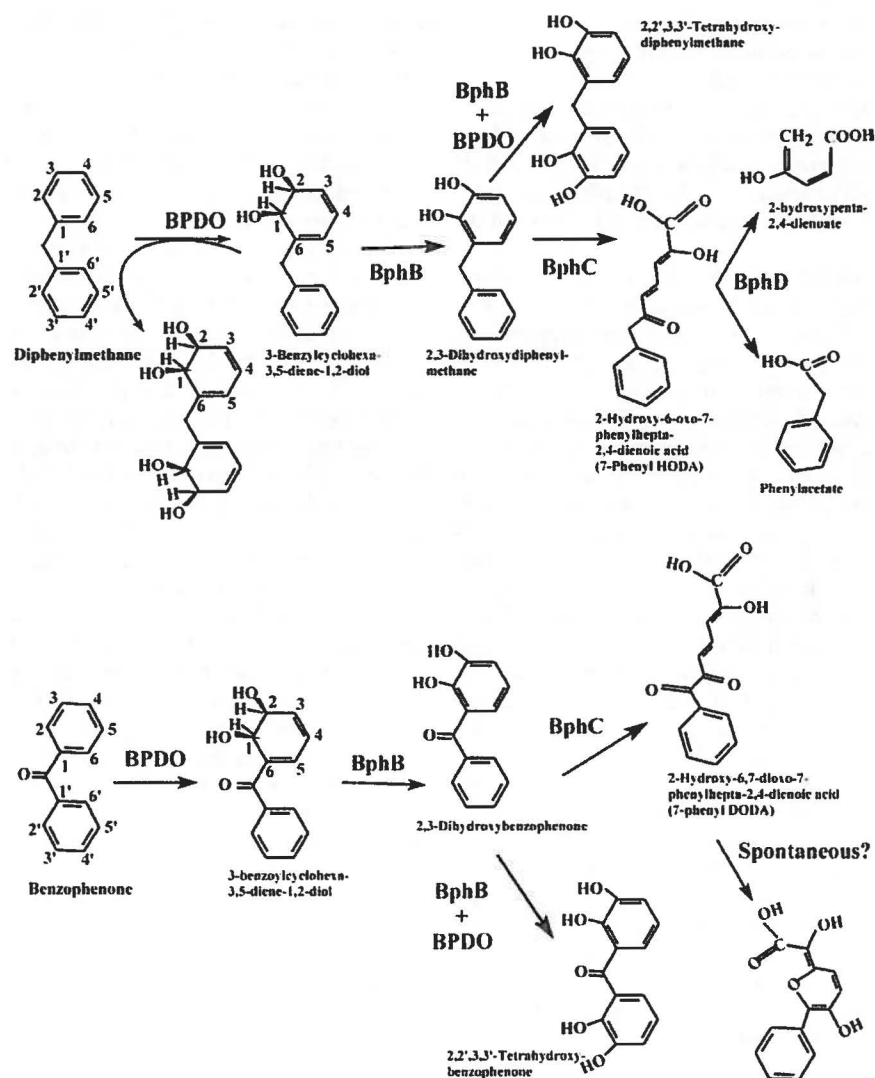


FIG 7 Profile of metabolites generated during the oxidation of diphenylmethane (upper) or benzophenone (lower) by diphenylmethane- or biphenyl-induced cells of strain B356 or by isolated enzymes of its biphenyl catabolic pathway.

DISCUSSION

Unlike *B. xenovorans* LB400, *P. promoenusa* B356 grew remarkably well on diphenylmethane, and many observations made in this work are supportive of the idea that it was metabolized by the enzymes of the biphenyl catabolic pathway to produce phenylacetate, which was further metabolized by a lower pathway. Cells of strain B356 produced the same metabolites from diphenylmethane during their growth on this substrate as those isolated from enzymes of the biphenyl catabolic pathway (Fig. 7). Furthermore, the kinetic parameters of BphAE_{B356} toward diphenylmethane were in the same range as those for biphenyl, suggesting this enzyme metabolizes diphenylmethane during growth on this substrate. It is noteworthy that when purified preparations of B356 BPDO or B356 BPDO plus BphB_{B356} were used to metabolize diphenylmethane, significant amounts of tetrahydroxylated metabolites were detected in the reaction medium. However, the tetrahydroxylated metabolites were present in very small amounts in

cultures of B356 growing on diphenylmethane (not shown). This shows that during growth of strain B356 on diphenylmethane, 3-benzylcyclohexa-3,5-diene-1,2-diol and subsequent metabolites were oxidized very efficiently by the downstream enzymes of the catabolic pathway, thus preventing further BPDO oxidation of the dihydrodiol and the catechol metabolites.

Judging by its steady-state kinetics toward diphenylmethane, BphAE_{LB400} metabolized this substrate as well as biphenyl. In addition, we found that BphC_{LB400} catalyzed the ring cleavage of 2,3-dihydroxydiphenylmethane, and the strain grew well on phenylacetate. However, unlike strain B356, cells of strain LB400 grown cometabolically on diphenylmethane plus sodium acetate were unable to metabolize 4-chlorobiphenyl, showing that diphenylmethane did not induce the biphenyl catabolic pathway of strain LB400. Therefore, the inability of diphenylmethane to induce the biphenyl catabolic pathway in strain LB400 most likely is the reason why this strain is unable to grow on this substrate.

Growth kinetics data provided strong evidence that both diphenylmethane and biphenyl induced the same catabolic enzymes during growth of strain B356. Uninduced cells grew poorly on diphenylmethane or biphenyl, which was the case when the inocula were prepared by growing the cells on sodium acetate. However, interchanging the growth substrates to prepare the inocula did not affect the growth kinetics on diphenylmethane or on biphenyl, which strongly suggests that both substrates induced the same catabolic pathway.

Remarkably, although further work will be needed to confirm the conclusion, data suggest that a benzoate pathway is induced when cells are grown on diphenylmethane. This was supported by the fact that 3-chlorobenzoate strongly inhibited growth on diphenylmethane. Based on a previous report (36), in order to inhibit growth on biphenyl, 3-chlorobenzoate must be converted to 3-chlorocatechol, which is a very potent inhibitor of BphC. In this study, we have not elucidated the enzymatic steps involved in phenylacetate catabolism during growth of strain B356 on diphenylmethane. However, since phenylacetate is a key metabolite in the metabolism of many aromatic chemicals, including phenylalanine, most bacteria have the ability to metabolize it through a pathway that proceeds via the formation of a coenzyme A (CoA)-thioester derivative (39). Strain LB400 can metabolize 3- and 4-hydroxyphenylacetate through the homogentisate pathway (40), but the ability of this strain to metabolize phenylacetate through this pathway has not been demonstrated. Focht and Alexander (22, 41) have described a *Hydrogenomonas* isolate that metabolizes diphenylmethane through a pathway that presumably involves the metacleaveage of a catechol metabolite, which is further metabolized to generate phenylacetate. Since cells grown on diphenylmethane readily metabolized homogentisate, they postulated that phenylacetate was metabolized via a homogentisic pathway in that *Hydrogenomonas* strain. However, neither the phenylacetyl-coenzyme A nor the homogentisate pathway involves production of a 2,3-catechol derivative, as is the case for the metabolism of benzoic acid in strain B356. Therefore, the growth inhibition caused by 3-chlorobenzoate suggests that diphenylmethane or one of its metabolites induces a pathway involving a benzoate 2,3-dioxygenase, namely, the biphenyl-associated benzoate pathway. Indeed, strain B356 carries two benzoate pathways, only one of which, the one induced when cells are grown on biphenyl, is able to produce 3-chlorocatechol from 3-chlorobenzoate (36).

Few investigations have assessed the ability of the bacterial biphenyl catabolic enzymes to metabolize diphenylmethane or one of its derivatives, such as DDT or 1,1-dichloro-2,2-(4-chlorophenyl)ethane (DDD) (16, 19, 42–44), but no studies have examined the ability of biphenyl-degrading bacteria to grow on diphenylmethane. Therefore, strain B356 might not be the only one with the ability to use the biphenyl catabolic pathway to grow on this substrate.

Neither strain B356 nor LB400 could use benzophenone as a growth substrate; however, BphAE_{B356} metabolized this diphenylmethane analog significantly more efficiently than BphAE_{LB400}. Structural analysis of the docked substrate showed that residues Phe336 and Gly321 were partly responsible for preventing productive binding of this substrate with BphAE_{LB400}. Structural analyses of substrate-bound crystals and docking experiments have shown that the combined effect of these two substitutions increases the space required in the catalytic pocket to accommo-

date bulkier substrates (8, 16). The replacement of Thr335 of BphAE_{LB400} by Gly333 in BphAE_{B356} produces a similar effect (16). However, other structural features that our docking experiments could not identify also may have an influence on the ability of the enzyme to metabolize this substrate, since, on the basis of their steady-state kinetics, BphAE_{B356} metabolized benzophenone more efficiently than BphAE_{P4}, which is a doubly substituted Thr335Ala/Phe336Met mutant of BphAE_{LB400}.

Generally, the investigations related to the biphenyl-degrading bacteria during the last 5 decades were initiated with the objective of designing a biological process to degrade PCBs and other chlorinated aromatics, such as chlorodibenzofurans (45, 46). These bacteria were obtained by enrichments on biphenyl, and traditionally it was believed that the four-enzymatic-step biphenyl pathway evolved in bacteria primarily to transform biphenyl into benzoic acid. However, data presented in the current and previous works (14) bring us to question this belief. Biphenyl is a naturally occurring chemical, but it is not universally distributed in nature. It is noteworthy that bacteria carrying the biphenyl catabolic pathway enzymes were obtained from pristine soils not exposed to biphenyl or chlorobiphenyls (10).

On the basis of their primary amino acid sequences, BphAE_{B356} and BphAE_{LB400} belong to distinct phylogenetic clusters of BphAE (9–11). Recent data suggested that each has acquired a distinct PCB-degrading pattern (9, 15), as well as distinct abilities to metabolize simple flavonoids (14), DDT (16), or DDD (43). In this work, we found that BphAE_{B356} and BphAE_{LB400} metabolized diphenylmethane similarly but benzophenone and 2,3-dihydroxybenzophenone very differently. Furthermore, the fact that the biphenyl catabolic pathway of strain B356 is inducible by diphenylmethane allows the strain to use it as a growth substrate. As a result, under natural conditions, strain B356 has the potential to metabolize or cometabolize many chemicals that strain LB400 metabolizes poorly.

Although the enzymes of the peripheral pathways, such as those of the biphenyl catabolic pathway, have evolved to metabolize a broad range of substrates, on the basis of the observations made in this work and a previous one (14), we postulate that the biphenyl catabolic pathway enzymes have evolved divergently in bacteria, in such a way that each phylogenetic branch has specialized to play distinct ecophysiological functions with regard to chemicals naturally found in nature.

ACKNOWLEDGMENTS

This work was supported by the Natural Sciences and Engineering Research Council of Canada (NSERC) (grant RGPIN/39579-2012).

We thank Sameer Al-Abdul-Wahid, QANUC NMR Facility (McGill University, Montreal, Quebec, Canada), for his help in NMR analysis. We also thank Eric Déziel, INRS-Institut Armand-Frappier, for the use of his Bioscreen C system.

REFERENCES

1. Sylvestre M. 2013. Prospects for using combined engineered bacterial enzymes and plant systems to rhizoremediate polychlorinated biphenyls. *Environ. Microbiol.* 15:907–915.
2. Boyd DR, Bugg TDH. 2006. Arene *cis*-dihydrodiol formation: from biology to application. *Org. Biomol. Chem.* 4:181–192.
3. Chun HK, Ohnishi Y, Shindo K, Misawa N, Furukawa K, Horinouchi S. 2003. Biotransformation of flavone and flavanone by *Streptomyces lividans* cells carrying shuffled biphenyl dioxygenase genes. *J. Mol. Catal. B Enzym.* 21:113–121.
4. Kagami O, Shindo K, Kyojima A, Takeda K, Ikenaga H, Furukawa K,

- Misawa N. 2008. Protein engineering on biphenyl dioxygenase for conferring activity to convert 7-hydroxyflavone and 5,7-dihydroxyflavone (chrysin). *J. Biosci. Bioeng.* 106:121–127.
5. Misawa N, Nakamura R, Kagiya Y, Ikenaga H, Furukawa K, Shindo K. 2005. Synthesis of vicinal diols from various arenes with a heterocyclic, amino or carboxyl group by using recombinant *Escherichia coli* cells expressing evolved biphenyl dioxygenase and dihydrodiol dehydrogenase genes. *Tetrahedron* 61:195–204.
6. Seeger M, Gonzalez M, Camara B, Munoz L, Ponce E, Mejias L, Mascayano C, Vasquez Y, Sepulveda-Boza S. 2003. Biotransformation of natural and synthetic isoflavonoids by two recombinant microbial enzymes. *Appl. Environ. Microbiol.* 69:5045–5050.
7. Seo J, Kang SI, Ryu JY, Lee YJ, Park KD, Kim M, Won D, Park HY, Ahn JH, Chong Y, Kanaly RA, Han J, Hur HG. 2010. Location of flavone B-ring controls regioselectivity and stereoselectivity of naphthalene dioxygenase from *Pseudomonas* sp. strain NCIB 9816-4. *Appl. Microbiol. Biotechnol.* 86:1451–1462.
8. Kumar P, Mohammadi M, Viger JF, Barriault D, Gomez-Gil L, Eltis LD, Bolin JT, Sylvestre M. 2011. Structural insight into the expanded PCB-degrading abilities of a biphenyl dioxygenase obtained by directed evolution. *J. Mol. Biol.* 405:531–547.
9. Standfuß-Gabisch C, Al-Halbouni D, Hofer B. 2012. Characterization of biphenyl dioxygenase sequences and activities encoded by the metagenomes of highly polychlorobiphenyl-contaminated soils. *Appl. Environ. Microbiol.* 78:2706–2715.
10. Vézina J, Barriault D, Sylvestre M. 2008. Diversity of the C-terminal portion of the biphenyl dioxygenase large subunit. *J. Mol. Microbiol. Biotechnol.* 15:139–151.
11. Witzig R, Junca H, Hecht HJ, Pieper DH. 2006. Assessment of toluene/biphenyl dioxygenase gene diversity in benzene-polluted soils: links between benzene biodegradation and genes similar to those encoding isopropylbenzene dioxygenases. *Appl. Environ. Microbiol.* 72:3504–3514.
12. Colbert CL, Agar NY, Kumar P, Chalko MN, Sinha SC, Powlowski JB, Eltis LD, Bolin JT. 2013. Structural characterization of *Pandora* *pnomenusa* B-356 biphenyl dioxygenase reveals features of potent polychlorinated biphenyl-degrading enzymes. *PLoS One* 8:e52550. doi:10.1371/journal.pone.0052550.
13. Furusawa Y, Nagarajan V, Tanokura M, Masai E, Fukuda M, Senda T. 2004. Crystal structure of the terminal oxygenase component of biphenyl dioxygenase derived from *Rhodococcus* sp. strain RHA1. *J. Mol. Biol.* 342:1041–1052.
14. Pham TTM, Tu Y, Sylvestre M. 2012. Remarkable ability of *Pandora* *pnomenusa* B356 biphenyl dioxygenase to metabolize simple flavonoids. *Appl. Environ. Microbiol.* 78:3560–3570.
15. Gomez-Gil L, Kumar P, Barriault D, Bolin JT, Sylvestre M, Eltis LD. 2007. Characterization of biphenyl dioxygenase of *Pandora* *pnomenusa* B-356 as a potent polychlorinated biphenyl-degrading enzyme. *J. Bacteriol.* 189:5705–5715.
16. L'Abbée JB, Tu YB, Barriault D, Sylvestre M. 2011. Insight into the metabolism of 1,1,1-trichloro-2,2-bis(4-chlorophenyl)ethane (DDT) by biphenyl dioxygenases. *Arch. Biochem. Biophys.* 516:35–44.
17. Anonymous. 2012. Some chemicals present in industrial and consumer products, food and drinking-water, p 285–305. IARC monographs on the evaluation of carcinogenic risks to humans, vol 101. World Health Organization Press, Geneva, Switzerland.
18. Hemshekhar M, Sunitha K, Santhosh MS, Devaraja S, Kemparaju K, Vishwanath BS, Niranjana SR, Girish KS. 2011. An overview on genus *Garcinia*: phytochemical and therapeutical aspects. *Phytochem. Rev.* 10:325–351.
19. Misawa N, Shindo K, Takahashi H, Suenaga H, Iguchi K, Okazaki H, Harayama S, Furukawa K. 2002. Hydroxylation of various molecules including heterocyclic aromatics using recombinant *Escherichia coli* cells expressing modified biphenyl dioxygenase genes. *Tetrahedron* 58:9605–9612.
20. Focht DD, Alexander M. 1971. Aerobic cometabolism of DDT analogues by *Hydrogenomonas* sp. *J. Agric. Food Chem.* 19:20–22.
21. Liu YS, Ying GG, Sharcef A, Kookana RS. 2012. Biodegradation of the ultraviolet filter benzophenone-3 under different redox conditions. *Environ. Toxicol. Chem.* 31:289–295.
22. Focht DD, Alexander M. 1970. DDT metabolites and analogs: ring fission by *Hydrogenomonas*. *Science* 170:91–92.
23. Lin JJ, Smith M, Jessee J, Bloom F. 1992. DH11s: an *E. coli* strain for preparation of single-stranded DNA from phagemid vectors. *Biotechniques* 12:718–721.
24. Miroux B, Walker JE. 1996. Over-production of proteins in *Escherichia coli*: mutant hosts that allow synthesis of some membrane proteins and globular proteins at high levels. *J. Mol. Biol.* 260:289–298.
25. Erickson BD, Mondello FJ. 1992. Nucleotide sequencing and transcriptional mapping of the genes encoding biphenyl dioxygenase, a multicomponent polychlorinated-biphenyl-degrading enzyme in *Pseudomonas* strain LB400. *J. Bacteriol.* 174:2903–2912.
26. Barriault D, Pelletier C, Hurtubise Y, Sylvestre M. 1997. Substrate selectivity pattern of *Comamonas testosteroni* strain B-356 towards dichlorobiphenyls. *Int. Biodeterior. Biodegradation* 39:311–316.
27. Hurtubise Y, Barriault D, Powlowski J, Sylvestre M. 1995. Purification and characterization of the *Comamonas testosteroni* B-356 biphenyl dioxygenase components. *J. Bacteriol.* 177:6610–6618.
28. Sambrook J, Fritsch EF, Maniatis T. 1989. Molecular cloning: a laboratory manual. Spring Harbor Laboratory Press, Cold Spring Harbor, NY.
29. Sylvestre M. 1980. Isolation method for bacterial isolates capable of growth on *p*-chlorobiphenyl. *Appl. Environ. Microbiol.* 39:1223–1224.
30. Toussaint JP, Pham TTM, Barriault D, Sylvestre M. 2012. Plant exudates promote PCB degradation by a rhodococcal rhizobacteria. *Appl. Microbiol. Biotechnol.* 95:1589–1603.
31. Mohammadi M, Viger JF, Kumar P, Barriault D, Bolin JT, Sylvestre M. 2011. Retuning Rieske-type oxygenases to expand substrate range. *J. Biol. Chem.* 286:27612–27621.
32. Hurtubise Y, Barriault D, Sylvestre M. 1996. Characterization of active recombinant his-tagged oxygenase component of *Comamonas testosteroni* B-356 biphenyl dioxygenase. *J. Biol. Chem.* 271:8152–8156.
33. Mohammadi M, Sylvestre M. 2005. Resolving the profile of metabolites generated during oxidation of dibenzofuran and chlorodibenzofurans by the biphenyl catabolic pathway enzymes. *Chem. Biol.* 12:835–846.
34. Morris GM, Huey R, Lindstrom W, Sanner MF, Belew RK, Goodsell DS, Olson AJ. 2009. AutoDock4 and AutoDockTools4: automated docking with selective receptor flexibility. *J. Comput. Chem.* 30:2785–2791.
35. Hein P, Powlowski J, Barriault D, Hurtubise Y, Ahmad D, Sylvestre M. 1998. Biphenyl-associated meta-cleavage dioxygenases from *Comamonas testosteroni* B-356. *Can. J. Microbiol.* 44:42–49.
36. Sondossi M, Sylvestre M, Ahmad D. 1992. Effects of chlorobenzoate transformation on the *Pseudomonas testosteroni* biphenyl and chlorobiphenyl degradation pathway. *Appl. Environ. Microbiol.* 58:485–495.
37. Barriault D, Durand J, Maaroufi H, Eltis LD, Sylvestre M. 1998. Degradation of polychlorinated biphenyl metabolites by naphthalene-catabolizing enzymes. *Appl. Environ. Microbiol.* 64:4637–4642.
38. Massé R, Messier F, Ayotte C, Lévesque Sylvestre M-FM. 1989. A Comprehensive gas chromatographic/mass spectrometric analysis of 4-chlorobiphenyl bacterial degradation products. *Biomed. Environ. Mass Spectrom.* 18:27–47.
39. Teufel R, Gantert C, Voss M, Eisenreich W, Haehnel W, Fuchs G. 2011. Studies on the mechanism of ring hydrolysis in phenylacetate degradation: a metabolic branching point. *J. Biol. Chem.* 286:11021–11034.
40. Romero-Silva MJ, Mendez V, Agullo L, Seeger M. 2013. Genomic and functional analyses of the gentisate and protocatechuate ring-cleavage pathways and related 3-hydroxybenzoate and 4-hydroxybenzoate peripheral pathways in *Burkholderia xenovorans* LB400. *PLoS One* 8:e56038. doi:10.1371/journal.pone.0056038.
41. Focht DD, Alexander M. 1970. Bacterial degradation of diphenylmethane, a DDT model substrate. *Appl. Microbiol.* 20:608–611.
42. Hay AG, Focht DD. 1998. Cometabolism of 1,1-dichloro-2,2-bis(4-chlorophenyl)ethylene by *Pseudomonas acidovorans* M3GY grown on biphenyl. *Appl. Environ. Microbiol.* 64:2141–2146.
43. Hay AG, Focht DD. 2000. Transformation of 1,1-dichloro-2,2-(4-chlorophenyl)ethane (DDD) by *Ralstonia eutropha* strain A5. *FEMS Microbiol. Ecol.* 31:249–253.
44. Nadeau LJ, Menn FM, Breen A, Sayler GS. 1994. Aerobic degradation of 1,1,1-trichloro-2,2-bis(4-chlorophenyl)ethane (DDT) by *Alcaligenes eutrophus* A5. *Appl. Environ. Microbiol.* 60:51–55.
45. Kumar P, Mohammadi M, Dhindwal S, Pham TT, Bolin JT, Sylvestre M. 2012. Structural insights into the metabolism of 2-chlorodibenzofuran by an evolved biphenyl dioxygenase. *Biochem. Biophys. Res. Commun.* 421:757–762.

46. Pieper DH, Seeger M. 2008. Bacterial metabolism of polychlorinated biphenyls. *J. Mol. Microbiol. Biotechnol.* 15:121–138.
47. Barriault D, Sylvestre M. 2004. Evolution of the biphenyl dioxygenase BphA from *Burkholderia xenovorans* LB400 by random mutagenesis of multiple sites in region III. *J. Biol. Chem.* 279:47480–47488.
48. Barriault D, Plante MM, Sylvestre M. 2002. Family shuffling of a targeted *bphA* region to engineer biphenyl dioxygenase. *J. Bacteriol.* 184:3794–3800.
49. Dhindwal S, Patil DN, Mohammadi M, Sylvestre M, Tomar S, Kumar P. 2011. Biochemical studies and ligand bound structures of biphenyl dehydrogenase from *Pandoraea pnomenusa* strain B-356 reveal a basis for broad specificity of the enzyme. *J. Biol. Chem.* 286:37011–37022.

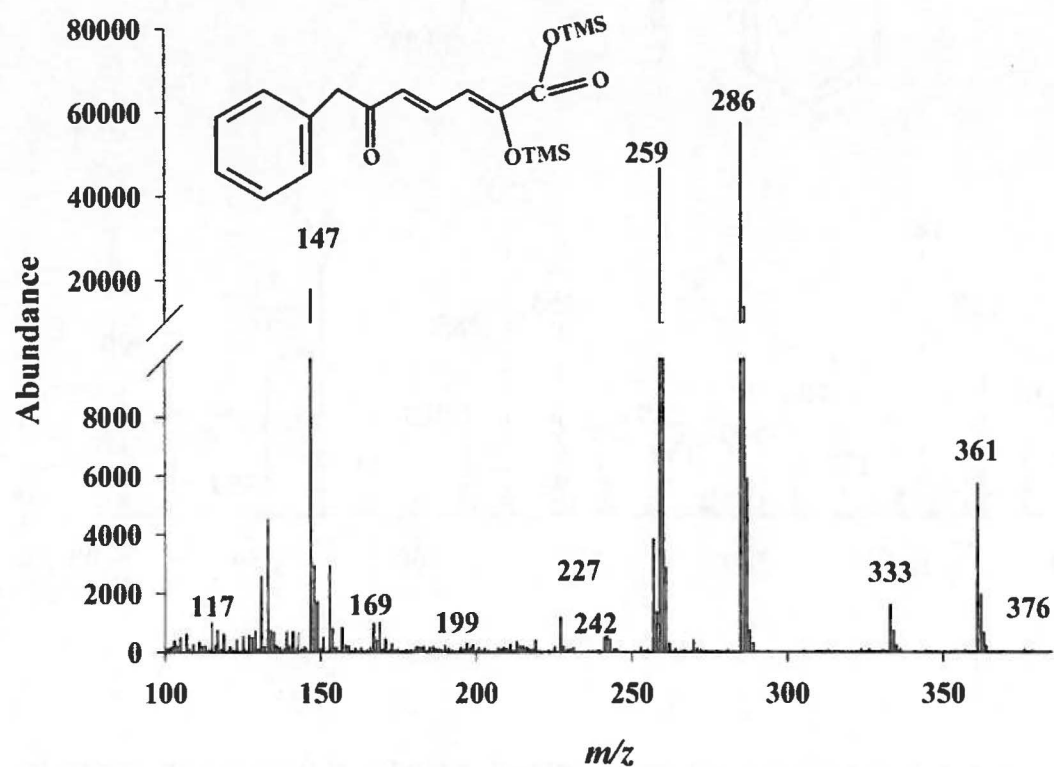


Fig. S1 Mass spectrum of the TMS-derived acidic metabolite produced from diphenylmethane by cells of strain B356 growing on diphenylmethane. Based on spectral features, the metabolite was identified as 2-hydroxy-6-oxo-7-phenylhepta-2,4-dienoic acid.

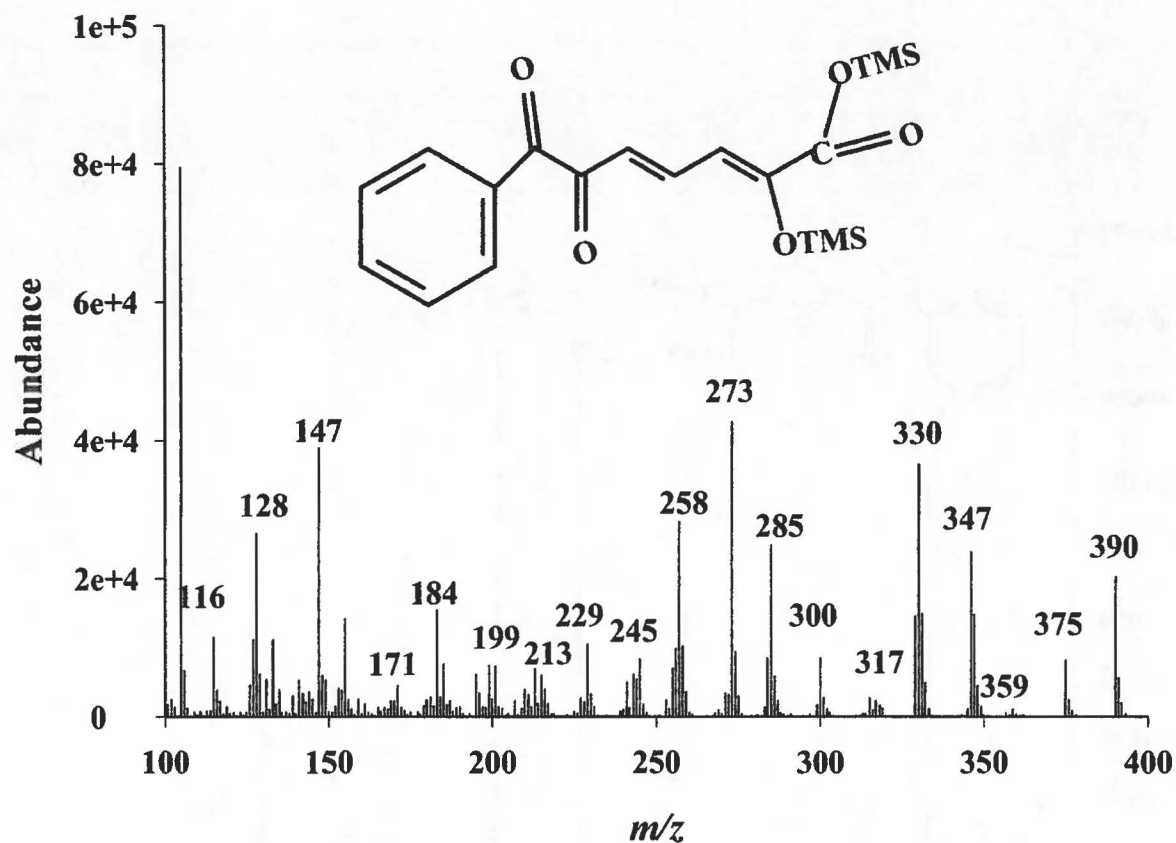


Fig. S2 Mass spectrum of a TMS-derived acidic metabolite produced from benzophenone by biphenyl-induced cells of strain B356. Based on spectral features, the metabolite was identified as 2-hydroxy-6,7-dioxo-7-phenylheptanoic acid.

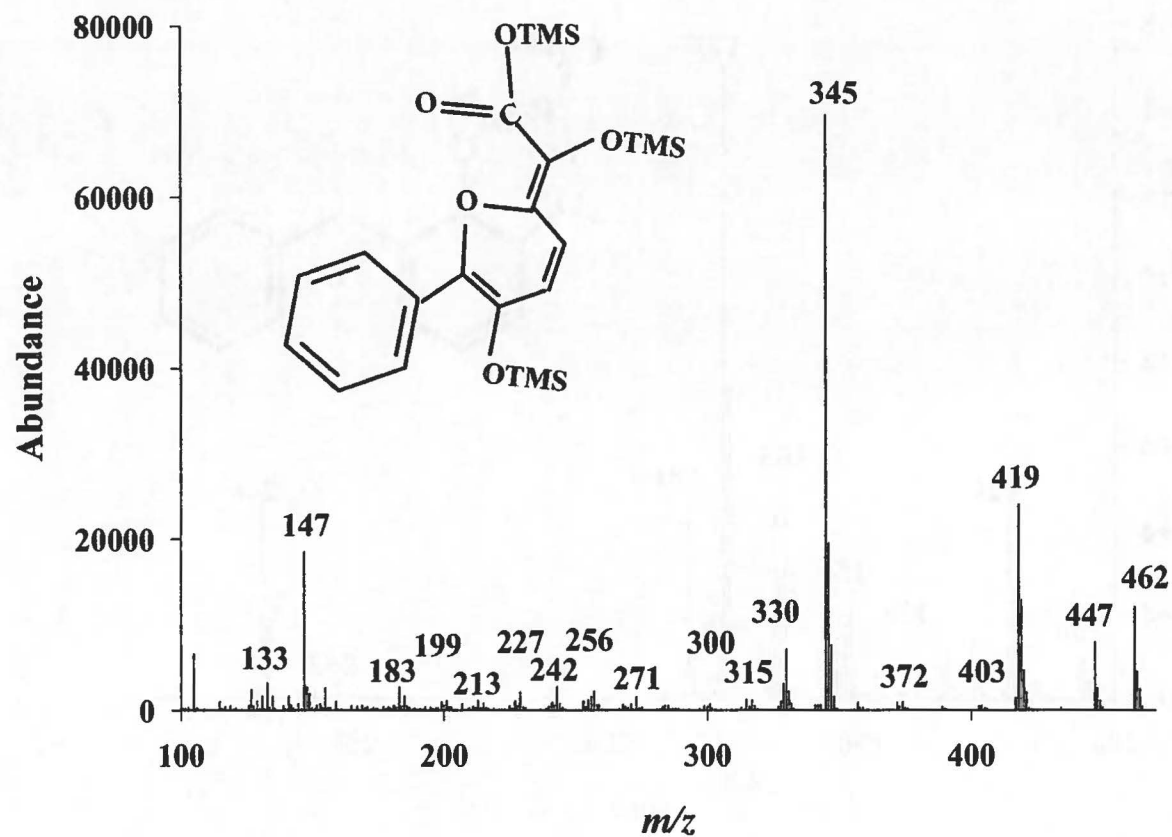


Fig. S3 Mass spectrum of a TMS-derived acidic metabolite produced from benzophenone by biphenyl-induced cells of strain B356. Based on spectral features, the metabolite was identified as a pyranol presumably generated from a cyclization reaction of 6,7-dioxo-7-phenylheptanoic acid.

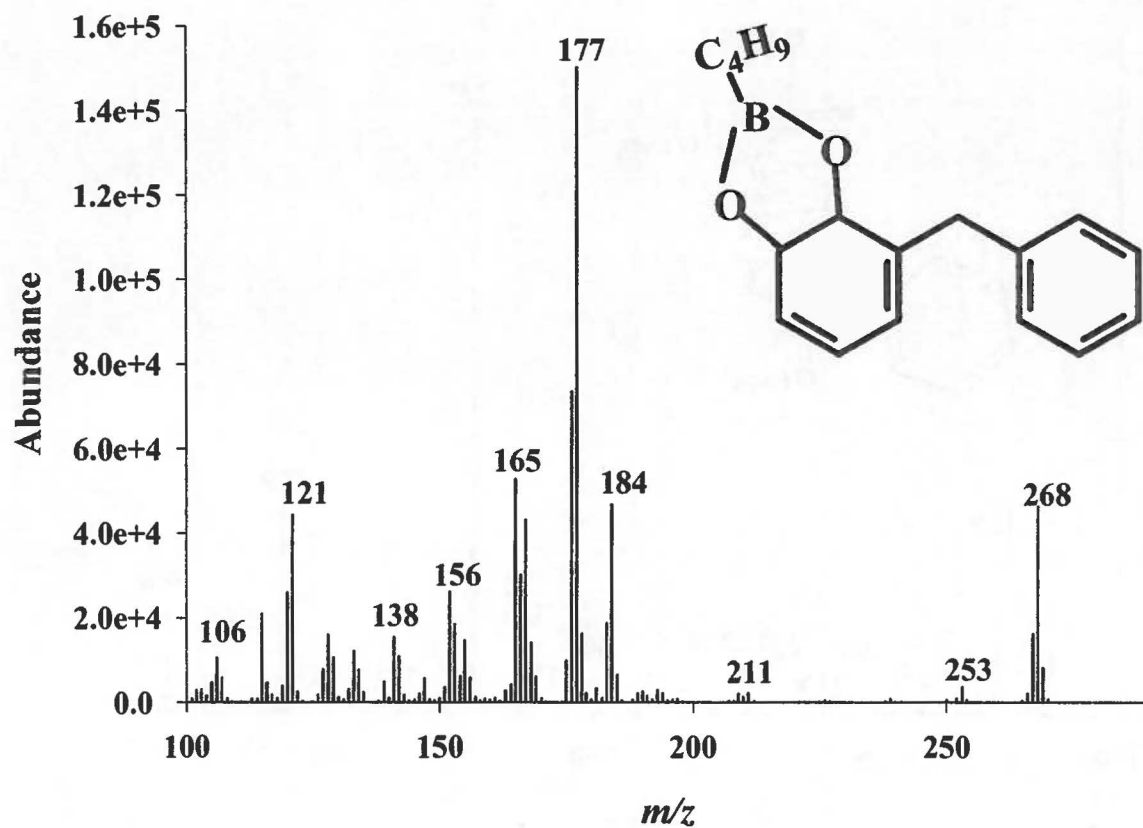


Fig. S4 Mass spectrum of a nBuB-derived metabolite produced from diphenylmethane by BphAE_{B356}. Based on spectral features, the metabolite was identified as 3-benzylcyclohexa-3,5-diene-1,2-diol.

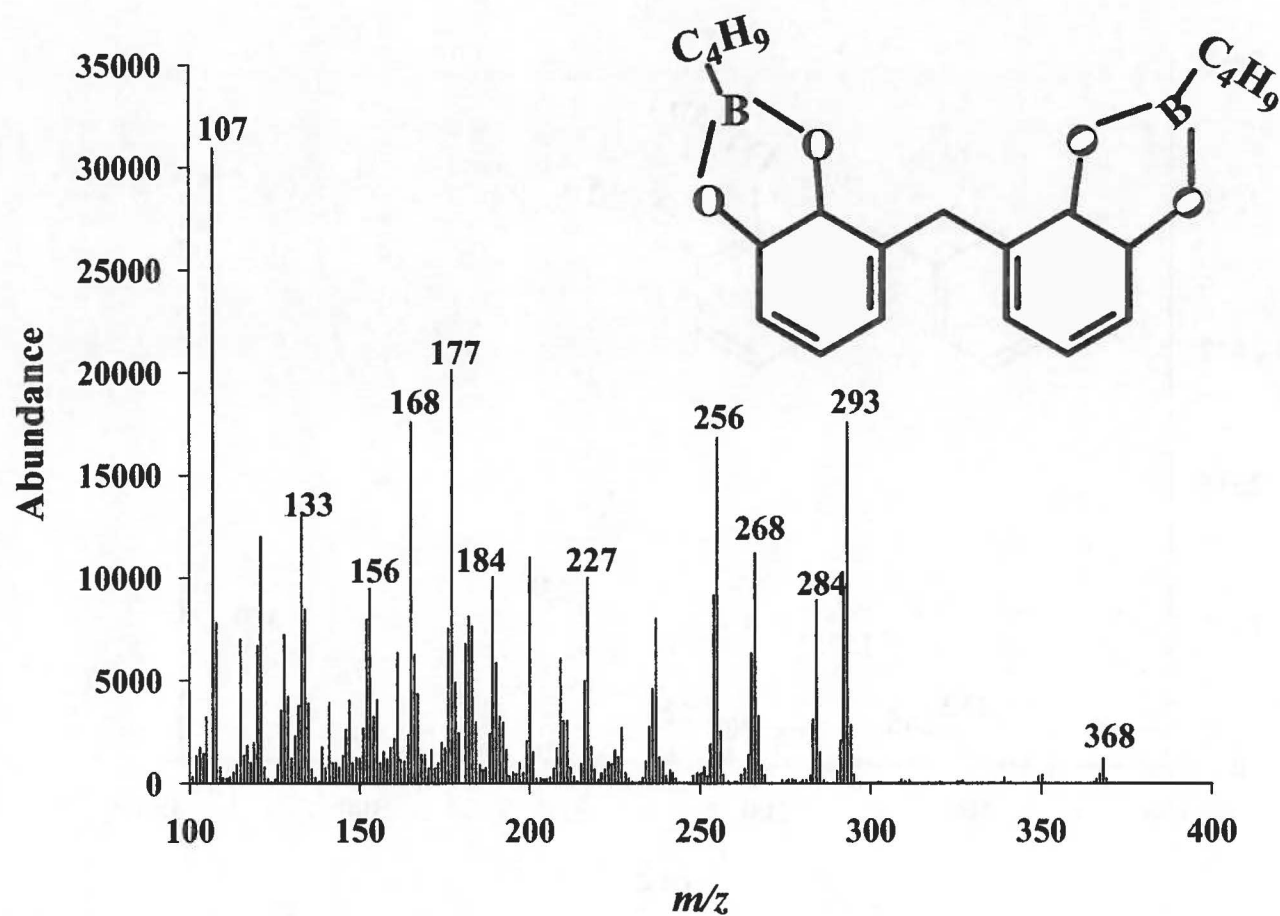


Fig. S5 Mass spectrum of a nBuB-derived metabolite produced from diphenylmethane by BphAE_{B356}. Based on spectral features, the metabolite was identified as 3-[(5,6-dihydroxycyclohexa-1,3-dien-1-yl)methyl]cyclohexa-3,5-diene-1,2-diol.

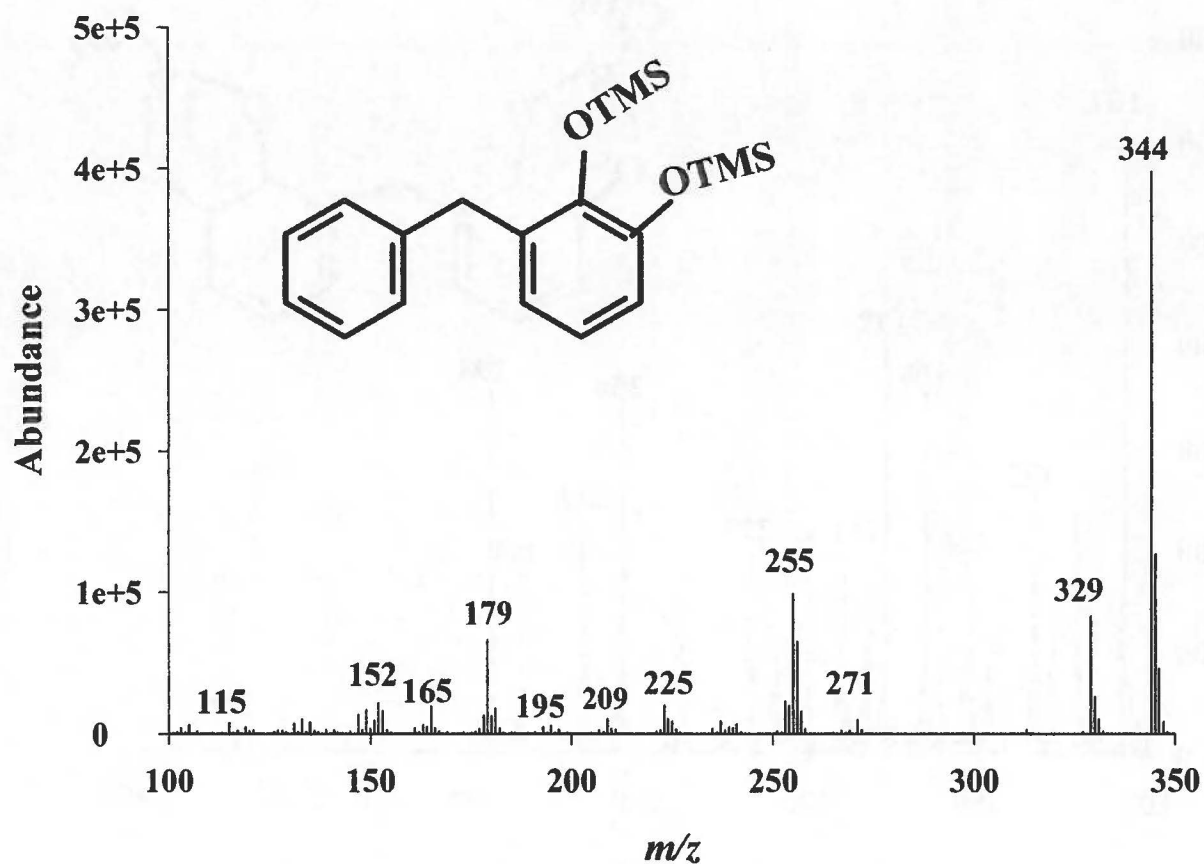


Fig. S6 Mass spectrum of the TMS-derived major metabolite produced from diphenylmethane by a coupled reaction composed of purified preparations of BphAE_{B356} plus BphB_{B356}. Based on spectral features, the metabolite was identified 2,3-dihydroxydiphenylmethane.

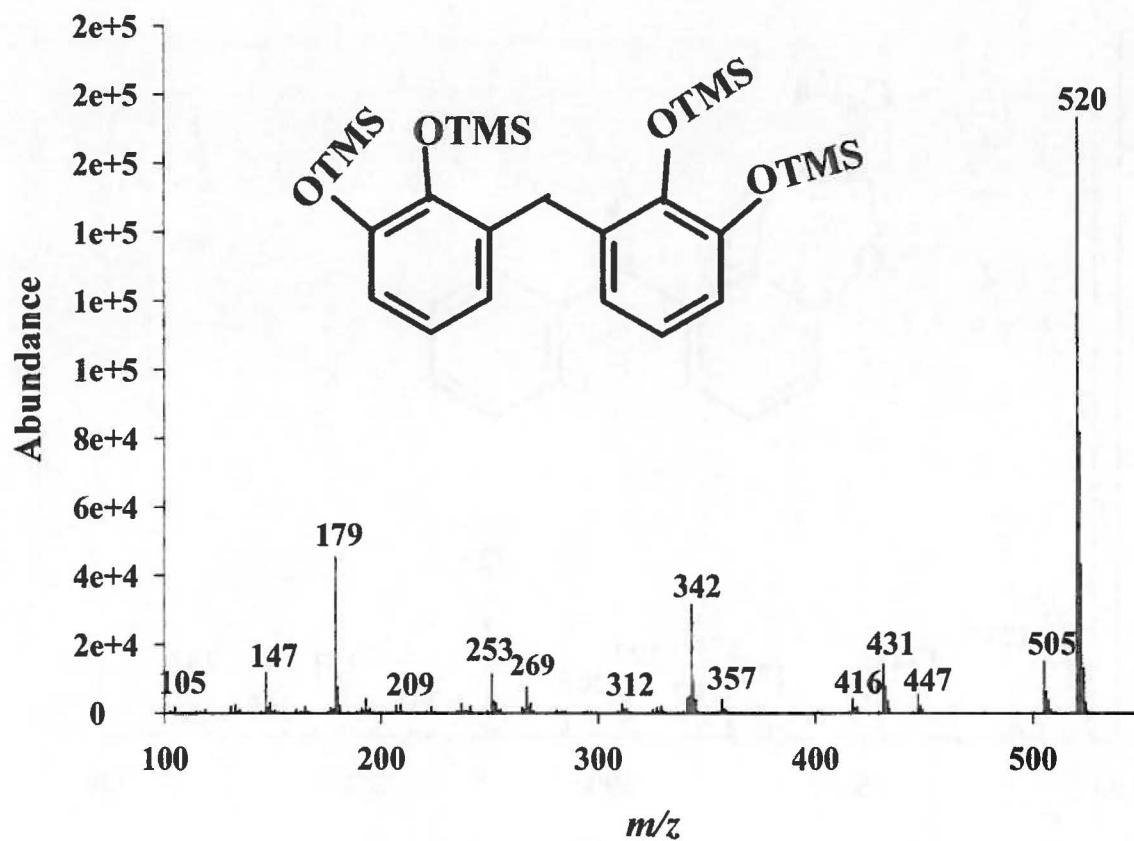


Fig. S7 Mass spectrum of the TMS-derived minor metabolite produced from diphenylmethane by a coupled reaction composed of purified preparations of BphAE_{B356} plus BphB_{B356}. Based on spectral features, the metabolite was identified 2,2',3,3'-tetrahydroxydiphenylmethane.

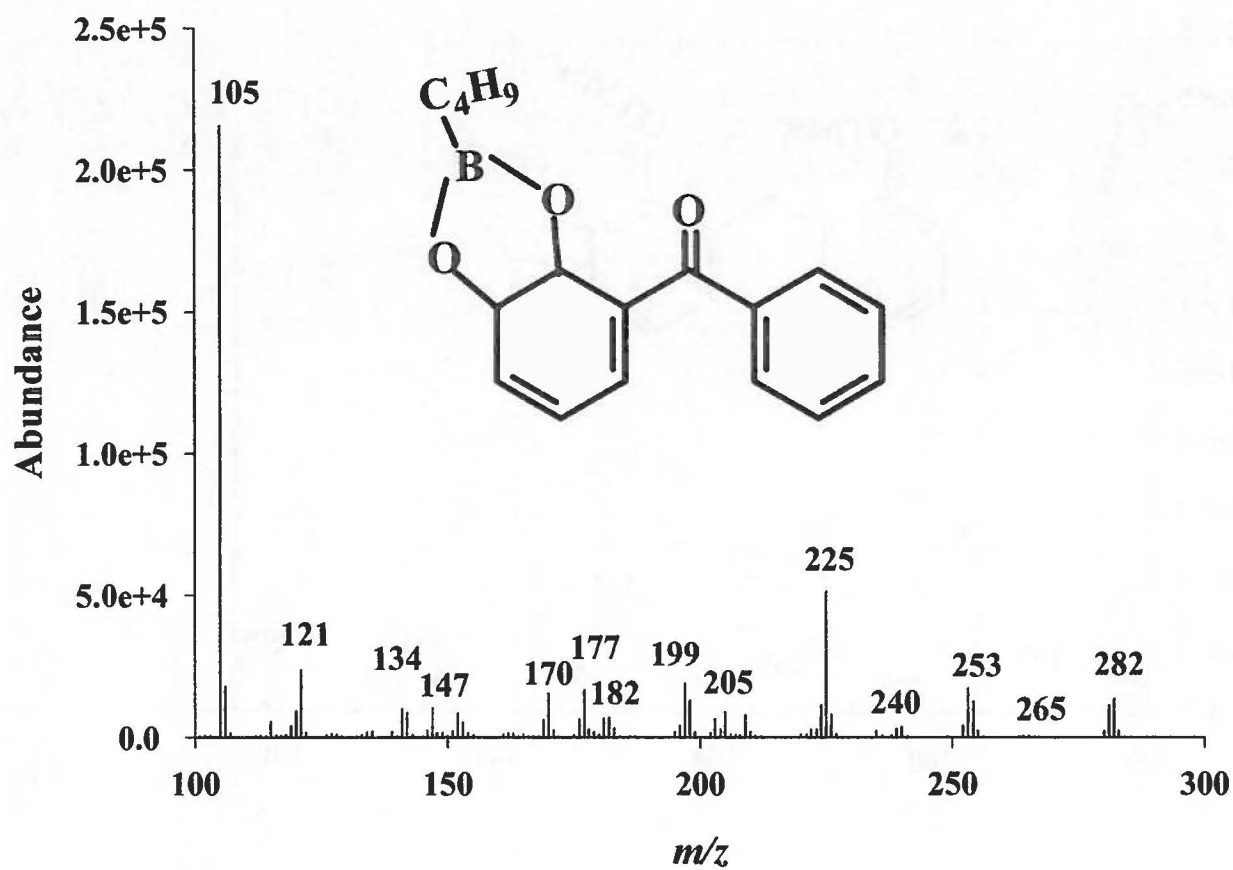


Fig. S8 Mass spectrum of the nBuB-derived metabolite produced from benzophenone by a BphAE_{B356}. Based on spectral features, the metabolite was identified 3-benzoylcyclohexa-3,5-diene-1,2-diol

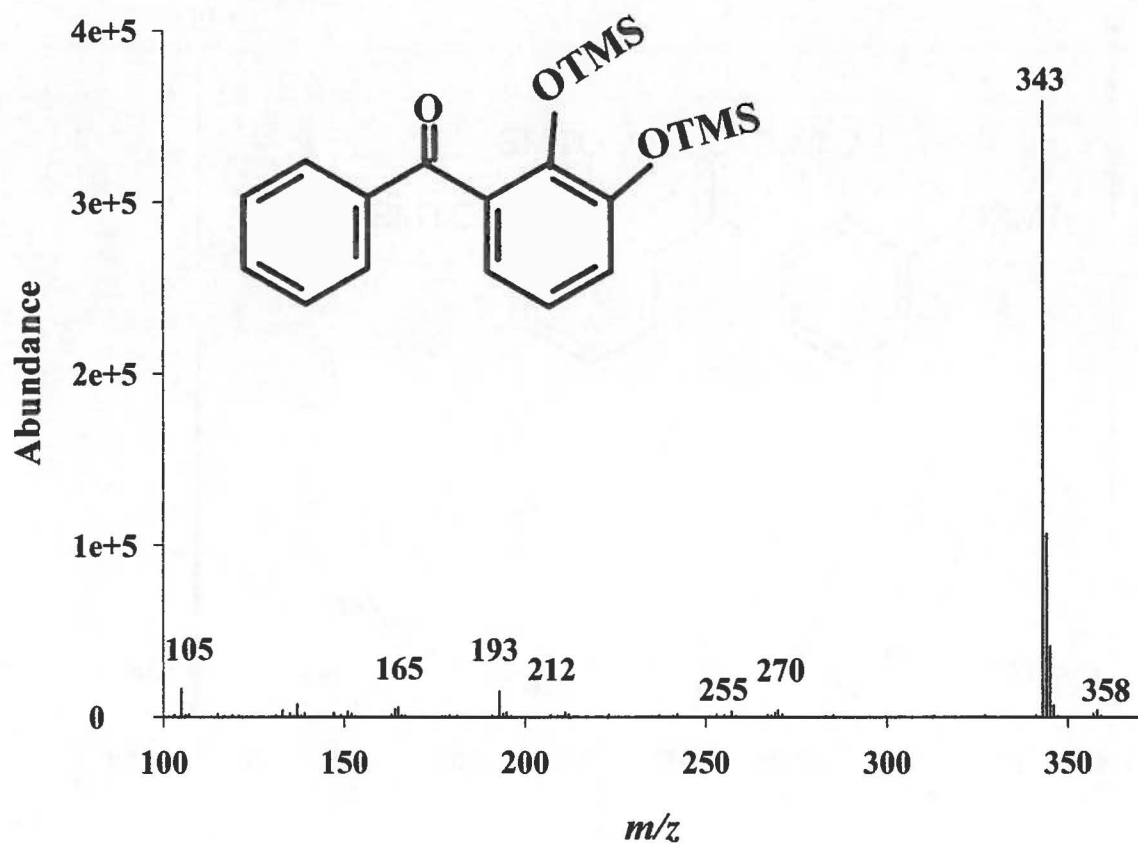


Fig. S9 Mass spectrum of the TMS-derived metabolite produced from 3-benzoylcyclohexa-3,5-diene-1,2-diol by BphB_{B356}. Based on spectral features, the metabolite was identified 2,3-dihydroxybenzophenone.

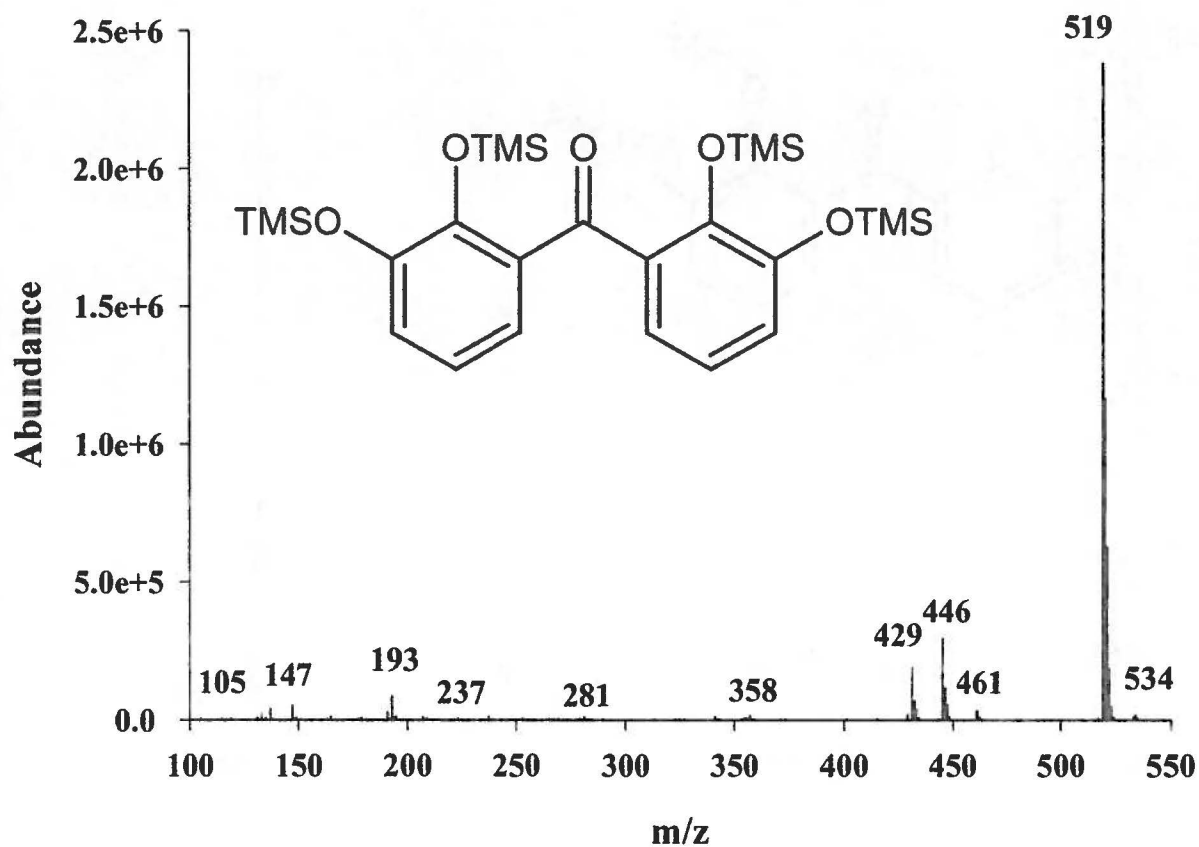
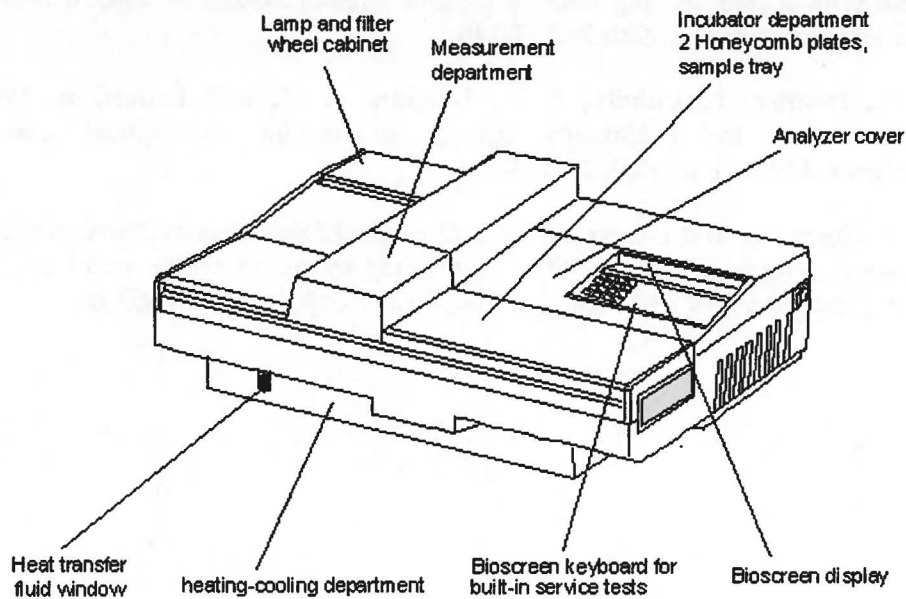


Fig. S10 Mass spectrum of the TMS-derived major metabolite produced from benzophenone by a coupled reaction composed of BphAE_{B356} plus BphB_{B356}. Based on spectral features, the metabolite was identified 2,2',3,3'-tetrahydroxybenzophenone.

Bioscreen C system

Bioscreen is an automated system manufactured by Labsystem, Helsinki, Finland, which is designed for high-throughput measurement of cell growth. Cells are inoculated in microplate wells and the plates are incubated in a computer-controlled incubator/shaker equipped with a sensitive spectrophotometer that can automatically follow cell growth by monitoring cell density or color production at a set frequency and at a desired wavelength. Data is exported to a computer that generates growth curves and may calculate accurate growth kinetic parameters. A diagram of the Bioscreen system is shown below.



The Bioscreen system diagram.

(Image was taken from the website <http://www.growthcurvesusa.com>)

Several studies using Bioscreen system can be cited :

- Begot et al. (1996) (2) used the system to calculate growth parameters of 9 bacterial strains.

- Augustin et al. (1999) (1) used the system to estimate the temperature dependent growth rate and lag time of 10 bacterial strains.

- Lebert et al. (1998) (3) used the system to study the effect of temperature, pH, and water activity on the growth of 59 bacterial strains isolated from meat products.

1. **Augustin, J. C., Rosso, L., and Carlier, V.** 1999. Estimation of temperature dependent growth rate and lag time of *Listeria monocytogenes* by optical density measurements. *J Microbiol Meth* **38**:137-146.
2. **Begot, C., Desnier, I., Daudin, J. D., Labadie, J. C., and Lebert, A.** 1996. Recommendations for calculating growth parameters by optical density measurements. *J Microbiol Meth* **25**:225-232.
3. **Lebert, I., Begot, C., and Lebert, A.** 1998. Growth of *Pseudomonas fluorescens* and *Pseudomonas fragi* in a meat medium as affected by pH (5.8-7.0), water activity (0.97-1.00) and temperature (7-25 degrees C). *Int J Food Microbiol* **39**:53-60.